EVALUATION OF FINGERPRINT PROFILE USING CHROMATOGRAPHIC TECHNIQUES OF BIOACTIVE HERBAL PHYTOCHEMICALS ISOLATED FROM *Paraboea paniculata*

TAN HOR YUE

MASTER OF SCIENCE

FACULTY OF SCIENCE
UNIVERSITI TUNKU ABDUL RAHMAN
MAY 2011

**EVALUATION OF FINGERPRINT PROFILE USING
CHROMATOGRAPHIC TECHNIQUES OF BIOACTIVE HERBAL
PHYTOCHEMICALS ISOLATED FROM *Paraboea paniculata***

By

TAN HOR YUE

A thesis submitted to the Department of Science,
Faculty of Science,
Universiti Tunku Abdul Rahman,
in partial fulfillment of the requirements for the degree of
Master of Science
May 2011

ABSTRACT

**EVALUATION OF FINGERPRINT PROFILE USING
CHROMATOGRAPHIC TECHNIQUES OF BIOACTIVE HERBAL
PHYTOCHEMICALS ISOLATED FROM *Paraboea paniculata***

TAN HOR YUE

Various attempts in isolating active pure compounds from potential plants by targeting a single compound have been practiced with the intention of developing a potent novel drug candidate. Yet, the possibilities of obtaining such novel substances are low from such approach. In view of this consideration, fingerprinting analysis of the bioactive compounds as a whole formulation to yield a common fingerprint profile in first dimension was aimed to establish in this study. The fingerprint profile established led to isolation and identification of active constituents for the first time from *Paraboea paniculata*.

An attempt to establish solid phase extraction (SPE) coupled with two-dimensional planar chromatographic (HPTLC) fingerprint profiles of *Paraboea paniculata* was demonstrated. The crude and SPE-fractionated extracts were screened at 50 μg/ml for cytotoxic activity against chronic myelogenous leukemic cell line, K-562 using MTT assay. The fingerprint profiles were developed with several optimised mobile systems and stationary phases. The HPTLC-DPPH method was applied to screen for free radical scavenging activity of the cytotoxic fractions. The active constituents were isolated with semi-preparative high

performance liquid chromatography (HPLC) and theirs structures were elucidated through spectroscopic data.

The segregation of the active group of constituents in both leaf and rhizome parts of *Paraboea paniculata* was clearly observed and each active fraction possesses its distinct set of fingerprint pattern. A common pattern of metabolites established from fractions 5 of leaf and rhizome indicates the presence of similar active group of constituents in both parts. The method was validated in term of precision, robustness, specificity and stability. Leaf and rhizome fractions 5 were both capable of scavenging DPPH free radicals, with corresponding inhibition rate of 84.5% and 79.7%. Three phenylpropanoid glycosides were isolated, namely 3,4-dihydroxyphenethyl-(3"-O-*β*-D-apiofuranosyl)-*β*-D-glucopyranoside (PP-1) from rhizome fraction 4; 3,4-dihydroxyphenethyl-(3"-O-*β*-D-apiofuranosyl-4"-O-caffeoyl)-*β*-D-glucopyranoside (PP-2), and 3,4-dihydroxyphenethyl-(3"-O-*α*-L-rhamnopyranosyl-4"-O-caffeoyl)-*β*-D-glucopyranoside (PP-3), from leaf fraction 5. PP-1, PP-2, and PP-3 exhibited strong cytotoxic activity against K-562 cell line with 50% of cell killing rate at the concentration of 18, 16.5, 17 µg/ml, respectively. As for DPPH free radical scavenging activity, PP-2 and PP-3 were as potent as quercitin and ascorbic acid and their IC_{50} values were determined as 15.3, 16.3, 7.5 and 11 µg/ml, correspondingly. Nevertheless, PP-1 attained an inhibition rate of 50% at the concentration of 34 µg/ml.

As a conclusion, the fingerprint profiles of *Paraboea paniculata* were successfully documented, which could be employed as an alternative rapid identification, and to interpret the bioactivities of similar species of plants through pattern recognition.

ACKNOWLEDGEMENT

Finally, I would like to express my utmost appreciation and gratitude to my parents for their untiring support and understanding all the while. And thank them for bringing me up throughout the years and unconditionally loving me. Same goes to my brother, my angels, and my friends for their love, moral support and encouragement all the while to bring the project to a successful completion.

APPROVAL SHEET

This thesis entitled **"EVALUATION OF FINGERPRINT PROFILE USING CHROMATOGRAPHIC TECHNIQUES OF BIOACTIVE HERBAL PHYTOCHEMICALS ISOLATED FROM _Paraboea paniculata_"** was prepared by TAN HOR YUE and submitted as partial fulfillment of the requirements for the degree of Master of Science at Universiti Tunku Abdul Rahman.

Approved by:

_____

(Assoc. Prof. Dr. Lim Yang Mooi)   Date: ……………………

Associate Professor/Supervisor

Department of Pre-Clinical Sciences

Faculty of Medicine and Health Sciences

Universiti Tunku Abdul Rahman

_____

(Assist. Prof. Dr. Lim Chan Kiang)   Date: ……………………

Assistant Professor/Co-Supervisor

Department of Chemical Science

Faculty of Science

Universiti Tunku Abdul Rahman

Date: _____

PERMISSION SHEET

It is hereby certified that **TAN HOR YUE** (ID NO: **08UEM08121**) has completed this dissertation entitled **"EVALUATION OF FINGERPRINT PROFILE USING CHROMATOGRAPHIC TECHNIQUES OF BIOACTIVE HERBAL PHYTOCHEMICALS ISOLATED FROM** *Paraboea paniculata***"** under supervision of **ASSOC. PROF. DR. LIM YANG MOOI** (Supervisor) from the Department of Pre-Clinical Sciences, Faculty of Medicine and Health Sciences and **ASSIST. PROF. DR. LIM CHAN KIANG** (Co-Supervisor) from the Department of Chemical Science, Faculty of Science.

I hereby give permission to my supervisor to write and prepare manuscript of these research findings for publishing in any form, if I did not prepare it within six (6) months time from this date provided that my name is included as one of the author for this article. Arrangement of the name depends on my supervisors.

Yours truly,

_____

(TAN HOR YUE)

DECLARATION

I hereby declare that the thesis is based on my original work except for quotations and citations which have been duly acknowledged. I also declare that it has not been previously or concurrently submitted for any other degree at UTAR or other institutions.

Name: <u>TAN HOR YUE</u>

Date: _____

FACULTY OF SCIENCE

UNIVERSITI TUNKU ABDUL RAHMAN

Date: _____

SUBMISSION OF DISSERTATION

It is hereby certified that **TAN HOR YUE** (ID NO: **08UEM08121**) has completed this dissertation entitled **"EVALUATION OF FINGERPRINT PROFILE USING CHROMATOGRAPHIC TECHNIQUES OF BIOACTIVE HERBAL PHYTOCHEMICALS ISOLATED FROM** *Paraboea paniculata***"** under supervision of **ASSOC. PROF. DR. LIM YANG MOOI** (Supervisor) from the Department of Pre-Clinical Sciences, Faculty of Medicine and Health Sciences and **ASSIST. PROF. DR. LIM CHAN KIANG** (Co-Supervisor) from the Department of Chemical Science, Faculty of Science.

I understand that the University will upload softcopy of my dissertation in pdf format into UTAR Institutional Repository, which may be made accessible to UTAR community and public.

Yours truly,

_____

(TAN HOR YUE)

TABLE OF CONTENTS

LIST OF TABLES

LIST OF FIGURES

LIST OF PLATES

LIST OF ABBREVIATIONS

1D	One dimensional
2D	Two dimensional
3D	Three dimensional
AHP	American Herbal Pharmacopoeia
ARBEC	ASEAN Review of Biodiversity and Environmental Conservation
ATP	Adenosine Triphosphate
C18	Carbon 18
CCD	Charge-coupled device
CD_3OD	Deuterated methanol
CD_3SOCD_3	Dimethyl sulfoxide
CH_3CN	Acetonitrile
CDK4	Cyclin dependent kinase 4
CDK6	Cyclin dependent kinase 6
CO_2	Carbon dioxide
CPGs	Caffeoyl phenylethanoid glycosides
D	Derivatization
D_2O	Deuterium oxide
DMSO	Dimethyl sulfoxide
DNA	Deoxyribonucleic acid
DPPH	2,2-diphenyl-2-picrylhydrazyl
DTP	Development Therapeutics Programme
EBV-EA	Epstein-Barr virus early antigen

EMEA	European Medicines Agency
FDA	Food and Drug administration
FT-IR	Fourier transform-infrared spectroscopy
GC-MS	Gas chromatography-mass spectroscopy
H	Hydrogen
H_2O	Water
HMBC	Heteronuclear Multiple-Bond Correlation
HMQC	Heteronuclear Multiple-Quantum Coherence
HPLC	High performance liquid chromatography
HPTLC	High performance thin layer chromatography
Hz	Hertz
IARC	International Agency for Research on Cancer
IC	Inhibitory concentration
INT	Iodonitrotetrazolium
IR	Infrared red
IVCLSP	*In vitro* cell line screening project
LDH	Lactate dehydrogenase enzyme
LLE	Liquid-liquid extraction
MAKNA	National Cancer Council
MIPs	Molecularly imprinted polymers
MP	Mobile phase
MS	Mass spectroscopy
MTS	3-(4,5-dimethylthiazol-2-yl)-5(3-carboxymethoxyphenyl)-2-(4-sulfophenyl)-2H-tetrazolium

MTT	(3-(4,5-dimethylthiazol-2-yl)-2, 5-diphenyltetrazolium bromide
NAD	Nicotinamide adenine dinucleotide
NCI	National Cancer Institute
NMR	Nuclear magnetic resonance
NO	Nitric oxide
O	Oxygen
pH	Potential of Hydrogen
PhGs	Phenylethanoid glycoside
PK-C	Protein kinase C
R_f	Retention factor
RNA	Ribonucleic acid
ROS	Reactive oxygen species
RP	Reversed phase
RPMI	Roswell Park Memorial Institute medium
SD	Standard deviation
Si	Silica
SP	Stationary phase
SPE	Solid phase extraction
TGF-β1	Tumour growth factor-beta1
TLC	Thin layer chromatography
U.S.	United States
USP	United States Pharmacopoeia
UV	Ultra violet
UV-vis	Ultra violet-visible

WHO	World Health Organization
XTT	2,3-bis(2-methoxy-4-nitro-5-sulfophenyl)-5-[(phenylamino) carbonyl]-2H-tetrazolium hydroxide
α-L-rhamnopyranosyl	alpha-L-rhamnopyranosyl
β-D-apiofuranosyl	beta-D-apiofuranosyl

CHAPTER 1

INTRODUCTION

International Agency for Research on Cancer (IARC) reported that 7.6 million of cancer death worldwide in 2008, and estimated 17 million of deaths by 2030 (American Cancer Society, 2008). The rate of cancer death is estimated to be 1 in 8 worldwide. In Malaysia, according to the report released in early of 2008, up to 70,000 new cancer cases were diagnosed in West Malaysia between 2003 and 2005 (MAKNA, 2008). Current cancer therapies are often inefficient due to the accompanied complications and side effects (Christian and Custodio, 2008). Thus, study aims to seek for more potent drug leads as a hope to counteract the problems posed by current cancer therapies should be emphasized.

Plants are well known as a common source of local medicinal remedy used today. Plant composed of a complex mixture, and often only a small amount of the compounds contributed to the pharmaceutical effects. Thus, determination of phytochemical compound(s) of every plant product is vital. The development of metabolite fingerprint proposed here is to create an alternative rapid identification and to interpret the bioactivities of similar species of plant(s) through pattern recognition.

Fingerprint analysis has been accepted by World Health Organization as a strategy in the assessment of the complex mixtures such as herbal medicines (WHO, 1991). A single herbal medicine composes of numerous substances, and chromatographic fingerprint profile allows a good integral representation of the chemical components as well as facilitates the dereplication and identification of active plant metabolites (Liang *et al*., 2004; Liu *et al.*, 2008). The employment of fingerprint profile by most studies serves the purpose of quality control and standardization of the herbal product since most of the target compounds present are known. In this study, the attempt to establish two-dimensional chromatographic fingerprint profiles of a novel plant product was demonstrated. The development of fingerprint profile using two-dimensional analysis aims to give a more reliable comprehensive chemical profile that represents the active group of constituent(s) in the plant.

Paraboea paniculata was screened and indicated to show cytotoxic effect against K-562 and HL-60 cell lines (Tan, 2008; Toi, 2008). A phytochemical investigation on *Paraboea glutinosa* has led to isolation of few triterpenes and sterols compounds (Wang *et al.*, 2009). However, at present there is no prior detailed literature of chemical composition and bioactivity of *P. paniculata* documented. And hence, this project was carried out to identify the cytotoxic constituent(s) of *P. paniculata.*

In addition, the fingerprint profiles of these cytotoxic constituents were documented. The offline hyphenated SPE-planar TLC technique was employed to facilitate the study. SPE was utilized in this study as an interface to fractionate the bioactive constituent(s) based on polarity. HPTLC was selected to establish and systematically document the two-dimensional fingerprint profiles due to its simplicity in sample preparation and the possibility of evaluating many samples simultaneously under same chromatographic condition (Reich and Schibli, 2007). HPTLC fingerprinting coupled with DPPH method was employed to screen for the free radical scavenging activity of the components present in *P. paniculata.*

Thus, the objectives of the present study are:

1. To evaluate the *in vitro* cytotoxic activity of *P. paniculata* against K-562 cell line by MTT assay.

2. To develop two-dimensional cytotoxic fingerprint profiles of both leaf and rhizome of *P. paniculata* with the employment of solid phase extraction (SPE) and advanced planar chromatography technique (HPTLC).

3. To validate the optimized method of HPTLC for establishment of cytotoxic fingerprint profiles.

4. To screen for the free radical scavenging activity of the components of *P. paniculata* via HPTLC-DPPH method and spectrophotometric DPPH method.

5. To isolate and structurally elucidate the cytotoxic pure constituents from both leaf and rhizome of *P. paniculata*.

CHAPTER 2

LITERATURE REVIEW

2.1 Overview of Cancer

Cancer is a group of diseases originates from normal cells that divide uncontrollably and invade other tissues (NCI, 2010). Normal mammalian cells only undergo division approximately 20 to 50 times before they age and die. Cancer occurs in the case where cell proliferation increases and decreases in the rate of cell death. The underlying causes that lead to cell mutation include down regulation of tumour suppressor gene, abnormal acceleration of cell senescence, and its self renewal property (Erenpreisa and Cragg, 2007). Human body is composed of millions of cells, the basic unit of structure and function. Genetic alteration causes increase of DNA damage, leads to malignant transformation. In addition, due to the defects of checkpoint in arrest phases of cell cycle, mutated genes (e.g. p53 genes) still trigger the DNA synthesis with a damaged template (Campbell and Reece, 2005; Melnick *et al*., 1993).
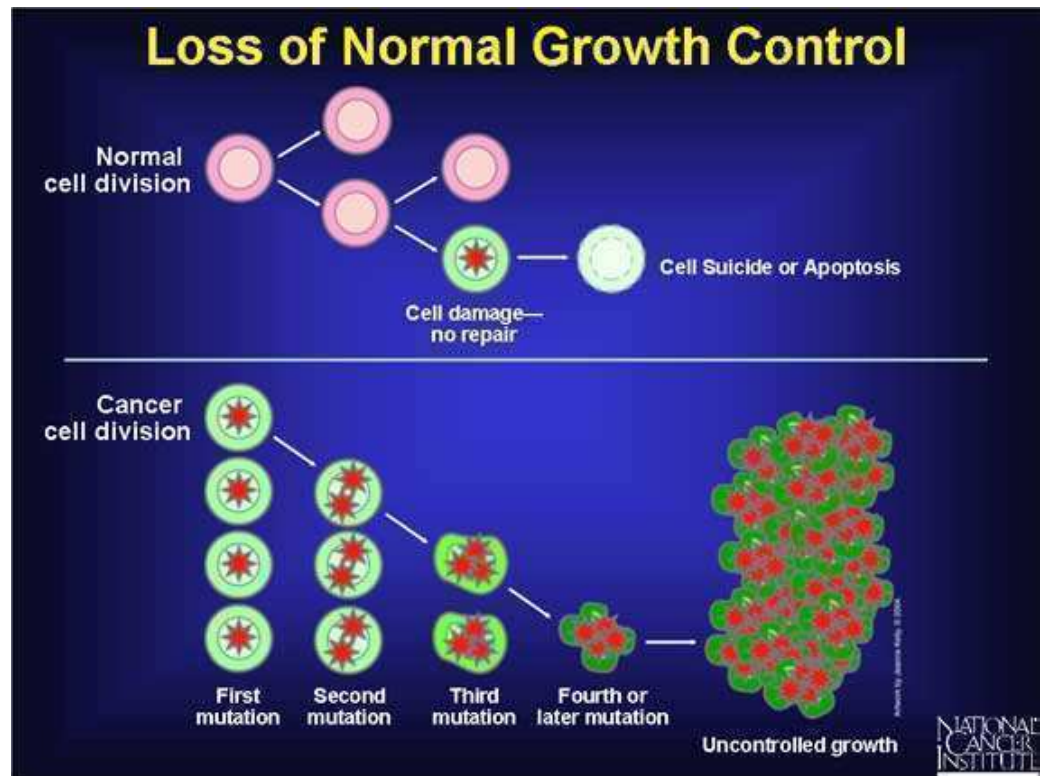
Figure 2.1: The loss of normal cell growth control, leads to cancer (NCI, 2006).

Not all tumours exhibit aggressive growth. Tumour development is divided into three categories that depend on its increasing severity: benign, malignant, and metastatic. Tumours that grow locally and remain on the original sites are benign tumours. These non-invasive tumours are not cancerous since they are harmless to their hosts and can be removed completely through surgery. As for malignant tumours, they are cancerous tumours that have the ability to invade nearby tissues and spawned metastases. They may enter hosts' bloodstream or lymph vessels and start to divide on the new target tissues.

There are five categories of malignant tumours: carcinoma, sarcoma, leukaemia, lymphoma/myeloma and central nervous system cancers. Carcinomas are the most common cancer, which arise from the epithelial tissues that line the internal organs. Tumours that arise from carcinomas include epithelial cells that lines gastrointestinal tract from mouth to large intestine, as well as the skin, mammary gland, pancreas, lung, liver, ovary, gallbladder and urinary bladder. Sarcomas are the non-epithelial cancers derived from connective or supportive tissues such as muscle, bone, tendon, cartilage, and fat. Lymphomas are tumours that start from the immune system while leukaemia is tumour that begins from the blood forming unit such as bone marrow. Central nervous system cancer is cancer that begins in the tissues of the brain and spinal cord (NCI, 2010).

Most current cancer therapies induce cancer cell death via two different processes, either apoptosis or necrosis. Apoptosis takes part actively in its own death process; as for necrosis, it is a passive process which serves to remove damaged cells from the organism. Normally, apoptosis and necrosis can be differentiated by their mode of cell death. Changes associated with apoptosis include membrane blebbing, cytoplasm shrinkage, nucleus condensed, and no inflammatory response triggered at last. In contrast, necrosis causes membrane integrity loss, swelling of cytoplasm and mitochondria followed by rupture of membrane, and lastly associated with inflammatory response (Tannock *et al*., 2005).

2.2   Current Cancer Treatment

According to NCI (2003), initial treatments given worldwide include the three common conventional therapies: chemotherapy, radiation therapy, surgery and other treatment approaches such as angiogenesis inhibitor, biological therapy, gene therapy, laser therapy and photodynamic therapy.

Chemotherapy is the primary treatment for inoperable diseases. Chemotherapy drugs work by targeting on DNA replication, DNA damage system, cell division mechanism and metabolic processes. Chemotherapy drugs can also use in combination to bring the synergistic effect between drugs (Gore and Russell, 2003). However, acute and long-term toxicities following chemotherapy bring the dose limiting factor in the patients (Pirozynski, 2006). Most chemotherapy drugs used are poorly selective to cancer cells and result in healthy cells damaged. Drug resistance also appears through mutation and selection. Schrijvers (2003) reported that extravasations increase the risk of chemotherapy as the chemotherapeutic agent escapes from vessels into tissue caused by drug leakage.

Radiotherapy works by directing the ionizing radiation to kill cancer cells selectively, while minimizing the damage of normal cells (Gore and Russell, 2003). However, tumour size becomes limiting factor for radiotherapy as the best result can only be seen in tumours with diameter less than 4cm (Pirozynski, 2006).

Surgical removal is another common way to perform, but it akin to radiotherapy, could not eradicate metastatic cancer (Chabner and Roberts, 2005). It is primarily used to remove melanoma *in situ* and stage I cancer.

2.3   Multistage Carcinogenesis

The development of tumour from single cells, undergoing expansion, forming foci and nodules and lastly proceeding to malignant stage is time dependent. The three typical stages of initiation, promotion and progression provide an important scaffold to understand the carcinogenesis.
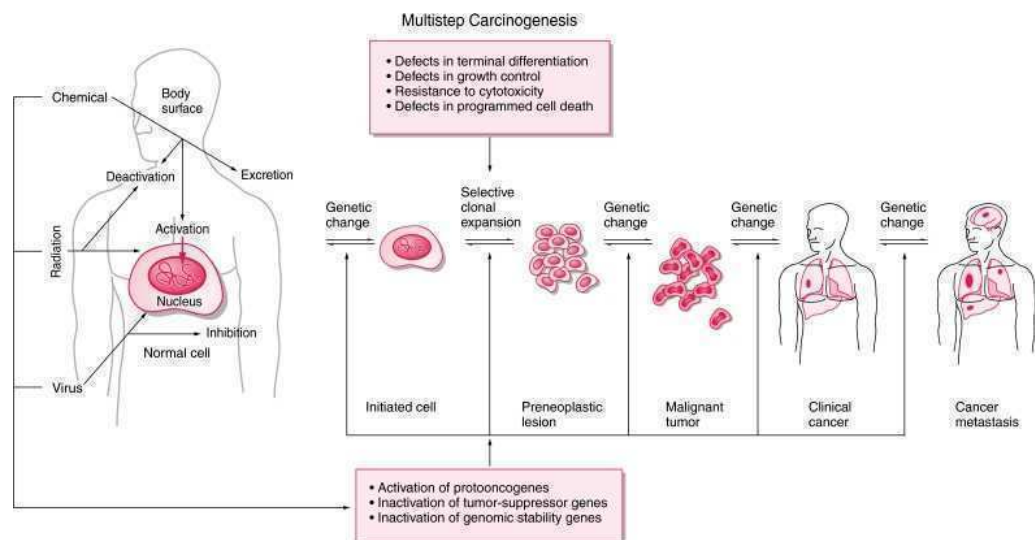
Figure 2.2: Multistage chemical carcinogenesis occurring in three phases, initiation, promotion and progression (Kufe *et al*., 2003).

2.3.1 Initiation

The administration route of carcinogens is an important factor that may influence the effects of carcinogens on initiated cells. Not only chemically acting carcinogens, but also hormones, irradiation, UV light and other physical agents are capable of instigating carcinogenesis. The carcinogens trigger genetic error and leading to mutation in DNA synthesis. However, presence of DNA adduct alone may not enough to bring about the initiation process, unless the cell proliferation implant in the genome and the DNA repair system declines. Initiated cells may not establish to become tumour, because most of the initiated cells will undergo apoptosis. Cells have protective mechanism by executing cell cycle arrest or even cell death if the damage is too extensive. DNA adduct formation that leads to mutation of proto-oncogenes, tumour suppressor genes and genes involved in damage repaired mechanism may disrupt the regulation of cell cycle and normal cell growth; thereby further stimulate tumour development (Kufe *et al*., 2003; Tysnes and Bjerkvig, 2007).

2.3.2 Promotion

Promotion stage is the only stage that is reversible (Weinberg, 2007). It does not involve changes of DNA structures but rather in gene expression. Tumour promotion is the clonal expansion of initiated cells via altered gene expression (Tannock *et al*., 2005). After the cells are initiated to proliferate, promoters are

involved to enhance the proliferation of altered cells, resulting formation of benign lesions such as papillomas, nodules and polyps. These lesions will relapse, unless the additional mutations are fortified to develop into malignant neoplasm. Tumour promoting agents reduce the tumour latency period once the tissue exposed to tumour initiator and induce formation of a population of initiated cells (Kufe *et al*., 2003). Sometimes, even when promoters have been removed, papillomas would collaborate with genetically modified initiator and continue to enlarge, eventually become carcinoma (Weinberg, 2007).

2.3.3 Progression

Progression indicates the evolution of cells to an increasingly malignant growth state (Weinberg, 2007). Population of malignant cells associated with abnormal karyotypes, and all the features of metastasis and invasion occur solely in progression stage. Transition of stable diploid to unstable aneuploid cells is one of the causes of karyotypic instability (Tysnes and Bjerkvig, 2007). Tumours with variety of genetic modifications create greater challenge to cancer therapy. Moreover, behaviour of cancer cells become metastatic, which means the abnormal cells are able to leave primary tumour to invade other cells by penetrating bloodstream or lymph circulation and begin to grow on other target organs. These aggressive cells are able to degrade extracellular matrix, develop suitable metabolism in order to escape from immunologic surveillance and subsequently invade and degrade the basement membranes (Lupulescu, 2001).

11

2.4 Plant Natural Product

Over 65% to 80% of the world's population use plants as their primary source of medicinal drugs (Cordell, 1995), which due to its structurally versatility, effectiveness and low cost. In Western Pharmacopoeia, approximately 7,000 medicinal compounds are derived from plants (ARBEC, 2003). U.S. Food and Drug Administration has also reported the growing interest on the evaluation of cancer targeted botanical drugs as there is an urgent medical need for new treatments (Chen *et al*., 2008). The anticancer property of plant natural product has been demonstrated in the early 1950s, where *Vinca* alkaloids with antidiabetic property are able to block tumour cell proliferation. Interest in plant natural products was further developed in year 1956 where a broad programme is established to collect and test plant and marine sources (Chabner and Roberts, 2005; Cragg and Newmann, 2005). In recent years, even with the advent of combinatorial chemistry and high-throughput screening, the discovery of new drug lead targeted on plant natural product is still demonstrated (Ortholand and Ganesan, 2004).

Secondary metabolites that produced by plant species are important for ecological functions such as chemical defence, allelopathy, and as attractants for pollination (Stepp and Moerman, 2001). Plants tend to produce toxic substances, for example tannins, alkaloids and terpenes to cause detrimental effects on other plants or predators. Interestingly, many of these compounds that produced by

plant might become the source of novel therapeutic candidate compounds. Aspirin, caffeine, pilocarpine, atropine, codeine, digoxin, eugenol, quinine, arteether, galantamine, nitisinone, tiotropium are examples of drug that derived from plants and currently in used for clinical practice. Vinca alkaloids, taxanes, podophyllotoxin, camptothecin are FDA-approved plant-derived anti-cancer compounds; and flavopiridol, homoharringtonine, β-lapachone and cambretastatin A4 are currently under investigation (Nobili *et al*., 2009; Lee *et al*., 2011).

2.5   Anticancer Drug Discovery and Development

In 1950s, U.S. National Cancer Institute has recognized the potential of natural product as anticancer agent by introducing the *in vitro* screening programme using a range of cancer cell lines (Cragg *et al*., 2005). In 1990, Development Therapeutics Programme (DTP) of National Cancer Institute has assisted anticancer drug discovery programme by implementing *In Vitro* Cell Line Screening Project (IVCLSP) (DTP, 2009). Roughly 85,000 compounds have been screened against 60 human tumour cell lines, representing leukaemia, melanoma, and cancers of lung, colon, brain, ovary, breast and prostate (Holbeck, 2004).

Route of developing a novel drug candidate is lengthy and time consuming. The whole process generally takes 12 years, including review and approval by FDA (Cashman, 1996). In United States, there are a series of three clinical trials before filing with FDA. In the phase I trial, candidate drugs are

13

tested for various doses, in order to yield a dose that are higher than that needed to elicit a therapeutic effect and lower than the maximum tolerated dose. Phase I clinical trial usually involved a small group of volunteers. Efficacy and dose range in patients are evaluated in phase II clinical trial. However, certain types of cancer would never be identified as target for drug treatment, as a result of many useful candidate drugs are discarded in this phase. Phase III trial is very costly, and yet critical. It is undertaken by huge population of patients. It shows the significant clinical response assigned to the drug (Weinberg, 2007). Before a lead compound passes through the three stages of clinical trials, it goes through the processes of lead identification, lead optimization (medicinal or combinatorial chemistry), and lead development (pharmacology, toxicology, pharmacokinetics, and ADME and drug delivery) (Balunas and Kinghorn, 2005).

An anticancer drug targeted at different levels, which include cancer cells, endothelium, extracellular matrix, immune system and the host cells. Classically, anticancer drugs can be classified as chemotherapy, hormone therapy and immunotherapy. However, Espinosa *et al*. (2003) has postulated another drug classification based on the kind of target, as the classical theory has failed to categorize all existing anti-cancer drugs. The proposed classification aims on DNA, RNA and protein level. Although DNA is the common target of anticancer chemotherapy, the efforts targeting on monoclonal antibodies and small molecules act at the level of protein of tumour cells and antisense

oligonucleotides directed towards the RNA level of cells also actively described in many studies (Avendano and Menendez, 2008).

Four main classes of anticancer chemotherapy agents in clinical use are vinca alkaloids, epipodophyllotoxins, taxanes, and camptothecins (Nobili *et al*., 2009). Vincristine and vinblastine, isolated from Madagascar periwrinkle, *Catharanthus roseus* block mitosis with metaphase arrest by binding specifically to tubulin as a consequence of depolymerisation. Podophyllotoxin, which isolated from resin of *Podophyllum peltatum* irreversibly inhibiting DNA topoisomerase II by binding to tubulin. Taxanes, extracted from the bark of *Taxus brevifolia* and camptothecin derived from the bark of *Camptotheca acuminata* represent a landmark in cancer research due to theirs significant anti-solid tumour efficacy (Rocha *et al*., 2001; Nobili *et al*., 2009).

2.6   Metabolic Fingerprinting

Plant chromatographic fingerprinting is a specific chromatographic pattern of recognizing a group of pharmacologically active and characteristic compounds derived from herbal medicine. A good chromatographic fingerprint profile could highlight the "integrity", "fuzziness", "sameness" and also "differences" of the plant investigated (Liang *et al*., 2004). The authentication and identification of all of the pharmacologically active compounds (Schaneberg *et al*., 2003), and their representative amount or concentration in the plant can be determined through an

15

informative fingerprint profile. Besides, fingerprint profiles of different samples with good separation can demonstrate their similarities and distinguish them from closely related species (Ni *et al.*, 2008).

Currently, the common practice is focusing on a single active marker for the purpose of identification and quality assessment; however, the therapeutic efficacy of herbal medicine is always featured by multiple ingredients in plant rather than single constituent. Thus, development of comprehensive multi-component fingerprint profile for an herbal drug is vital (Chen *et al.*, 2006). Fingerprint analysis has been accepted by World Health Organization as a strategy in the assessment of the complex mixtures such as herbal medicines (1991). Besides, FDA (U.S. FDA, 2000), EMEA (European Medicines Agency, 2001) and Committee of National (Chinese) Pharmacopoeia (2000) have also denoted the employment of chromatographic fingerprinting as the quality control of botanical medicines. Fingerprint method is a comparably easier, faster, less expensive and less labour-intensive screening tool (Chen *et al.*, 2007).

Plant fingerprint profile becomes primary tool for the standardization and quality control of the plant product (Gong *et al.*, 2008), especially in the lack of authentic standards for identification of all of the active substances in herbal medicine (Kumar *et al.*, 2008). The bioactivities and possible side effects of active compounds may modify due to the variation of herbal product at different harvest season, geographical origin and processing process. Thus, determination

of phytochemical compounds in every herbal product by fingerprinting technique is essential, in order to ensure the repeatability and reliability of production. Moreover, conventional research emphasizes on the isolation of the most active compound and this may neglect many possible bioactive metabolites due to large dynamic range, for example masking of major compounds and different polarity of compounds present in the plant (Yuliana *et al*., 2011). Fingerprint provides the full picture of the herbal product. It explains the interaction among the compounds through pattern recognition, meanwhile offering the integral characterization of the complex mixture with high level of reliability (Cao *et al*., 2006). An optimized fingerprint profile should demonstrate as much compounds as possible. However, it may be impossible to develop an all-embracing chromatographic fingerprint in practice; a representative fingerprint is acceptable to yield the preliminary evidence of compounds (Xie *et al*., 2006).

A paramount analytical methods include chromatographic and electrophoretic methods, particularly hyphenated chromatography such as GC-MS (Fiehn, 2008), HPLC coupled with atomic emission spectroscopy (Ni *et al*., 2008), HPLC-FTICR/MS (Suzuki *et al*., 2008), HPLC-MS (Yang *et al*., 2008), pressurized capillary electro chromatography (Xie *et al*., 2007) and hyphenated capillary electrophoresis (García-Pérez *et al*., 2008), that coupled with spectroscopic method are employed in most studies to obtain a chemical fingerprinting that provide qualitative analysis and structural elucidation. Liu *et al*. (2008) has demonstrated effective identification of active constituents in treating

atherosclerosis by establishment of semi-purified plant library via HPLC-DAD-MS. The screening and differentiation between different genera performed in the region of chromatogram via HPTLC also reported by Di *et al*. (2003). Every analytical method has its own advantages and limitations. The potential pitfalls and focus on finding conditions to minimize these problems for more reliable analysis is essential (Micheal, 2006). More methodological validation such as specificity, reproducibility and applicability is required in order to obtain a stable and official fingerprint profile.

2.7   Separation Methods

2.7.1 Solid Phase Extraction (SPE)

By definition, solid phase extraction (SPE) is a method for rapid sample preparation in which the solid stationary phase is pre-packed into a syringe cartridge. It is an alternative method to liquid-liquid extraction (LLE) and used to selectively separate, concentrate and purify the target analytes. LLE aims to separate compounds between two liquid phases, whereas analytes in SPE are separated between solid and liquid phases. In SPE, analytes with greater affinity to solid phase will tend to retain on stationary phase. The retained compounds are removed from stationary phase by eluting the appropriate mobile phase with higher affinity to analytes.

Usually, SPE is used to clean up sample by removing the impurities from the sample matrices, to concentrate the target analyte as well as to reduce sample complexity before chromatographic analysis (Cho *et al.*, 2009). The applicability of SPE mainly depend on the use of different solid sorbents (stationary phase) such as silica gel, chemically bonded silica phase, florisil, ion exchangers, and polymers (Phenomenex, 2008). The physiological interactions among the analyte/sample, sorbent and mobile phase have to be properly controlled in order to achieve the great separation power of SPE. The polarity or ionic strength of mobile phase will determine the separation selectivity of the sorbent.

The use of molecularly imprinted polymers (MIPs) with combination of SPE has been practiced to selectively extract specific analytes from complex samples (Claude *et al.*, 2008). Rochfort *et al.* (2006) also reported the isolation of glucoraphanin from broccoli seeds by the employment of C18 and protonated amino propyl anion exchange cartridges connected in series before preparative HPLC analysis. Lategan *et al.* (2009) discovered the increase activity of SPE fractions compared to the isolated compounds, which suggests the synergism of different compounds in extract of *Siphonochilus aethiopicus*.

2.7.2 Planar Chromatographic Technique (HPTLC)

Planar chromatography has been employed as a method of analysis for natural products, particularly to separate constituents in crude and partially

separated plant extracts. By term of planar chromatography, the stationary phase is a plane layer of material coated on an inert support, for example, aluminium, glass or polyester. The significant differences between the planar and column chromatography is the way of expression retention and mobile phase flow. Separation of planar chromatography is based on the variable migration distance at the fixed time, while separation of column chromatography is in either way. In TLC, movement of mobile phase is depending on the capillary flow, while mobile phase of GC and HPLC are maintained at optimal velocity by gas pressure and pump pressure (Reich and Schibli, 2007). Planar chromatography performs in the theory of adsorption chromatography, which retains substances based on their type and number of functional groups.

Thin layer chromatography (TLC) is the only chromatographic technique that presenting the result as a picture-like image with all detected bands seen as a sequence of dark, colour or fluorescent zones. The visual result and simplicity of TLC method allow inexperienced analyst to easily perform the chromatographic process. TLC gives the possibility of analysing many samples at the same time under the same chromatographic condition, which leads to rapid results. TLC is flexible in terms of a series of operational parameters can be optimised especially the unlimited combination of mobile phases together with the stationary phases. Every TLC plate can only be used once, without clean-up complications and consumption of mobile phase for TLC plate is greatly reduced if compared to other chromatographic techniques. The same developed TLC plate can be

visualized and evaluated repeatedly using different light sources (Gallo *et al.*, 2008; Kumar *et al.*, 2008; Rumalla *et al.*, 2008; Tian *et al.*, 2009). Commonly, TLC analysis is employed for the purpose of comparison of column fractions, optimization of solvent system for column chromatography, screening for certain biological assay and others.

In recent years, modern planar chromatographic technique (HPTLC) seems to become renaissance of interest for many chromatographic analysts. It becomes the alternative technique to classical TLC, as special plates and automated applicator are employed while documentation and quantitative evaluation of separation is aided by TLC visualizer and densitometer (Di *et al.*, 2003). HPTLC is the combination of modern equipment, solid theoretical formula and standardized methodology (Reich and Schibli, 2007). High performance plates have three fold numbers of theoretical plates and narrower particle size distribution, allowing higher separation power and sensitivity detection. As compared to classical TLC, HPTLC gives better resolution, and thus minimizing errors that might occur in manual TLC techniques (Pozharitskaya *et al.*, 2006). HPTLC technique has been recognized as an ideal tool for routine fingerprint analysis due to its rapidity, convenience (Sunita and Abhishek, 2008; Rathi *et al.*, 2008) and good post-chromatography visualization with standardized methodology (Pereira *et al*, 2004). As reported by Pereira *et al.* (2004), HPTLC technique is reliable as species identification through fingerprint analysis is fully concurrent with the microscopic (morphological) identification of the plant. In

addition, detection of adulteration and quantitative determination of marker compounds in sample are widely employed (Ankli *et al*., 2008; Jadhav *et al*., 2007). European Pharmacopoeia, American Herbal Pharmacopoeia (AHP), United States Pharmacopoeia (USP) and Pharmacopoeia of the People's Republic of China have also accepted HPTLC together with scanning densitometry as the general chromatographic analysis method for herbal products (AHP, 2009; Reich and Widmer, 2009). Budding advances in instrumentation, stationary phases, different types of force flow planar chromatography and the hyphenation of planar chromatography with MS or other ionization techniques will definitely make TLC an essential herbal analytical tool in near future (Kemsley, 2009).

2.8   Multidimensional Analysis Approach

Generally, two-dimensional (2D) separations are techniques where the sample is subjected to two displacement processes, one along each axis (Giddings, 1984). There are two types of separative displacements, simultaneously or sequentially. For simultaneous displacement process, the displacement is carried out in the same channel under same condition. As for sequential displacement, the sample is carried out in first displacement with optimum conditions, followed by the second displacement with modified optimum condition. Sequential displacement is more often employed, especially in the 2D liquid chromatography coupled with two different columns (Chen *et al*., 2004; Jiang *et al*., 2005).

The highest resolution can be achieved with the combination of two comprehensive systems with different separation modes (Ciesla *et al*., 2008). The separation power of chromatography greatly increases when the outcome variability of 1D multiplies with the system's dimensionality. For instance, the peak capacity (number of resolvable peaks) in 2D is N^2, where N is the peak capacity of 1D. Thus, the resolving power can be enhanced by choosing the appropriate combination of techniques, with both displaying high peak capacity. Due to the multiplicative effect, multidimensional separation is especially important for complex mixtures and plants containing structurally analogous substances (Hawryl *et al*., 2000). Fingerprint with only one dimensional chromatographic information may not sufficient to provide the whole chemical profile of an herbal medicine, as plant is composed of myriads of constituents (Yang *et al*., 2008). Many of the researches emphasize on the combination of analytical methods with different selectivity, yet it is complicated and time-consuming due to the systems' feasibility and detection.

In planar chromatography, two-dimensional thin layer chromatography can be established by employing different eluent systems on one adsorbent, different sorbents (bi-layer plate or graft-TLC) (Tuzimski and Soczewinski, 2002), and hyphenated techniques such as HPLC-TLC (Hawryl *et al*., 2000). However, several downsides of the methods may easily take place, for instance, the lack of proper instrumentation for qualitative analysis and the possibility of artefact formation during chromatographic process (Ciesla and Waksmundzka-hajnos,

2009). To date, there are only a few reports on the identification and separation of herbal product using multidimensional approach. Therefore, in this study, the offline two-dimensional separation with the use of two stationary phases, which normal phase in first dimension for crude extract separation and reverse phase in second dimension for semi-purified fractions separation was performed.

2.9   Antioxidant Activity

Free radicals are species with one or more unpaired electrons, and highly reactive oxygen species (ROS) is electron acceptors that react with free radical to form radicals. Both are believed to involve in several chronic disease including cardiovascular disease and cancer, tissue injuries and also acceleration of the aging process (Lee *et al*., 1998). Over exposure of human to carcinogenic xenobiotic and microorganisms induce the production of highly reactive oxygen species and free radicals, and lead to oxidative stress when the balanced state of antioxidants and free radicals is altered (Tsuda *et al*., 2004). Oxidative damage provokes deleterious effects on human body such as DNA alterations causing abnormal signalling, peroxidation of lipid membranes, and oxidation of lipids and proteins in body. The important role of antioxidant is to suppress the formation of free radicals or scavenge the free radicals, thus reduce the risk of oxidative damage to human body. As stated by Saha *et al.* (2004), antioxidant may function by reducing oxygen level, intercepting the singlet oxygen, terminating the first chain initiation by scavenging the initial radical, binding metal ion catalysts,

decomposing the product to reduced form, and chain-breaking to halt the further hydrogen subtraction from substrates.

2.9.1 DPPH-Free Radical Scavenging Assay and Fingerprinting via DPPH Free Radical Scavenging Activity

The molecule of 1, 1-diphenyl-2-picrylhydrazyl (DPPH) is a stable free radical that possesses an odd electron, with a maximum absorbance of 517nm. This strong absorption contributes to the deep violet colour due to the presence of unpaired electron of DPPH radical. When this free radical pairs off in the presence of a free radical scavenger and gives rise to reduced form DPPH-H, the absorption vanishes and the resulting loss of violet colour is stoichiometric with respect to the number of electrons captured (Figure 2.3). This assay provides a picture of the reactions take place in the oxidization in human body. The DPPH molecule represents the free radicals formed in human system, and its action is suppressed by the antioxidant (Molyneux, 2003). The spectrophotometric DPPH free radical scavenging method is useful as a primary screening method, for its ability to evaluate a large amount of samples in a short time and its sensitivity in detecting the active substances at low concentration (Russo *et al.*, 2005).

The combination of thin layer chromatography and post chromatographic DPPH free radical derivatization is a detection of antioxidant activity *in situ* after substances separation by TLC. This method involves TLC separation of the analyte mixture, followed by the detection of radical scavenging activity by

staining of the TLC plate with 0.05% DPPH solution in methanol. The active compounds are visualised as yellow bands under violet background. In the past few years, TLC-DPPH technique has been widely employed to rapidly identify the radical scavenging activity of the herbal drugs (Ravishankara *et al*., 2002; Pozharitskaya *et al*., 2007; Kancheva *et al*., 2010). Yrjonen *et al.* (2003) also demonstrated the similar method on reversed-phase TLC, and suggested the use of CCD video camera for the detection of activity due to the instability of colour developed on reversed phase TLC plate. The estimation of synergistic action between active compounds through the slope of the tangent of calibration curves is proposed by Pozharitskaya *et al.* (2008). DPPH test that performed directly on the TLC plates is informative as it demonstrates the quenching of DPPH radical by different compounds separated on TLC in the mixture (Simonovska, 2003).
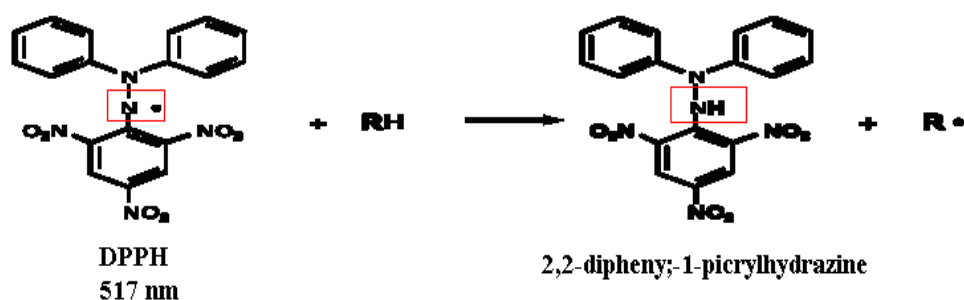
Figure 2.3: Structure of free radical DPPH and its reduction by an antioxidant (Prakash, 2001).

2.10 Cytotoxicity

Assessment of a compound's toxicology to various cell types can be made using *in vitro* cytotoxicity assay. The selection of cytotoxicity assays is complicated because the variation of assays depends on different physiological mechanisms and end-points. Neutral red assay measures the ability of metabolically active cells to take up supravital dye, neutral red in lysosomes. It has been found to be more sensitive than MTT assay (Babich and Borenfreund, 1991). LDH leakage assay is based on the conversion of lactate to pyruvate by cytoplasmic lactate dehydrogenase enzyme (LDH) simultaneous with reduction of NAD upon plasma membrane damaged (Fotakis and Timbrell, 2005). Abe and Matsuki (2000) have reported that, MTT reduction, an index of cellular activity, and LDH release, an index of cell membrane damage, can be measured using the same dye MTT.

Alamar blue is a commercial preparation of dye resazurin, which reduced to fluorescent resorufin by reductase localized in mitochondrial membrane and in cytosol once diffused into living cells (Gonzalez and Tarloff, 2001). Another short term based assay, ATP assay is depending on the detection of ATP by luciferase-luciferin reaction (Cree and Andreotti, 1997). Although ATP based assay is the most sensitive assay among the others, with high tumour evaluability rate and technical simplicity (Tam *et al*., 2004), however, the luminescence-

readout could be easily influenced by the quenching effect of the samples (Weyermann *et al*., 2005).

2.10.1 MTT Assay

Formazans are produced when tetrazolium salts such as MTS (3-(4,5-dimethylthiazol-2-yl)-5(3-carboxymethoxyphenyl)-2-(4-sulfophenyl)-2H-tetrazolium), MTT (3-(4,5-dimethylthiazol-2-yl)-2,5-diphenyl tetrazolium bromide), INT (Iodonitrotetrazolium) and XTT (2,3-bis(2-methoxy-4-nitro-5-sulfophenyl)-5-[(phenylamino) carbonyl]-2H- tetrazolium hydroxide) are reduced by naturally occurring enzymes. Formazan is impermeable to cell membrane and thus it accumulates in healthy cells. They range in a variety of colours from dark blue to deep red to orange, depending on the tetrazolium salt.

MTT is used to determine the disruption of biochemical function and cell viability in assays of cytotoxicity, cell proliferation and cell activation (Mosmann, 1983; Gerlier and Thomasset, 1986). Hordegen *et al*. (2006) reported that MTT can also be used to measure anti-helmintic activity. This assay utilizes the concept of conversion of purple, water-insoluble end product (formazan) from yellow, water-soluble substrate (MTT), by mitochondrial succinate dehydrogenase that present only in living cells. This involves reduction of tetrazolium ring in MTT (Figure 2.4). The coloured formazan yielded is in proportion to the amount of

metabolically active cells (Mosmann, 1983). A decrease in cellular MTT reduction indicates occurrence of cell damage.
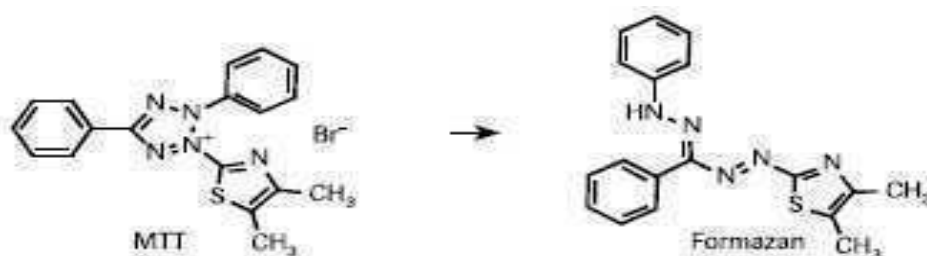
Figure 2.4: Metabolism of MTT to formazan salt by viable cells (Roche Applied Science, 2005).

2.11 Limestone Species

Limestone is a hard sedimentary rock composed largely of calcium carbonate. It is formed by the shells and small creatures under the sea in the early period and the rock under the sea is fortified through movements of earth's crust and become the limestone land now (Royal Horticulture Society, 2004). Approximately 20 percent of the 1200 limestone plant species in Malaysia are endemic and 10 percent of them are strictly limestone species (Yong, 2003). In Malaysia, limestone hill is gigantic, towering, and has steep-sided surface, and sharp peak. Limestone is mostly found in Sabah, Sarawak and northern part of Peninsular Malaysia (Soepadmo, 1998). Perak, a state in Malaysia is known to have large number of limestone tree species, as the hills are ecologically isolated with localised habitats. *Prismatomeris albiflora*, a limestone species commonly found in Vietnam, Burma, Thailand, and Malaysia has been reported to possess

compounds of anthraquinone and mitoxantrone with high anti-neoplastic value (Wiart, 2007).

2.11.1 Plant of Interest- *Paraboea paniculata*

There are around 87 species of *Paraboea* found in Bhutan, China, Indonesia, Malaysia, Myanmar, Philippines, Thailand and Vietnam. Among them, few of the species are localized in limestone rocks and cliffs; include *P. velutina*, *P. peltifolia*, *P. filipes*, *P. nutans*, *P. changjiangensis*, *P. rufescens*, *P. paramartinii*, *P. clavisepala*, *P. martini*, *P. neurophylla*, *P. tribracteata* (Wang *et al.*, 1998). Prior detailed literatures on bioactivities of *Paraboea* species have identified several metabolites, i.e. acteoside from *P. dictyoneura*, and *P. treubii* (Kvist and Pedersen, 1986), anthocyanins from *P. cordata* (Lowry, 1972), triterpenes, triterpene glycosides and sterols from *P. glutinosa* (Wang *et al.*, 2009). Recent research by Gao *et al.* (2006) reported the pollination ecology of the species, *Paraboea rufescens*. Another report by Ueda *et al.* (2002), *Paraboea treubii* is described as a therapeutic agent to treat cough and fever.

Paraboea paniculata belongs to the family of Gesneriaceae. It is wild and rare, as its population is small and can be found only in very few places in Malaysia. The herbaceous *Paraboea paniculata* is stacked on the exposed limestone cliffs and adapted to the hot, dry condition of exposed cliff surfaces. It has been reported to have special secretion glands for excess calcium carbonate,

for adaptation purpose (Soepadmo, 1998). It is a perennial and rhizomatous plant. Its leaves are clustered at stem apex and spirally arranged. The leaf blade is adaxially and abaxially woolly and it has five petals in purple colour (Figure 2.5).

Paraboea paniculata serves as a prime example of botanical in current work where metabolite fingerprinting method is developed. Prior screening on this plant showed a great potential in exhibiting cytotoxic effects against K-562 and HL-60 cell lines. In a preliminary study, both rhizome and leaf of *Paraboea paniculata* exhibited promising cytotoxic effect with cell viability of 5.74% and 12.10%, respectively against K-562 cell line (Tan, 2008). Another preliminary screening done by Toi (2008) also showed that *Paraboea paniculata* has strong cell killing effect with cell viability of 21.65% for leaf and 8.21% for root against HL-60 cell line. Besides, Tan (2009) also reported methanol crude extract of this plant exhibited potent anti-tumour-promoting activity on Epstein-Barr virus early antigen (EBV-EA). *Paraboea paniculata* was reported by Soepadmo (1998) to be local medicinal plant in Malaysia, but the detailed chemical composition, toxicity and pharmacological effect have not been investigated.

Figure 2.5: Plant of *Paraboea paniculata* collected by Dr. Lim Yang Mooi and her research team at SamPoh Cave, Ipoh in October, 2007.

CHAPTER 3

MATERIAL AND METHODS

3.1   Collection of Plant Materials

Paraboea paniculata was collected from limestone cave in Gunung Rapat, Ipoh, Perak, Malaysia. The voucher specimen is deposited in Faculty of Medicine and Health Sciences of UTAR, with voucher number of HCT 001. Herbarium of the plant was authenticated by Dr. Lee Chin Yoong from PK Herbal Research Center, Ipoh. The freshly collected plants were washed, separated into two parts: leaf and rhizome and dried at room temperature for three days. Dried leaves were ground with blender (Panasonic) while dried rhizomes were crushed with mortar and pestle. Powdered parts were accurately weighed and macerated with methanol (Merck) at room temperature for 3 days. The crude extracts were filtered and evaporated *in vacuo* using rotary evaporator (BUCHI, Rotavapor R-2000). The process of extraction was repeated three times. Dried concentrated crude extracts were weighed and percentage yields were obtained. The crude extracts were subjected to MTT assay for cytotoxic activity evaluation.

3.2 Purification by Solid Phase Extraction (SPE)

The dried crude extract was reconstituted in water and methanol with 9:1 (v/v) ratio. The Strata C18 SPE cartridge (Phenomenex) was first conditioned with methanol, and equilibrated with water: methanol (9:1, v/v). The crude extract was loaded onto conditioned SPE column. The column was washed with water: methanol (9.5: 0.5, v/v) with a vacuum pressure of 1ml/min to remove impurities. The extract was eluted with a gradient of solvent system in decreasing polarity (water, methanol, dichloromethane). The gradient profiles employed were previously optimized. The sample loading capacity and eluting volume depend on column size and amount of sorbent packed. All SPE-collected fractions were subjected to cytotoxic activity evaluation using MTT assay.

3.3 Fingerprint Development by Planar Thin Layer Chromatography (HPTLC)

3.3.1 Sample Application and Development

5 µl of active cytotoxic plant samples (5 mg/ml) and standard solutions (1mg/ml) were applied as band of 8 mm, with 2 mm apart, 8 mm from the lower edge, and 15 mm from the right and left edges of 10 x 10 cm pre-coated HPTLC plate (Merck) by Linomat IV sample applicator (Camag). The sample loaded plate was dried at cold air with hair dryer (Panasonic). 10ml of respective developing solvent was added into a 10 x 10 cm twin-trough chamber, and conditioned with

filter paper in one trough for 20 minutes. Applied plate was pre-equilibrated for another 20 minutes in the saturated chamber. Plate was developed upward to a distance of 70 mm, from the lower edge of plate. The developed plate was dried under cold air. The chromatographic condition was optimized previously to obtain the best peak resolution and reproducible results.

3.3.2 Plate Derivatization and Evaluation

After plate development, the dried plates were separately stained with (i) 10% of sulphuric acid in cold methanol and (ii) 2 g of vanillin in 1% of sulphuric acid-ethanol for 5 seconds, and the immersed plates were heated on a plate heater (Camag) at 100°C for 5 minutes. Images of the plates under white light were captured and documented by means of TLC visualizer (Camag). The plates were also evaluated at wavelength of 200 nm to 700 nm via Camag Scanner 3 with winCATS integrated software.

Figure 3.1: Images of Camag Linomat V sample applicator, Camag TLC visualizer, and Camag TLC Scanner 3 for the purpose of sample application and band documentation in automated manner.

3.4 Method Validation

The method of HPTLC fingerprint profile establishment was validated in terms of precision, robustness, specificity and stability (EMEA, 2006; Reich and Schibli, 2007). For precision and robustness of the method, two significant peaks of the fingerprint profile of each sample were selected as reference peaks and analyzed on the basis of retention time of the peaks. They were analysed in term of standard deviation and relative standard deviation of the R_f values (EMEA, 2006). The percentage of relative standard deviation was calculated as followed:

RSD (%) = 100 (standard deviation of R_f / average of R_f)

3.4.1 Precision

The precision of the method was expressed as multiple applications on the same plate (repeatability), on different plates (intermediate precision), and on different days (reproducibility). Precision on the same plate was evaluated by individually applying three aliquots of sample on one plate. The average of R_f values of the two selected zones across the plate in the parallel analysis do not vary more than 0.01. Intermediate precision was accessed by applying three aliquots of sample on three individual plates. The average of R_f values of the two selected zones from plate to plate do not vary more than 0.02. Reproducibility was determined on two other days (one plate prepared during repeatability test,

two plates on different days). The average R_f values between plates on different days do not vary more than 0.05.

3.4.2 Robustness

The robustness is the ability of the method to tolerate variation of parameters without significantly changing the result. It was determined by evaluating the parameters in terms of volume of developing solvent, equilibration time between gas phase and stationary phase, type of chamber, development distance and dosage speed of sample application. Volume of developing solvent was performed in 5 ml, and 15 ml in place of 10 ml. Equilibration times of gas phase and stationary phase was performed in 10 minutes and 30 minutes, instead of 20 minutes. A flat bottom chamber in comparable size was employed to replace the twin-trough chamber. The developing distance was extended to 75 mm and 80 mm, rather than 70 mm from the lower edge of the plate. Dosage speed of sample applicator was performed in 150 nl/s and 200 nl/s, which normally in 100 nl/s to observe any significant difference.

3.4.3 Specificity

The specificity ensures constituents with similar identity give similar result as raw sample, and deviate from other samples with different identity. The crude fraction was applied on track 1 and 2, followed by the respective SPE-

separated fraction applied on track 3 and 4. Isolated compound was served as marker, and applied on the following tracks. All samples were applied on the same plate and developed with optimized mobile phase. The fingerprint profiles of raw material samples were compared with the isolated compounds (marker) in terms of the number, position, colour and intensity of zone.

3.4.4 Stability

The stability is commonly accessed to investigate the possibility of sample degradation. The stability of method was evaluated as before chromatography (different batches of isolated fractions and different time of application), during chromatography (including the drying step), and after chromatography. The stability of analyte before chromatography was accessed by applying the previously isolated sample on track 1, and set aside for three hours. After 3 hours, the sample solution was applied to track 2 and track 3. Another batch of exactly weighed isolated sample was prepared and applied in the same way as the first batch of sample solution. The zones of each fingerprint profile were compared to investigate any decomposition product. A 2-dimensional chromatogram was used to confirm the stability of analyte during chromatography. The sample solution was applied as spot at right bottom of the plate, and allowed to dry and develop. After the first development, the plate is turned 90° to the right and developed for second time with a fresh portion of developing solvent. Any zones of the sample that located aside from the diagonal connecting to the application position were

examined. Lastly, to investigate the stability of analyte after chromatography, the chromatographic result was repeatedly reviewed. The chromatogram was evaluated after 10 minutes, 30 minutes and 1 hour. Any changes of the result were observed.

3.5 HPTLC-DPPH Method

5 µl of active cytotoxic plant samples (0.5 mg/ml) were applied on HPTLC plate and developed with respective developing solvent system following the standard protocol as described in Section 3.3.1. Curcumin and quercitin (0.5 mg/ml) (Sigma) were served as standard control. After plate development, the developed plates were immersed into 0.05% solution of DPPH in methanol for 5 seconds. The plates were dried at room temperature for 1 minute in fume hood. The dried plates were stored in darkness for 30 minutes and examined under white light and images captured with TLC visualizer (Camag).

3.6 DPPH Free Radical Scavenging Assay

DPPH radical scavenging assay was performed in 96-wells micro-plate (Orange scientific). All plant extracts to be tested were dissolved in methanol (Merck) to give the concentration of 100 µg/ml. 95 µl of methanol was added into each well, followed by 100 µl of tested sample (100 µg/ml) to give a final concentration of 50 µg/ml, and final volume of 195 µl in each well. Methanol was

used as blank solution while L-ascorbic acid and Quercitin (Sigma) dissolved in methanol was used as positive control. 5 µl of 4 mg/ml DPPH (1, 1-diphenyl-2-picrylhydrazyl) (Sigma) solution in methanol was added to each well of micro-plate. The plate was kept and incubated in dark for 30 minutes. All measurements were carried out in triplicate. The decrease in absorbance at 517 nm was measured by micro-plate reader (Bio-Rad, Model 680 with Micro plate Manager Software). This assay was carried out in three independent experiments. The percentage inhibition of the DPPH radical by the sample was calculated as followed:

Percentage of inhibition = $[(A_0-A_1)/A_0] * 100$

Where A_0 = absorbance of blank solution

A_1 = absorbance of test sample

3.7 Isolation by Semi-preparative High Performance Liquid Chromatography (HPLC)

The chosen cytotoxic SPE-separated fractions were subjected to semi-preparative high performance liquid chromatography to isolate the active constituents. The semi-preparative HPLC isolation was performed using Shimadzu model LC-20AD gradient HPLC instrument, equipped with two LC-20AD pumps controlled by a CBM-20A interface module and a photodiode array detector SPD-M20A. Deionised water and HPLC-grade acetonitrile (Merck) employed were pre-filtered using a Millipore (Bedford, MA) system and analyses

were performed on Merck RP-C18 Chromolith performance reverse-phase column (100 x 10 i. d.). The flow rate was 4 ml/min. The separation was performed after optimization using binary gradient system to yield few significant peaks. The fractions collected were dried in fume hood and subjected to MTT assay for the activity evaluation.

3.7.1 Compound Identification

The structures of isolated compounds were identified with the aid of liquid chromatography-mass spectrometry (LC-MS), Fourier-transform infrared (FT-IR), and nuclear magnetic resonance (NMR) spectroscopic data. The liquid chromatography-mass spectra were recorded using a Finnigan model LCQ mass spectrometer with ion trap mass analyser (available at National University of Singapore). Ionisation was induced by electron impact. The infrared spectra were obtained from a Perkin-Elmer FT-IR model RX 1 spectrophotometer. Proton NMR spectra (400 MHz), Carbon NMR spectra (100 MHz), HMQC, and HMBC correlation experiments were obtained using a Jeol ECX series 400 NMR spectrometer. Deuterated methanol (CD_3OD), dimethyl sulfoxide (CD_3SOCD_3), deuterium oxide (D_2O) (Merck) were used for NMR test samples preparation.

3.8 Cell Culture

3.8.1 Medium Preparation

The Roswell Park Memorial Institute, RPMI-1640 medium was prepared by dissolving 10.4 g of RPMI-1640 powder (Sigma) and 2 g/L of sodium bicarbonate (Goodrich Chemical Enterprise) in 1 L of ultra-pure water. The pH of the medium was adjusted to pH range of 7.2 to 7.6 by 1 M hydrochloric acid or 1 M sodium hydroxide. The medium was filter-sterilized with 0.2 µm membrane (Sartorius) and kept at 4^oC. 2 ml of newly prepared medium was cultured in culture dish and incubated overnight. The incubated medium was checked under inverted microscope (Nikon, Eclipse TS100) for any possible contamination. The sterilised medium was supplemented with 10% of foetal bovine serum (HyClone) prior to use.

3.8.2 Cell Culture and Cell Line Maintenance

Human chronic myelogenous leukaemia cell line, K-562 employed was a suspension-growing cell line purchased from RIKEN Cell Bank, Japan. Cell line was maintained in RPMI-1640 medium with 10% FBS. It was cultured in 10 ml or 50 ml tissue culture flask (Orange Scientific) and maintained in 5% CO_2 humidified incubator (Nuaire) at 37^oC. Cell culture was sub-cultured every 2 or 3 days and observed under inverted microscope. The cell concentration and

viability were determined using the trypan blue (GIBCO, Invitrogen) dye exclusion method.

3.8.3 Freezing and Thawing of Cell Culture

70% of confluent cells were removed from tissue culture flask and transferred into a 50 ml of centrifuge tube. Cell suspensions were spun down at 1000 rpm for 5 minutes using a bench centrifuge (Heraeus, Biofuge Primo). The supernatant, RPMI-1640 medium was removed. 1 ml of growth medium was added, followed by 10% of DMSO (dimethyl sulfoxide, Fisher Scientific) as cryoprotectant. The cell mixture was re-suspended and transferred into 1ml cryopreservative vial (Nalgene). The vial was stored in freezer (Sanyo) at $-86^{o}C$ overnight before transfer into $-196^{o}C$ liquid nitrogen tank (Locator).

A vial of cells was removed from liquid nitrogen tank and rapidly thawed in $37^{o}C$ water bath (Memmert). The cells were then transferred into pre-incubated tissue culture flask containing RPMI-1640 medium supplemented with 10% foetal bovine serum. Cell culture was incubated in 5% CO_2 humidified incubator at $37^{o}C$ overnight. The culture was spun down at 1000 rpm for 5 minutes and the DMSO-containing medium was replaced with new growth medium in the following day.

3.9 MTT Cytotoxicity Assay

The MTT reduction assay employed is based on the protocols described by Mosmann (1983). MTT assay was carried out in 96-wells micro-plate (Orange scientific). All plant extracts to be assayed were prepared with RPMI-1640 medium in the concentration of 100 µg/ml. 100 µl of cell culture (7.0×10^4 cells/ml) was added to each well, followed by 100 µl of plant extracts (100 µg/ml) to give a final concentration of 50 µg/ml of samples, and final volume of 200 µl in each well. Each of the samples was done in triplicates. For the positive control, 100 µl of medium instead of plant extract was used, and 200 µl of medium was served as negative control. The plate was incubated for 72 hours at 37°C in 5% CO_2 humidified incubator (Sanyo).

After 72 hours of incubation, 20 µl of 5 mg/ml MTT (3-(4, 5-dimethylthiazol-2-yl)-2, 5-diphenyl tetrazolium bromide) (AMRESCO®) solution in PBS (Phosphate Buffered Saline, GIBCO, Invitrogen) was added to each well of micro-plate. After 3 hours of incubation, the plate was spun at 3000 rpm for 10 minutes (Heraeus, Multifuge 1 S-R). Approximately 70% of supernatant was removed from each well and 150 µl of DMSO was added to dissolve the remaining formazan crystal. The plate was placed on orbital shaker, in dark condition at room temperature for 15 minutes. The absorbance was determined by micro-plate reader (Bio-Rad, Model 680 with Micro plate Manager Software) at wavelength of 550 nm. Percentage of cell viability was calculated from the

44

absorbance values. Three plates were used for each plant extract to give three independent determinations within one experiment. The percentage of cell viability was calculated as followed:

$$\text{Cell viability, \%} = \frac{\text{Average S} - \text{Average B}}{\text{Average A} - \text{Average B}} \times 100\%$$

Where, S = Absorbance of sample

A = Absorbance of blank cell (untreated cells)

B = Absorbance of blank medium (background)

3.9.1 Determination of Optimal Cell Seeding Density for MTT Assay

The MTT assay described previously was performed in a six-point serial dilution, which ranging from 0.25 to 8.0 x 10^5 cells/ml in order to determine the optimal K-562 cell seeding density. The cells at various concentrations were incubated for 72 hours at 37^oC in 5% CO_2 humidified incubator. After 72 hours of incubation, 20 µl of 5 mg/ml MTT solution in PBS was added to all wells of micro- plate. After 3 hours of incubation, the plate was spun at 3000 rpm for 10 minutes. Approximately 70% of supernatant was removed from each well and 150 µl of DMSO was added to dissolve the remaining formazan crystal. The plate was placed on orbital shaker, in dark condition at room temperature for 15 minutes. The absorbance was determined by micro-plate reader at wavelength of 550 nm. The graph of absorbance against each point of cell concentration was plotted. The

optimal cell seeding density was determined as cell concentration with absorbance value that is approximately 1.0 from the plotted graph.

3.9.2 IC$_{50}$ Determination of Cytotoxicity against K-562 Cell Line

The isolated compounds, doxorubicin and cisplastin were subjected to five-point serial dilution of MTT assay, in order to determine the concentration at which 50% of cells are killed. The MTT assay protocols were performed as described in Section 3.9. The compounds to be subjected to five-point serial dilution (50 μg/ml, 25 μg/ml, 12.5 μg/ml, 6.25 μg/ml, and 3.125 μg/ml) were prepared with RPMI-1640 medium from initial concentration of 100 μg/ml. The following concentrations were prepared as illustrated in Figure 3.2. Reference compounds, doxorubicin and cisplastin were prepared in initial concentrations of 2 μg/ml and 20 μg/ml, and assayed in six-point serial dilution (1 μg/ml, 0.5 μg/ml, 0.25 μg/ml, 0.125 μg/ml, 0.0625 μg/ml, and 0.03125 μg/ml) and (10 μg/ml, 5 μg/ml, 2.5 μg/ml, 1.25 μg/ml, 0.625 μg/ml, and 0.3125 μg/ml). Triplicates were done for each point of tested concentrations. The graph of percentage viability against five-point compound concentrations was constructed and IC$_{50}$ value was determined from the plotted graph. The percentage of cell viability (adjusted) was calculated as followed:

$$\text{Adjusted cell viability, \%} = \frac{\text{Average S - Average C}}{\text{Average A – Average B}} \times 100\%$$

Where, S = Absorbance of sample

A = Absorbance of blank cell (untreated cells)

B = Absorbance of blank medium (background)

C = Absorbance of medium and sample
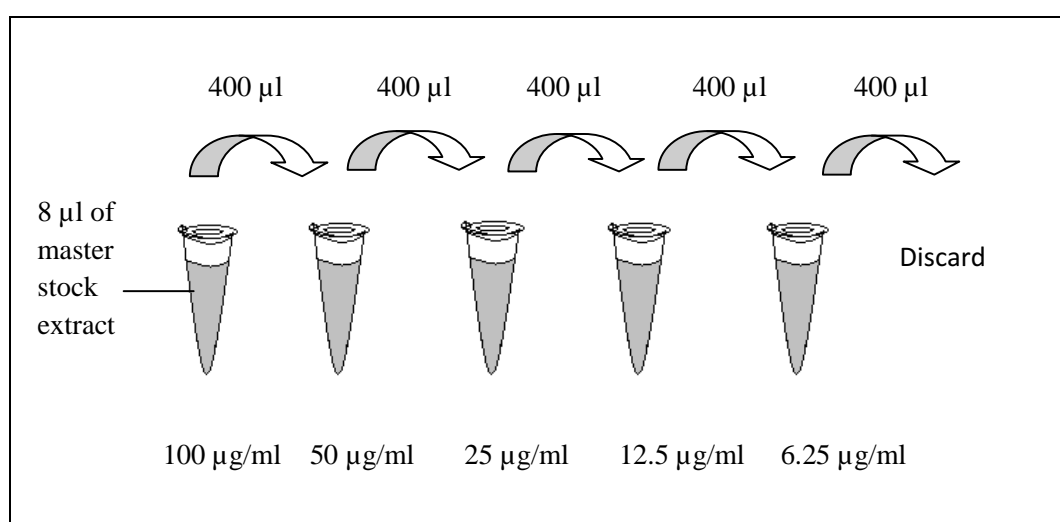
Figure 3.2: Five points serial dilution in varying concentrations of plant extract.

3.10 IC$_{50}$ Determination of DPPH Free Radical Scavenging Activity

The isolated compounds, together with quercitin and L-ascorbic acid were subjected to five-point serial dilution of DPPH scavenging assay, in order to determine the concentration at which 50% of free radical inhibited. The DPPH scavenging assay protocols were performed as described in Section 3.6. The isolated and standard compounds to be subjected to five-point serial dilution (50 µg/ml, 25 µg/ml, 12.5 µg/ml, 6.25 µg/ml, and 3.125 µg/ml) were prepared in methanol with initial concentration of 100 µg/ml. The following concentrations were prepared as illustrated in Figure 3.2. Triplicates were done for each point of tested concentrations. The graph of percentage inhibition against five-point compound concentrations was constructed and IC$_{50}$ value was determined from the plotted graph.

CHAPTER 4

RESULTS

Paraboea paniculata (Gesneriaceae) was collected from the limestone cliffs located in Ipoh, Malaysia. The plant was separated into two parts, dried, and extracted with methanol. The initial screening of the plant on the cytotoxic activity against K-562 cell line showed that the methanolic extracts of leaf and rhizome of Paraboea paniculata were both toxic toward K-562 cell line (Table 4.1). The results obtained from the MTT assay were classified into 3 categories. The categories include, strongly cytotoxic with cell viability less than 30%, moderately cytotoxic with cell viability between 30% and 70%, and non-cytotoxic with cell viability more than 70%.

Table 4.1: Percentage yield of crude leaf and rhizome of *Paraboea paniculata* after extraction with methanol and cell viability of K-562 cell line after treatment.

Plant Species	Plant part	Dried weight	Percentage yield	Cell viability ± SD (%)
Paraboea paniculata	Leaf	806 g	13.45%	7.15 ± 1.29
	Rhizome	555 g	9.41%	9.85 ± 0.90

Cell viability was expressed as percentage ± standard deviation value of three independent experiments.

4.1 Development of First Dimensional Fingerprint Profiles

The planar TLC peak patterns of both leaf and rhizome of *Paraboea paniculata* were developed, and documented as the first dimensional fingerprint profiles. The chromatographic profile was documented as peak profile from wavelength of 200 nm to 700 nm in both three dimensional and two dimensional angles, and at 250 nm (Figures 4.1 and 4.2) as well as picture-liked image at 254 nm, 365 nm, and under white light after derivatization by sulphuric and vanillin reagents (Figure 4.3).
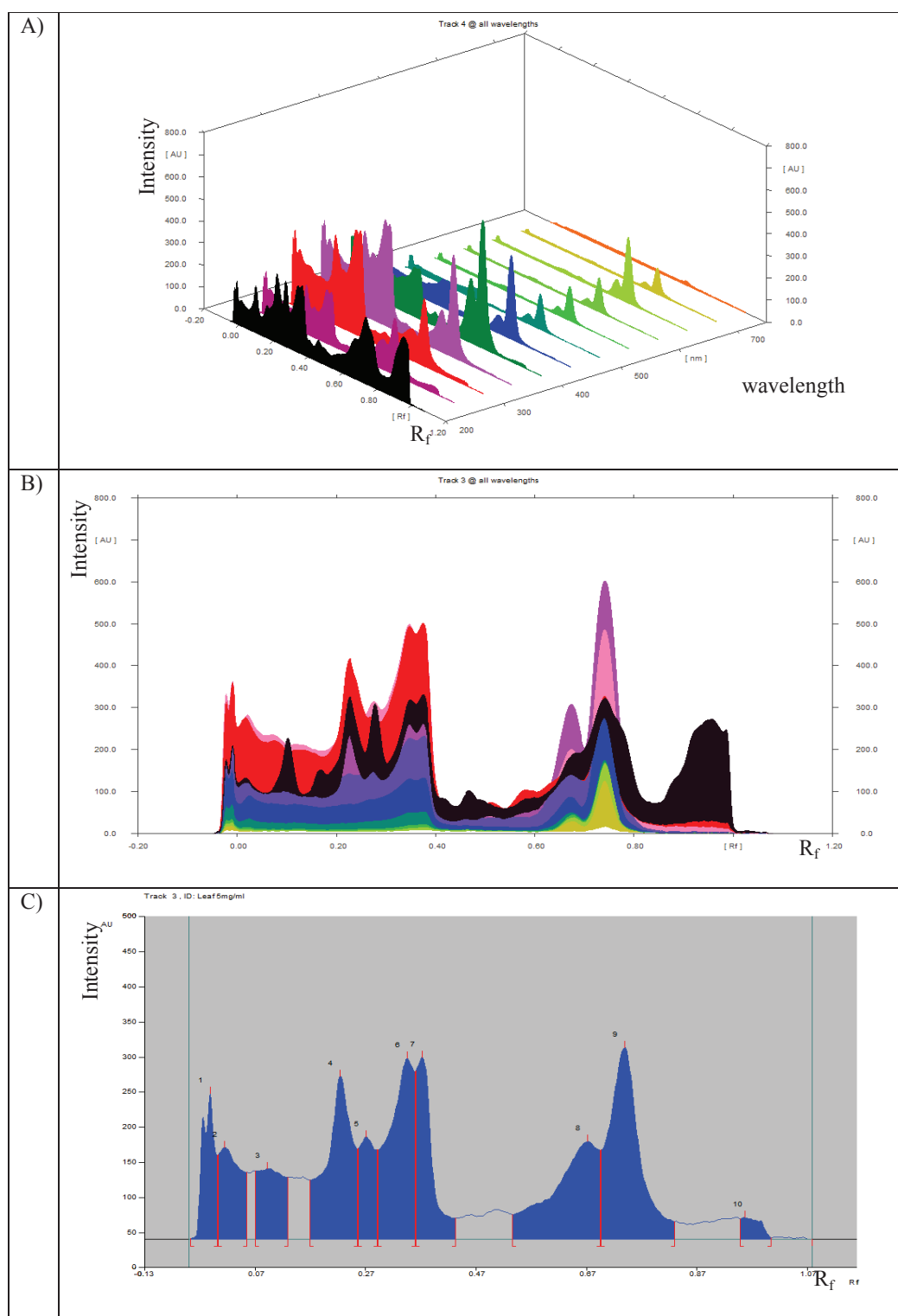
Figure 4.1: HPTLC first dimensional fingerprint profile of leaf crude extract. Stationary Phase: HPTLC Si 60 F$_{254}$. Mobile Phase: ethyl acetate: methanol: water (75.27%: 13.98%: 10.75%). (A) Spectral scans 200-700 nm in 3D (B) Spectral scans 200-700 nm in 2D (C) 250 nm.
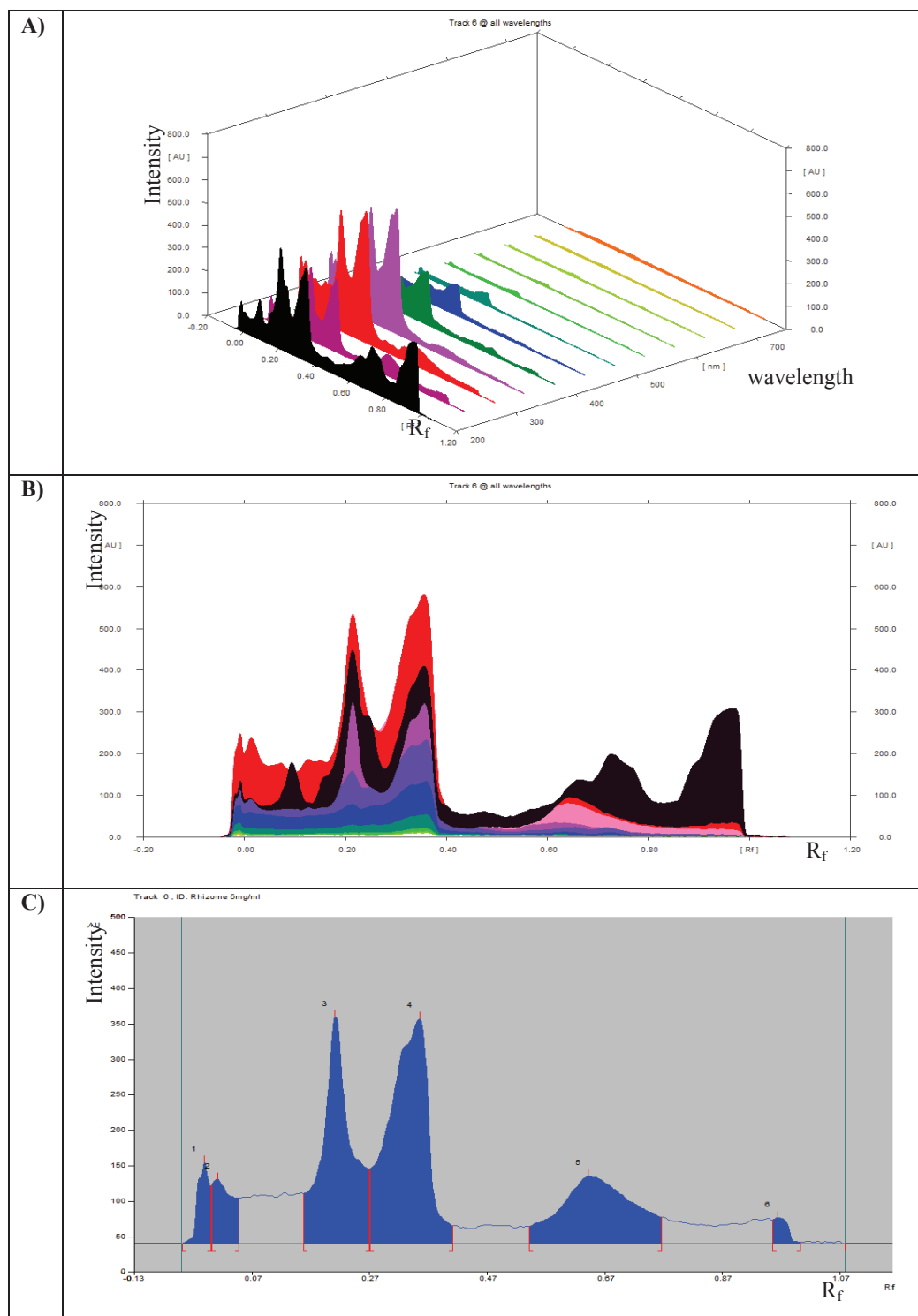
Figure 4.2: HPTLC first dimensional fingerprint profile of rhizome crude extract. Stationary Phase: HPTLC Si 60 F_{254}. Mobile Phase: ethyl acetate: methanol: water (75.27%: 13.98%: 10.75%). (A) Spectral scans 200-700 nm in 3D (B) Spectral scans 200-700 nm in 2D (C) 250 nm.
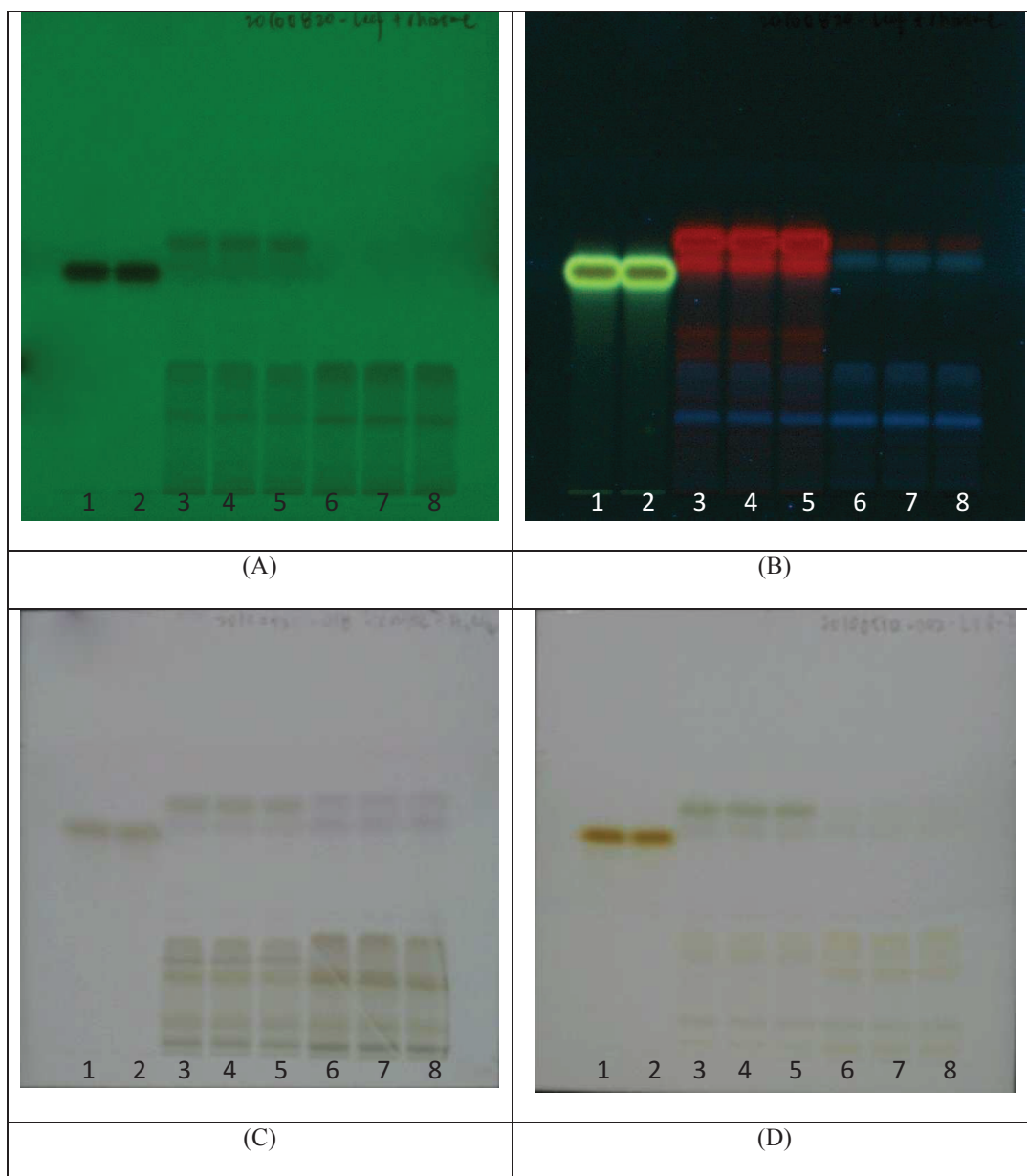
Figure 4.3: HPTLC first dimensional fingerprint profile of leaf and rhizome crude extracts. Stationary Phase: HPTLC Si 60 F$_{254}$. Mobile Phase: ethyl acetate: methanol: water (75.27%: 13.98%: 10.75%). (A) UV 254 nm. (B) UV 365 nm. D: (C) Sulphuric reagent, white light. (D) Vanillin reagent, white light. From left to right: Track 1 to 2, curcumin; track 3 to 5, leaf crude fraction; track 6 to 8, rhizome crude fraction.

4.2 Development of Second Dimensional Fingerprint Profiles

The crude leaf extract of *Paraboea paniculata* was fractionated by solid phase extraction method with C18 octadecyl as stationary phase. 19 fractions were yielded from leaf crude extract and the fractions were eluted with a gradient of decreasing polarity with water, methanol and dichloromethane. All SPE-separated fractions were subjected to MTT assay against K-562 cell line (Table 4.2). Leaf SPE-separated fractions 5 and 12 exhibited strong cytotoxic activity (cell viability <30%), which their cell viability were 18.90% and 3.42%, correspondingly (Figure 4.4). The second dimensional fingerprint profiles of active fractions 5 and 12 were documented based on their optimized mobile phases. The chromatographic profile was documented as peak profile from wavelength of 200 nm to 700 nm in both three dimensional and two dimensional angles, and at 250 nm (Figures 4.5 and 4.7) as well as picture-liked image at 254 nm, 365 nm, and under white light after derivatization by sulphuric reagent and vanillin reagent (Figures 4.6 and 4.8). Quercitin and stigmasterol are served as standard control, according to their suitability on the respective developing solvent systems.

Table 4.2: Percentage yield and cell viability of K-562 cell line after treated with 19 SPE-separated leaf fractions of *Paraboea paniculata* via MTT assay.

Fraction	Solvent systems employed	Percentage yield	Cell viability ± SD (%)
1	Sample applied	9.84%	96.34 ± 9.04
2	Sample washed (95% water: 5% methanol)	22.98%	86.27±5.19
3	100% water	0.50%	93.51 ± 4.40
4	80% water: 20% methanol	5.27%	51.56 ± 10.50
5	60% water: 40% methanol	33.99%	**18.90 ± 3.25**
6	40% water: 60% methanol	16.53%	65.33 ± 14.39
7	20% water: 80% methanol	0.76%	73.69 ± 2.17
8	100% methanol	2.65%	47.90 ± 6.24
9		1.73%	69.11 ± 5.01
10		0.40%	34.16 ± 6.44
11	80% methanol: 20% dichloromethane	0.60%	38.73 ± 8.72
12		1.28%	**3.42 ± 4.36**
13		0.11%	26.96 ± 0.85
14	60% methanol: 40% dichloromethane	0.88%	84.01 ± 4.94
15		0.41%	80.02 ± 10.75
16	40% methanol: 60% dichloromethane	0.47%	82.42 ± 4.46
17	20% methanol: 80% dichloromethane	0.30%	90.70 ± 6.66
18	100% dichloromethane	0.20%	97.05 ± 3.12
19	Acidified methanol with 2M of nitric acid	1.54%	83.10 ± 8.02

Cell viability was tested at the concentration of 50 µg/ml.
Separation of sub fractions based on different extract colour of bands eluted (refer to Appendix A).
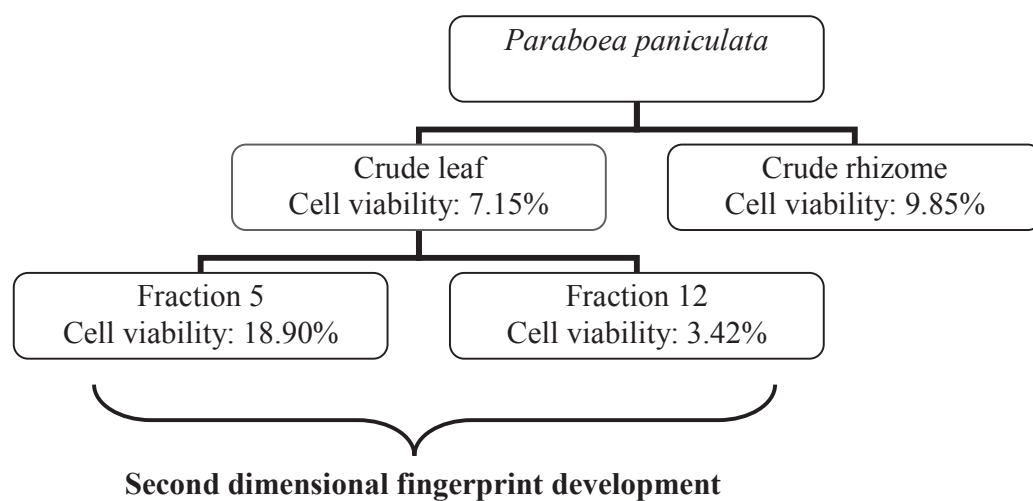
Figure 4.4: Cytotoxic leaf SPE-separated fractions for second dimensional fingerprint profile development.
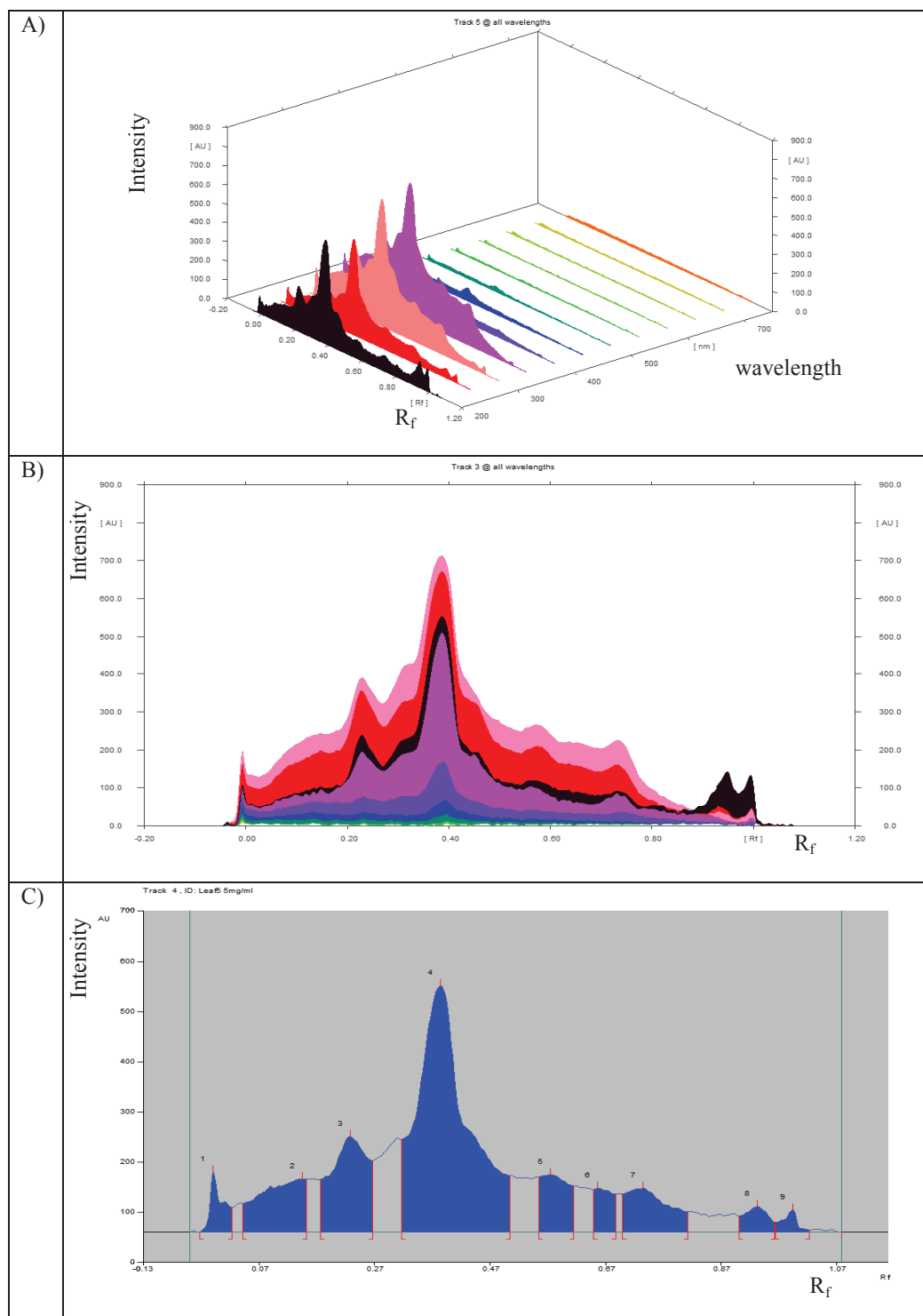
Figure 4.5: HPTLC second dimensional fingerprint profile of leaf SPE-separated fraction 5. Stationary Phase: TLC Si 60 RP18 $F_{254}S$. Mobile Phase: ethyl acetate: methanol: water (5%: 35%: 60%). (A)Spectral scans 200-700 nm in 3D (B) Spectral scans 200-700 nm in 2D (C) UV 250 nm.
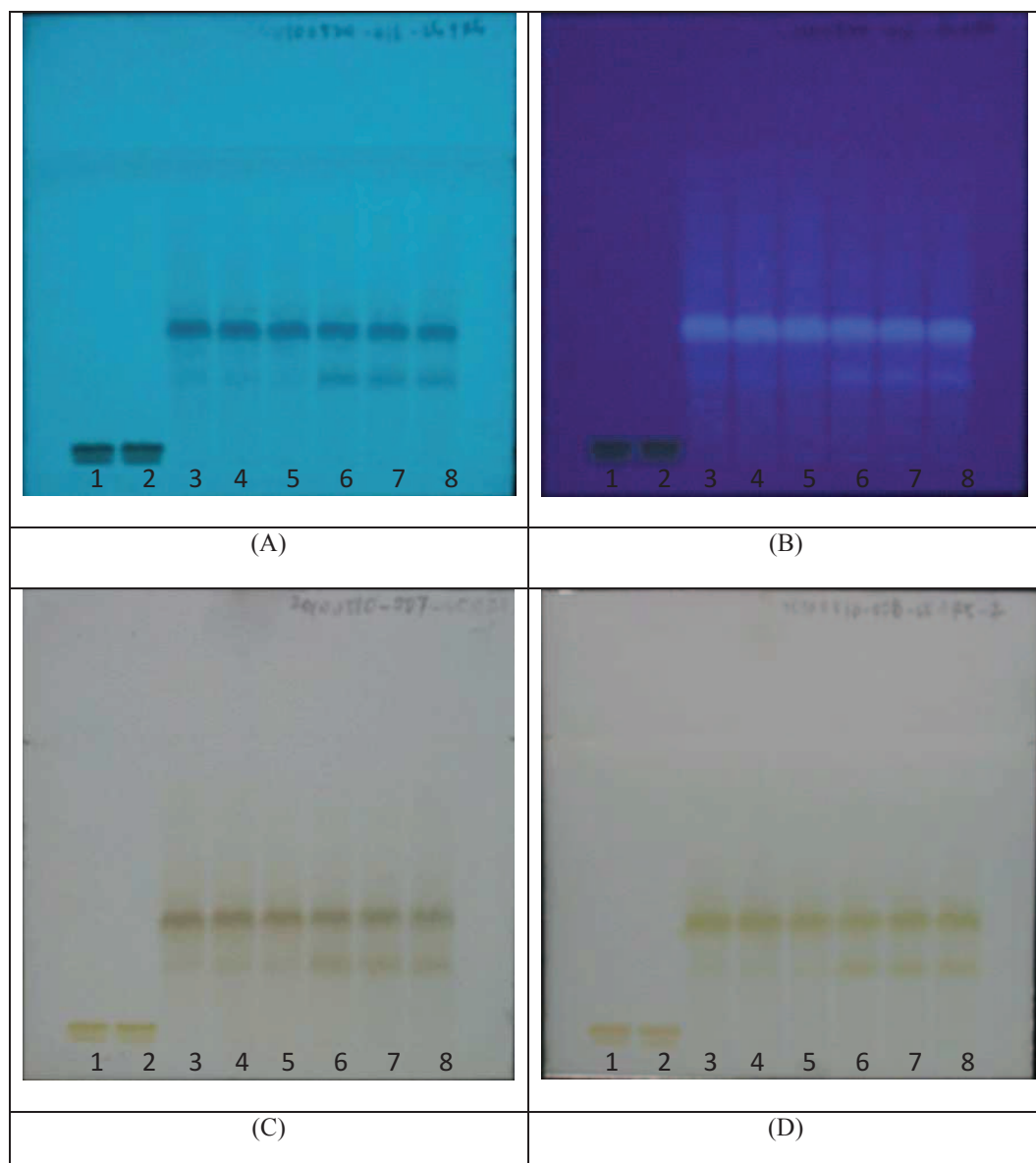
Figure 4.6: HPTLC second dimensional fingerprint profile of leaf and rhizome SPE-separated fractions 5. Stationary Phase: TLC Si 60 RP18 F_{254}S. Mobile Phase: ethyl acetate: methanol: water (5%: 35%: 60%). (A) UV 254 nm. (B) UV 365 nm. D: (C) Sulphuric reagent, white light. (D) Vanillin reagent, white light. From left to right: Track 1 to 2, quercitin; track 3 to 5, leaf SPE-separated fraction 5; track 6 to 8, rhizome SPE-separated fraction 5.

A)

Track 5 @ all wavelengths

Intensity

wavelength

R_f

B)

Track 4 @ all wavelengths

Intensity

R_f

C)

All tracks @ 200 nm

Intensity

Leaf F-12

stigmasterol

R_f

D)

All tracks @ 350 nm

Intensity

1000.0 [AU]

Leaf F-12

stigmasterol
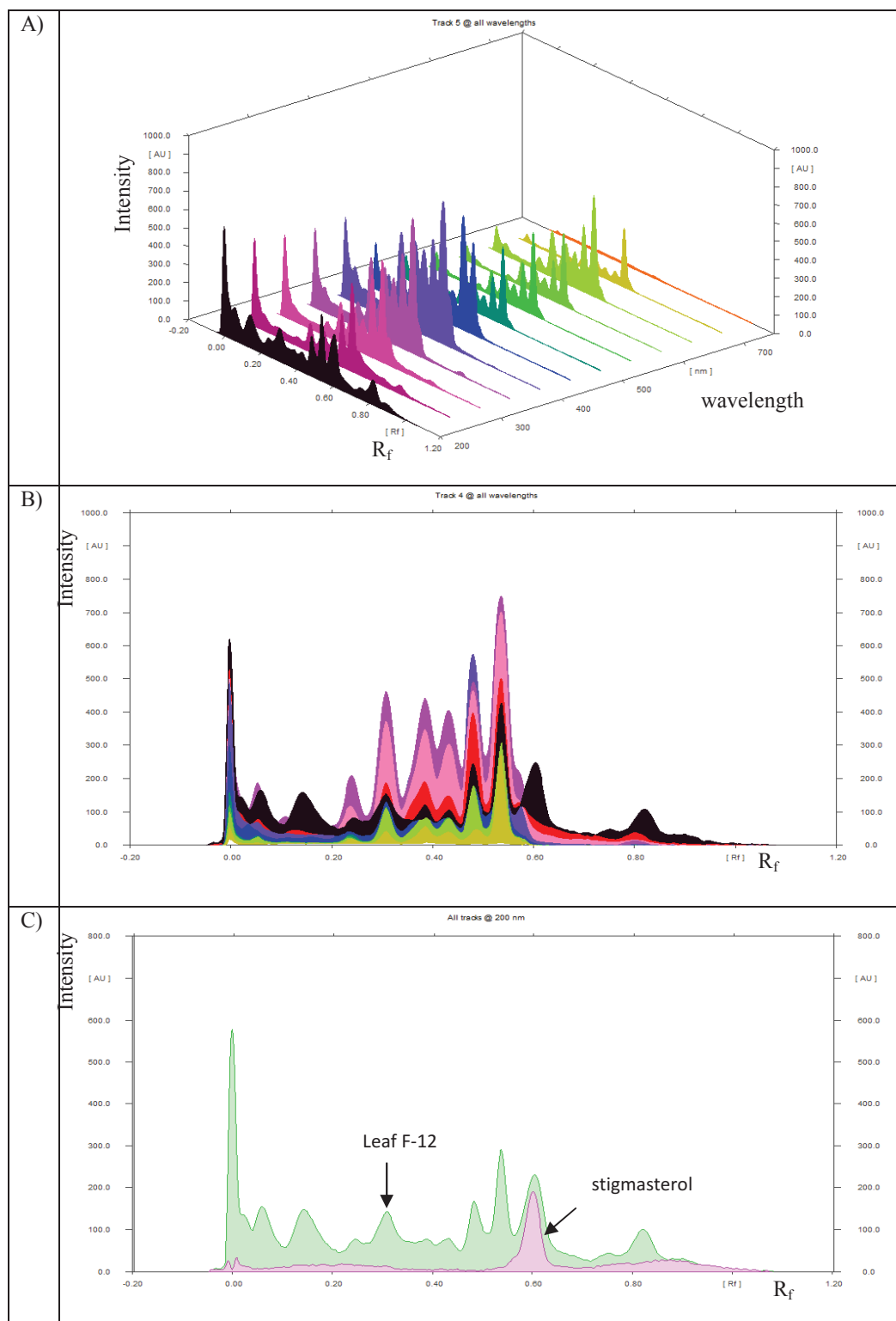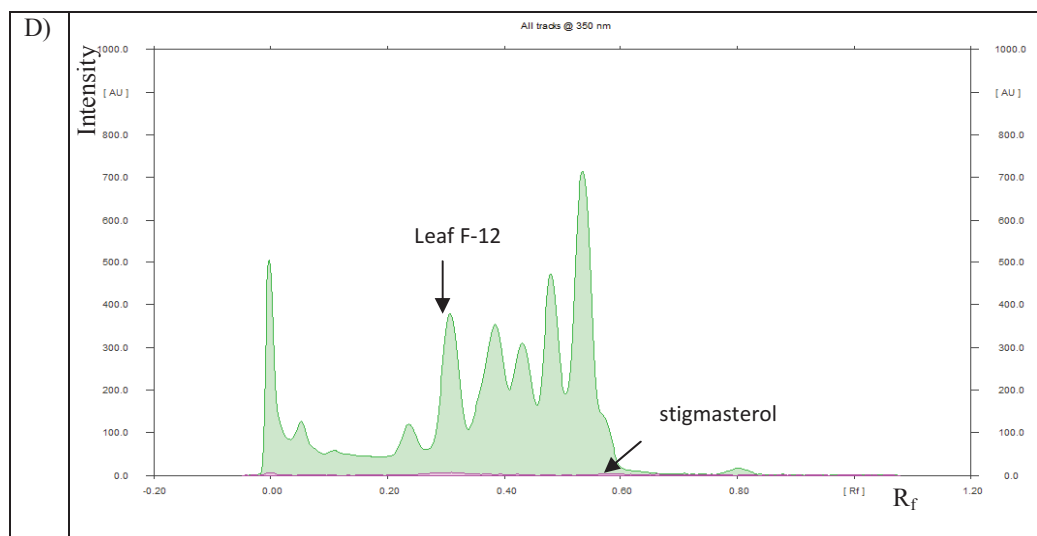
Figure 4.7: HPTLC second dimensional fingerprint profile of leaf SPE-separated fraction 12. Stationary Phase: HPTLC Si 60 F_{254}. Mobile Phase: hexane: acetone (70%: 30%). (A) Spectral scans 200-700 nm in 3D (B) Spectral scans 200-700 nm in 2D (C) UV 200 nm (D) 350 nm. In C and D, Pink track: stigmasterol; Green track: Leaf SPE-separated fraction 12.
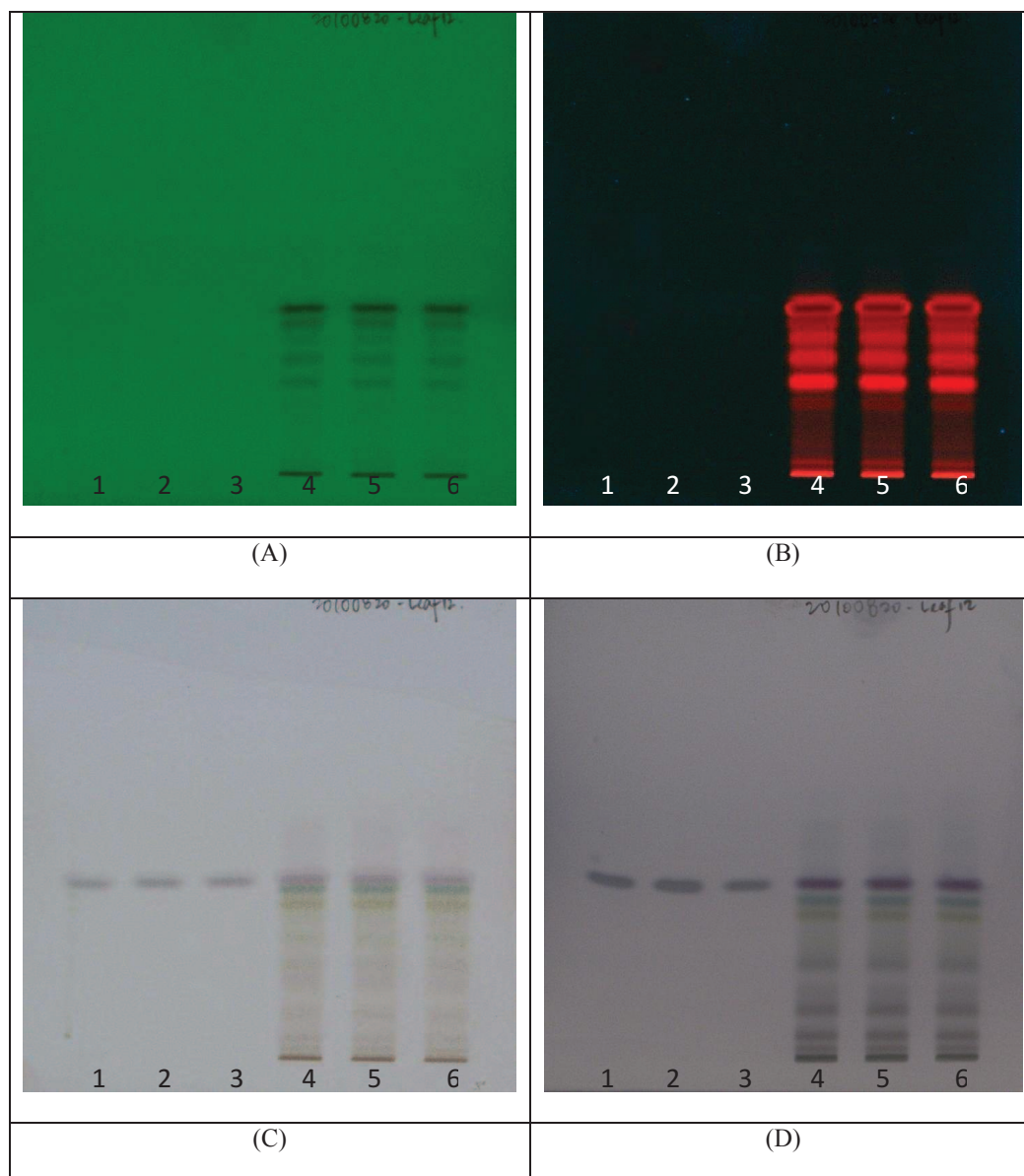
Figure 4.8: HPTLC second dimensional fingerprint profile of leaf SPE-separated fraction 12. Stationary Phase: HPTLC Si 60 F_{254}. Mobile Phase: hexane: acetone (70%: 30%). (A) UV 254 nm. (B) UV 365 nm. D: (C) Sulphuric reagent, white light. (D) Vanillin reagent, white light. From left to right: Track 1 to 3, stigmasterol; track 4 to 6, leaf SPE-separated fraction 12.

The crude rhizome extract of *Paraboea paniculata* was fractionated using solid phase extraction method with C18 octadecyl as stationary phase. 14 fractions were obtained from rhizome crude extract. All fractions were subjected to MTT assay against K-562 cell line (Table 4.3). Rhizome SPE-separated fractions 4, 5 and 7 demonstrated strong cytotoxic activity (cell viability <30%), with cell viability of 5.22%, 15.59% and 16.27%, respectively. The second dimensional fingerprint profiles of cytotoxic fractions 4, 5 and 7 were developed owing to the polarity nature of the active fractions (Figure 4.9). The chromatographic profiles were documented as peak profile from wavelength of 200 nm to 700 nm in both three dimensional and two dimensional angle, and in 250 nm (Figures 4.10, 4.12 and 4.13) as well as picture-liked image in 254 nm, 365 nm, and under white light after derivatization by sulphuric and vanillin reagents (Figures 4.6, 4.11 and 4.14). Quercitin and curcumin are served as standard control, according to their suitability on the respective developing solvent systems.

Table 4.3: Percentage yield and cell viability of K-562 cell line after treated with 14 SPE-separated rhizome fractions of *Paraboea paniculata* via MTT assay.

Fraction	Solvent systems employed	Percentage yield	Cell viability ± SD (%)
1	Sample applied	12.77%	86.88 ± 5.07
2	Sample washed		
	(95% water: 5% methanol)	29.93%	85.23 ± 5.52
3	100% water	0.39%	85.43 ± 4.42
4	80% water: 20% methanol	8.84%	**5.22 ± 1.76**
5	60% water: 40% methanol	31.50%	**15.59 ± 0.6**9
6	40% water: 60% methanol	21.43%	62.95 ± 12.95
7	20% water: 80% methanol	0.81%	**16.27 ± 0.54**
8	100% methanol	3.54%	39.21 ± 3.68
9	80% methanol: 20% dichloromethane	3.48%	73.17 ± 6.04
10	60% methanol: 40% dichloromethane	1.45%	85.24 ± 3.88
11	40% methanol: 60% dichloromethane	0.57%	83.04 ± 5.61
12	20% methanol: 80% dichloromethane	0.21%	91.56 ± 6.05
13	100% dichloromethane	0.10%	82.75 ± 4.88
14	Acidified methanol with 2M of nitric acid	0.16%	71.69 ± 2.11

Cell viability was tested at the concentration of 50 µg/ml.
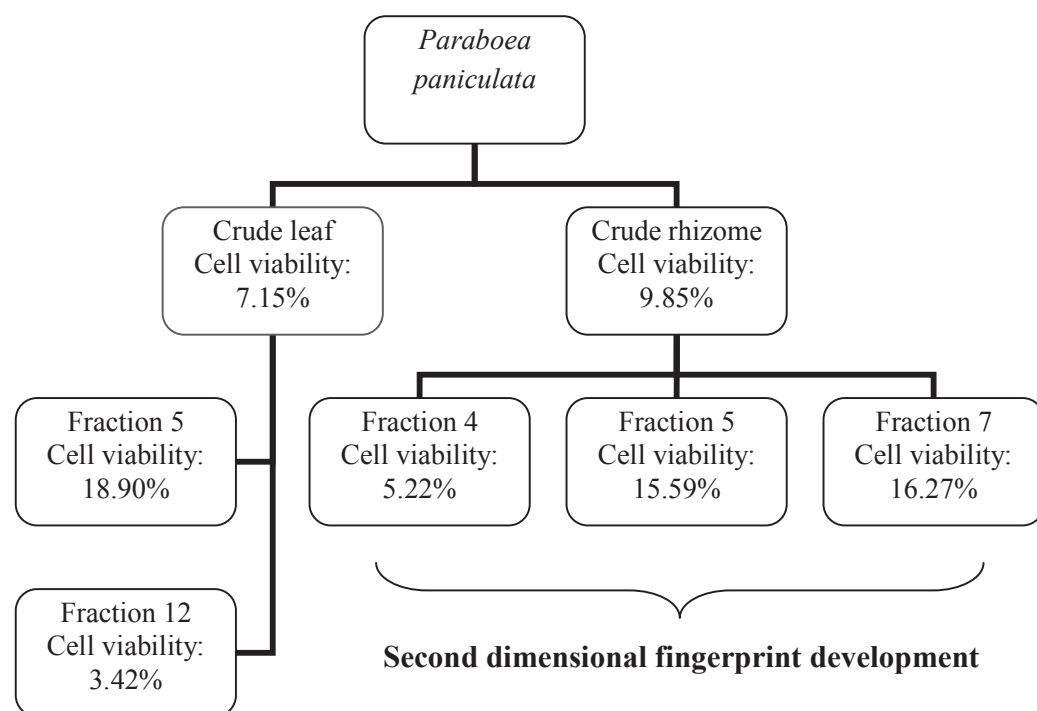
Figure 4.9: Cytotoxic leaf and rhizome SPE-separated fractions for second dimensional fingerprint profile development.
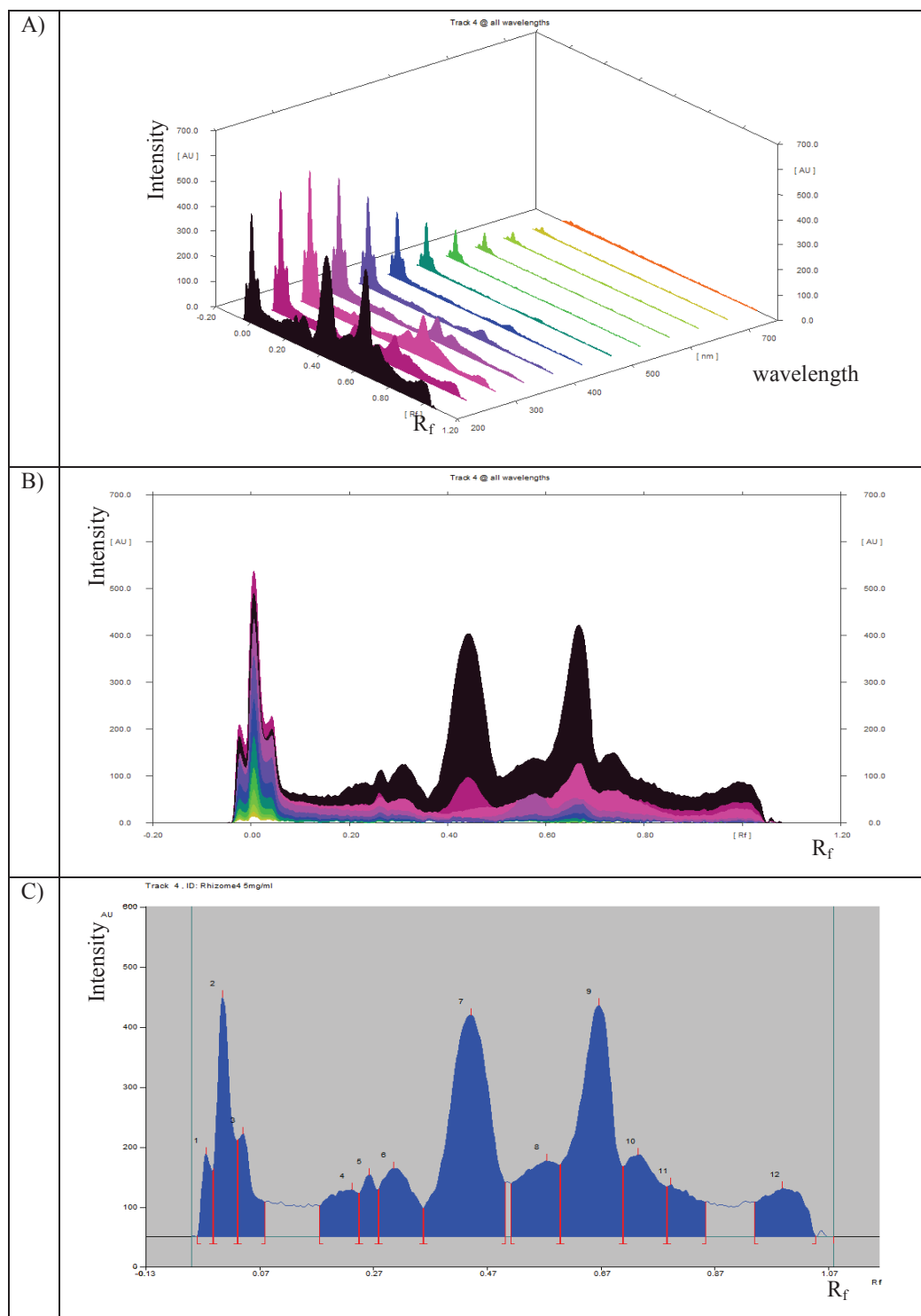
Figure 4.10: HPTLC second dimensional fingerprint profile of rhizome SPE-separated fraction 4. Stationary Phase: TLC Si 60 RP18 F_{254}S. Mobile Phase: ethyl acetate: methanol: water (75%: 15%: 10%). (A)Spectral scans 200-700 nm in 3D (B) Spectral scans 200-700 nm in 2D (C) 200 nm.
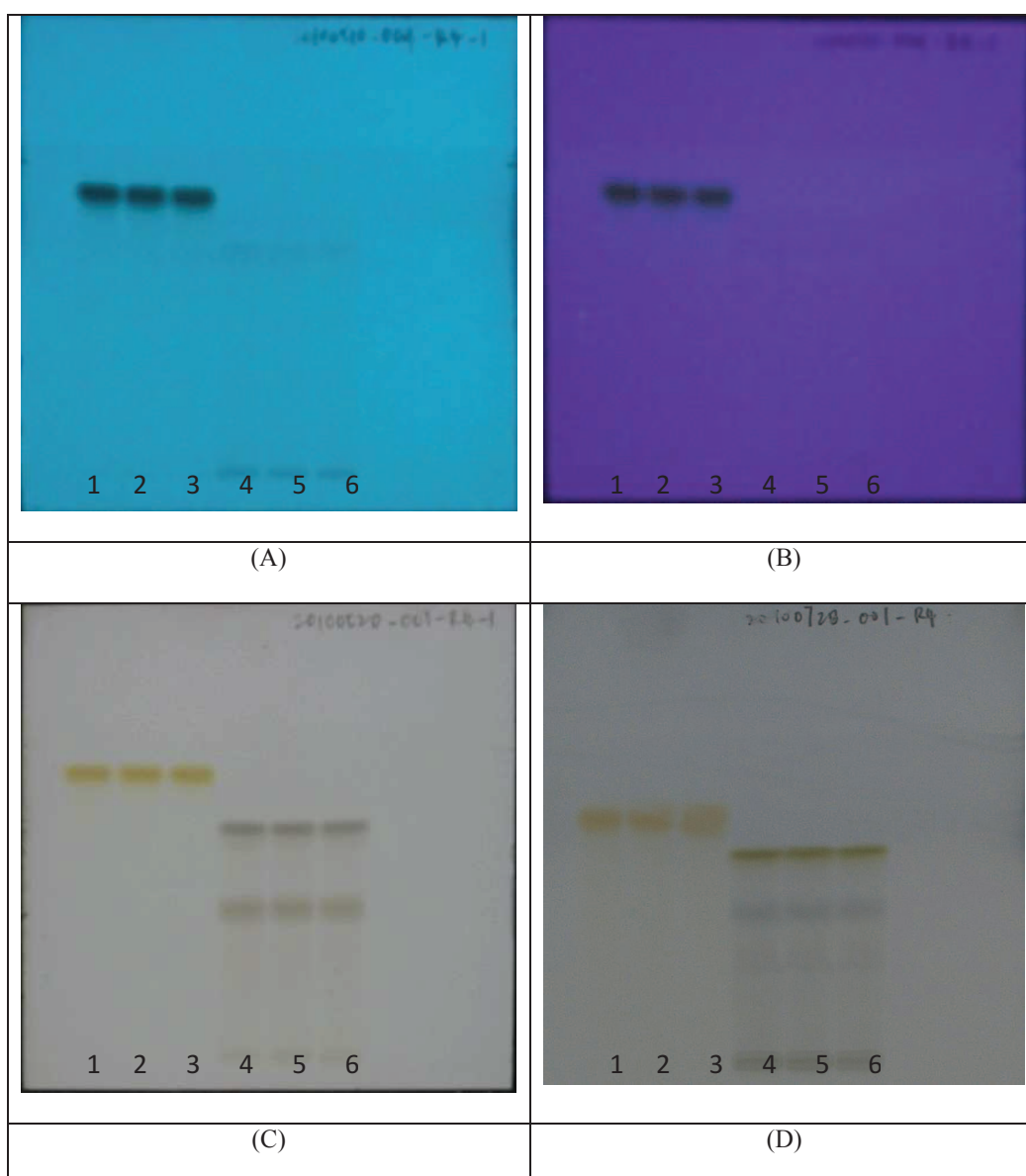
Figure 4.11: HPTLC second dimensional fingerprint profile of rhizome SPE-separated fraction 4. Stationary Phase: TLC Si 60 RP18 F_{254}S. Mobile Phase: ethyl acetate: methanol: water (75%: 15%: 10%). (A) UV 254 nm. (B) UV 365 nm. D: (C) Sulphuric reagent, white light. (D) Vanillin reagent, white light. From left to right: Track 1 to 3, quercitin; track 4 to 6, rhizome SPE-separated fraction 4.
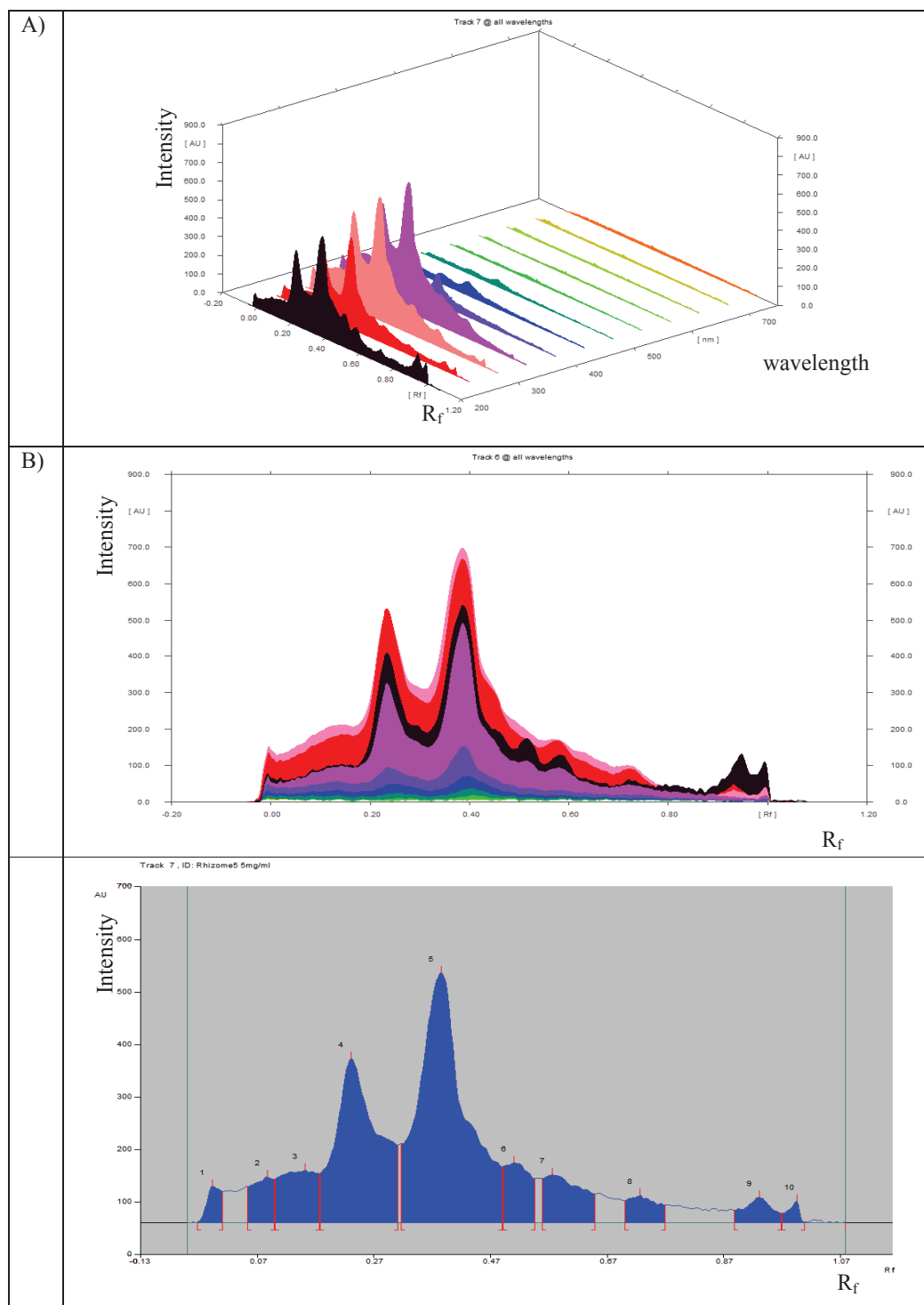
Figure 4.12: HPTLC second dimensional fingerprint profile of rhizome SPE-separated fraction 5. Stationary Phase: TLC Si 60 RP18 $F_{254}S$. Mobile Phase: ethyl acetate: methanol: water (5%: 35%: 60%). (A)Spectral scans 200-700 nm in 3D (B) Spectral scans 200-700 nm in 2D (C) UV 250 nm. Please refer to Figure 4.6, for the HPTLC second dimensional fingerprint profiles of the fraction on TLC plate.
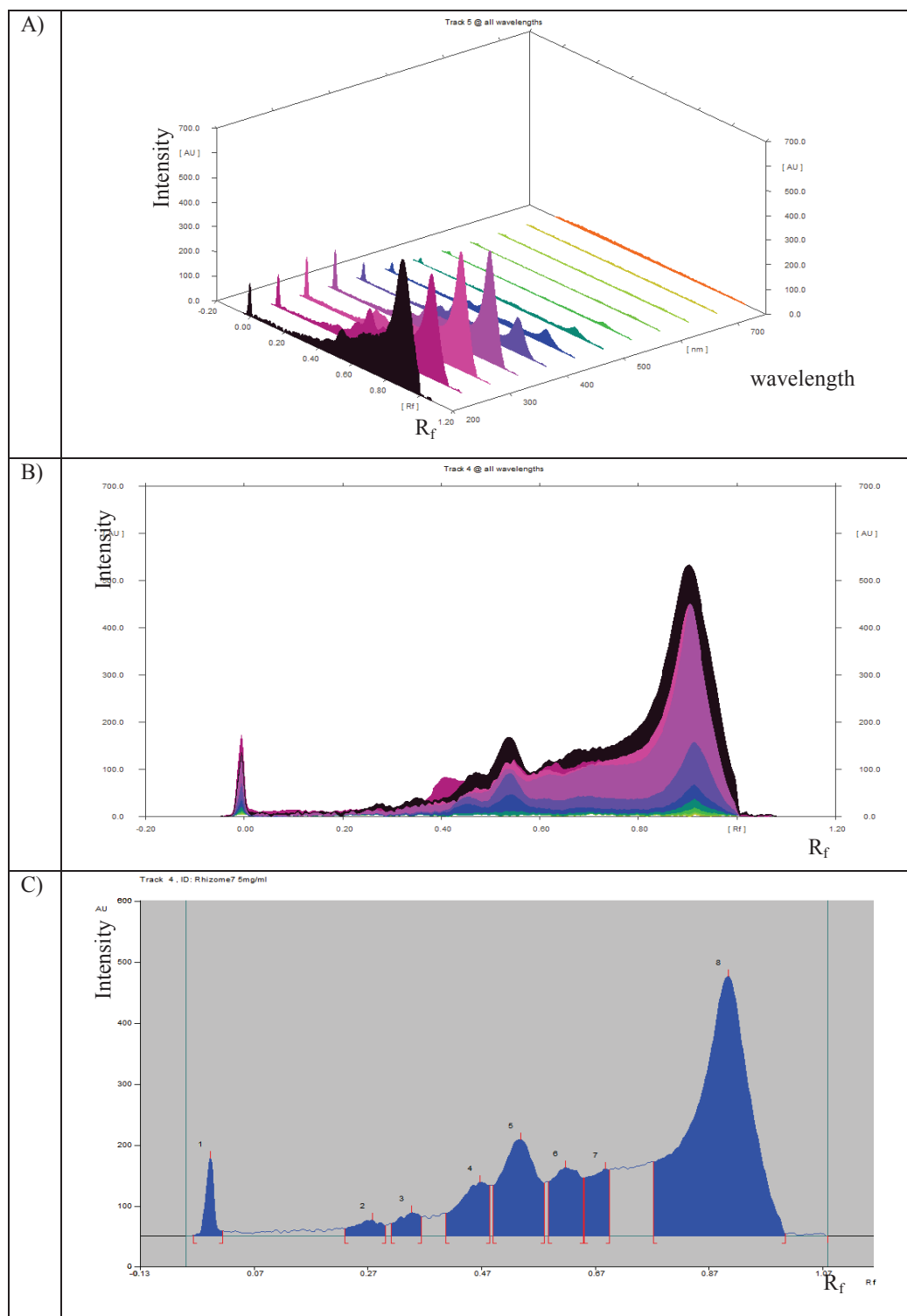
Figure 4.13: HPTLC second dimensional fingerprint profile of rhizome SPE-separated fraction 7. Stationary Phase: TLC Si 60 RP18 $F_{254}S$. Mobile Phase: ethyl acetate: methanol: water (40%: 30%: 30%). (A) Spectral scans 200-700 nm in 3D (B) Spectral scans 200-700 nm in 2D (C) UV 250 nm.
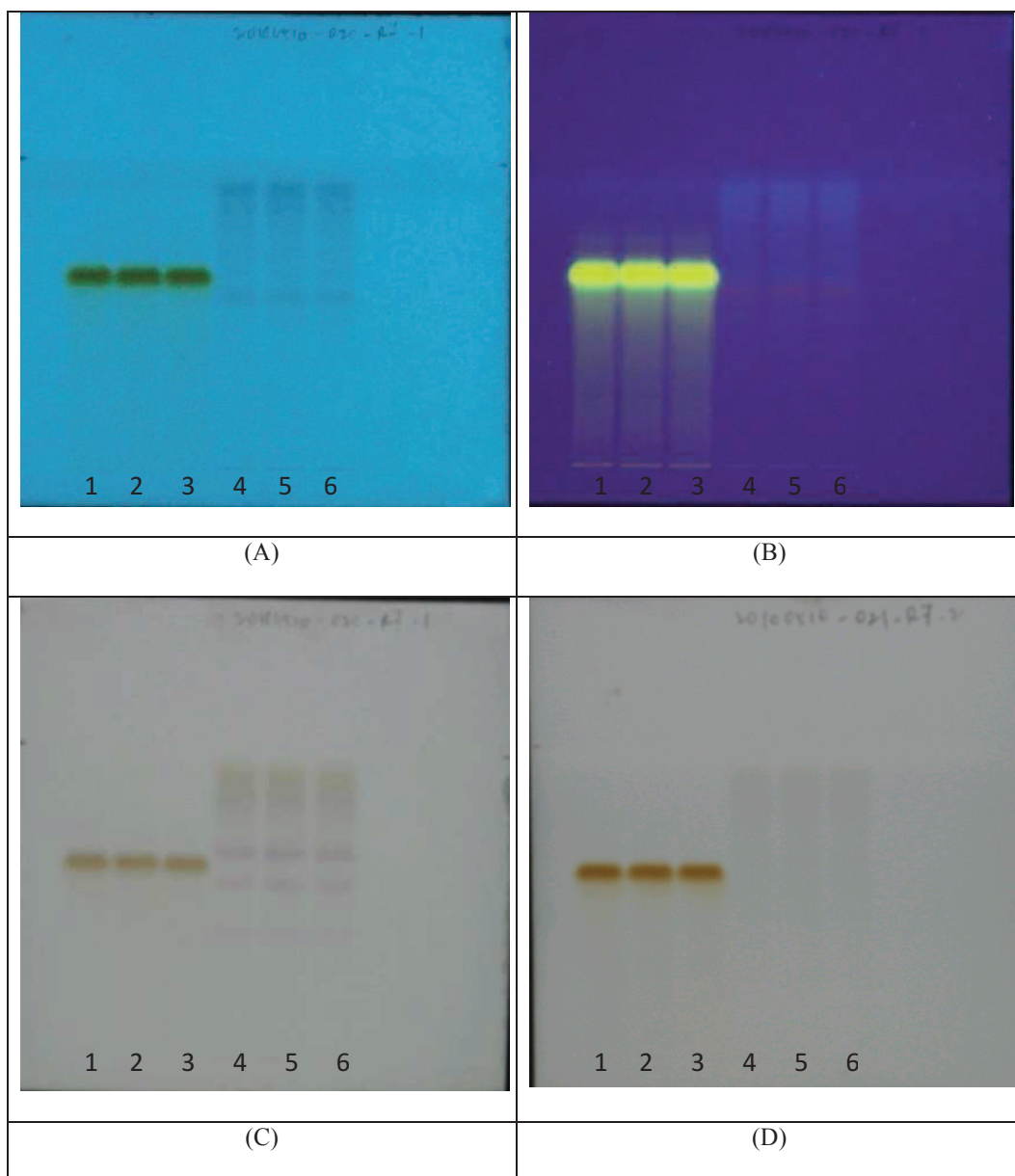
Figure 4.14: HPTLC second dimensional fingerprint profile of rhizome SPE-separated fraction 7. Stationary Phase: TLC Si 60 RP18 $F_{254}S$. Mobile Phasse: ethyl acetate: methanol: water (40%: 30%: 30%). (A) UV 254 nm. (B) UV 365 nm. D: (C) Sulphuric reagent, white light. (D) Vanillin reagent, white light. From left to right: Track 1 to 3, curcumin; track 4 to 6, rhizome SPE-separated fraction 7.

4.3   Validation of the Method

Validation is the formal proof that a method is suitable for its particular usage. The repeatability, intermediate precision, reproducibility, robustness, specificity and stability of the analyte before, during and after chromatography were validated according to the general validation procedure.

4.3.1   Precision on A Plate (Repeatability) is expressed from the average of R_f values of prominent peaks of the fingerprints in parallel analysis of replicates (n=3). An acceptable measure is that the R_f values across the plate do not deviate more than 0.01. The repeatability of the method is acceptable for all fractions (Table 4.4).

Table 4.4: Precision of R_f values of the replicate zones of all fractions together with respective standard compound on an individual plate.

Fractions	Reference peaks	Track 1	Track 2	Track 3	Average	Standard deviation	RSD (%)	Repeatability
Curcumin	Peak1	0.71	0.71	0.71	0.710	0.000	0.00	Accepted
Leaf	Peak1	0.37	0.38	0.38	0.377	0.006	1.59	Accepted
	Peak2	0.79	0.79	0.79	0.790	0.000	0.00	
Rhizome	Peak1	0.25	0.25	0.25	0.250	0.000	0.00	Accepted
	Peak2	0.38	0.39	0.39	0.387	0.006	1.55	
Quercitin	Peak1	0.05	0.05	0.05	0.050	0.000	0.00	Accepted
Leaf F5	Peak1	0.26	0.26	0.26	0.260	0.000	0.00	Accepted
	Peak2	0.41	0.42	0.42	0.417	0.006	1.44	
Rhizome F5	Peak1	0.26	0.26	0.26	0.260	0.000	0.00	Accepted
	Peak2	0.39	0.4	0.39	0.393	0.006	1.53	
Stigmasterol	Peak1	0.58	0.58	0.58	0.580	0.000	0.00	Accepted
Leaf F12	Peak1	0.4	0.41	0.41	0.407	0.006	1.47	Accepted
	Peak2	0.48	0.48	0.49	0.483	0.006	1.24	
Quercitin	Peak1	0.93	0.92	0.92	0.923	0.006	0.65	Accepted
Rhizome F4	Peak1	0.51	0.51	0.52	0.513	0.006	1.17	Accepted
	Peak2	0.77	0.77	0.78	0.773	0.006	0.78	
Curcumin	Peak1	0.63	0.63	0.63	0.630	0.000	0.00	Accepted
Rhizome F7	Peak1	0.55	0.55	0.55	0.550	0.000	0.00	Accepted
	Peak2	0.89	0.89	0.89	0.890	0.000	0.00	

The two significant peaks of the fingerprint profile of each sample were selected as reference peaks and analyzed on the basis of retention time of the peaks. Refer to Appendix B for the prominent peaks referring. RSD: relative standard deviation in percentage

4.3.2 Precision on Different Plates (Intermediate Precision) is expressed from the average of R_f values of prominent peaks of the fingerprints on different plates (n=9). An acceptable criterion is that the R_f values from plate to plate do not differ more than 0.02. The intra-day precision of the method is accepted (Table 4.5).

Table 4.5: Precision of R_f values of the replicate zones of the tested fractions on three individual plates.

Fractions	Reference peaks	Plate 1	Plate 2	Plate 3	Average	Standard deviation	RSD (%)	Intra-day precision
Curcumin	Peak1	0.700	0.705	0.710	0.705	0.005	0.71	Accepted
Leaf	Peak1	0.243	0.240	0.253	0.246	0.007	2.85	Accepted
	Peak2	0.790	0.790	0.820	0.800	0.017	2.13	
Rhizome	Peak1	0.250	0.240	0.260	0.250	0.010	4.00	Accepted
	Peak2	0.387	0.380	0.403	0.390	0.012	3.08	
Quercitin	Peak1	0.055	0.050	0.040	0.145	0.008	5.51	Accepted
Leaf F5	Peak1	0.260	0.267	0.260	0.262	0.004	1.53	Accepted
	Peak2	0.417	0.417	0.410	0.414	0.004	0.97	
Rhizome F5	Peak1	0.260	0.243	0.247	0.250	0.009	3.60	Accepted
	Peak2	0.393	0.383	0.390	0.389	0.005	1.29	
Stigmasterol	Peak1	0.580	0.570	0.590	0.580	0.010	1.72	Accepted
Leaf F12	Peak1	0.407	0.387	0.380	0.391	0.014	3.58	Accepted
	Peak2	0.483	0.487	0.470	0.480	0.009	1.88	
Quercitin	Peak1	0.923	0.925	0.910	0.919	0.008	0.87	Accepted
Rhizome F4	Peak1	0.513	0.497	0.497	0.502	0.010	1.99	Accepted
	Peak2	0.773	0.780	0.760	0.771	0.010	1.30	
Curcumin	Peak1	0.630	0.610	0.620	0.620	0.010	1.61	Accepted
Rhizome F7	Peak1	0.550	0.570	0.553	0.558	0.011	1.97	Accepted
	Peak2	0.890	0.880	0.907	0.892	0.013	1.46	

Triplicates were done for each point of R_f value.

4.3.3 Precision on Different Days (Reproducibility) is expressed from the average of R_f values of prominent peaks of the fingerprint on different plates in different days (n=9). An acceptable criterion is that the R_f values between plates on different days do not vary more than 0.05. The inter-day precision of the method is acceptable across all fractions tested (Table 4.6).

Table 4.6: Precision of R_f values of the replicate zones of the tested fractions between plates from different days.

Fractions	Reference peaks	Plate 1	Plate 4	Plate 5	Average	Standard deviation	RSD (%)	Inter-day Precision
Curcumin	Peak1	0.700	0.690	0.725	0.705	0.018	2.55	Accepted
Leaf	Peak1	0.243	0.243	0.243	0.243	0.000	0.00	Accepted
	Peak2	0.790	0.793	0.807	0.797	0.009	1.13	
Rhizome	Peak1	0.250	0.237	0.237	0.241	0.008	3.32	Accepted
	Peak2	0.387	0.387	0.390	0.388	0.002	0.52	
Quercitin	Peak1	0.055	0.040	0.040	0.045	0.009	20.00	Accepted
Leaf F5	Peak1	0.260	0.257	0.233	0.250	0.015	6.00	Accepted
	Peak2	0.417	0.400	0.380	0.399	0.018	4.51	
Rhizome F5	Peak1	0.260	0.237	0.257	0.251	0.013	5.18	Accepted
	Peak2	0.393	0.373	0.397	0.388	0.013	3.35	
Stigmasterol	Peak1	0.580	0.585	0.665	0.610	0.048	7.88	Accepted
Leaf F12	Peak1	0.407	0.383	0.440	0.410	0.028	6.83	Accepted
	Peak2	0.483	0.480	0.490	0.484	0.005	1.03	
Quercitin	Peak1	0.923	0.833	0.873	0.877	0.045	5.13	Accepted
Rhizome F4	Peak1	0.513	0.470	0.460	0.481	0.028	5.82	Accepted
	Peak2	0.773	0.703	0.717	0.731	0.037	5.06	
Curcumin	Peak1	0.630	0.635	0.570	0.612	0.036	5.88	Accepted
Rhizome F7	Peak1	0.550	0.553	0.517	0.540	0.020	3.70	Accepted
	Peak2	0.890	0.910	0.890	0.897	0.012	1.34	

Triplicates were done for each point of R_f value. Plates 4 and 5 were established after every 3 days.

4.3.4 Robustness is the ability to tolerate variation of parameters, without significant changes in the fingerprint profiles. It is expressed in term of volume of developing solvent, equilibration time between gas phase and stationary phase, type of chamber, development distance and dosage speed of sample application.

4.3.4.1 Volume of Developing Solvent was performed in 5 ml, and 15 ml in place of 10 ml. The acceptable criterion for the variation of R_f values as a function of volume of developing solvent would be less than 0.05. No significant difference was seen when the plates were developed in different volume of developing solvents (Table 4.7), except for leaf F-5 and rhizome F-4, where the changes are varied more than 0.05.

Table 4.7: Changes in the fingerprint analysis of the tested fractions as function of volume of developing solvent.

Fractions	Reference peaks	5ml	10ml	15ml	Average	Standard deviation	RSD (%)	Robustness (Volume)
Curcumin	Peak1	0.710	0.690	0.700	0.700	0.010	1.43	Accepted
Leaf	Peak1	0.247	0.243	0.240	0.243	0.003	1.23	Accepted
	Peak2	0.830	0.807	0.807	0.814	0.013	1.60	
Rhizome	Peak1	0.250	0.247	0.233	0.243	0.009	3.70	Accepted
	Peak2	0.390	0.390	0.373	0.384	0.010	2.60	
Quercitin	Peak1	0.050	0.050	0.070	0.057	0.012	21.05	Accepted
Leaf F5	Peak1	0.223	0.280	0.337	0.280	0.057	20.35	Not Accepted
	Peak2	0.387	0.450	0.500	0.446	0.057	12.78	
Rhizome F5	Peak1	0.257	0.293	0.290	0.280	0.020	7.14	Accepted
	Peak2	0.400	0.433	0.417	0.417	0.017	4.08	
Stigmasterol	Peak1	0.580	0.610	0.577	0.589	0.018	2.13	Accepted
Leaf F12	Peak1	0.350	0.400	0.360	0.370	0.026	7.03	Accepted
	Peak2	0.453	0.510	0.477	0.480	0.028	5.83	
Quercitin	Peak1	0.950	0.830	0.757	0.846	0.098	11.58	Not Accepted
Rhizome F4	Peak1	0.490	0.473	0.420	0.461	0.037	4.37	Not Accepted
	Peak2	0.800	0.713	0.610	0.708	0.095	13.42	
Curcumin	Peak1	0.663	0.625	0.600	0.629	0.032	5.09	Accepted
Rhizome F7	Peak1	0.570	0.530	0.523	0.541	0.025	4.62	Accepted
	Peak2	0.927	0.917	0.940	0.928	0.012	1.29	

Triplicates were done for each point of R_f value.

4.3.4.2 Equilibration Time of gas phase and stationary phase was performed in 10 minutes and 30 minutes, instead of 20 minutes. The acceptable criterion for the difference of R_f values as a function of equilibration time would be less than 0.05. The separation was not affected by the increased time of equilibration (Table 4.8).

Table 4.8: Changes in the fingerprint analysis of the tested fractions as function of equilibration time of gas phase and stationary phase.

Fractions	Reference peaks	10 min	20 min	30 min	Average	Standard deviation	RSD (%)	Robustness (E. time)
Curcumin	Peak1	0.680	0.690	0.700	0.690	0.010	1.45	Accepted
Leaf	Peak1	0.240	0.243	0.263	0.249	0.013	5.22	Accepted
	Peak2	0.787	0.807	0.807	0.800	0.012	1.50	
Rhizome	Peak1	0.243	0.247	0.250	0.247	0.003	1.21	Accepted
	Peak2	0.380	0.390	0.397	0.389	0.008	2.06	
Quercitin	Peak1	0.070	0.050	0.055	0.058	0.010	17.24	Accepted
Leaf F5	Peak1	0.300	0.280	0.263	0.281	0.018	6.41	Accepted
	Peak2	0.463	0.450	0.417	0.443	0.024	5.42	
Rhizome F5	Peak1	0.227	0.293	0.247	0.256	0.034	13.28	Accepted
	Peak2	0.350	0.433	0.387	0.390	0.042	10.77	
Stigmasterol	Peak1	0.607	0.610	0.607	0.608	0.002	0.33	Accepted
Leaf F12	Peak1	0.383	0.400	0.390	0.391	0.008	2.05	Accepted
	Peak2	0.493	0.510	0.493	0.499	0.010	2.00	
Quercitin	Peak1	0.900	0.830	0.870	0.867	0.035	4.04	Accepted
Rhizome F4	Peak1	0.477	0.473	0.453	0.468	0.013	2.78	Accepted
	Peak2	0.740	0.713	0.710	0.721	0.016	2.22	
Curcumin	Peak1	0.663	0.625	0.600	0.629	0.032	5.09	Accepted
Rhizome F7	Peak1	0.570	0.530	0.523	0.541	0.025	4.62	Accepted
	Peak2	0.927	0.917	0.940	0.928	0.012	1.29	

Triplicates were done for each point of R_f value.

4.3.4.3 Type of Chamber was performed in flat bottom chamber in comparable size, instead of twin-trough chamber. The acceptable criterion for the difference of R_f values as a function of chamber type would be less than 0.05. The different type of chamber has affected the fingerprint analysis, as the R_f values of most fractions are deviate more than 0.05 (Table 4.9).

Table 4.9: Changes in the fingerprint analysis of the tested fractions as function of type of chamber.

Fractions	Reference peaks	Twin-trough	Flat bottom	Average	Standard deviation	RSD (%)	Robustness (Chamber)
Curcumin	Peak1	0.690	0.800	0.745	0.078	10.47	Not accepted
Leaf	Peak1	0.243	0.300	0.272	0.040	14.71	Not accepted
	Peak2	0.807	0.903	0.855	0.068	7.95	
Rhizome	Peak1	0.247	0.300	0.273	0.038	13.92	Accepted
	Peak2	0.390	0.460	0.425	0.049	11.53	
Quercitin	Peak1	0.050	0.030	0.040	0.014	35.00	Accepted
Leaf F5	Peak1	0.280	0.200	0.240	0.057	23.75	Not Accepted
	Peak2	0.450	0.373	0.412	0.054	13.11	
Rhizome F5	Peak1	0.293	0.220	0.257	0.052	20.23	Not Accepted
	Peak2	0.433	0.390	0.412	0.031	7.52	
Stigmasterol	Peak1	0.610	0.567	0.588	0.031	5.27	Accepted
Leaf F12	Peak1	0.400	0.340	0.370	0.042	11.35	Not Accepted
	Peak2	0.510	0.403	0.457	0.075	16.41	
Quercitin	Peak1	0.830	0.943	0.887	0.080	9.02	Not Accepted
Rhizome F4	Peak1	0.473	0.553	0.513	0.057	11.11	Not Accepted
	Peak2	0.713	0.823	0.768	0.078	10.16	
Curcumin	Peak1	0.625	0.573	0.599	0.037	6.18	Accepted
Rhizome F7	Peak1	0.530	0.527	0.528	0.002	0.38	Accepted
	Peak2	0.917	0.930	0.923	0.009	0.98	

Triplicates were done for each point of R_f value.

4.3.4.4 The **Developing Distance** was extended to 75 mm and 80 mm, rather than 70 mm from the lower edge of the plate. The acceptable criterion for the difference of R_f values as function of developing distance would be less than 0.05. No significant difference was seen by the increased developing distance (Table 4.10).

Table 4.10: Changes in the fingerprint analysis of the tested fractions as function of developing distance.

Fractions	Reference peaks	70mm	75mm	80mm	Average	Standard deviation	RSD (%)	Robustness (distance)
Curcumin	Peak1	0.690	0.750	0.700	0.713	0.032	4.49	Accepted
Leaf	Peak1	0.243	0.287	0.260	0.263	0.022	8.37	Accepted
	Peak2	0.807	0.860	0.820	0.829	0.028	3.38	
Rhizome	Peak1	0.247	0.290	0.260	0.266	0.022	8.27	Accepted
	Peak2	0.390	0.423	0.400	0.404	0.017	4.21	
Quercitin	Peak1	0.050	0.035	0.065	0.050	0.015	30.00	Accepted
Leaf F5	Peak1	0.280	0.283	0.280	0.281	0.002	0.71	Accepted
	Peak2	0.450	0.437	0.430	0.439	0.010	2.28	
Rhizome F5	Peak1	0.293	0.270	0.300	0.288	0.016	5.56	Accepted
	Peak2	0.433	0.427	0.455	0.438	0.015	3.42	
Stigmasterol	Peak1	0.610	0.547	0.570	0.576	0.032	5.56	Accepted
Leaf F12	Peak1	0.400	0.363	0.390	0.384	0.019	4.95	Accepted
	Peak2	0.510	0.460	0.450	0.473	0.032	6.77	
Quercitin	Peak1	0.830	0.920	0.905	0.885	0.048	5.42	Accepted
Rhizome F4	Peak1	0.473	0.503	0.493	0.490	0.015	3.06	Accepted
	Peak2	0.713	0.777	0.767	0.752	0.034	4.52	
Curcumin	Peak1	0.625	0.647	0.640	0.637	0.011	1.73	Accepted
Rhizome F7	Peak1	0.530	0.557	0.543	0.543	0.013	2.39	Accepted
	Peak2	0.917	0.927	0.93	0.924	0.007	0.76	

Triplicates were done for each point of R_f value.

4.3.4.5 Dosage Speed of Sample Applicator was performed in 150 nl/s and 200 nl/s, which normally in 100 nl/s to observe any significant difference. The acceptable criterion for the difference of R_f values as function of dosage speed would be less than 0.05. No significant difference was seen by the increased dosage speed of the sample applicator (Table 4.11).

Table 4.11: Changes in the fingerprint analysis of the tested fractions as function of dosage speed of sample applicator.

Fractions	Reference peaks	100nl/s	150nl/s	200nl/s	Average	Standard deviation	RSD (%)	Robustness (Dosage speed)
Curcumin	Peak1	0.710	0.690	0.670	0.690	0.020	2.90	Accepted
Leaf	Peak1	0.260	0.243	0.240	0.248	0.011	4.44	Accepted
	Peak2	0.820	0.807	0.780	0.802	0.020	2.49	
Rhizome	Peak1	0.260	0.247	0.240	0.249	0.010	4.02	Accepted
	Peak2	0.400	0.390	0.377	0.389	0.012	3.08	
Quercitin	Peak1	0.055	0.050	0.050	0.052	0.003	5.77	Accepted
Leaf F5	Peak1	0.307	0.280	0.293	0.293	0.013	4.44	Accepted
	Peak2	0.467	0.450	0.460	0.459	0.008	1.74	
Rhizome F5	Peak1	0.297	0.293	0.263	0.284	0.018	6.34	Accepted
	Peak2	0.453	0.433	0.410	0.432	0.022	5.09	
Stigmasterol	Peak1	0.560	0.610	0.557	0.576	0.030	5.21	Accepted
Leaf F12	Peak1	0.383	0.400	0.393	0.392	0.008	2.04	Accepted
	Peak2	0.490	0.510	0.490	0.497	0.012	2.41	
Quercitin	Peak1	0.895	0.830	0.990	0.905	0.080	8.84	Accepted
Rhizome F4	Peak1	0.470	0.473	0.500	0.481	0.016	3.33	Accepted
	Peak2	0.737	0.713	0.810	0.753	0.050	6.64	
Curcumin	Peak1	0.580	0.625	0.663	0.623	0.042	6.74	Accepted
Rhizome F7	Peak1	0.540	0.530	0.577	0.549	0.025	4.55	Accepted
	Peak2	0.957	0.917	0.923	0.932	0.021	2.25	

Triplicates were done for each point of R_f value.

4.3.5　Stability before Chromatography

Stability of the analytes on a plate before chromatography was assessed in term of the consistency of the same samples prepared in solution at different time and from different batches. The first batch of isolated sample solutions was applied at track 1, and then applied at tracks 2 and 3 after set aside for 3 hours at room temperature. The same goes to the second batch of sample solutions, at track 4 to track 6. The reasonable criterion would be the samples are stable prior to chromatography and no additional zones or decomposition of analytes is observed. Both batches of samples are stable for at least 3 hours prior to chromatography (Figure 4.15 to Figure 4.19).
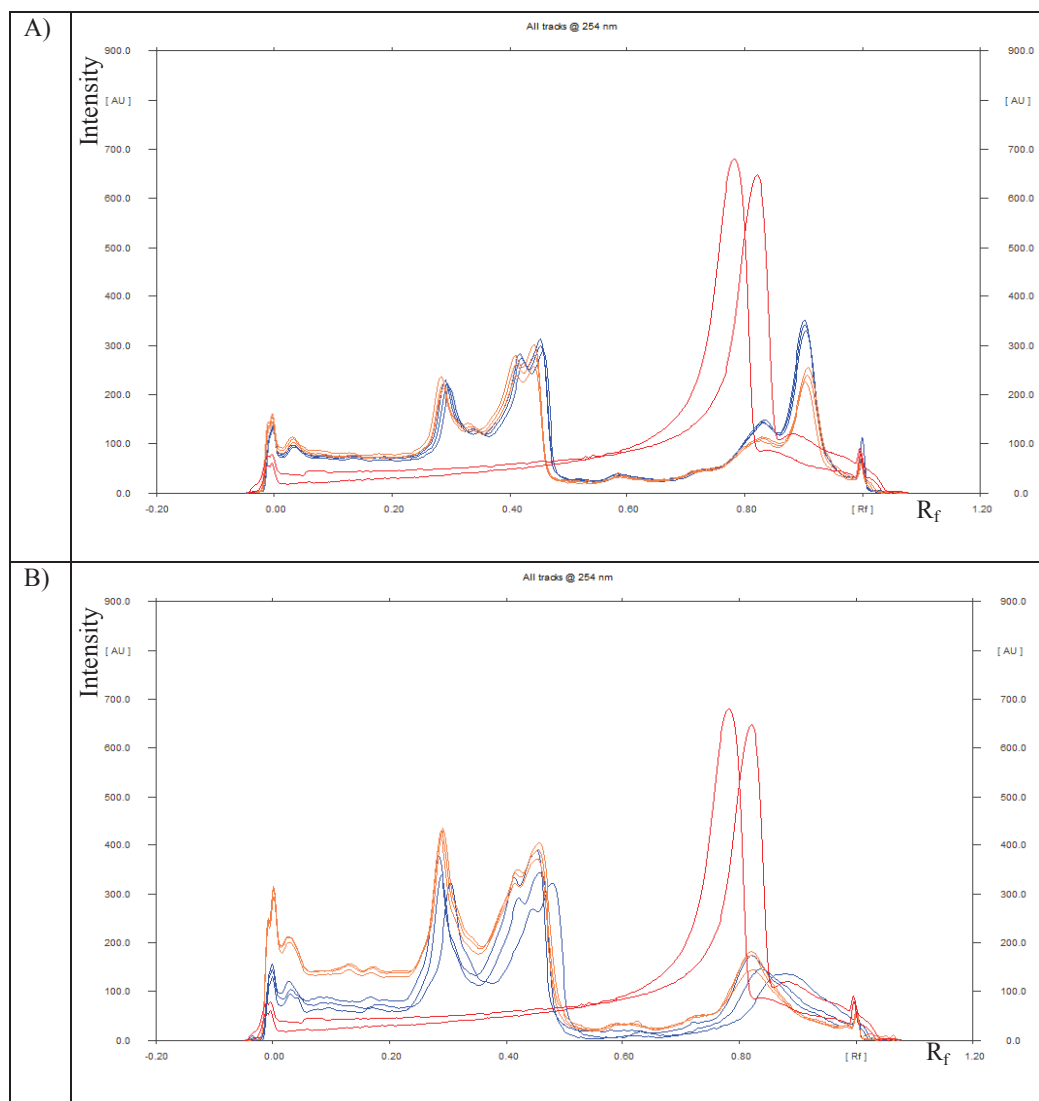
Figure 4.15: Stability of leaf and rhizome crude fraction of different batches of extraction. Stationary Phase: HPTLC Si 60 F_{254}. Mobile Phase: ethyl acetate: methanol: water (75.27%: 13.98%: 10.75%). UV 254 nm. A) Leaf crude fraction. B) Rhizome crude fraction. Red tracks, quercitin; Brown tracks, First batch of extraction; Blue tracks, Second batch of extraction.
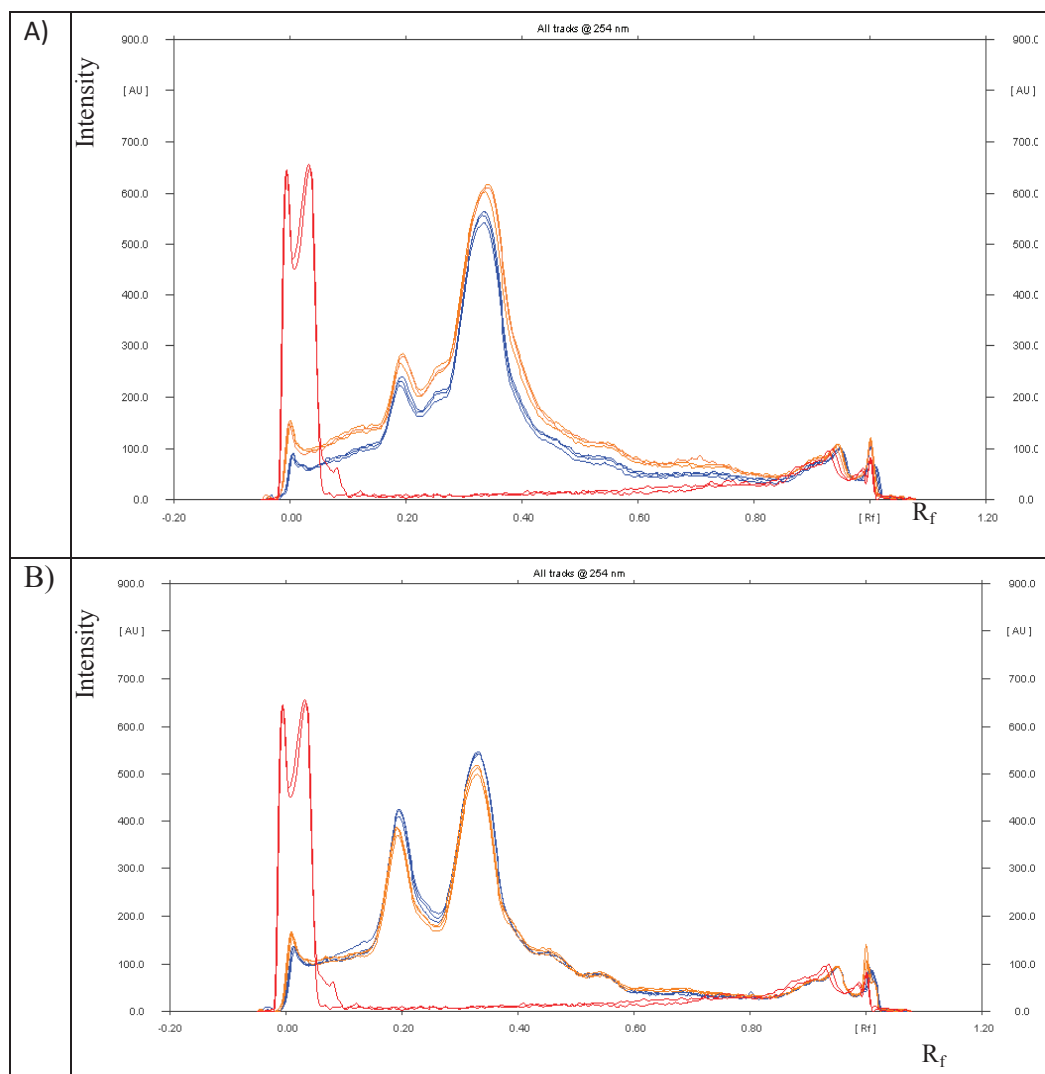
Figure 4.16: Stability of leaf and rhizome SPE-separated fraction 5 of different batches of isolation. Stationary Phase: TLC Si 60 RP18 $F_{254}S$. Mobile Phase: ethyl acetate: methanol: water (5%: 35%: 60%). UV 254 nm. A) Leaf SPE-separated fraction 5. B) Rhizome SPE-separated fraction 5. Red tracks, quercitin; Brown tracks, first batch of fractionation; Blue tracks, second batch of fractionation.
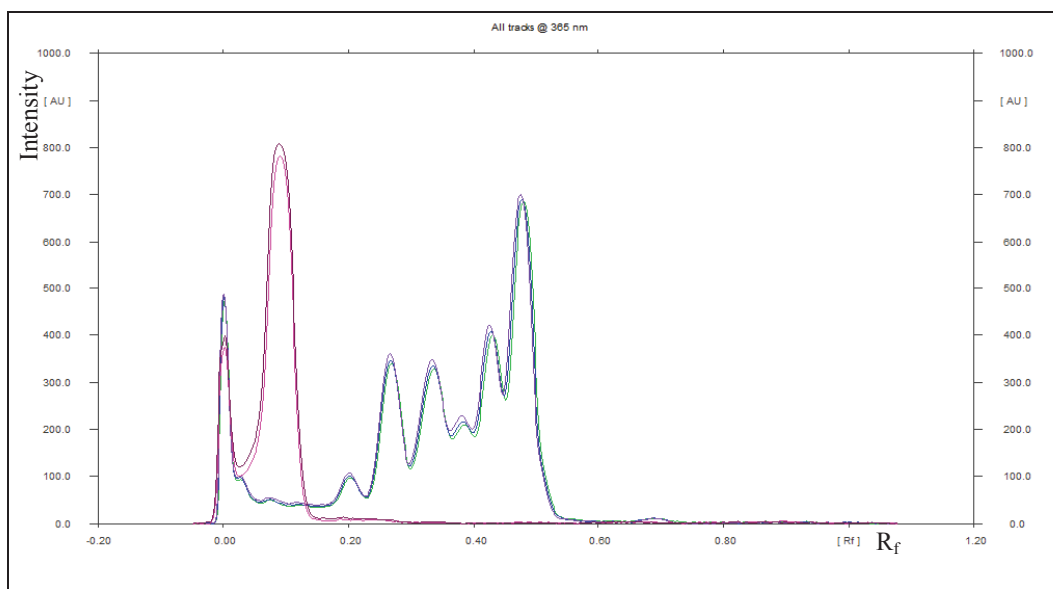
Figure 4.17: Stability of leaf SPE-separated fraction 12 of different batches of isolation. Stationary Phase: HPTLC Si 60 F_{254}. Mobile Phase: hexane: acetone (70%: 30%). UV 365 nm. Purple tracks, curcumin; Brue tracks, first batch of fractionation; Green tracks, second batch of fractionation.
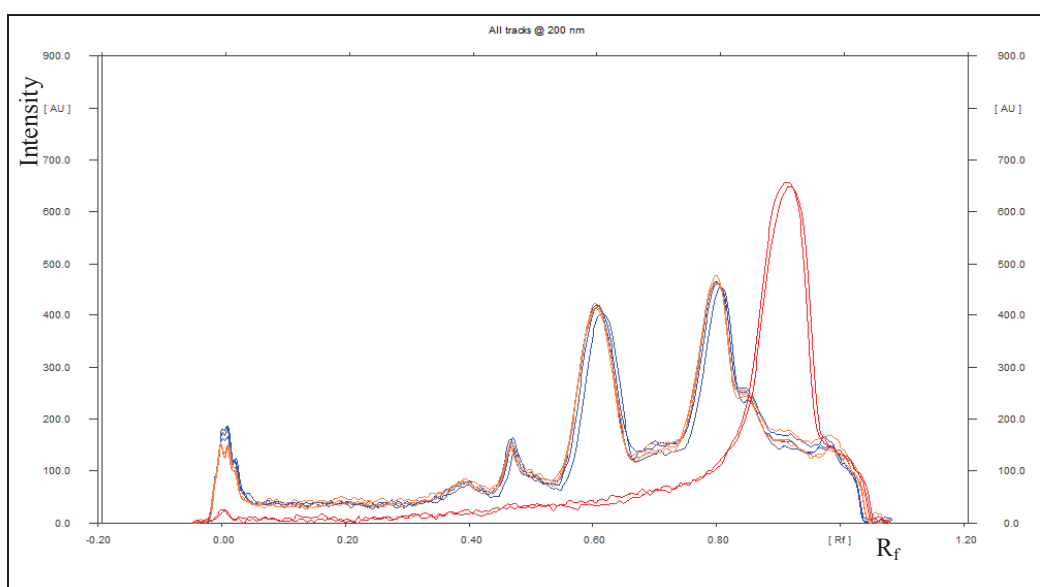
Figure 4.18: Stability of rhizome SPE-separated fraction 4 of different batches of isolation. Stationary Phase: TLC Si 60 RP18 $F_{254}S$. Mobile Phase: ethyl acetate: methanol: water (75%: 15%: 10%). UV 200 nm. Red tracks, quercitin; Brown tracks, first batch of fractionation; Blue tracks, second batch of fractionation.
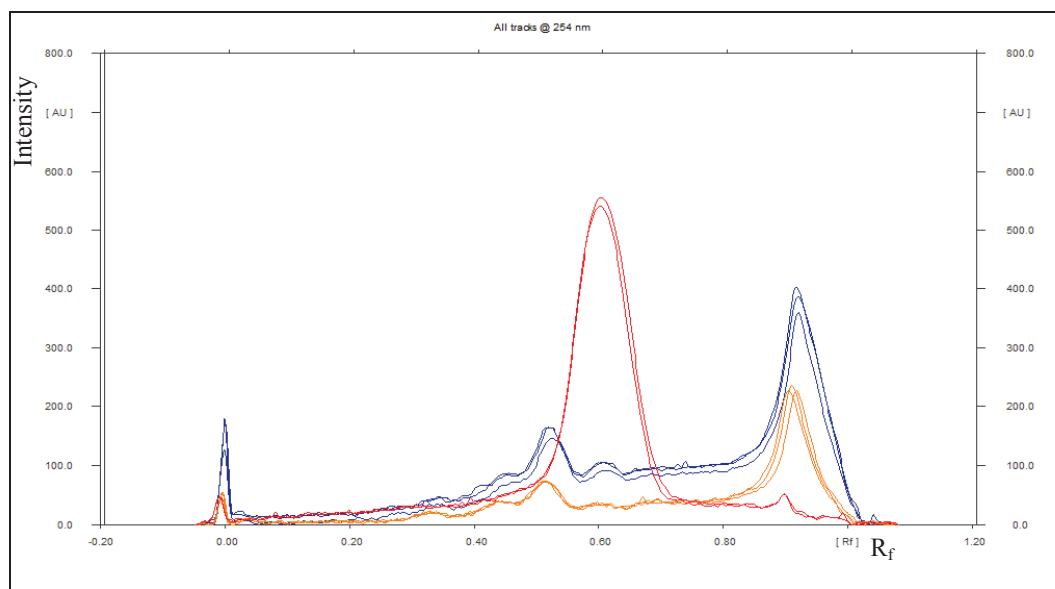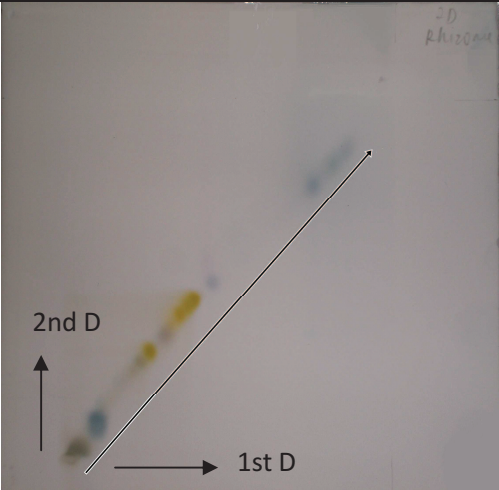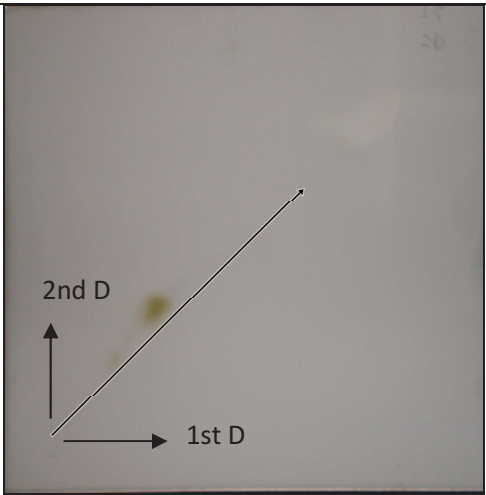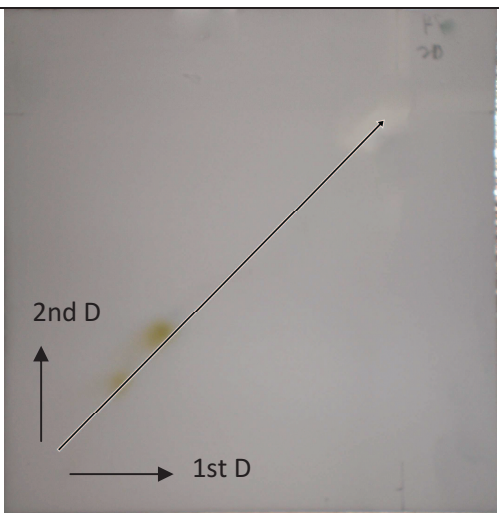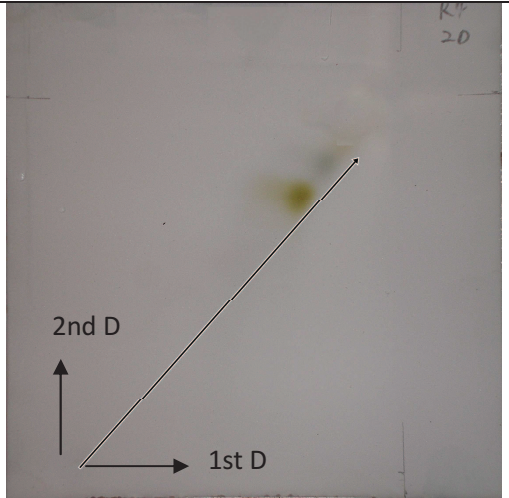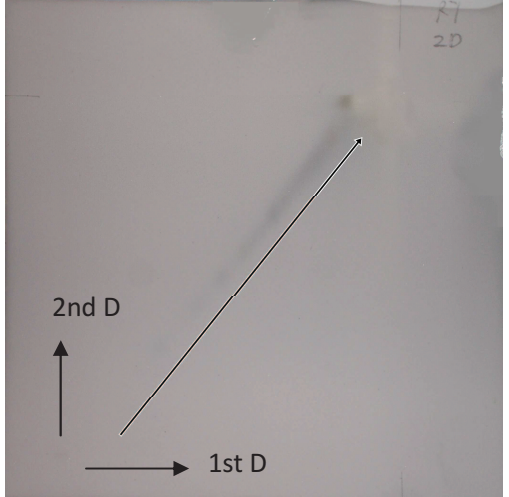
Figure 4.19: Stability of rhizome SPE-separated fraction 7 of different batches of isolation. Stationary Phase: TLC Si 60 RP18 F_{254}S. Mobile Phase: ethyl acetate: methanol: water (40%: 30%: 30%). UV 254 nm. Red tracks, curcumin; Brown tracks, first batch of fractionation; Blue tracks, second batch of fractionation.

4.3.6 Stability during Chromatography

Stability of analytes during chromatography was investigated by turning the plate 90 degrees to the right and developed with fresh similar developing solvent. The sample would be considered stable during chromatography if all zones are located at the diagonal connecting to the application position with the intersection of the two solvent fronts. Results showed the samples were stable during chromatography and no zone was located aside of the diagonal (Figure 4.20 to Figure 4.26).

Figure 4.20: Stability of leaf crude fraction during chromatography with 2D chromatography. Stationary Phase: HPTLC Si 60 F_{254}. Mobile Phase: ethyl acetate: methanol: water (75.27%: 13.98%: 10.75%). D: vanillin reagent, white light.

Figure 4.21: Stability of rhizome crude fraction during chromatography with 2D chromatography. Stationary Phase: HPTLC Si 60 F_{254}. Mobile Phase: ethyl acetate: methanol: water (75.27%: 13.98%: 10.75%). D: vanillin reagent, white light.

Figure 4.22: Stability of leaf SPE-separated fraction 5 during chromatography with 2D chromatography. Stationary Phase: TLC Si 60 RP18 F_{254}S. Mobile Phase: ethyl acetate: methanol: water (5%: 35%: 60%). D: vanillin reagent, white light.

Figure 4.23: Stability of rhizome SPE-separated fraction 5 during chromatography with 2D chromatography. Stationary Phase: TLC Si 60 RP18 F_{254}S. Mobile Phase: ethyl acetate: methanol: water (5%: 35%: 60%). D: vanillin reagent, white light.

Figure 4.24: Stability of leaf SPE-separated fraction 12 during chromatography with 2D chromatography. Stationary Phase: HPTLC Si 60 F_{254}. Mobile Phase: hexane: acetone (70%: 30%). D: vanillin reagent, white light.

Figure 4.25: Stability of rhizome SPE-separated fraction 4 during chromatography with 2D chromatography. Stationary Phase: TLC Si 60 RP18 F_{254}S. Mobile Phase: ethyl acetate: methanol: water (75%: 15%: 10%). D: vanillin reagent, white light.

Figure 4.26: Stability of rhizome SPE-separated fraction 7 during chromatography with 2D chromatography. Stationary Phase: TLC Si 60 RP18 F_{254}S. Mobile Phase: ethyl acetate: methanol: water (40%: 30%: 30%). D: vanillin reagent, white light.

4.3.7 Stability after Chromatography

Stability of analytes after chromatography was assessed by evaluating the chromatographic result repeatedly: right after, 10 minutes, 30 minutes, and 1hour after plate development. The samples are considered stable after separation if there are no significant changes of chromatogram within the time frame. Results showed the samples were stable after chromatography as no significant changes was seen within 1 hour (Figure 4.27 to Figure 4.33).
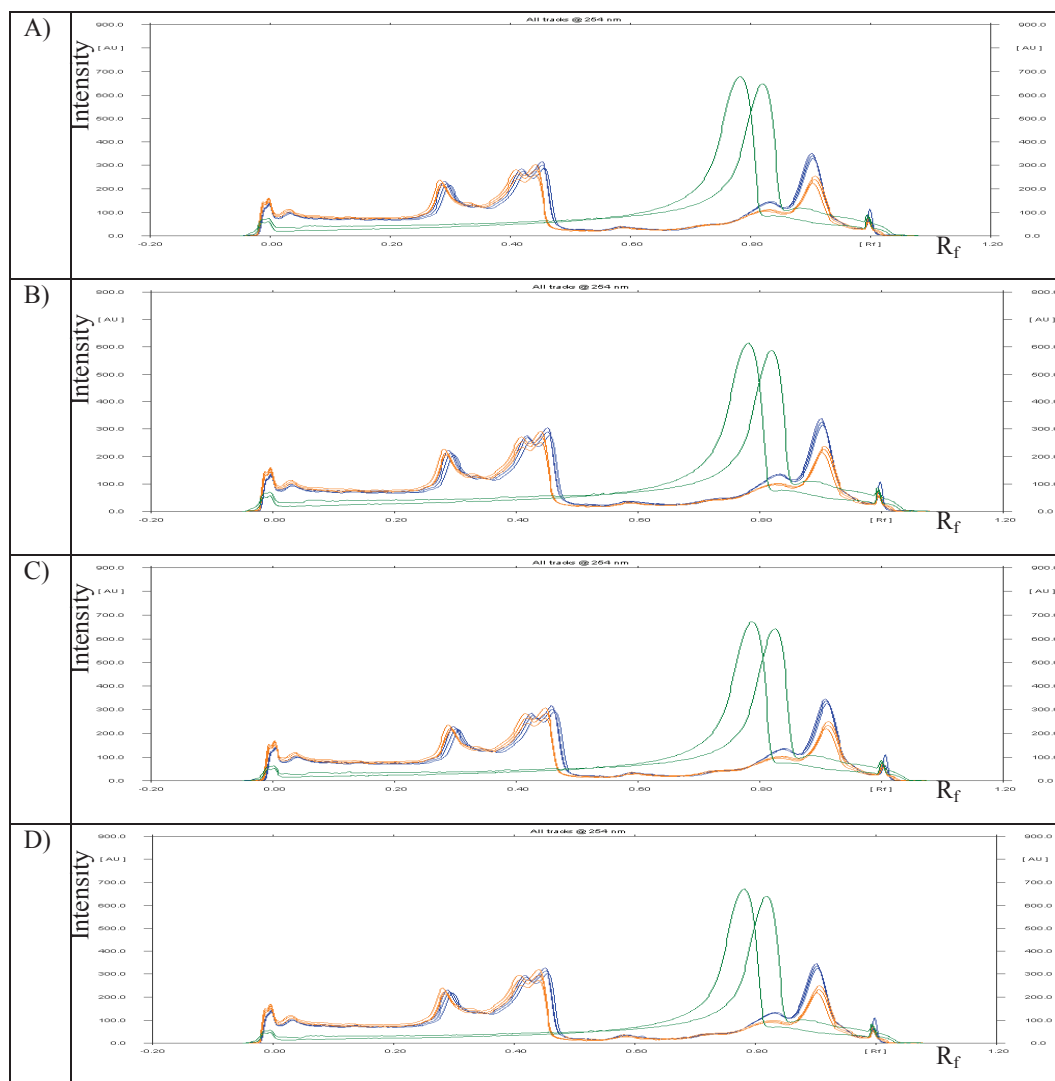
Figure 4.27: Stability of the chromatographic result of leaf crude fraction. Stationary phase: HPTLC Si 60 F$_{254}$. Mobile phase: ethyl acetate: methanol: water (75.27%: 13.98%: 10.75%). UV 254 nm. (A) Right after development. (B) After 10 minutes. (C) After 30 minutes. (D) After 1 hour. Green tracks, quercitin; Brown tracks, first batch of extraction; Blue tracks, second batch of extraction.
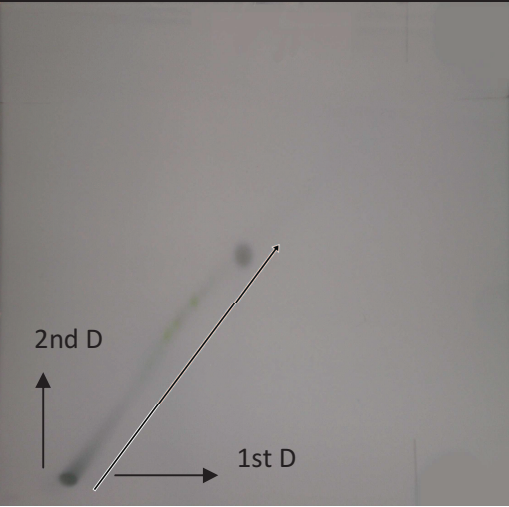
A)

B)

C)

D)
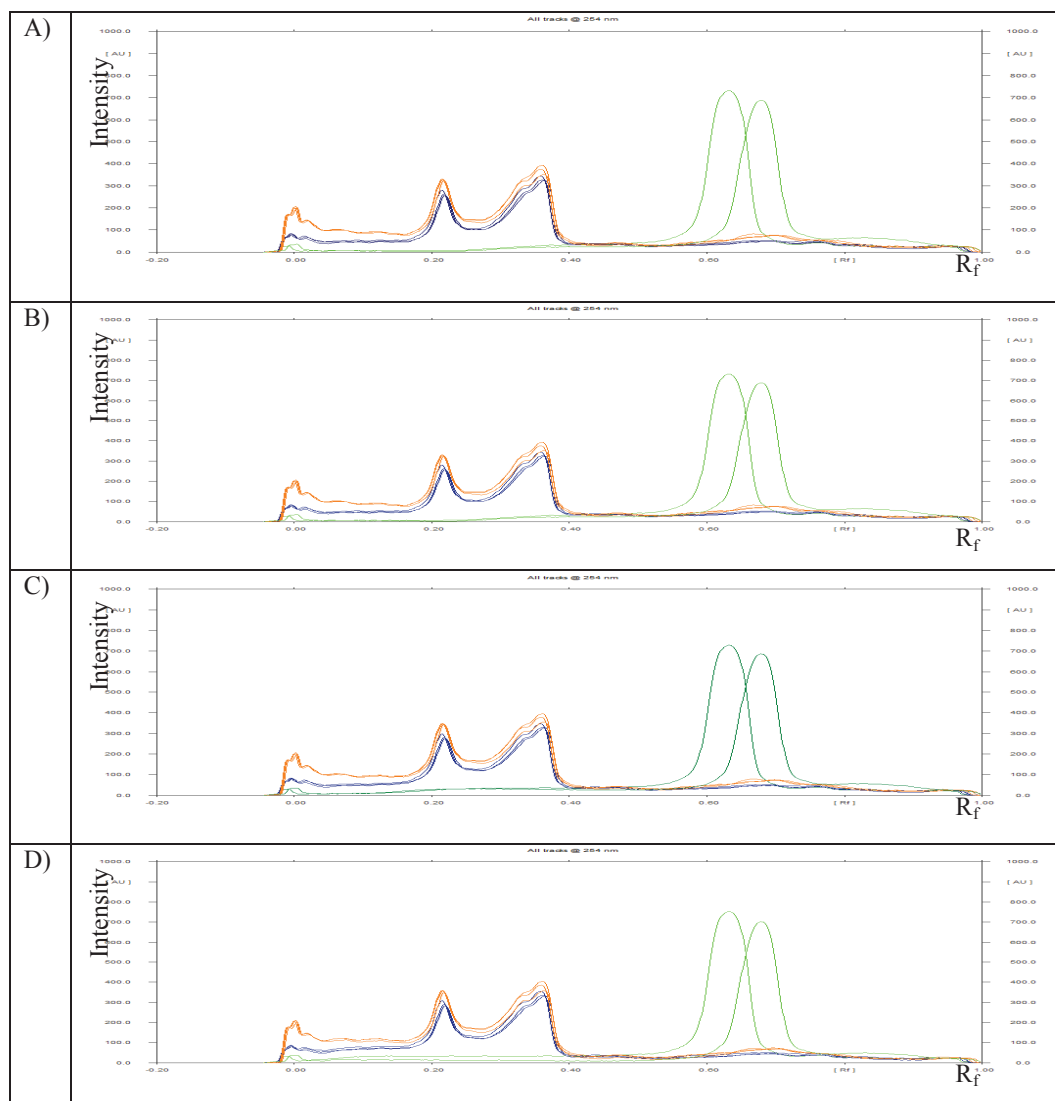
Figure 4.28: Stability of the chromatographic result of rhizome crude fraction. Stationary phase: HPTLC Si 60 F_{254}. Mobile phase: ethyl acetate: methanol: water (75.27%: 13.98%: 10.75%). UV 254 nm. (A) Right after development. (B) After 10 minutes. (C) After 30 minutes. (D) After 1 hour. Green tracks, quercitin; Brown tracks, first batch of extraction; Blue tracks, second batch of extraction.
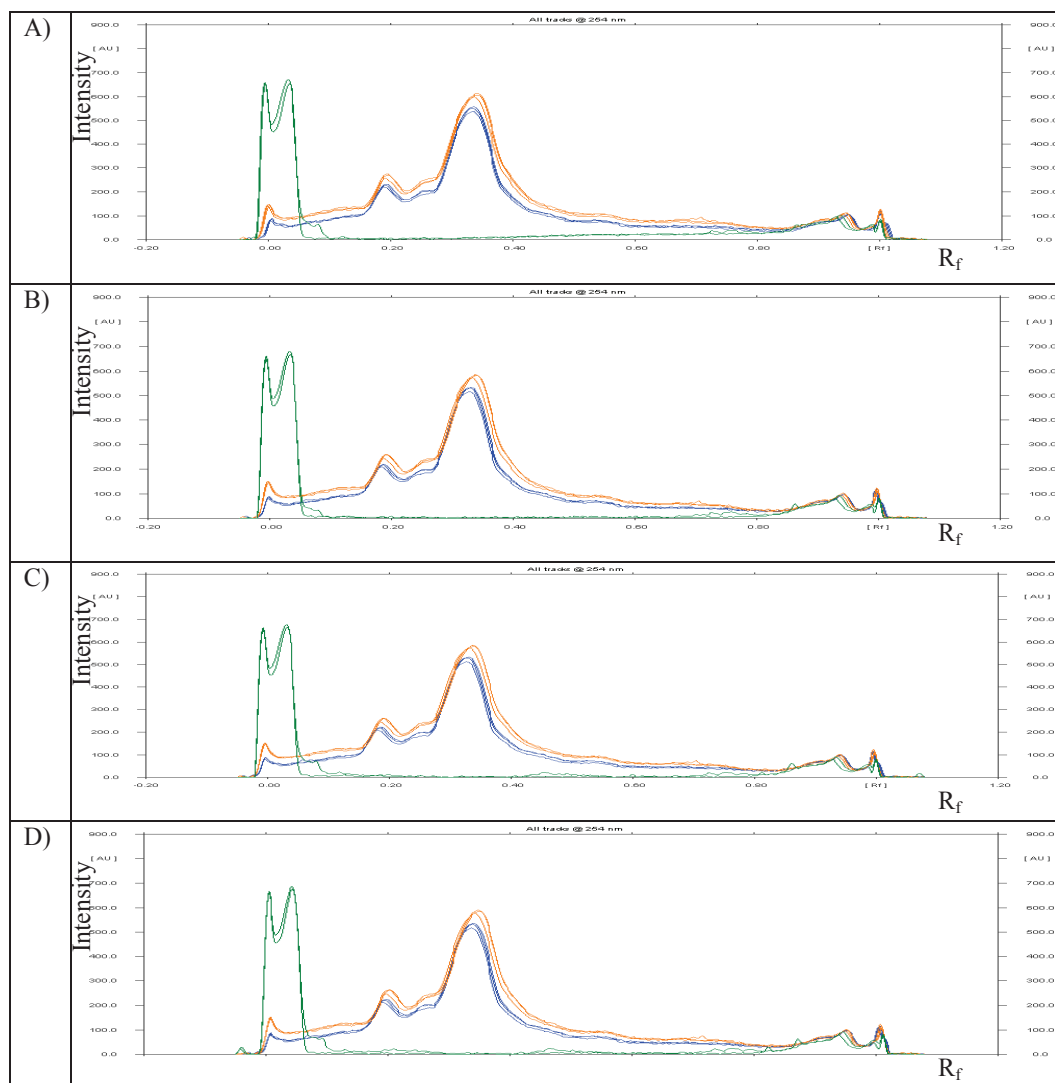
Figure 4.29: Stability of the chromatographic result of leaf SPE-separated fraction 5. Stationary phase: TLC Si 60 RP18 $F_{254}S$. Mobile phase: ethyl acetate: methanol: water (5%: 35%: 60%). UV 254 nm. (A) Right after development. (B) After 10 minutes. (C) After 30 minutes. (D) After 1 hour. Green tracks, quercitin; Brown tracks, first batch of fractionation; Blue tracks, second batch of fractionation.
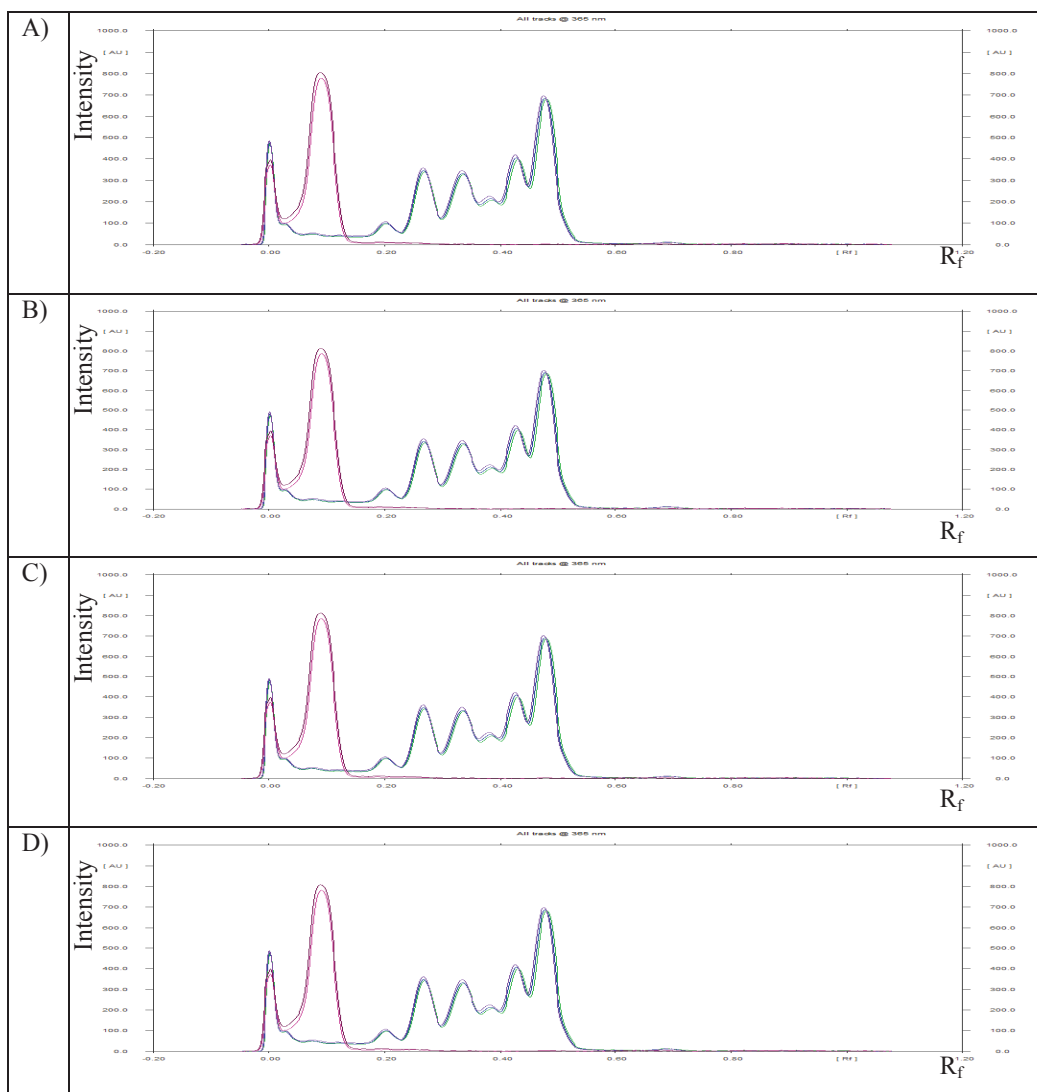
Figure 4.30: Stability of the chromatographic result of leaf SPE-separated fraction 12. Stationary phase: HPTLC Si 60 F$_{254}$. Mobile phase: hexane: acetone (70%: 30%). UV 365 nm. (A) Right after development. (B) After 10 minutes. (C) After 30 minutes. (D) After 1 hour. Purple tracks, curcumin; Brue tracks, first batch of fractionation; Green tracks, second batch of fractionation.
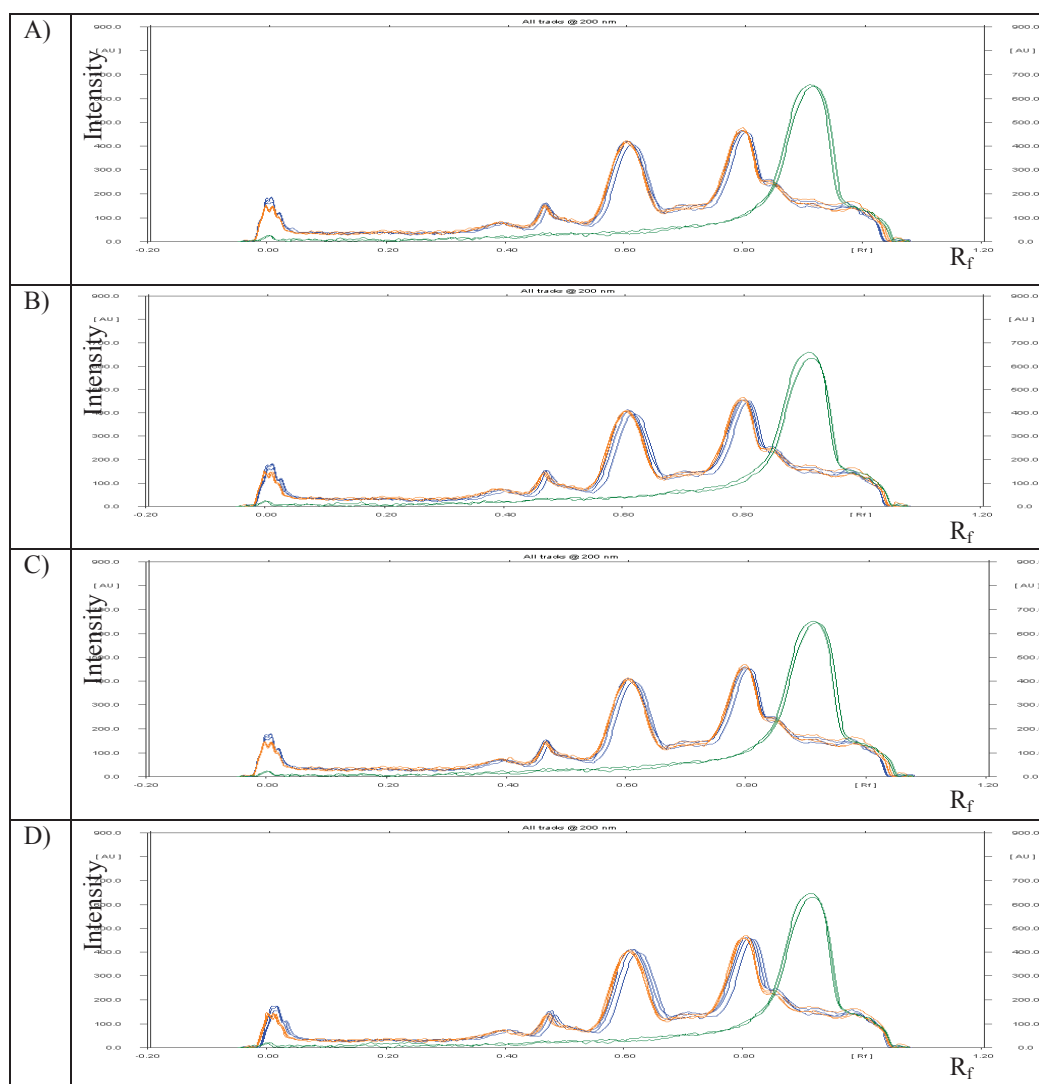
Figure 4.31: Stability of the chromatographic result of rhizome SPE-separated fraction 4. Stationary Phase: TLC Si 60 RP18 F$_{254}$S. Mobile Phase: ethyl acetate: methanol: water (75%: 15%: 10%). UV 200 nm. (A) Right after development. (B) After 10 minutes. (C) After 30 minutes. (D) After 1 hour. Green tracks, quercitin; Brown tracks, first batch of fractionation; Blue tracks, second batch of fractionation.
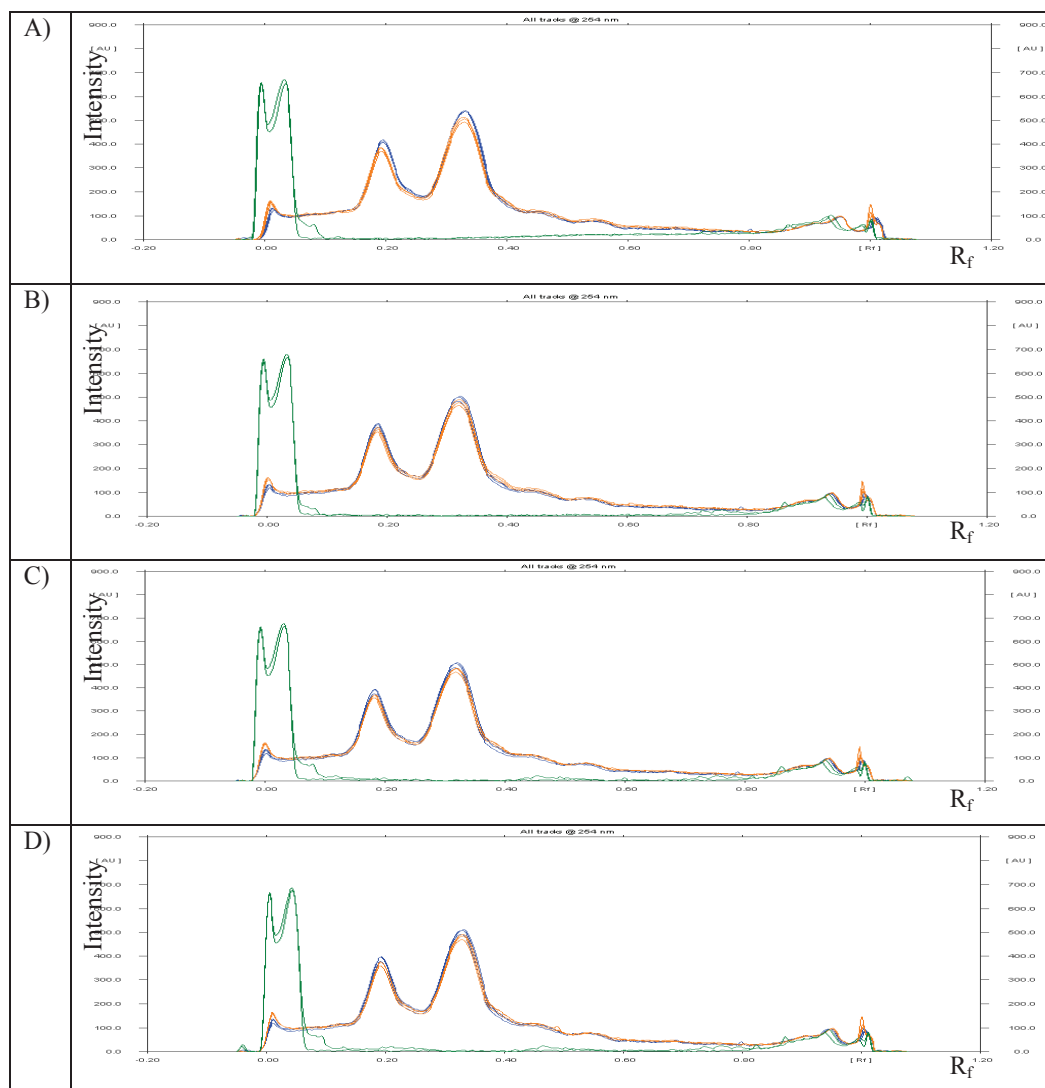
Figure 4.32: Stability of the chromatographic result of rhizome SPE-separated fraction 5. Stationary phase: TLC Si 60 RP18 F$_{254}$S. Mobile phase: ethyl acetate: methanol: water (5%: 35%: 60%). UV 254 nm. (A) Right after development. (B) After 10 minutes. (C) After 30 minutes. (D) After 1 hour. Green tracks, quercitin; Brown tracks, first batch of fractionation; Blue tracks, second batch of fractionation.
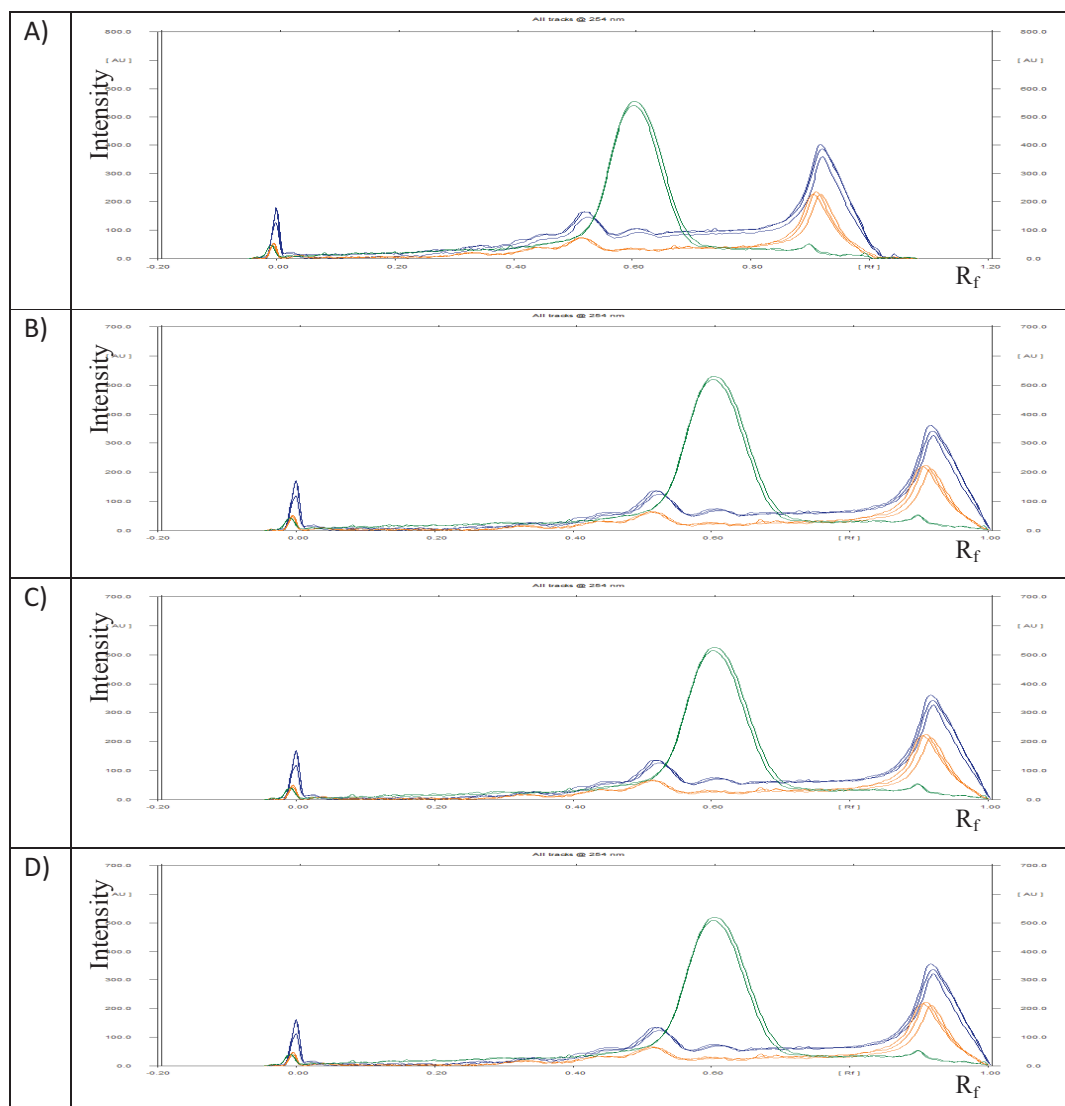
Figure 4.33: Stability of the chromatographic result of rhizome SPE-separated fraction 7. Stationary phase: TLC Si 60 RP18 F$_{254}$S. Mobile phase: ethyl acetate: methanol: water (40%: 35%: 35%). UV 254 nm. (A) Right after development. (B) After 10 minutes. (C) After 30 minutes. (D) After 1 hour. Green tracks, curcumin; Brown tracks, first batch of fractionation; Blue tracks, second batch of fractionation.

4.3.8 Specificity

Specificity of the method was assessed by comparing the different sets of same sample, in order to investigate the similarity in their identity. The samples of same identity were expected to give similar result and can be distinguished from the samples of different identity. Fingerprint of the samples are compared in term of number, position, colour and intensity of the zones. In Figures 4.34 and 4.35, active isolated compounds, PP-1 from rhizome SPE-separated F-4; PP-2, and PP-3 from leaf SPE-separated F-5 were compared to the crude extracts and semi-purified fractions. The crude extract and semi-purified fractions showed the bands corresponding with PP-1, PP-2 and PP-3 under UV 254 nm, 365 nm and after derivatization by sulphuric reagent. In order to investigate the similarity in their identity of the three isolated constituents, they were evaluated on the same TLC plates in two different developing solvent systems (Figure 4.36; mobile phase: ethyl acetate: methanol: water (5%: 35%: 60%) and Figure 4.37; mobile phase: ethyl acetate: methanol: water (75%: 15%: 10%)). Different sequences of bands were observed for PP-1, PP-2, and PP-3, although they were very close to each other.

Figure 4.34: Specificity of the method for identification of active constituent from rhizome of *Paraboea paniculata*. Mobile phase: ethyl acetate: methanol: water (75%: 15%: 10%). Stationary phase: TLC Si 60 RP18 $F_{254}S$. (A) UV 254 nm. (B) 365 nm. (C) D: Sulphuric reagent, white light. From left to right: Track 1 to 2, Crude rhizome; Track 3 to 4, Rhizome SPE-separated fraction 4; Track 5 to 6, Compound PP-1.

Figure 4.35: Specificity of the method for identification of active constituents from leaf of *Paraboea paniculata*. Mobile phase: ethyl acetate: methanol: water (5%: 35%: 60%). Stationary phase: TLC Si 60 RP18 F_{254}S. (A) UV 254 nm. (B) 365 nm. (C) D: Sulphuric reagent, white light. From left to right: Track 1 to 2, Crude leaf; Track 3 to 4, Leaf SPE-separated fraction 5; Track 5 to 6, Compound PP-2; Track 7 to 8, Compound PP-3.

Figure 4.36: Comparison of isolated compounds from leaf and rhizome of *Paraboea paniculata*. Mobile phase: ethyl acetate: methanol: water (5%: 35%: 60%). Stationary phase: TLC Si 60 RP18 F_{254}S. (A) UV 254 nm. (B) 365 nm. (C) D: Sulphuric reagent, white light. From left to right: Track 1 to 2, Mixture of three compounds; Track 3 to 4, Compound PP-2; Track 5 to 6, Compound PP-3; Track 7 to 8, Compound PP-1. Note: Compound PP-1 is only detected after derivatization.

Figure 4.37: Comparison of isolated compounds from leaf and rhizome of *Paraboea paniculata*. Mobile phase: ethyl acetate: methanol: water (75%: 15%: 10%). Stationary phase: TLC Si 60 RP18 F_{254}S. (A) UV 254 nm. (B) 365 nm. (C) D: Sulphuric reagent, white light. From left to right: Track 1 to 2, Mixture of three compounds; Track 3 to 4, Compound PP-2; Track 5 to 6, Compound PP-3; Track 7 to 8, Compound PP-1. Note: Compound PP-1 is only detected after derivatization.
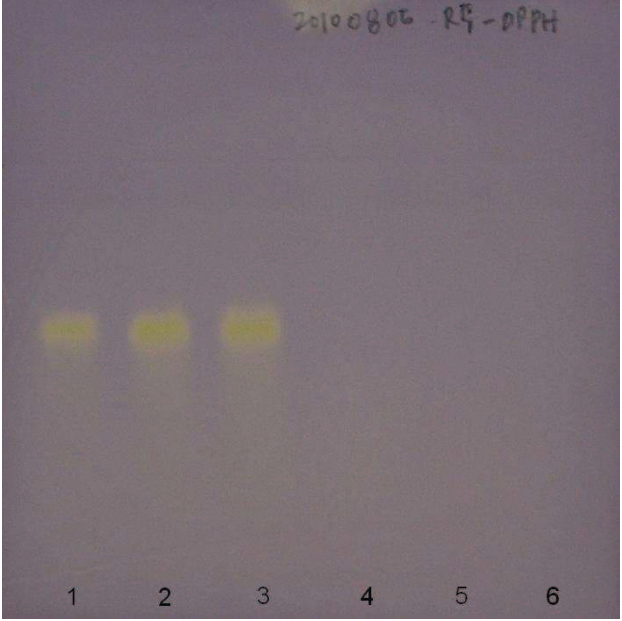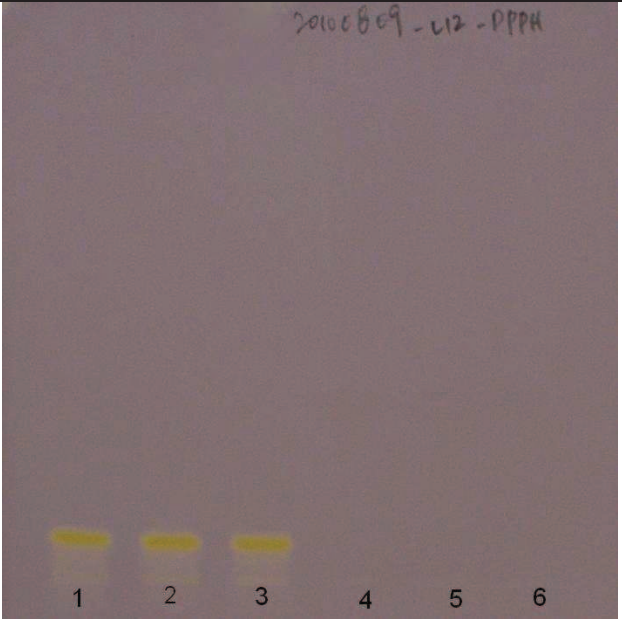
4.4 Determination of Radical Scavenging Activity by HPTLC-DPPH *in situ* Method

The DPPH free radical scavenging activity of the target fractions was determined by immersing the developed TLC plate into 0.05% solution of DPPH in methanol (Figure 4.38 to Figure 4.42). The fractions that suggested being active would be the fractions with yellow zones against violet background (Figures 4.39 and 4.40).

Figure 4.38: Screening of antioxidant activity of leaf and rhizome crude extract; curcumin as reference standard. Stationary phase: HPTLC Si 60 F_{254}. Mobile phase: ethyl acetate: methanol: water (75.27%: 13.98%: 10.75%). Under white light. From left to right: Track 1 to 2, Curcumin; Track 3 to 5, Leaf crude extract; Track 6 to 8, rhizome crude extract. No yellow bands observed on sample tracks.

Figure 4.39: Screening of antioxidant activity of leaf SPE-separated fraction 5 and rhizome SPE-separated fraction 5; quercitin as reference standard. Stationary phase: TLC Si 60 RP18 F_{254}S. Mobile phase: ethyl acetate: methanol: water (5%: 35%: 60%). Under white light. From left to right: Track 1 to 2, Quercitin; Track 3 to 5, leaf SPE-separated F-5; Track 6 to 8, rhizome SPE-separated F-5. Red bracket indicates the yellow zones observed.

Figure 4.40: Screening of antioxidant activity of rhizome SPE-separated fraction 4; quercitin as reference standard. Stationary phase: TLC Si 60 RP18 F_{254}S. Mobile phase: ethyl acetate: methanol: water (75%: 15%: 10%). Under white light. From left to right: Track 1 to 3, Quercitin; Track 4 to 6, rhizome SPE-separated F-4. Thin yellow bands observed in red bracket.

Figure 4.41: Screening of antioxidant activity of rhizome SPE-separated fraction 7; curcumin as reference standard. Stationary phase: TLC Si 60 RP18 F_{254}S. Mobile phase: ethyl acetate: methanol: water (40%: 35%: 35%). Under white light. From left to right: Track 1 to 3, Curcumin; Track 4 to 6, rhizome SPE-separated F-7. No yellow bands observed on sample tracks.

Figure 4.42: Screening of antioxidant activity of leaf SPE-separated fraction 12; curcumin as reference standard. Stationary phase: HPTLC Si 60 F_{254}. Mobile phase: hexane: acetone (70%: 30%). Under white light. From left to right: Track 1 to 3, Curcumin; Track 4 to 6, leaf SPE-separated F-12. No yellow bands observed on sample tracks.

4.5 Determination of Radical Scavenging Activity by Spectrophotometric DPPH Method

DPPH free radical scavenging assay was carried out to further determine the antiradical activity of the fractions. The crude extracts and SPE-separated fractions with the concentration of 50 µg/ml were screened, while quercitin and L-ascorbic acid were served as reference standard in the assay. Table 4.12 showed both the leaf and rhizome SPE-separated fractions 5 exhibited strong antiradical activity (84.46% and 79.69%), which are comparable to both reference standards.

Table 4.12: Percentage of inhibition of active cytotoxic fractions of *Paraboea paniculata* via DPPH-free radical scavenging assay.

Fractions assayed	Percentage of inhibition ± SD (%)
Quercitin (Reference standard)	**92.90 ± 0.11**
L-ascorbic acid (Reference standard)	**93.80 ± 0.06**
Leaf crude extract	34.40 ± 5.46
Rhizome crude extract	27.73 ± 6.20
Leaf SPE separated fraction 5	**84.46 ± 4.03**
Leaf SPE separated fraction 12	-8.22 ± 8.41
Rhizome SPE separated fraction 4	30.64 ± 2.08
Rhizome SPE separated fraction 5	**79.69 ± 10.26**
Rhizome SPE separated fraction 7	44.26 ± 8.76

DPPH free radical scavenging activity was expressed as percentage inhibition ± standard deviation value of three independent experiments.

4.6   Bioassay-Guided-Isolation of Active Cytotoxic Compounds from *Paraboea paniculata*

The former part of study in the establishment of fingerprint profile led to the isolation and identification of the active constituent(s) in *Paraboea paniculata*. The cytotoxic SPE-separated fractions 4 (F-4), 5 (F-5), and 7 (F-7) from rhizome and fractions 5 (F-5) and 12 (F-12) from leaf were investigated for the active constituents (Figure 4.43). The study on rhizome F-4 has afforded phenylethanoid glycosides, namely 3, 4-dihydroxyphenethyl-(3"-O-*β*-D-apiofuranosyl)-*β*-D-glucopyranoside (PP-1). As for leaf F-5, the study has yielded two known caffeoyl phenylethanoid glycosides (CPGs), namely 3,4-dihydroxyphenethyl-(3"-O-*β*-D-apiofuranosyl-4"-O-caffeoyl)-*β*-D-glucopyranoside (PP-2), and 3,4-dihydroxyphenethyl-(3"-O-*α*-L-rhamnopyranosyl-4"-O-caffeoyl)-*β*-D-glucopyranoside (PP-3). Since the rhizome F-5 has a similar peak profile as leaf F-5, both of the fractions could be presumed of having similar type of constituents. A total of 28.9 mg (1.28%) of leaf F-12 was obtained; it was identified as a mixture of phytosterols by gas chromatography analysis (Figure 4.44). As for rhizome F-7 (0.81%), due to its scarce amount in crude fraction, it was not subjected for further isolation.
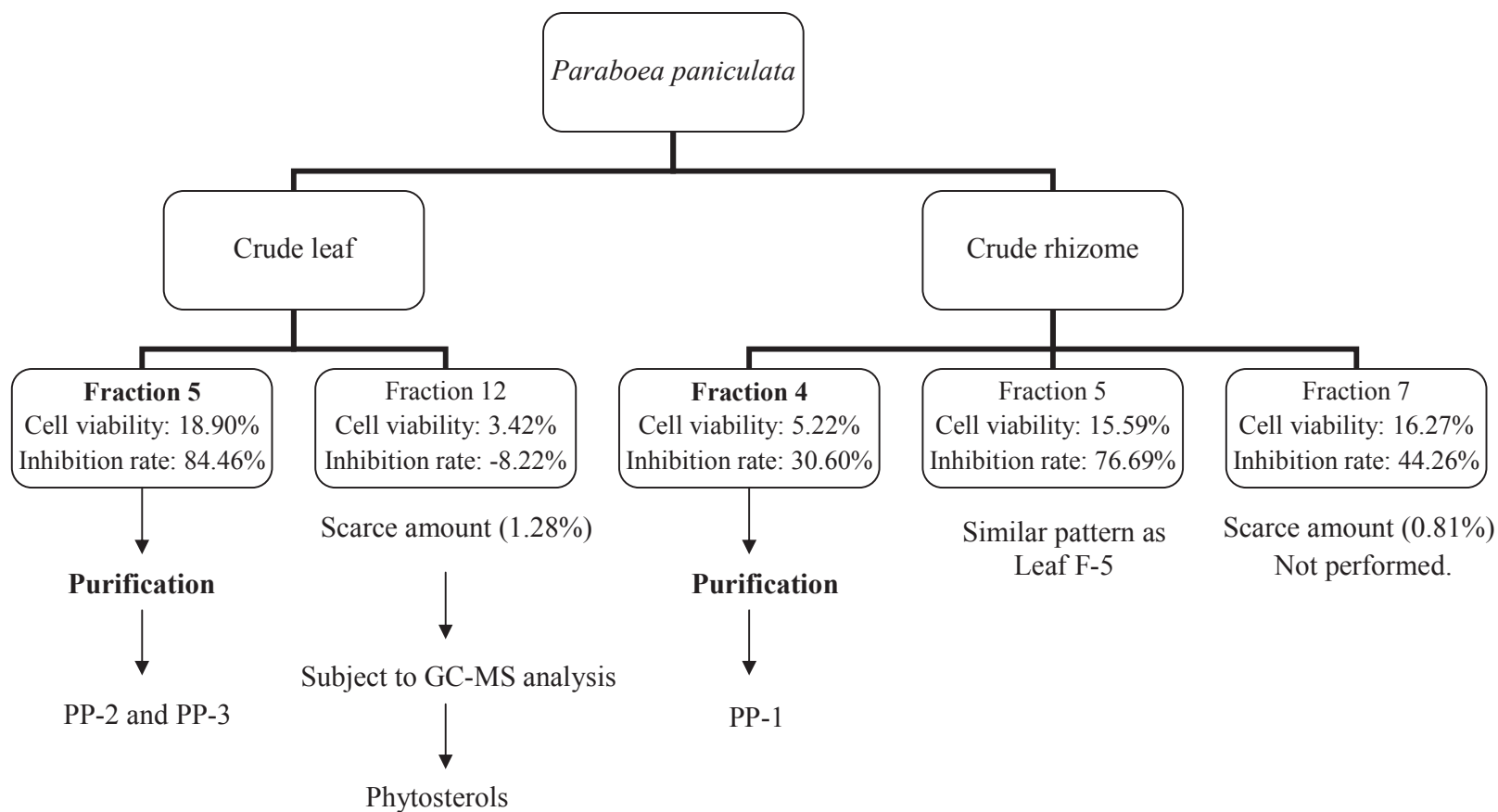
Figure 4.43: Flow chart of cytotoxic fractions of *Paraboea paniculata*.
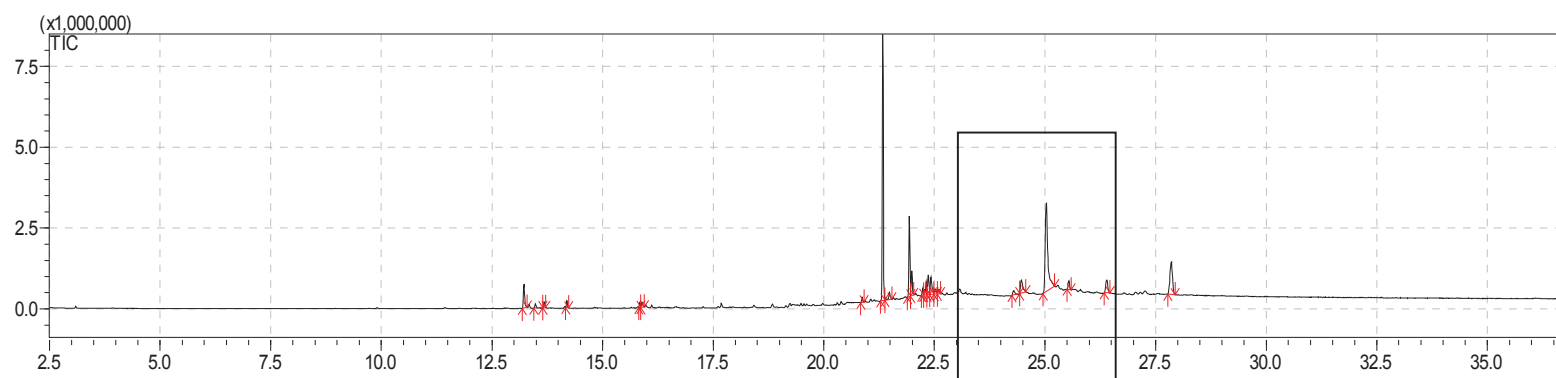
Figure 4.44a: Gas chromatography analysis of Leaf F-12.
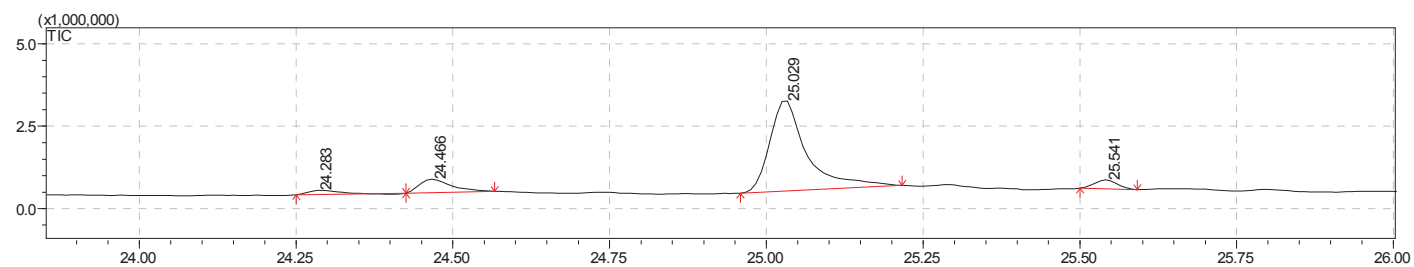
Figure 4.44b: Gas chromatography analysis of Leaf F-12 (extended view). RT (retention time) 24.466 = stigmasterol, and RT 25.029 = beta-sitosterol.
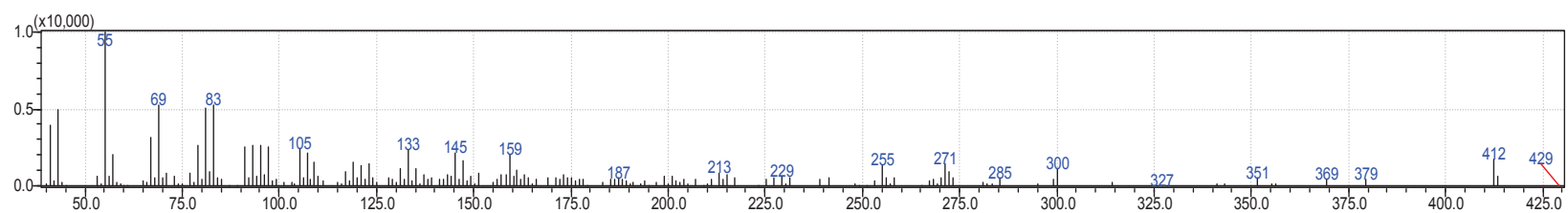
Figure 4.44c: Mass spectrum of stigmasterol (RT 24.466), with 91% of compound similarity.
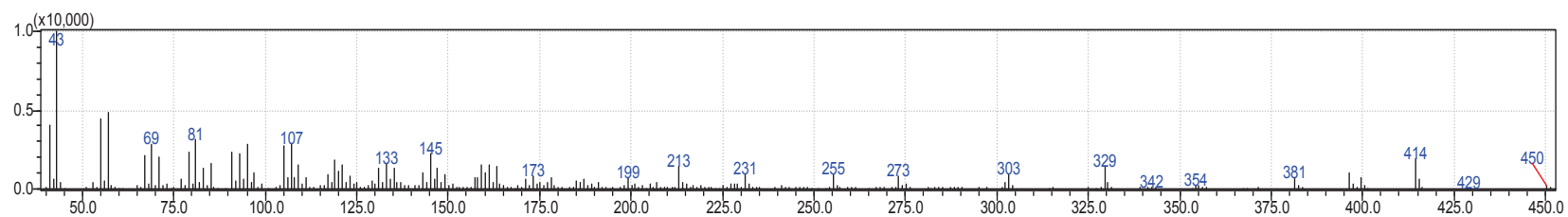
Figure 4.44d: Mass spectrum of beta-sitosterol (RT 25.029), with 92% of compound similarity.

4.6.1 Purification and Identification of 3, 4-Dihydroxyphenethyl-(3"-O-*β*-D-apiofuranosyl)-*β*-D-glucopyranoside (PP-1)

A total of 199 mg (9.95%) of rhizome F-4 was fractionated from crude rhizome extract eluted with a mixture of water: methanol (v/v, 4:1). The rhizome F-4 was subjected to semi-preparative HPLC separation and 5 sub-fractions were obtained (Figure 4.45). HPLC collected sub-fractions 4 and 5 were found to exhibit strong cytotoxic activity, with corresponding cell viability of 15.56% and 26.99% (Table 4.13). The sub-fraction 4 was subjected to second time of semi-preparative HPLC isolation (Figure 4.46), to yield pure compound of PP-1 (Figure 4.47). 24.7 mg of PP-1 (12.4%) was isolated in the form of white amorphous powder. The LC-mass spectrum gave a molecular ion peak at m/z 447 [M-H]$^-$ and dimeric signal at m/z 894.9 [2M-H]$^-$ in negative ion mode with calculated molecular weight of 448, corresponding to the molecular formula of $C_{19}H_{28}O_{12}$. Other fragment ion peaks were observed at 402, 315 [M-pentose]$^-$, 274, and 135 [315-hexose-H_2O]$^-$ (Figures 4.48 and 4.49). The UV-Vis spectrum exhibited absorption maxima at 197, 217, and 279 nm (Figure 4.50). Examination of the IR spectrum demonstrated bands at 3422 (hydroxyl groups), 2918 (C-H), 2848, 1637 (C=C), 1447, 1155 (C-O stretching), 1118, 1084, 1045, 1030, and 811 cm^{-1} (Figure 4.51).

The structural assignment was facilitated by ^{1}H NMR, ^{13}C NMR, HMQC and HMBC spectroscopic data (Figures 4.52, 4.53, 4.54, and 4.55). Analysis of signals in the ^{1}H-NMR spectrum of PP-1 revealed the presence of a 3, 4-

dihydroxyphenyl unit, and two sugar units. The three signals at δ 6.59 (dd, *J*=8.0, 1.8 Hz), δ 6.70 (d, *J*=8.0 Hz) and δ 6.69 (br. s) were attributed to protons H-6, H-5 and H-2, respectively in a 1, 3, 4-trisubstituted aromatic ring. The anomeric proton signal at δ 4.31 (d, *J*=7.9 Hz) indicated the presence of *β*-glucosyl unit, because of its resonance at 4.4 to 4.8 ppm and large coupling constant in range of 6 to 8 Hz (Agrawal, 1992; Ishii and Yanagisawa, 1998). Hu and Fan (2008) has reported the comparison of anomeric carbon signals in *α-D-*(δ 104.5) and *β-D-*apiofuranosides (δ 111.5), thus the second ring carbon was determined as *β-*apiosyl unit from its chemical shift of C-1' (δ 109.2). The HMBC correlation between proton H-1" (δ 4.31) and carbon C-8 (δ 70.9) shows the attachment of 3, 4-dihydroxyphenethoxy moiety to carbon C-1" of the central glucose unit. The HMBC correlation of the anomeric proton H-1' (δ 5.15) to the deshielded carbon C-3" (δ 82.6) of glucopyranoside, indicated the interglycosidic linkage between C-3" of glucose and C-1' of apiose sugar.

The structure assessment and comparison of spectral data with other literatures are summarized in Tables 4.15 to 4.16. 3, 4-Dihydroxyphenylethanol-8-O-[*β*-D-apiofuranosyl(1→3)]-*β*-D-glucopyranoside isolated from *Corallodiscus flabellata* (Zheng *et al.*, 2003) was found to possess structural similarity as compound PP-1. The difference of Cuneataside C (Chang and Case, 2005) and compound PP-1 is the attachment position of apiosyl unit to core glucose unit in the structure. The downfield shift of glucose C-6" signal (δ 69.8) of Cuneataside C indicated the 1→6 glycosidic bond between glucose and apiose. As for PP-1,

the downfield shift of C-3" signal (δ 82.6) and HMBC correlation suggested the glucose and apiose were linked through 1→3 glycosidic bond. Based on the data obtained, PP-1 was established as 3, 4-dihydroxyphenethyl-(3"-O-*β*-D-apiofuranosyl)-*β*-D-glucopyranoside (Figure 4.56).
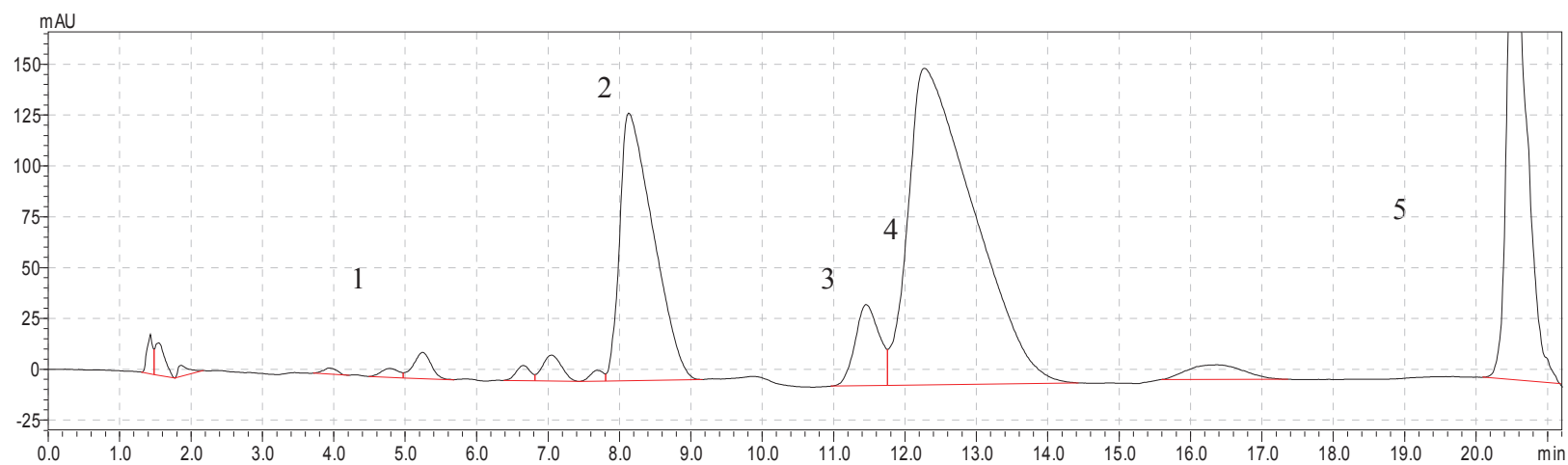
Figure 4.45: Semi-preparative high performance liquid chromatography analysis of rhizome F-4. Stationary phase: Chromolith RP-18 semi preparative column 100-10 mm. Mobile phase: 0-20 min (3% CH_3CN: 97% H_2O); 20-22 min (100% ACN). Flow rate: 4.0 ml/min. Spectral scans 210-800 nm.

Table 4.13: Cell viability of K-562 cell line after treated with five semi-preparative HPLC separated fractions of rhizome F-4 of *Paraboea paniculata* via MTT assay.

Sub-Fractions	Cell viability ± SD (%)
R-F4-1	75.79 ± 5.85
R-F4-2	85.95 ± 1.05
R-F4-3	56.48 ± 1.89
R-F4-4	**15.56 ± 5.71**
R-F4-5	26.99 ± 4.34
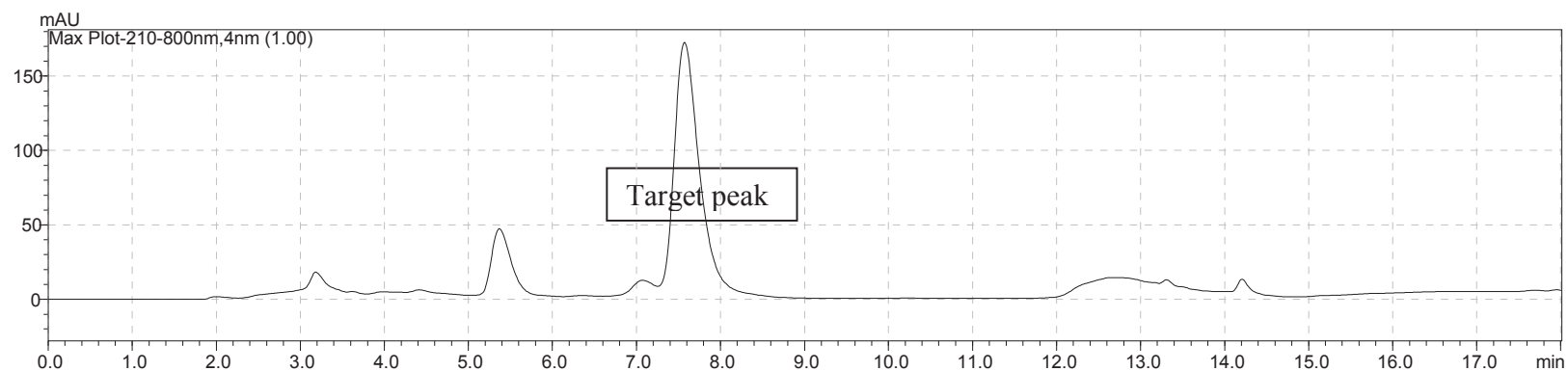
Figure 4.46: Second time of semi-preparative high performance liquid chromatography analysis of rhizome F-4 sub-fraction 4. Stationary phase: Chromolith RP-18 analytical column 100-4.6 mm. Mobile phase: 0-3 min (8% CH_3CN: 92% H_2O); 3-10 min (80% CH_3CN: 20% H_2O); 12.5-17 min (100% CH_3CN); 19-23 min (8% CH_3CN: 92% H_2O). Flow rate: 0.5 ml/min. Spectral scans 210 nm to 800 nm.
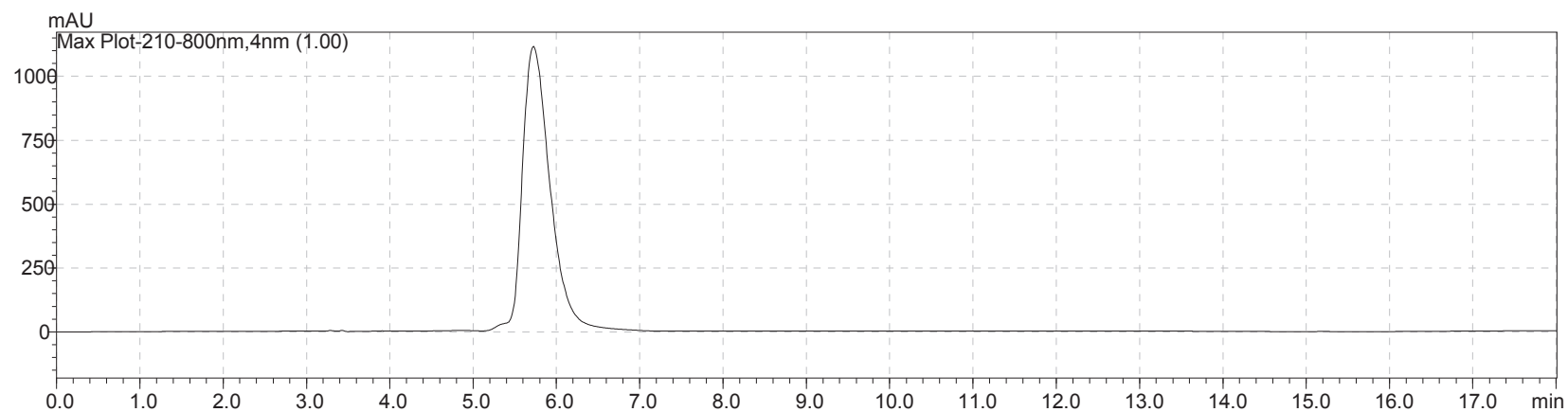
Figure 4.47: High performance liquid chromatography analysis of Compound PP-1. Stationary phase: Chromolith RP-18 analytical column 100-4.6 mm. Mobile phase: 0-3 min (8% CH₃CN: 92% H₂O); 3-10 min (80% CH₃CN: 20% H₂O); 12.5-15 min (100% CH₃CN); 15.5-18 min (8% CH₃CN: 92% H₂O). Flow rate: 0.5 ml/min. Spectral scans 210 nm to 800 nm. About 98% of peak purity was achieved.
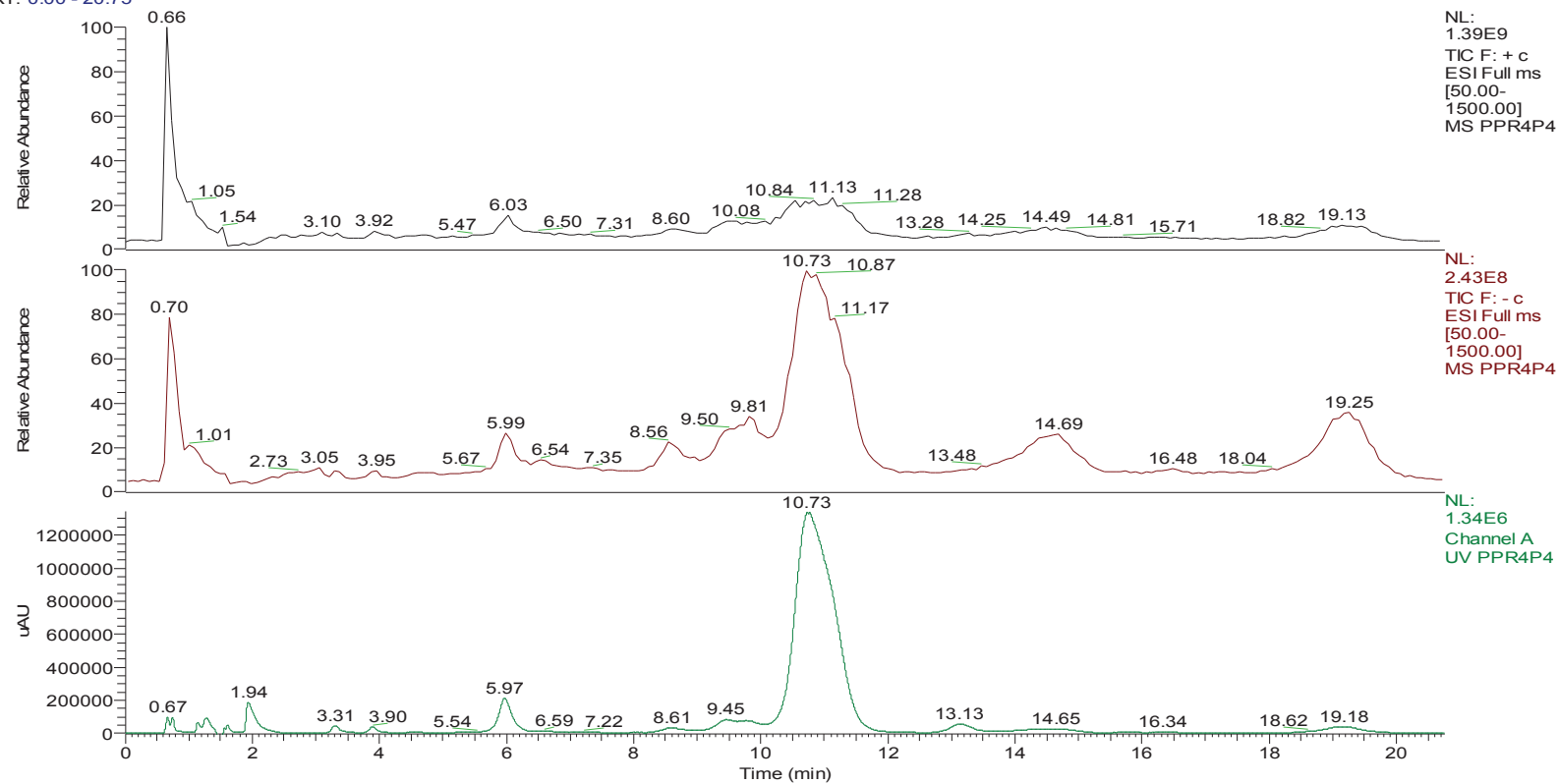
Figure 4.48: Liquid chromatography-mass spectroscopy analysis of Compound PP-1. (-)-ESI showed stronger peak signal than (+)-ESI does. From top to bottom: positive ion mode-ESI, negative ion mode-ESI, UV liquid chromatography.

PPR4P4 #269-276 RT: 10.80-11.02 AV: 4 SB: 5 7.31-7.67 NL: 1.12E8
F: - c ESI Full ms [50.00-1500.00]
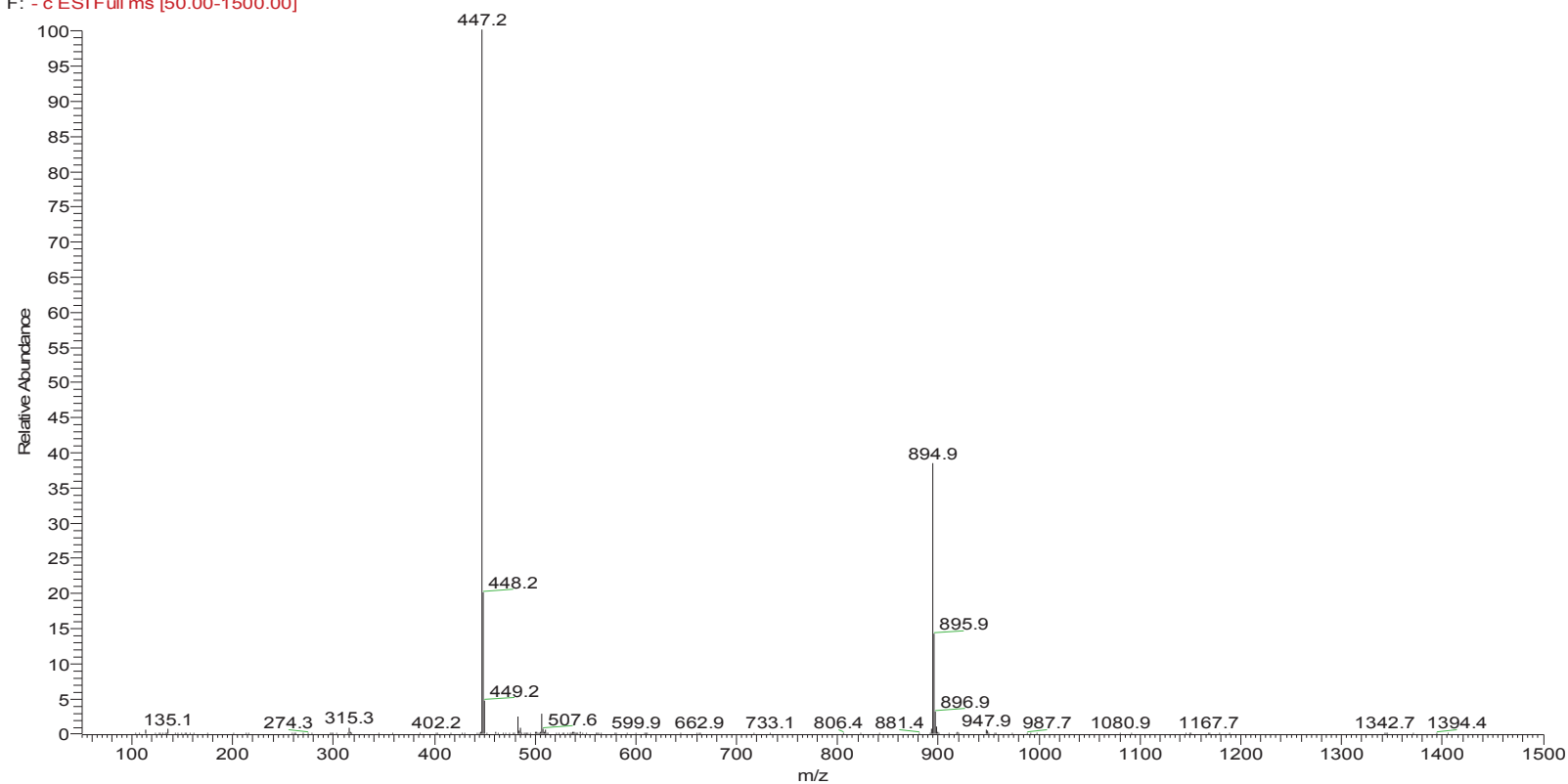
Figure 4.49: Mass spectrum of Compound PP-1, with a molecular ion peak at m/z 447 [M-H]⁻ and dimeric signal ion at m/z 894.9 [2M-H]⁻ in negative ion mode.
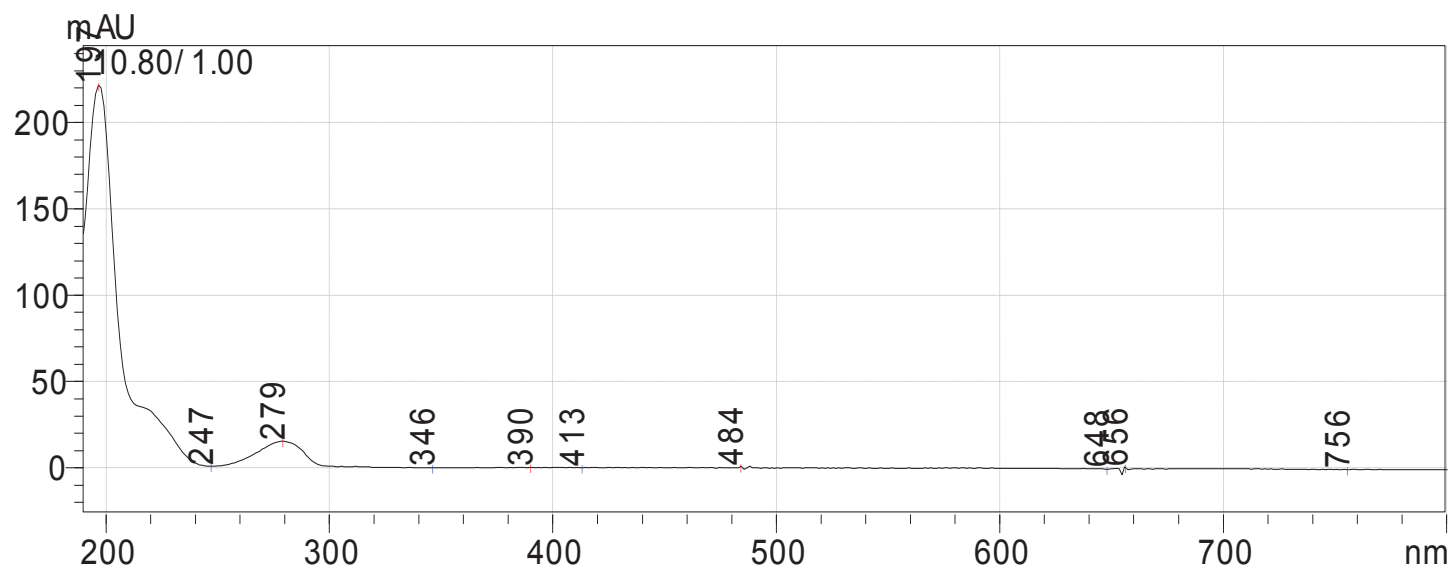
Figure 4.50: UV-Vis Spectrum of Compound PP-1.
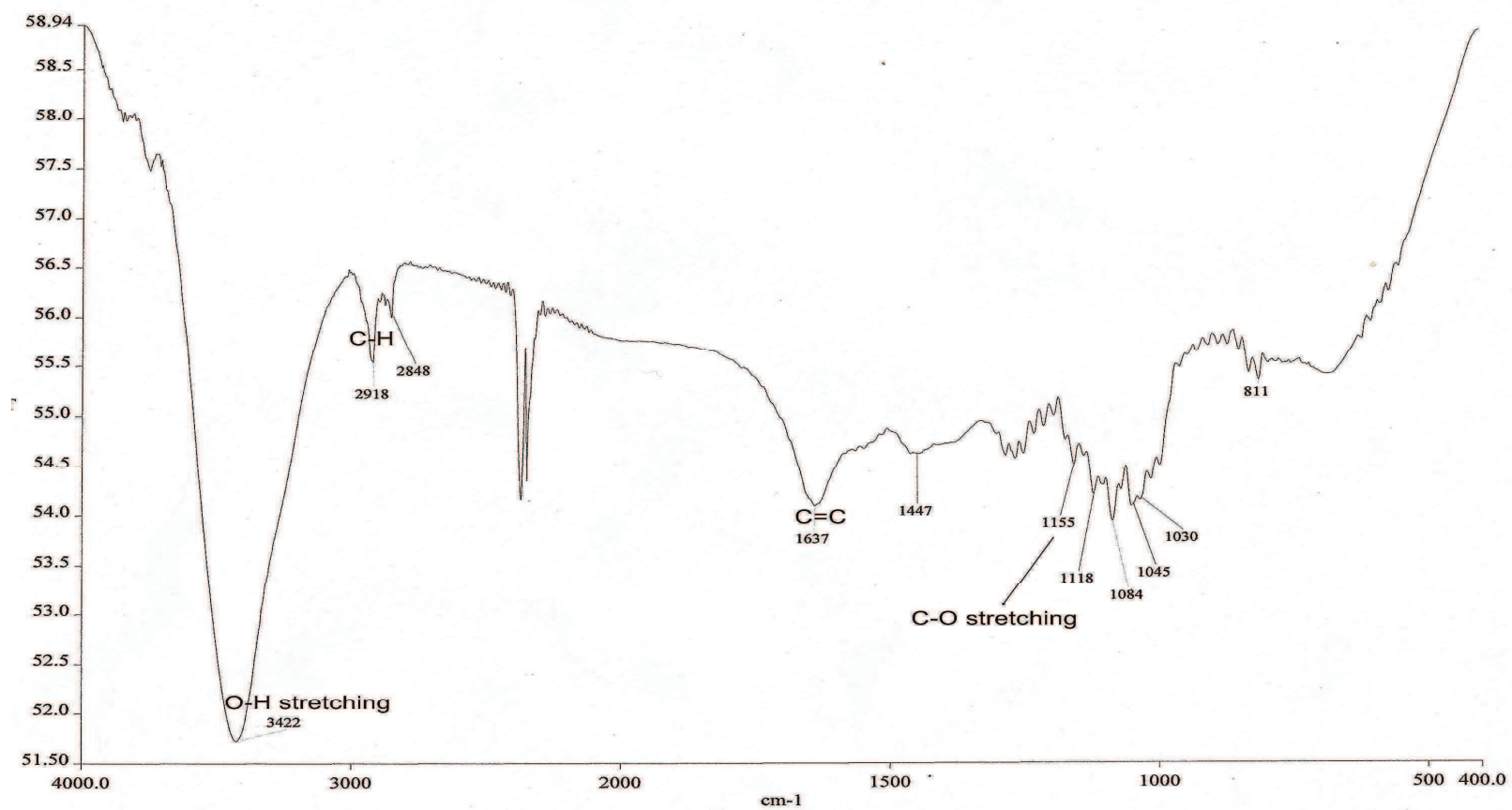
Figure 4.51: Infrared spectrum of Compound PP-1.
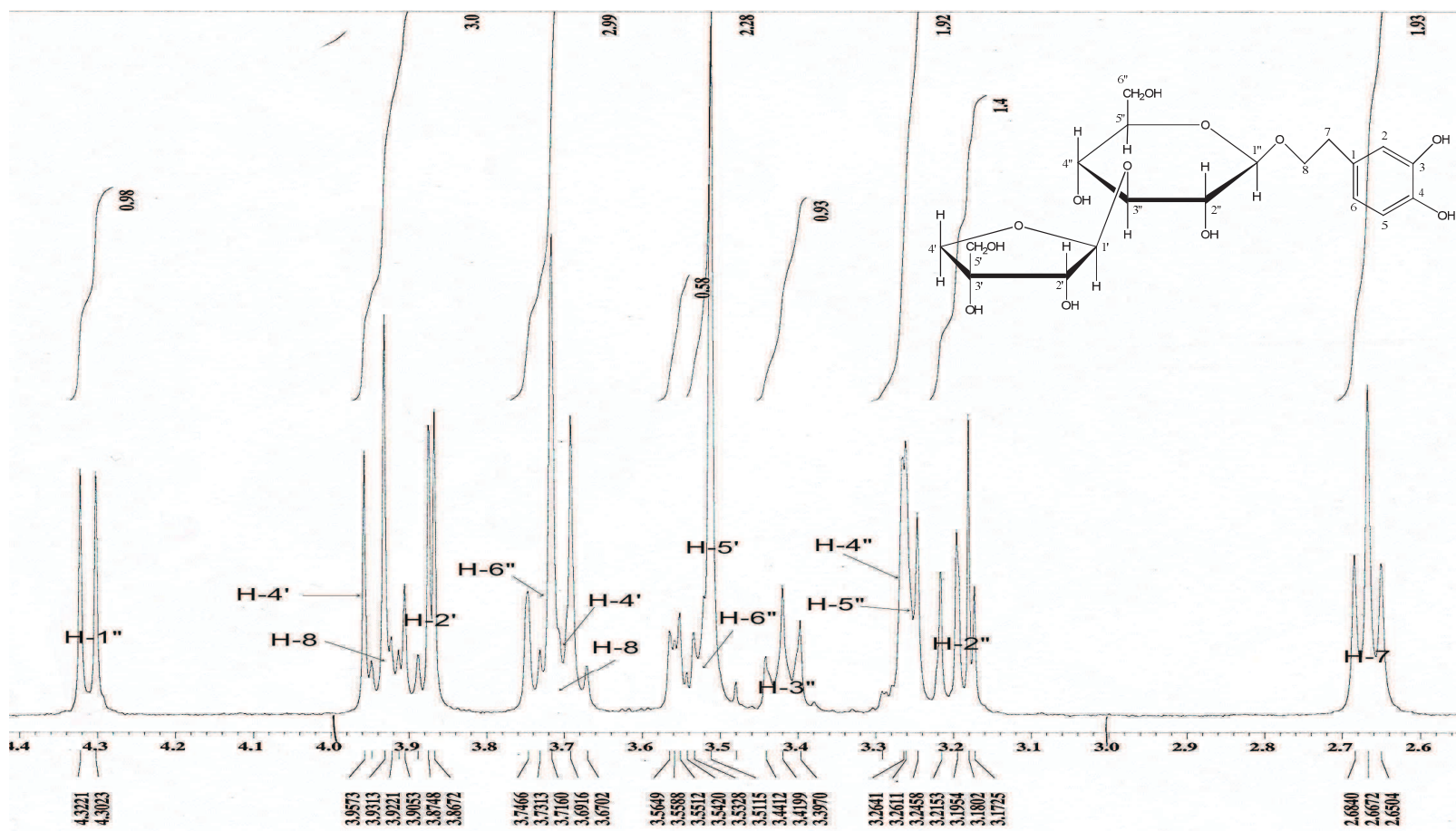
Figure 4.52 (a): Proton NMR spectrum of Compound PP-1.
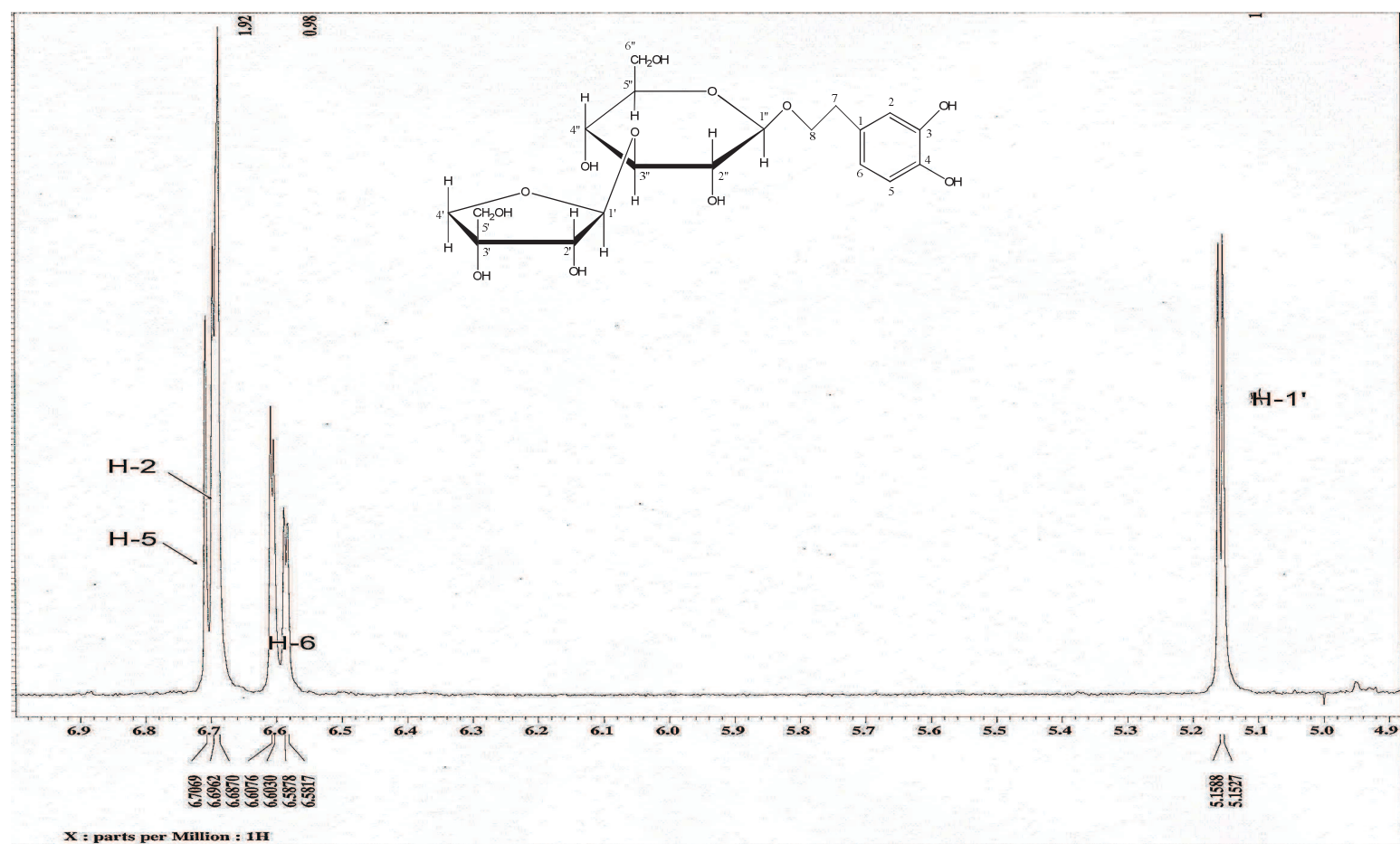
Figure 4.52 (b): Proton NMR spectrum of Compound PP-1.
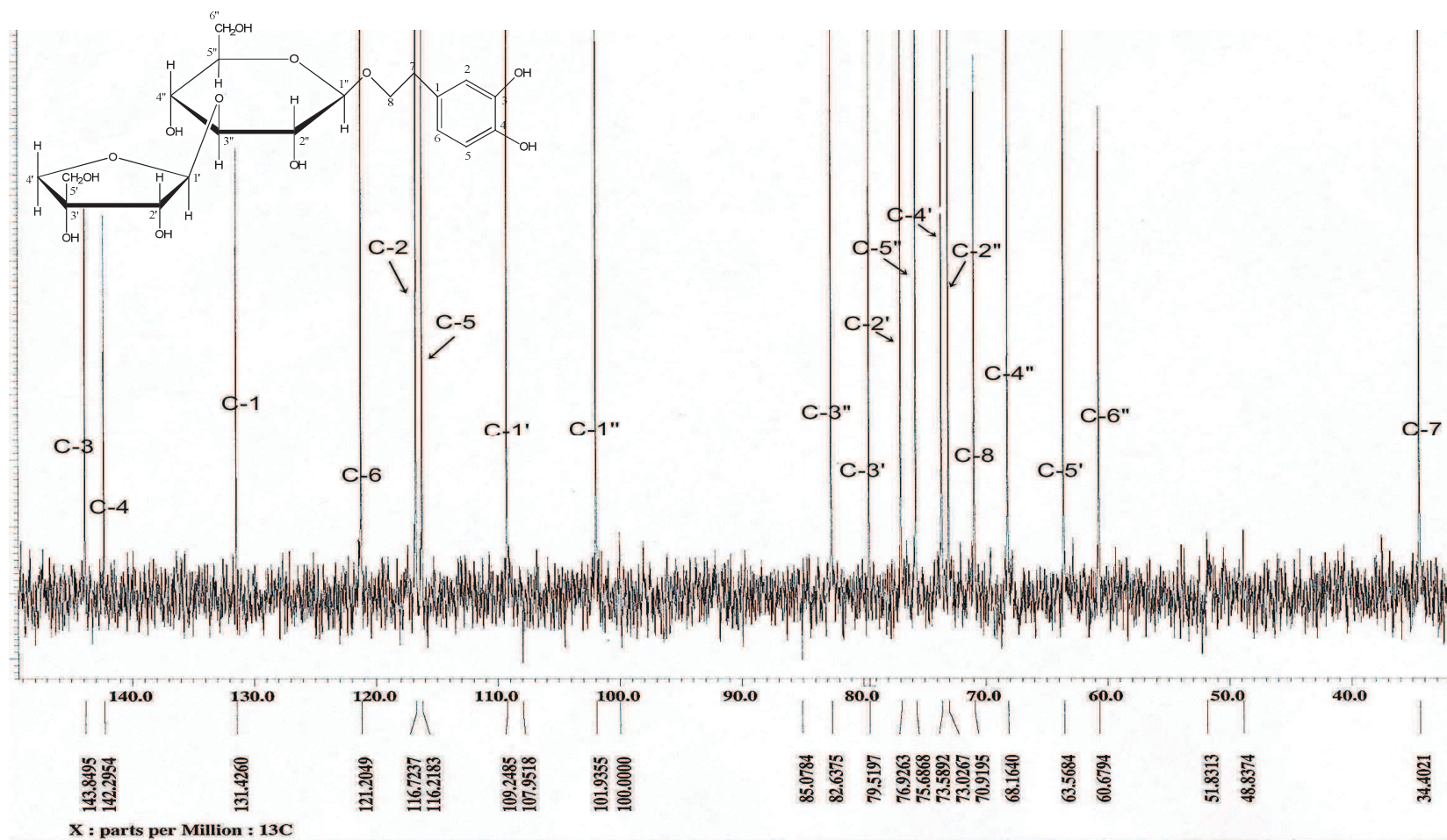
Figure 4.53: Carbon NMR spectrum of Compound PP-1.
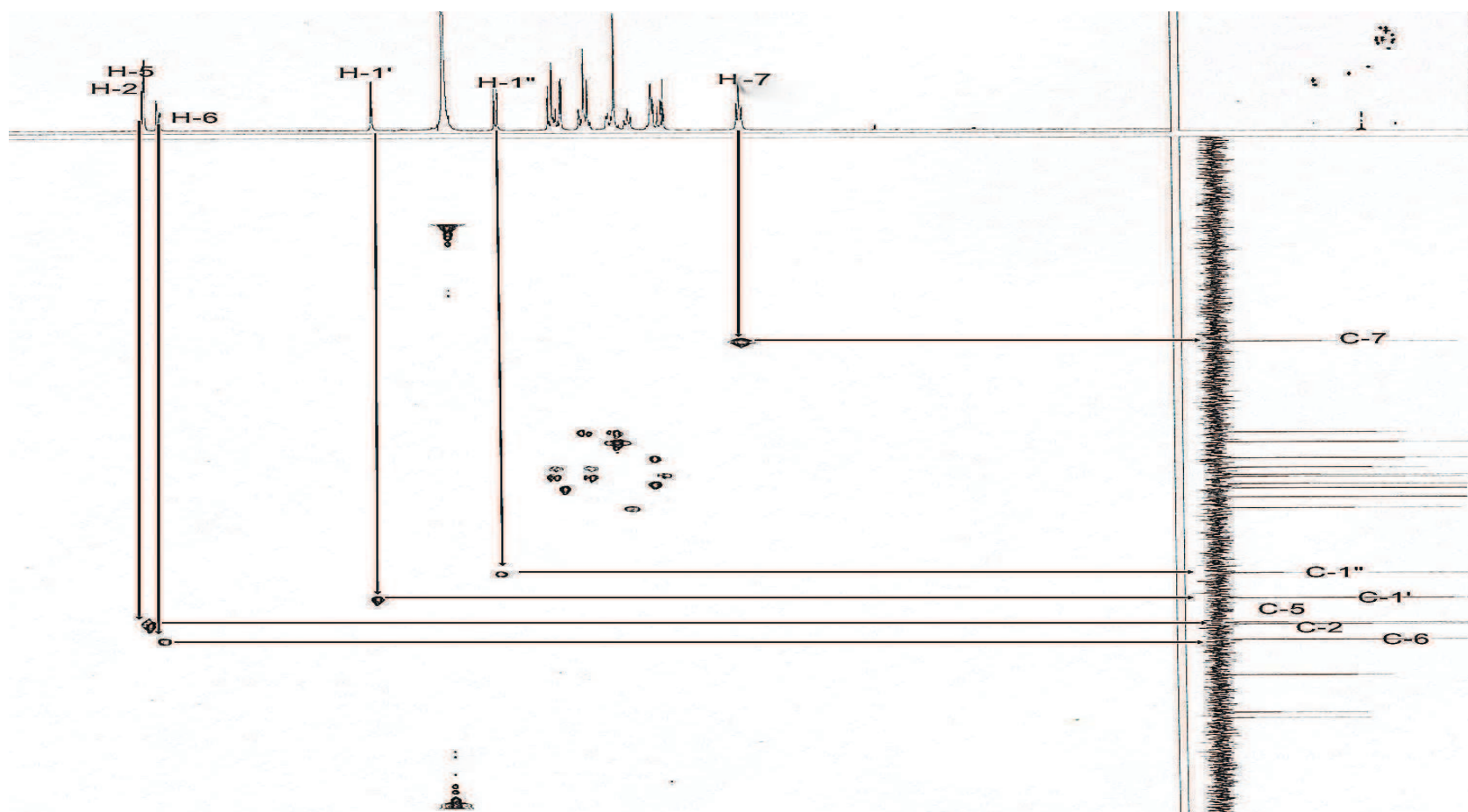
Figure 4.54: HMQC spectrum of Compound PP-1. Refer to Appendix C: Figures 7.9 (a, b) for enlarged spectra.
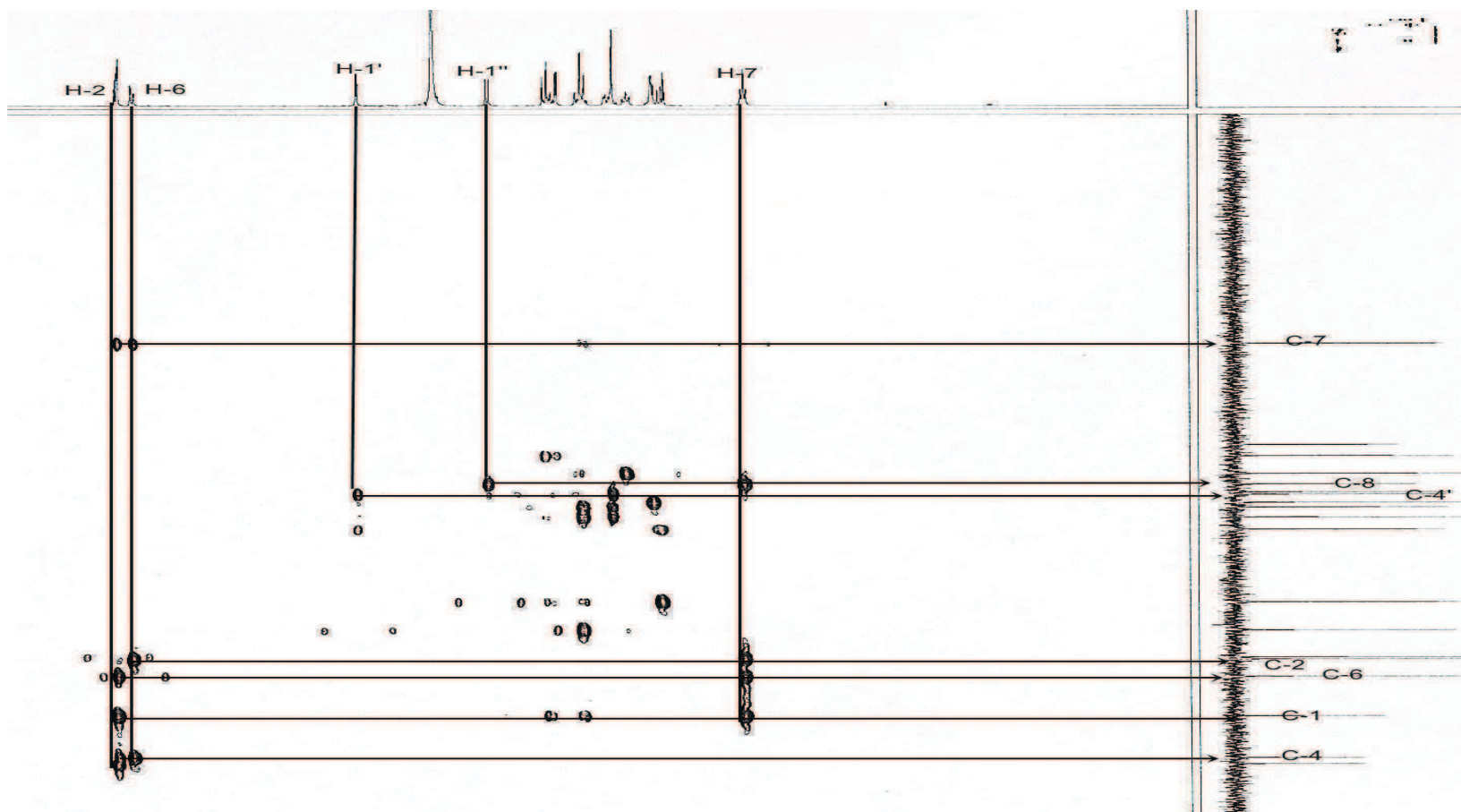
Figure 4.55: HMBC spectrum of Compound PP-1. Refer to Appendix C: Figures 7.10 (a-e) for enlarged spectra.

Table 4.14: Carbon and proton chemical shifts and HMBC correlation for PP-1.

	^{13}C NMR	^{1}H NMR	HMBC
		Aglycone	
C-1	131.4		
CH-2	116.7	6.69, br. s	C-1, C-4, C-6, C-7
C-3	143.8		
C-4	142.3		
CH-5	116.2	6.70, d (J=8.0)	C-3
CH-6	121.2	6.59, dd (J=8.0, 1.8)	C-2, C-4, C-7
CH$_2$-7	34.4	2.66, t (J=6.7)	C-1, C-2, C-6, C-8
CH$_2$-8	70.9	3.69-3.71; 3.92, m	C-1, C-1"
		Core sugar	
CH-1"	101.9	4.31, d (J=7.9)	C-8
CH-2"	73.0	3.17-3.19, m	C-1", C-3"
CH-3"	82.6	3.41, t (J=8.8)	C-4"
CH-4"	68.2	3.25-3.26, m	C-5"
CH-5"	75.7	3.21-3.25, m	
CH$_2$-6"	60.7	3.5; 3.6-3.7, m	
		Apiosyl unit	
CH-1'	109.2	5.15, d (J=2.7)	C-3", C-4'
CH-2'	76.9	3.87, d (J=2.7)	C-1'
C-3'	79.5	Quartenary C	
CH$_2$-4'	73.6	3.70; 3.94, m	C-2', C-3'
CH$_2$-5'	63.6	3.51, br. s	C-2', C-3', C-4'

Chemical shifts are in (δ) in ppm, multiplicities and coupling constant in Hz in parentheses.
Multiplicity caused by overlapping and poorly-resolved ^{1}H signals.

Table 4.15: Carbon chemical shifts of PP-1, 3,4-dihydroxyphenylethanol-8-O-[β-D-apiofuranosyl (1→3)]-β-D-glucopyranoside (Zheng *et al*., 2003), and Cuneataside C (Chang and Case, 2005).

	^{13}C NMR		
	PP-1	**3,4-dihydroxyphenylethanol-8-O-[β-D-apiofuranosyl (1-->3)]-β-D-glucopyranoside**	**Cuneataside C**
Aglycone			
C-1	131.4	132.1	131.5
CH-2	116.7	117.4	116.9
C-3	143.8	144.5	146.1
C-4	142.3	142.9	146.4
CH-5	116.2	116.9	118.1
CH-6	121.2	121.9	121.3
CH$_2$-7	34.4	35.1	37.0
CH$_2$-8	70.9	71.6	73.2
Core sugar			
CH-1"	101.9	102.6	104.5
CH-2"	73.0	73.7	75.2
CH-3"	82.6	83.3	78.0
CH-4"	68.2	68.8	71.9
CH-5"	75.7	76.3	77.2
CH$_2$-6"	60.7	61.3	69.8
Apiosyl unit			
CH-1'	109.2	109.9	111.0
CH-2'	76.9	77.6	79.1
C-3'	79.5	80.2	81.2
CH$_2$-4'	73.6	74.2	75.8
CH$_2$-5'	63.6	64.2	65.9

PP-1, 3, 4-dihydroxyphenylethanol-8-O-[β-D-apiofuranosyl (1→3)]-β-D-glucopyranoside and Cuneataside C (400 MHz for ^{1}H and 100 MHz for ^{13}C) were measured in D$_2$O.

Table 4.16: Proton chemical shifts of PP-1, 3, 4-dihydroxyphenylethanol-8-O-[β-D-apiofuranosyl (1→3)]-β-D-glucopyranoside (Zheng *et al.*, 2003), and Cuneataside C (Chang and Case, 2005).

	¹H NMR		
	PP-1	**3,4-dihydroxyphenylethanol-8-O-[β-D-apiofuranosyl (1-->3)]-β-D-glucopyranoside**	**Cuneataside C**
		Aglycone	
C-1			
CH-2	6.69 br. s	6.68 br. s	6.88 d(1.6)
C-3			
C-4			
CH-5	6.70 d(8.0)	6.70 d(8.0)	6.9 d(8.0)
CH-6	6.59 dd(8.0, 1.8)	6.57 d(8.0)	6.79 dd(8.0,1.6)
CH_2-7	2.66 t(6.7)	2.66 t(6.8)	2.85 t(6.8)
CH_2-8	3.69-3.71; 3.92 m	3.96; 3.68 m	3.89, 4.10 m
		Core sugar	
CH-1"	4.31 d(7.9)	4.29 d(8.0)	4.49 d(8.0)
CH-2"	3.17-3.19 m	3.19 t(8.8)	3.28 dd(9.0,8.0)
CH-3"	3.41 t(8.8)	3.51 t(9.6)	3.48 dd(9.1,9.0)
CH-4"	3.25-3.26 m	3.26 m	3.42 dd(9.4,9.1)
CH-5"	3.21-3.25 m	3.24 m	3.59 m
CH_2-6"	3.5; 3.6-3.7 m	3.74; 3.56 m	3.75 dd(11.5,6.2); 4.03 d(11.5)
		Apiosyl unit	
CH-1'	5.15 d(2.7)	5.15 d(2.8)	5.12 d(3.3)
CH-2'	3.87 d(2.7)	3.87 d(2.8)	4.01 d(3.3)
C-3'			
CH_2-4'	3.70; 3.94 m	3.70 br. s	4.07, 3.90 d(10.1)
CH_2-5'	3.51 br. s	3.42 br. s	3.68 s

Chemical shifts are in (δ) in ppm, multiplicities and coupling constant in Hz in parentheses.
PP-1, 3, 4-dihydroxyphenylethanol-8-O-[β-D-apiofuranosyl (1→3)]-β-D-glucopyranoside and Cuneataside C (400 MHz for ¹H and 100 MHz for ¹³C) were measured in D_2O.
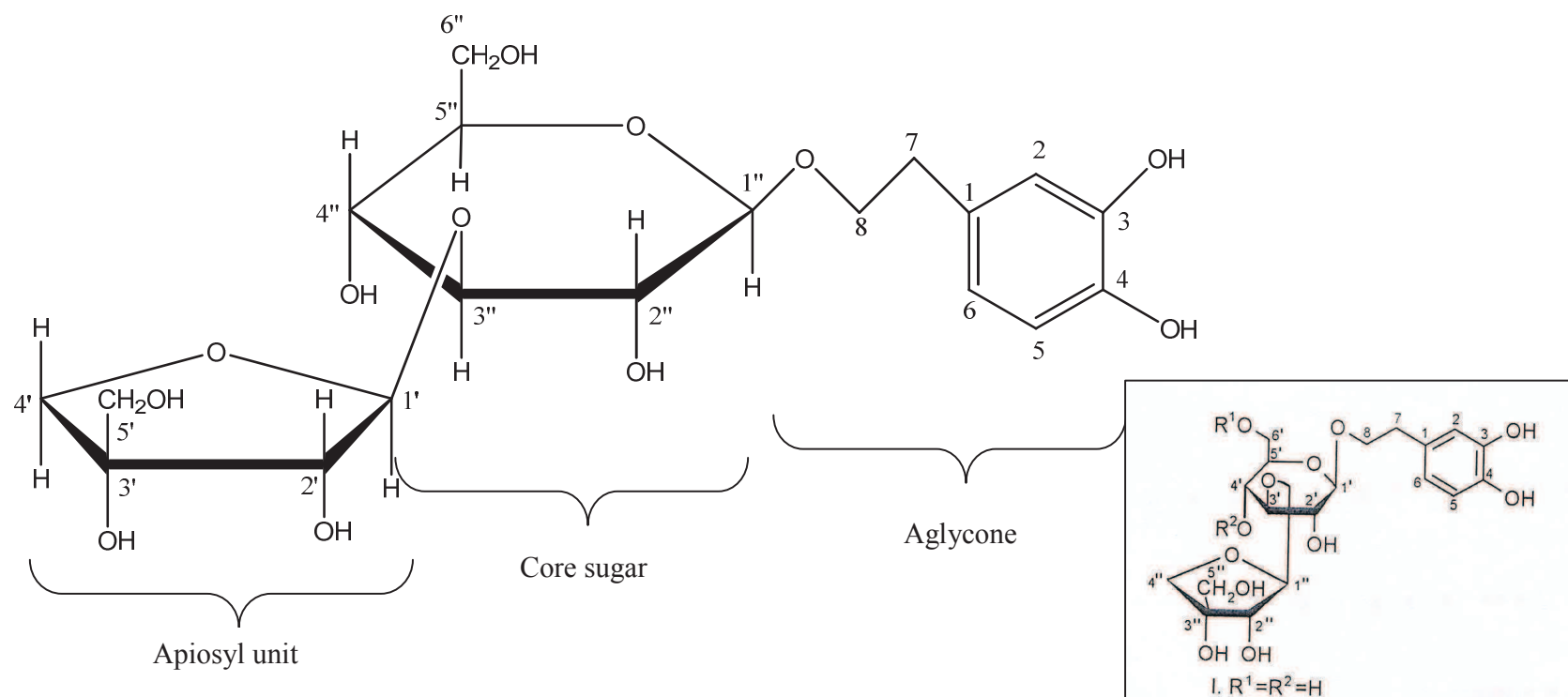
Figure 4.56: Molecular structure of PP-1, 3, 4-dihydroxyphenethyl-(3''-O-*β*-D-apiofuranosyl)-*β*-D-glucopyranoside. The structure on right bottom is 3, 4-dihydroxyphenylethanol-8-O-[β-D-apiofuranosyl (1→3)]-β-D-glucopyranoside isolated from *Corallodiscus flabellata* (Zheng *et al.*, 2003).

4.6.2 Purification and Identification of 3,4-Dihydroxyphenethyl-(3"-O-β-D-apiofuranosyl-4"-O-caffeoyl)-β-D-glucopyranoside (PP-2) and 3,4-dihydroxyphenethyl-(3"-O-α-L-rhamnopyranosyl-4"-O-caffeoyl)-β-D-glucopyranoside (PP-3)

A total of 764.8 mg (33.99%) of fraction 5 was fractionated from crude leaf extract at mixture of water: methanol (3:2). The leaf F-5 was subjected to semi-preparative HPLC separation and 4 sub-fractions were yielded (Figure 4.57). HPLC isolated sub-fractions 2 (PP-2) and 3 (PP-3) were exhibiting strong cytotoxic activity, with corresponding cell viability of 24.44% and 24.65% (Table 4.17).

49.5 mg of PP-2 (23.57%) was isolated from 210 mg of leaf F-5 in the form of brownish amorphous powder. The LC-mass spectrum showed a molecular ion peak at m/z 609 [M–H]$^-$ and dimeric signal at m/z 1218.9 [2M-H]$^-$ in negative ion mode with calculated molecular weight of 610, suggesting the molecular formula of $C_{28}H_{34}O_{15}$. Other fragment ion peaks were observed at 535, 448, 447 [M-caffeoyl unit-H]$^-$, 415, 315 [447-pentose]$^-$, 258, 162, 161 [315-aglycone-H$_2$O]$^-$, and 133 [315-hexose-H$_2$O-2H]$^-$ (Figures 4.59 and 4.60). Supporting evidence was obtained from the UV spectrum (Figure 4.61) with absorption maxima at 199, 217, and 329nm, which indicated the presence of aromatic moieties. Examination of the IR spectrum (Figure 4.62) demonstrated bands at 3423 (hydroxyl groups), 2929 (C-H), 1690 (C=O), 1623 (C=C), 1524 (aromatic ring), 1443, 1369, 1280, 1160 (C-O stretching), 1118, 1026, 809, and 668 cm^{-1}.

The signals in ^{1}H-NMR spectrum (Figure 4.63) of PP-2 revealed the presence of two aromatic rings, and two sugar units. Initial identification showed the common key features: signals (δ 6.6-7.1) for a set of ABX spin system and a set of AMX spin system as well as the presence of a methylene group (δ 2.81) and a carbonyl carbon (δ 167.7), suggesting the presence of a 3, 4-dihydroxyphenylethanol residue and a caffeoyl unit; two anomeric protons at δ 4.46 (d; J=8.0 Hz) and δ 5.29 (d; J=2.4 Hz), which assignable to β-glucosyl and β-apiosyl units, respectively. The coupling constant (J=15.9 Hz) between H-7''' and H-8''' of caffeoyl moiety suggested its *trans*-configuration. The glycosidic site was established by HMBC experiment in which the long-range correlation between H-1'' (δ 4.46) and C-8 (δ 71.1) was observed. H-4'' of glucose was shifted downfield (δ 4.89) indicating that C-4'' of glucose was singly bonded to the oxygen atom in the ester group of caffeoyl unit and this was further confirmed by the HMBC correlation between H-4'' and C-9''' (δ 167.7). The down-field shift of the glucose C-3'' signal (δ 80.8) indicated that glucose and apiose were linked through a 1$\rightarrow$3 glycosidic bond. The interglycosidc linkage was also determined through the HMBC correlation between C-3'' and H-1' (δ 5.29).

Figure 4.69 demonstrated the evaluation of proton NMR spectrum of PP-2, dissolved in (A) D_2O and CD_3OD (Figure 4.63) (B) CD_3SOCD_3 (Figure 4.67). The ^{1}H NMR of PP-2 that measured in D_2O and CD_3OD has the chemical shift of solvent signals at δ 4.8 and δ 4.87, which the solvent area has the possibility of masking the target signal. However, it was confirmed by examining the proton

NMR spectrum of PP-2 measured in CD_3SOCD_3, where the region of δ 4.4 to δ 5.2 was found to display only 3 groups of individual signals. The sugar region of ^{1}H NMR spectrum measured in CD_3SOCD_3 was overlapped by a large moisture signal, which has restricted the spectrum analysis.

A comparison of the ^{1}H and ^{13}C NMR spectral data of PP-2 with the literature data reported (Tables 4.19 and 4.20), points to its high similarity to calceoralarioside E (Damtoft *et al*., 1993), nuomioside A (Kasai *et al*., 1991), and cusianoside A (Tanaka *et al*., 2004). However, an α-apiosyl unit was seen in cusianoside A instead of β-apiosyl unit as in calceoralarioside E, nuomioside A, and PP-2. The stereochemistry of anomeric carbon of the apiosyl moiety of cusianoside A was in α-configuration as observed from its singlet proton signal (δ 5.25, s). As stated by Ishii and Yanagisawa (1998), anomeric protons of α-glycosides resonate at lowest field with coupling constant close to 1 Hz. On the basis of these data, the structure of PP-2 was established as 3,4-dihydroxyphenethyl-(3''-O-*β*-D-apiofuranosyl-4''-O-caffeoyl)-*β*-D-glucopyranoside (Figure 4.70).
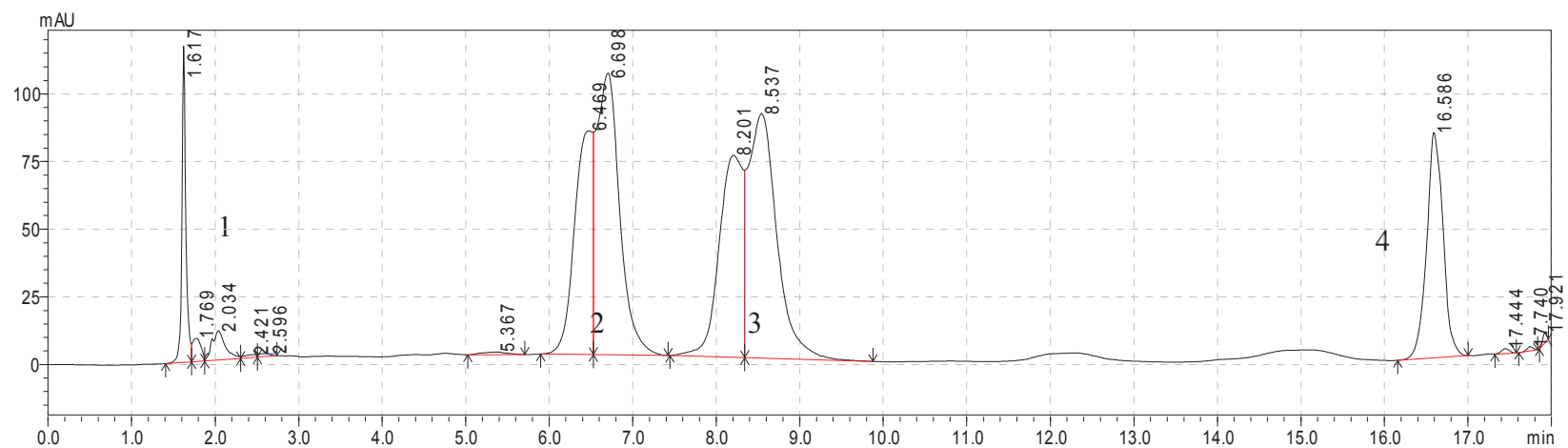
Figure 4.57: Semi-preparative high performance liquid chromatography analysis of leaf F-5. Stationary phase: Chromolith RP-18 semi-preparative column 100-10 mm. Mobile phase: 0-13 min (15% CH₃CN: 85% H₂O); 13-18 min (100% CH₃CN). Flow rate: 4.0 ml/min. Spectral scan 210-800 nm.

Table 4.17: Cell viability of K-562 cell line after treated with four semi-preparative HPLC separated fractions of leaf F-5 of *Paraboea paniculata* via MTT assay.

Sub-Fractions	Cell viability ± SD (%)
L-F5-1	62.32 ± 0.86
L-F5-2	24.44 ± 2.55
L-F5-3	24.65 ± 7.85
L-F5-4	28.98 ± 2.09
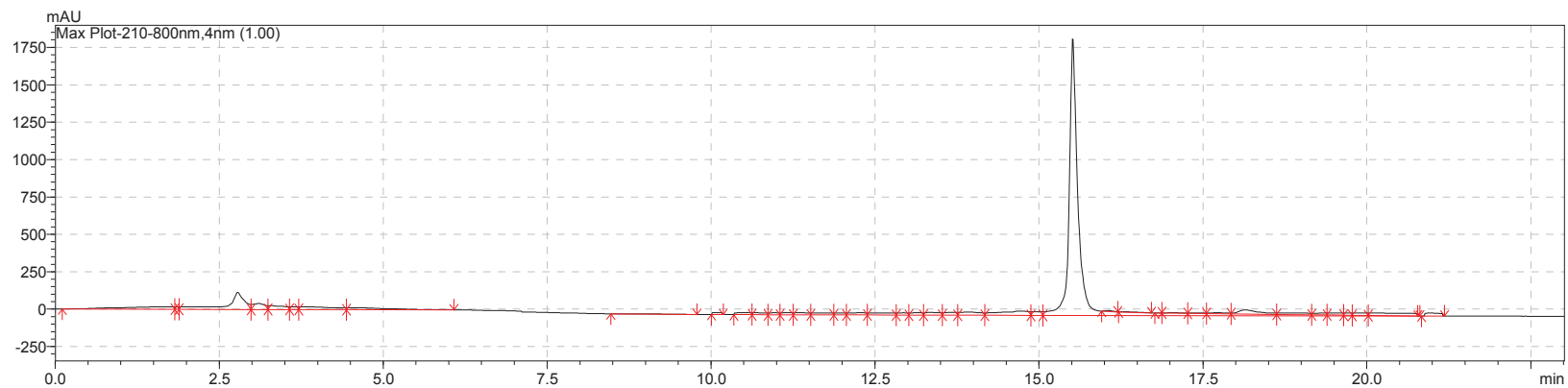
Figure 4.58: High performance liquid chromatography analysis of Compound PP-2. Stationary phase: Chromolith RP-18 analytical column 100-4.6 mm. Mobile phase: 0-7 min (7% CH_3CN: 93% H_2O); 7-10 min (20% CH_3CN: 80% H_2O); 10-15 min (35% CH_3CN: 65% H_2O); 15-17 min (60% CH_3CN: 40% H_2O); 17-23 min (7% CH_3CN: 93% H_2O). Flow rate: 0.6 ml/min. Spectral scan 210 nm to 800 nm. About 89% of peak purity was achieved.
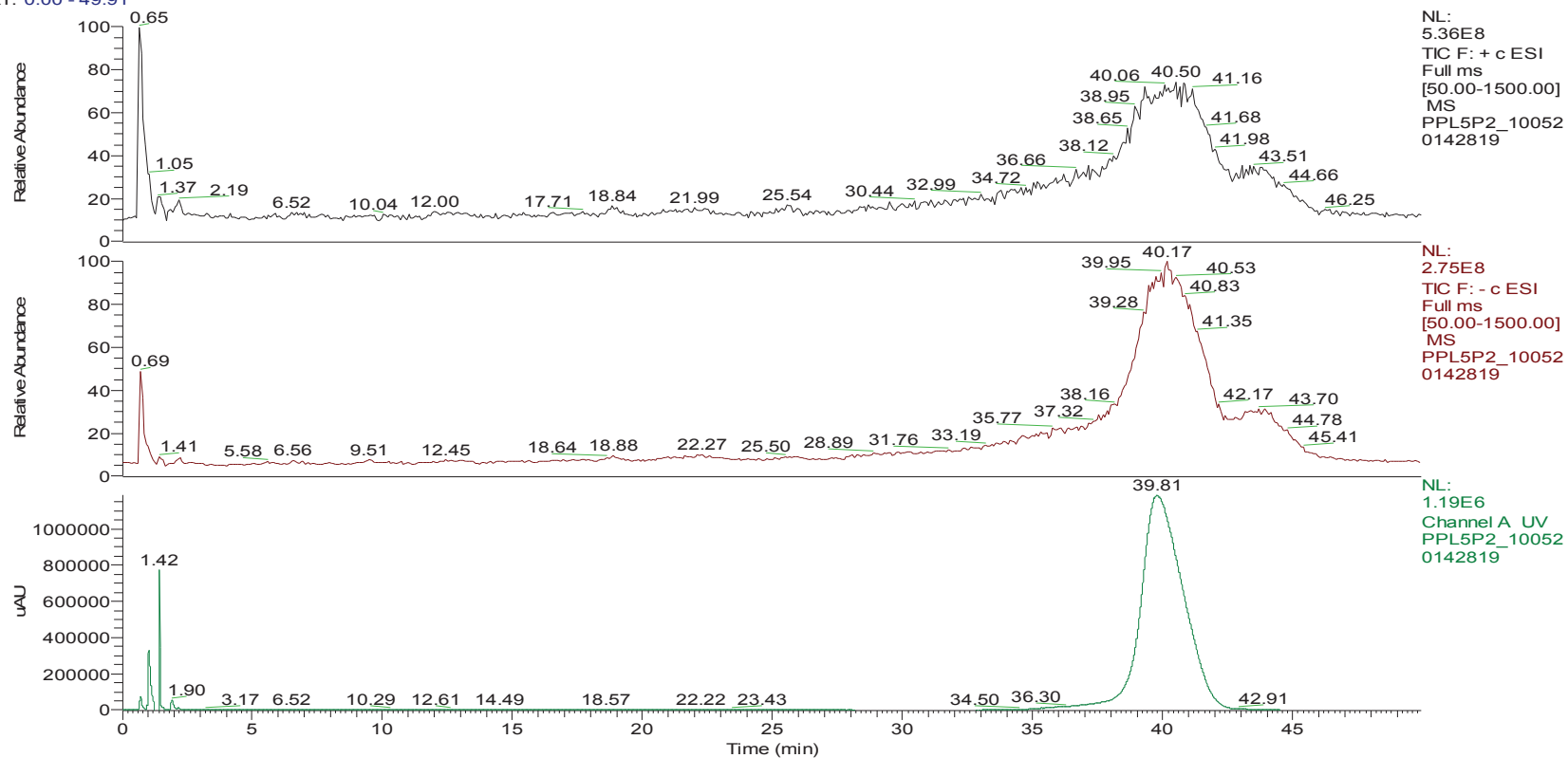
Figure 4.59: Liquid chromatography-mass spectroscopy analysis of Compound PP-2. (-)-MS showed stronger peak signal than (+)-MS does. From top to lowest: positive ion mode-ESI, negative ion mode-ESI, UV liquid chromatography.
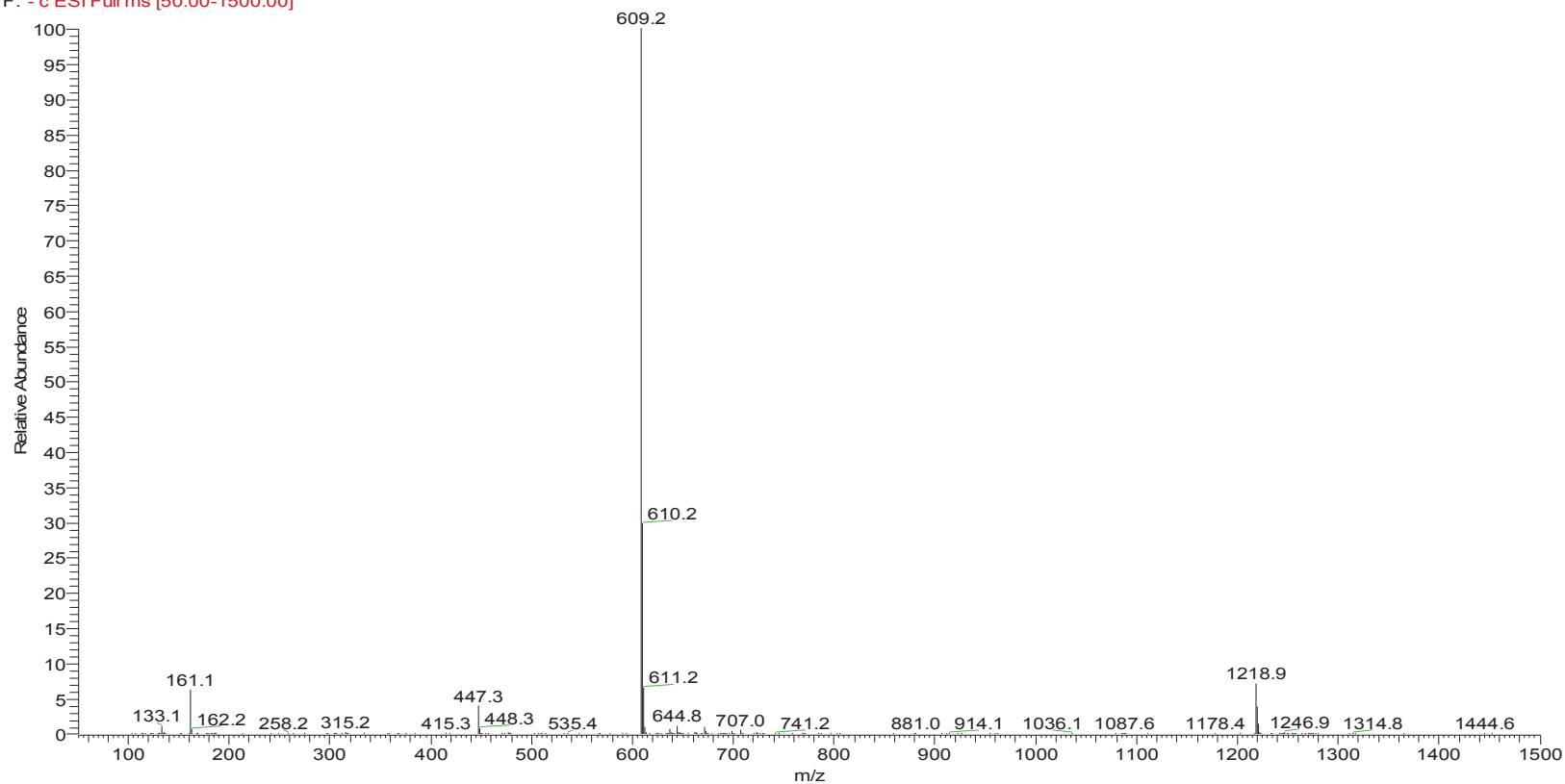
Figure 4.60: Mass spectrum of Compound PP-2, with a molecular ion peak at m/z 609 [M–H]⁻ and dimeric signal ion at m/z 1218.9 [2M-H]⁻ in negative ion mode.
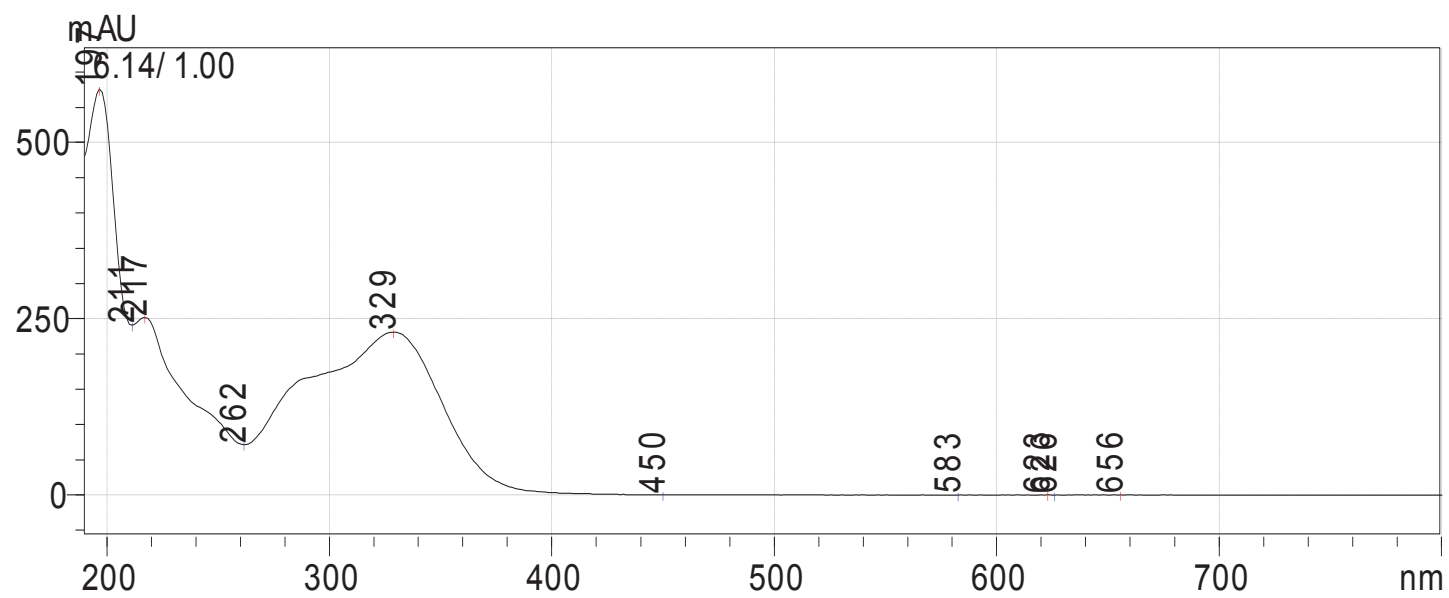
Figure 4.61: UV-Vis spectrum of PP-2.
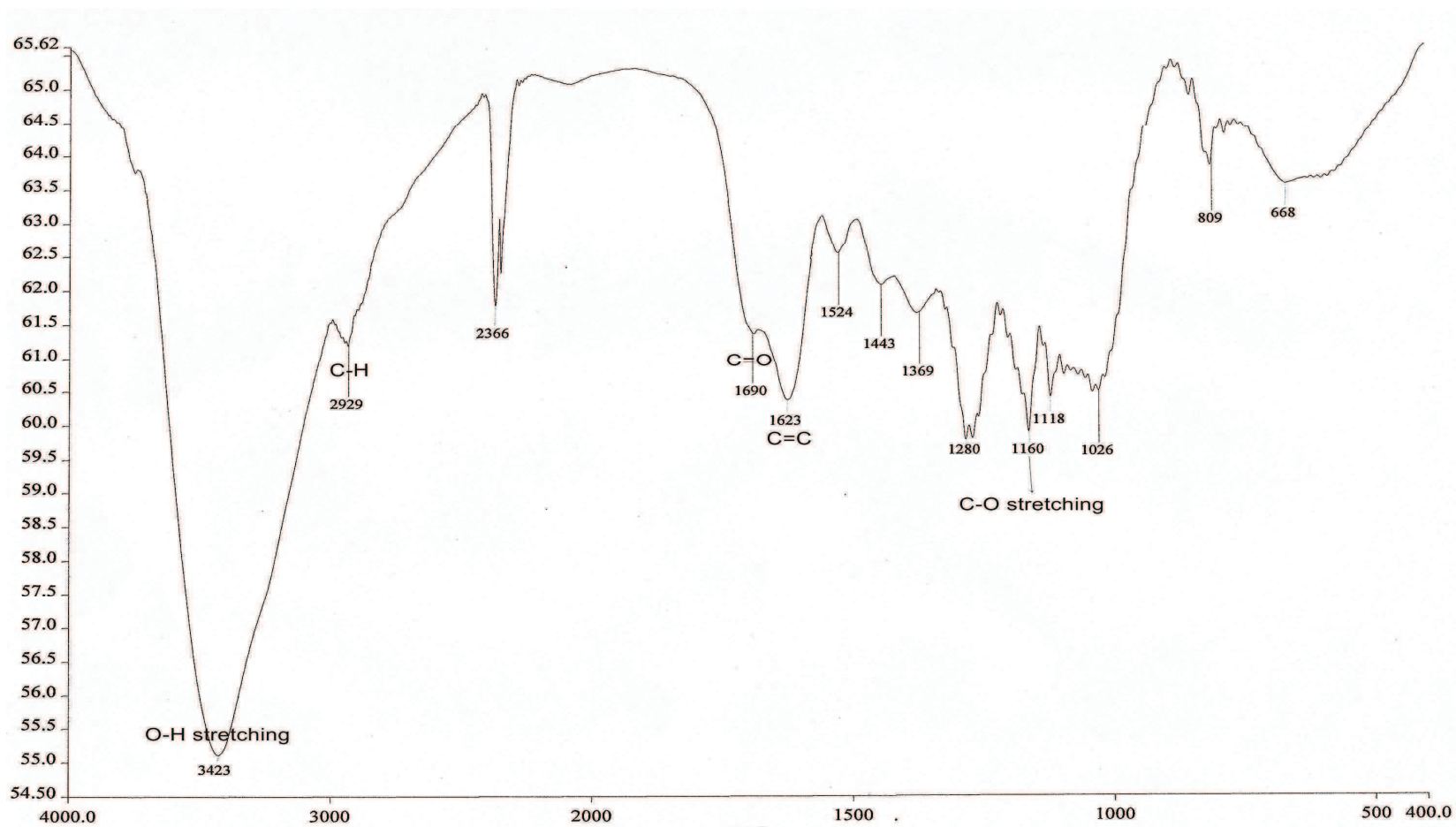
Figure 4.62: Infrared spectrum of Compound PP-2.
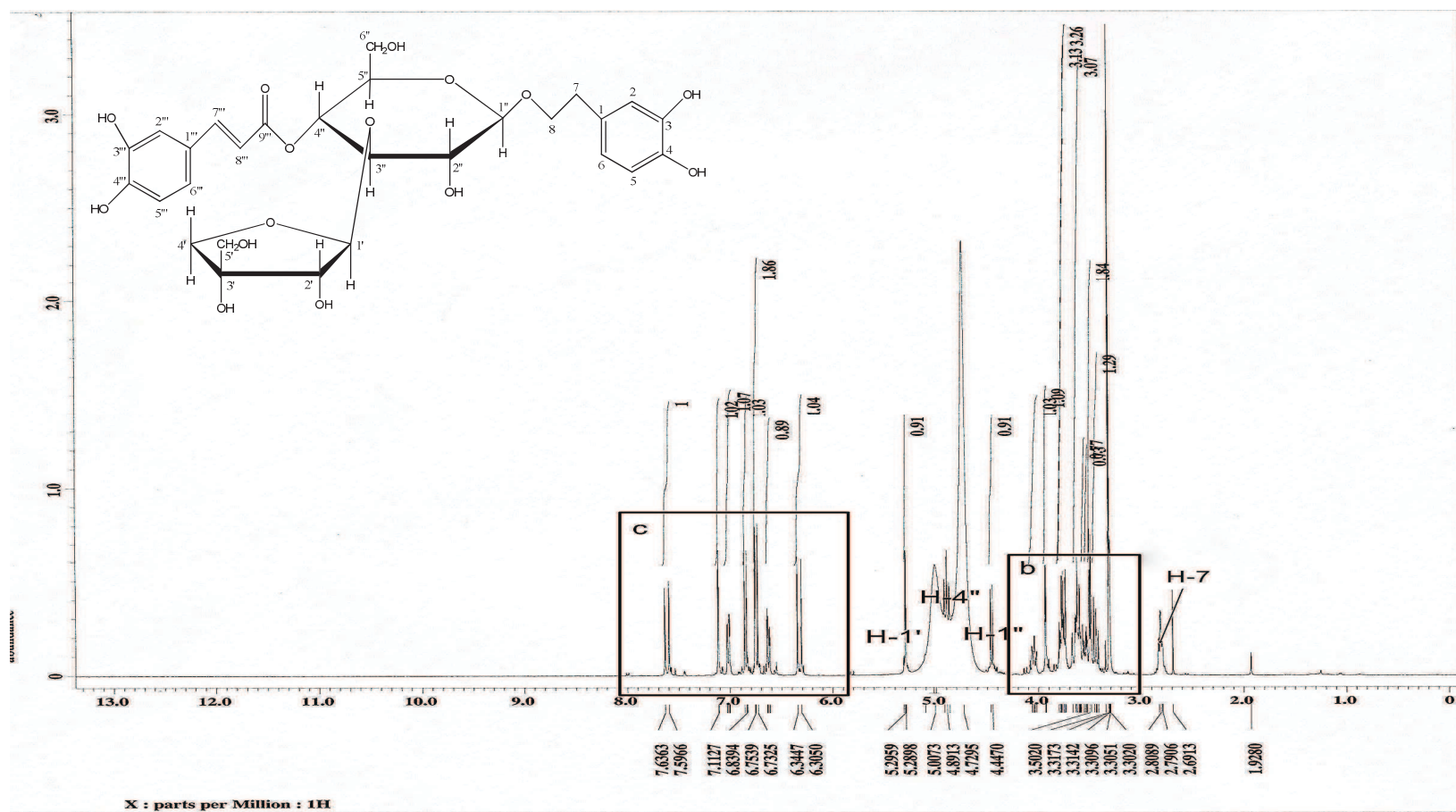
Figure 4.63 (a): Proton NMR spectrum of Compound PP-2 (measured in D_2O and CD_3OD). Please refer to following figures (b) and (c) for enlarged spectra.
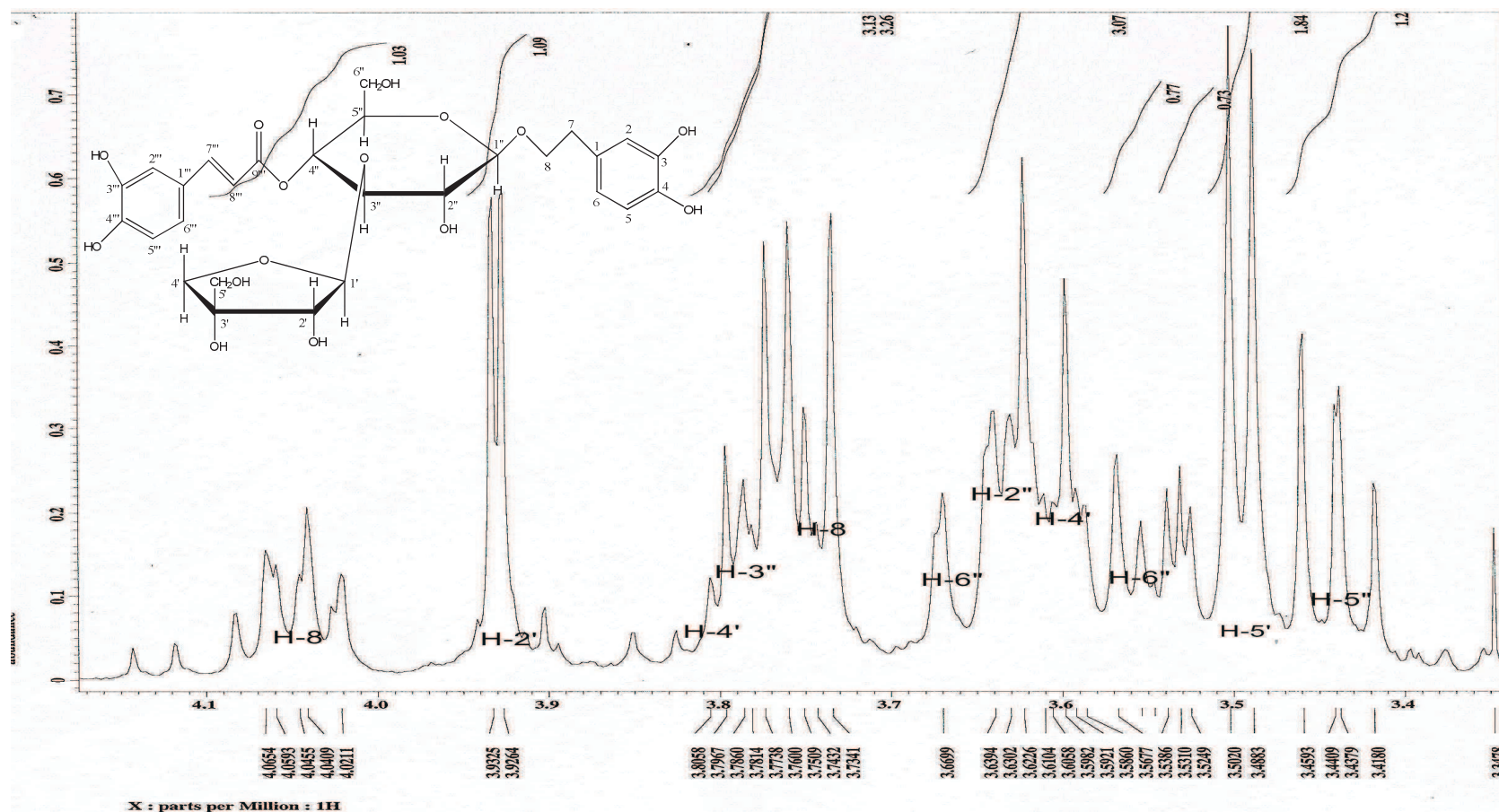
Figure 4.63 (b): Proton NMR spectrum of Compound PP-2 (measured in D_2O and CD_3OD) (extended view).
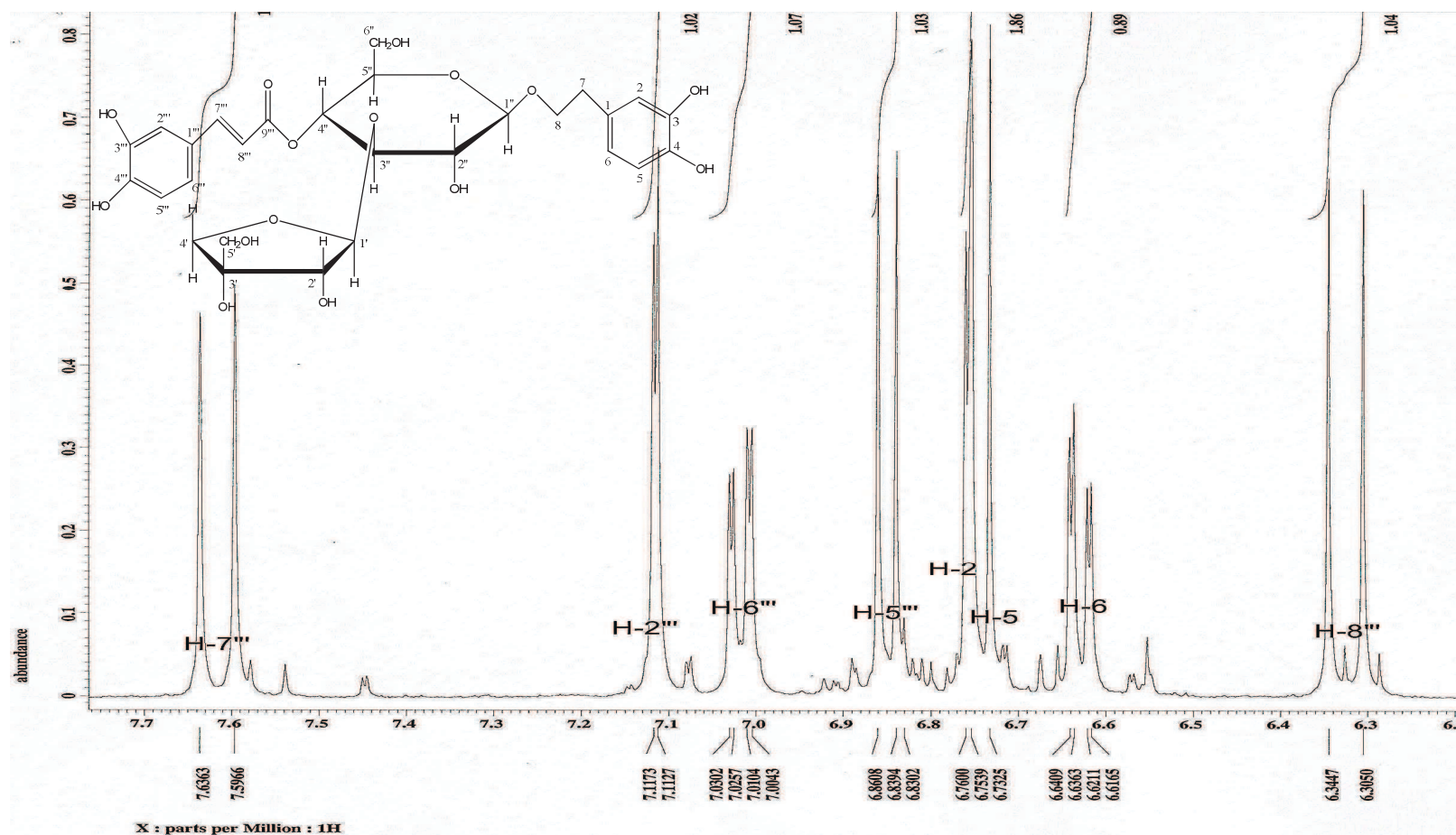
Figure 4.63 (c): Proton NMR spectrum of Compound PP-2 (measured in D$_2$O and CD$_3$OD) (extended view).
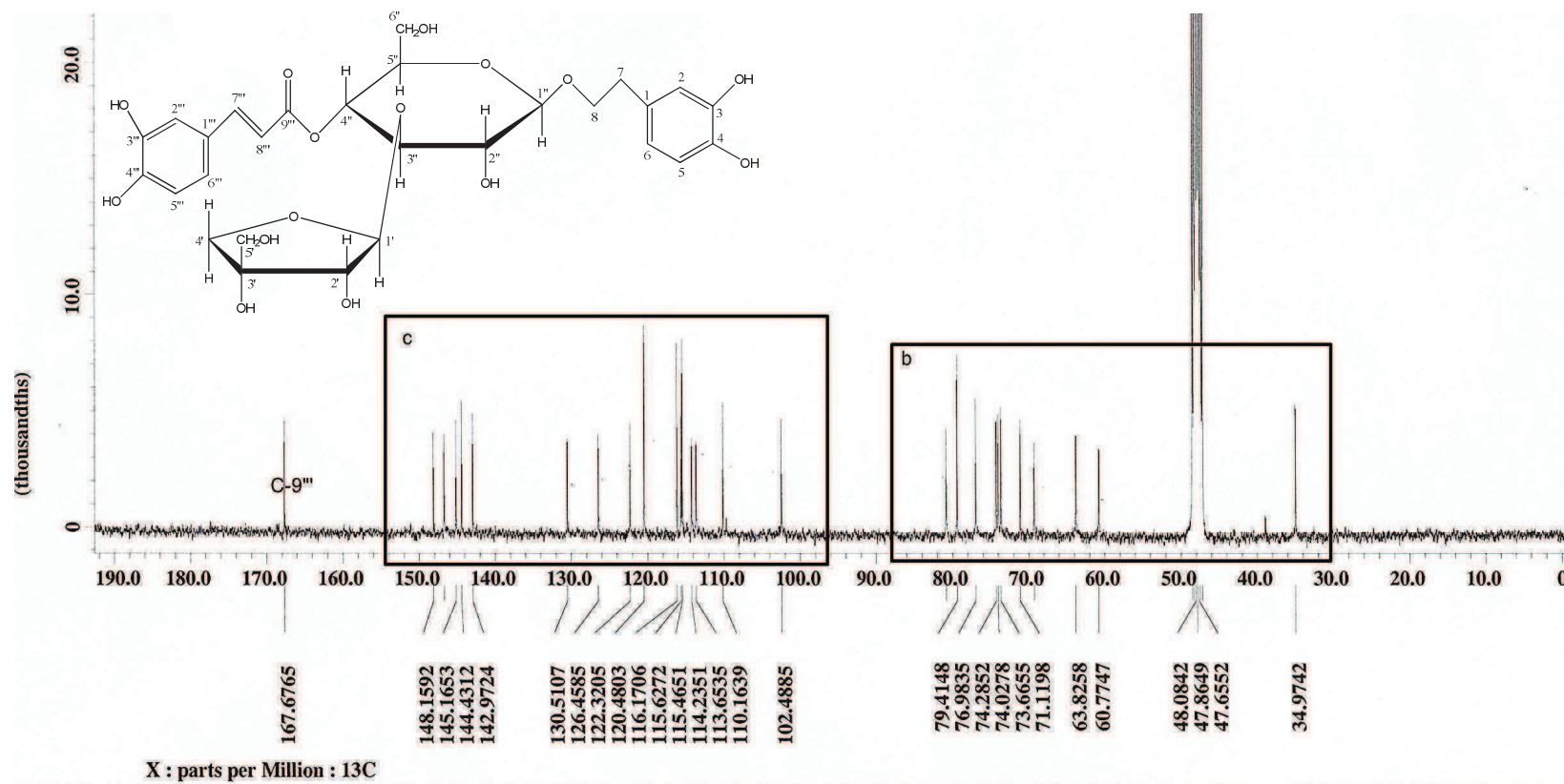
Figure 4.64 (a): Carbon NMR spectrum of Compound PP-2 (measured in D₂O and CD₃OD). Please refer to the following figures (b) and (c) for enlarged spectra.
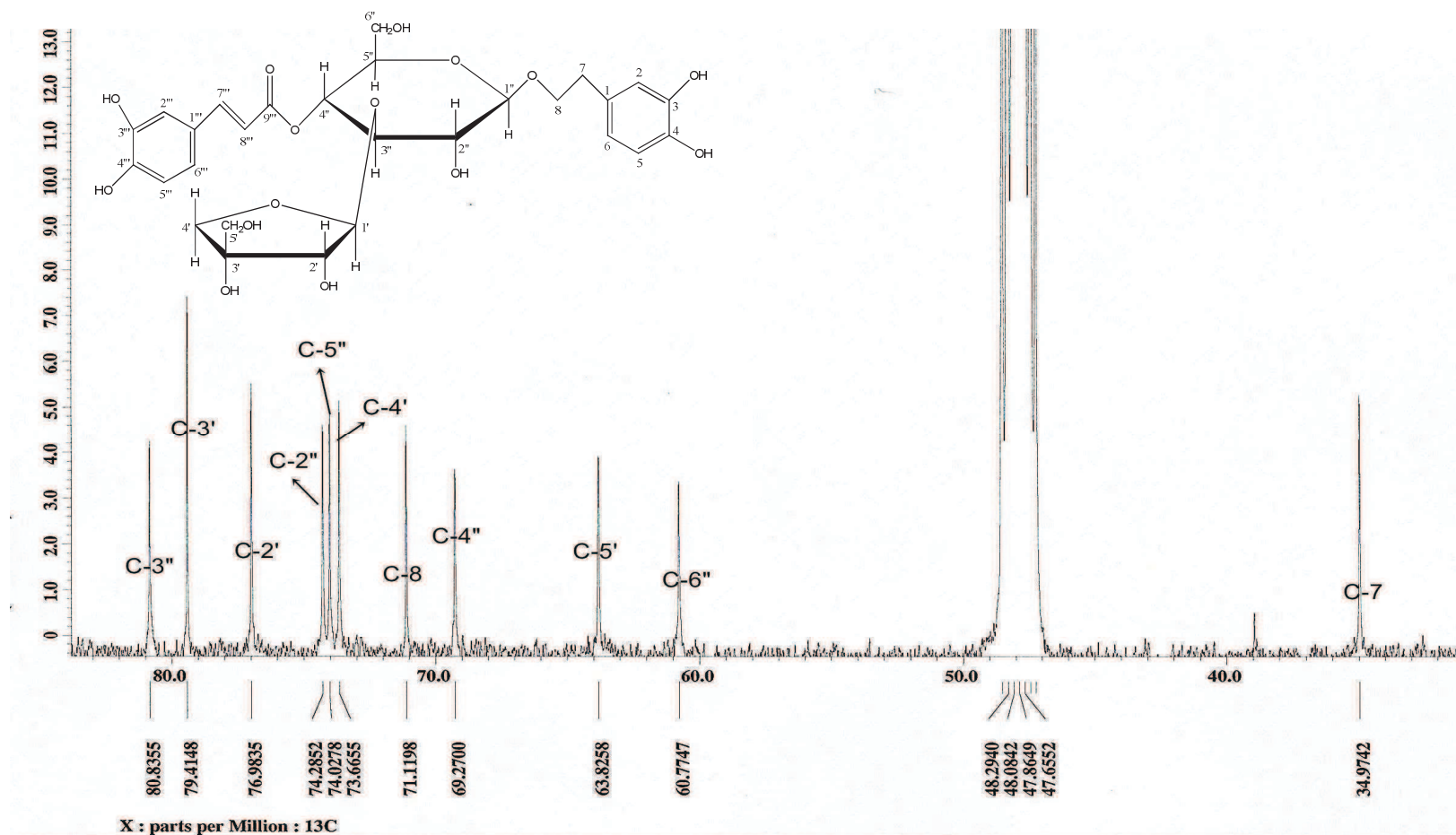
Figure 4.64 (b): Carbon NMR spectrum of Compound PP-2 (measured in D_2O and CD_3OD) (extended view).
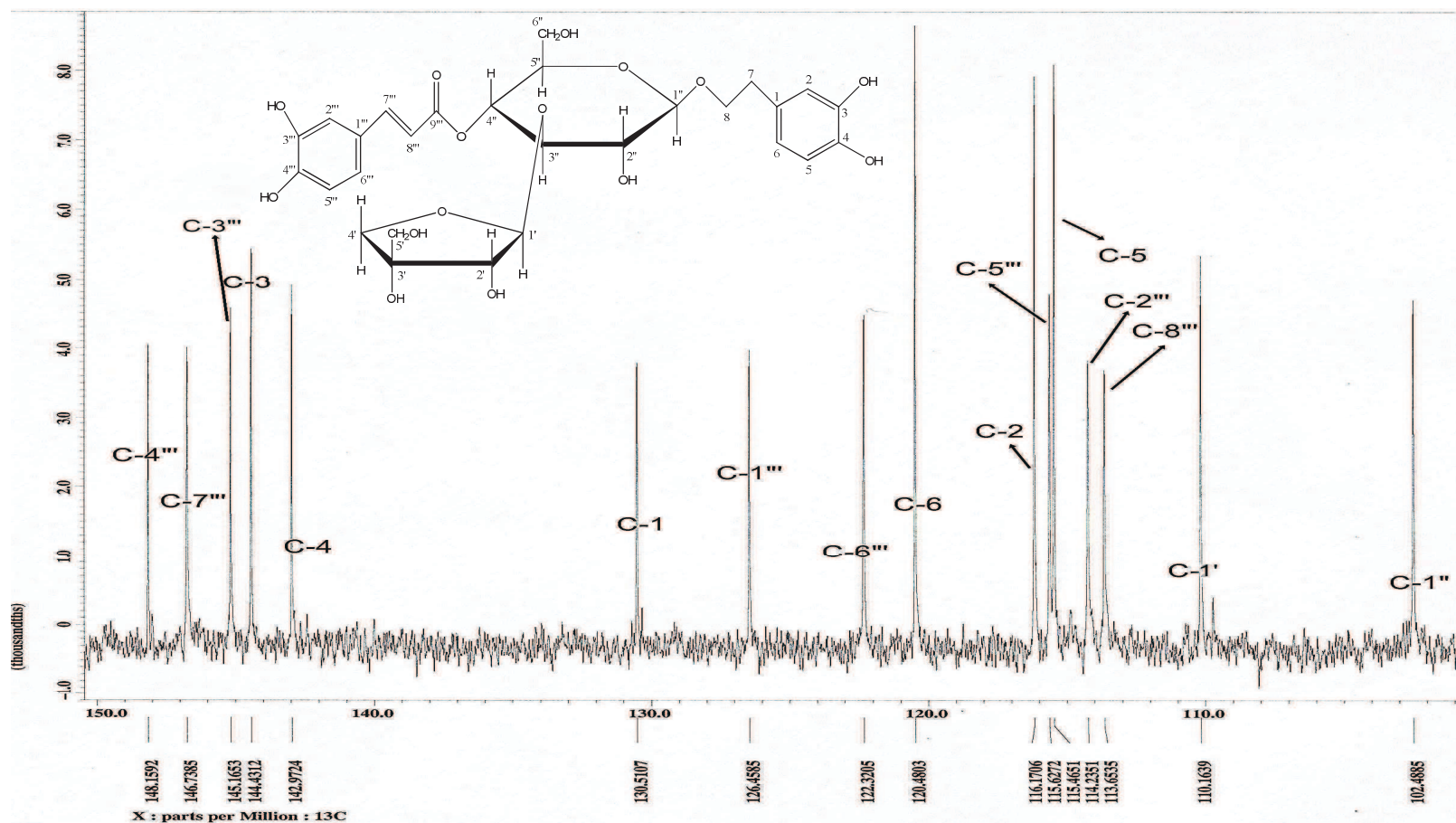
Figure 4.64 (c): Carbon NMR spectrum of Compound PP-2 (measured in D_2O and CD_3OD) (extended view).
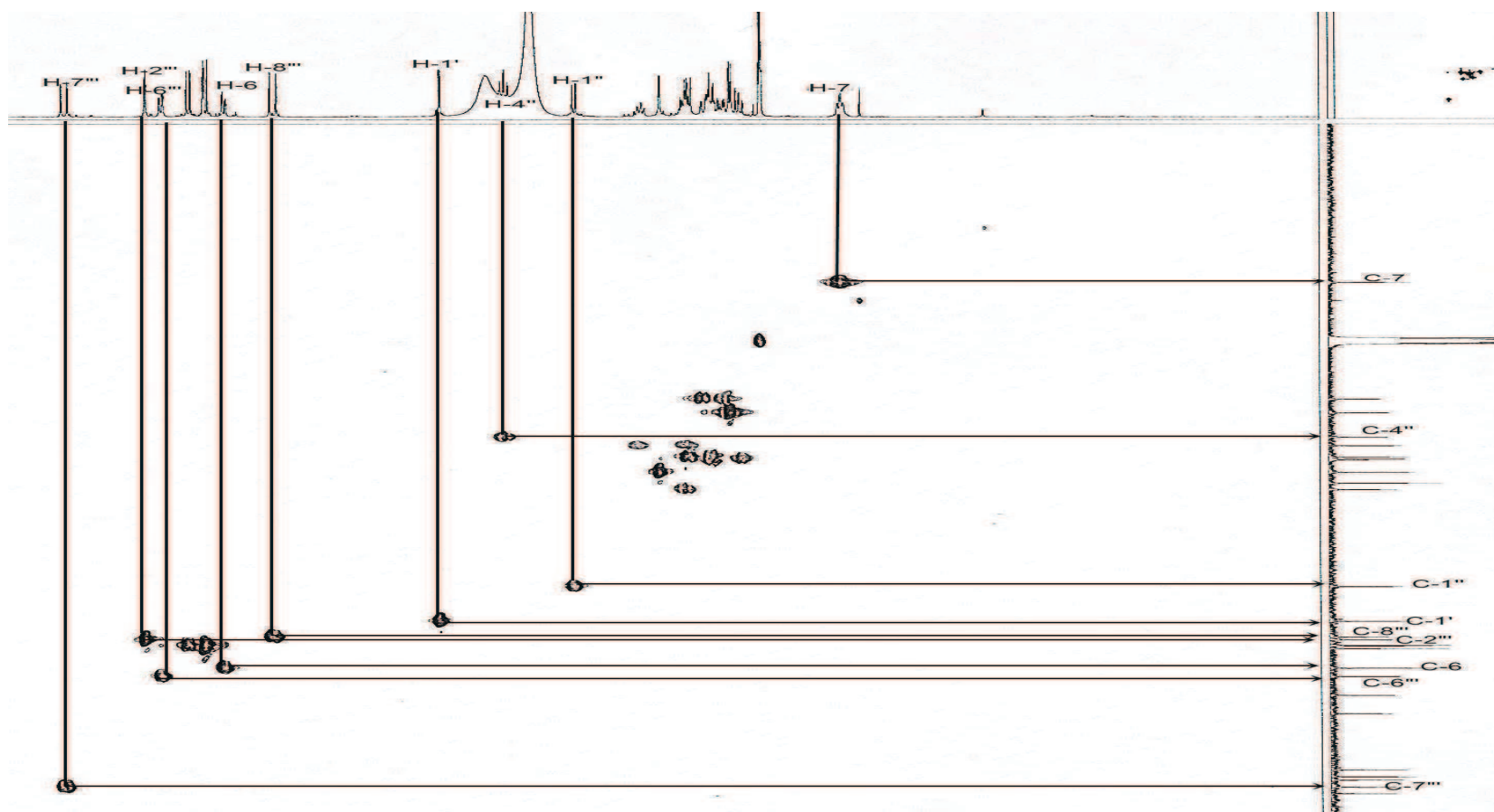
Figure 4.65: HMQC spectrum of Compound PP-2. Please refer to Appendix C: Figures 7.11 (a-d) for enlarged spectra.
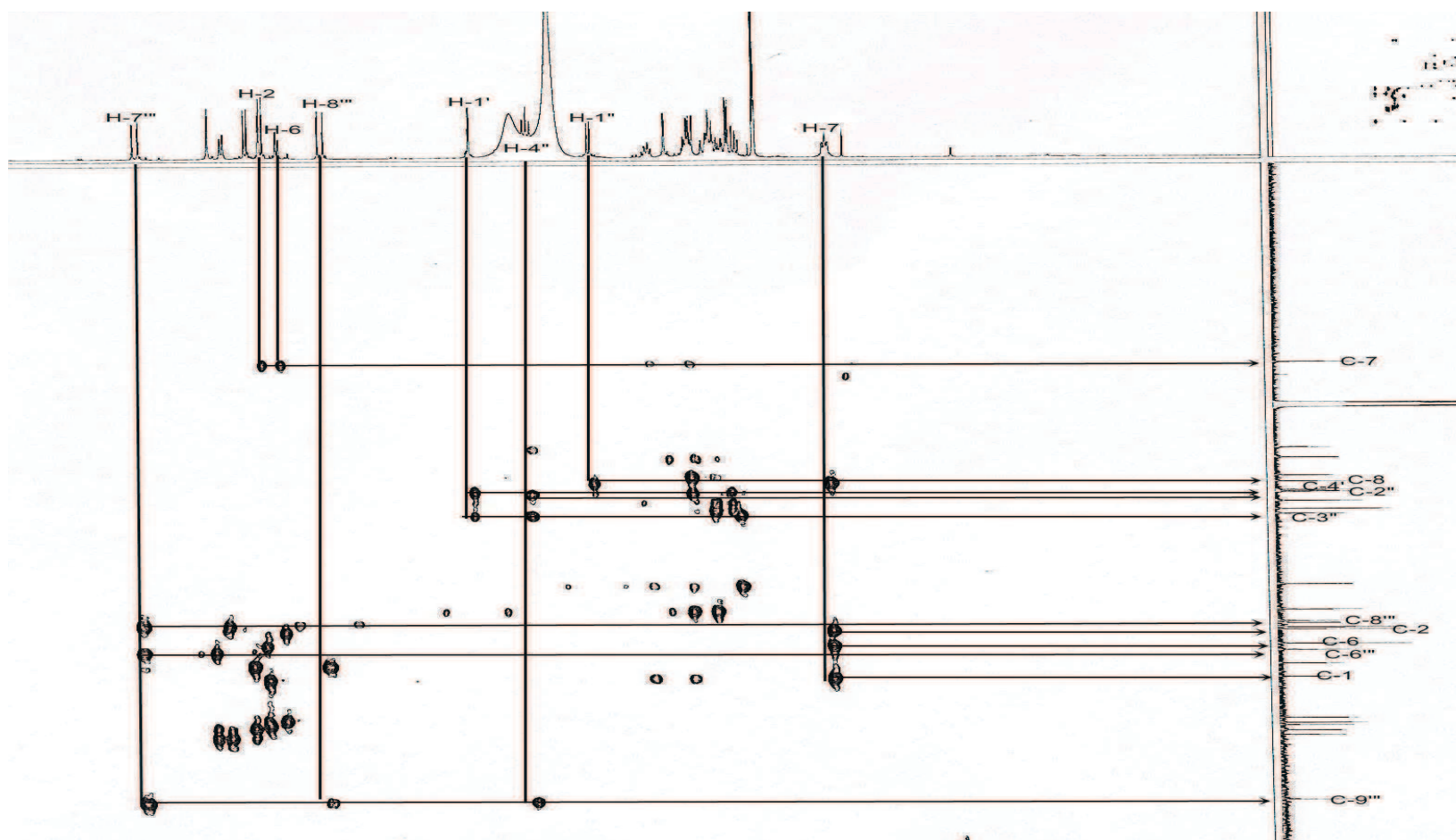
Figure 4.66: HMBC spectrum of Compound PP-2. Please refer to Appendix C: Figures 7.12 (a-d) for enlarged spectra.
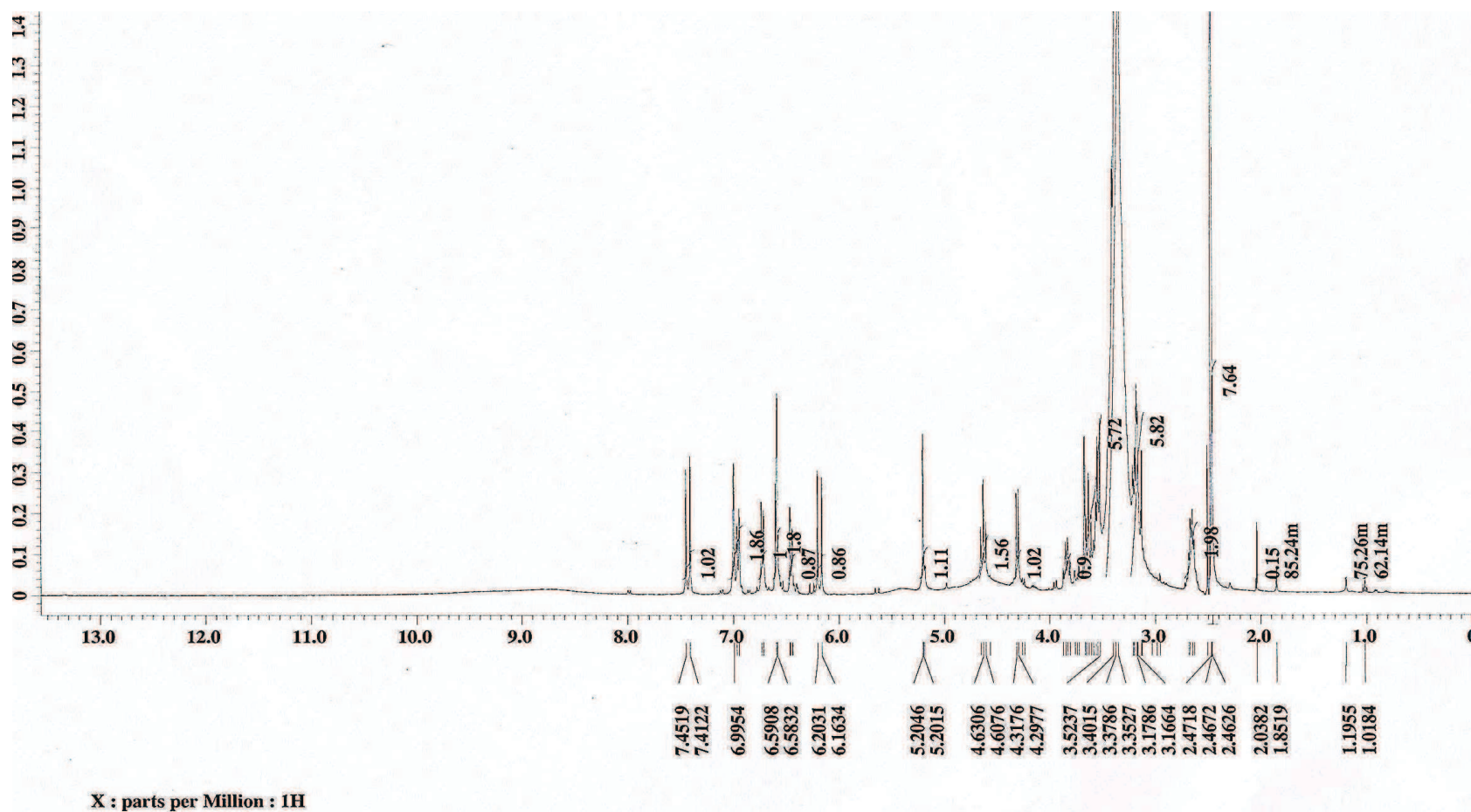
Figure 4.67: Proton NMR spectrum of Compound PP-2 (measured in CD_3SOCD_3).
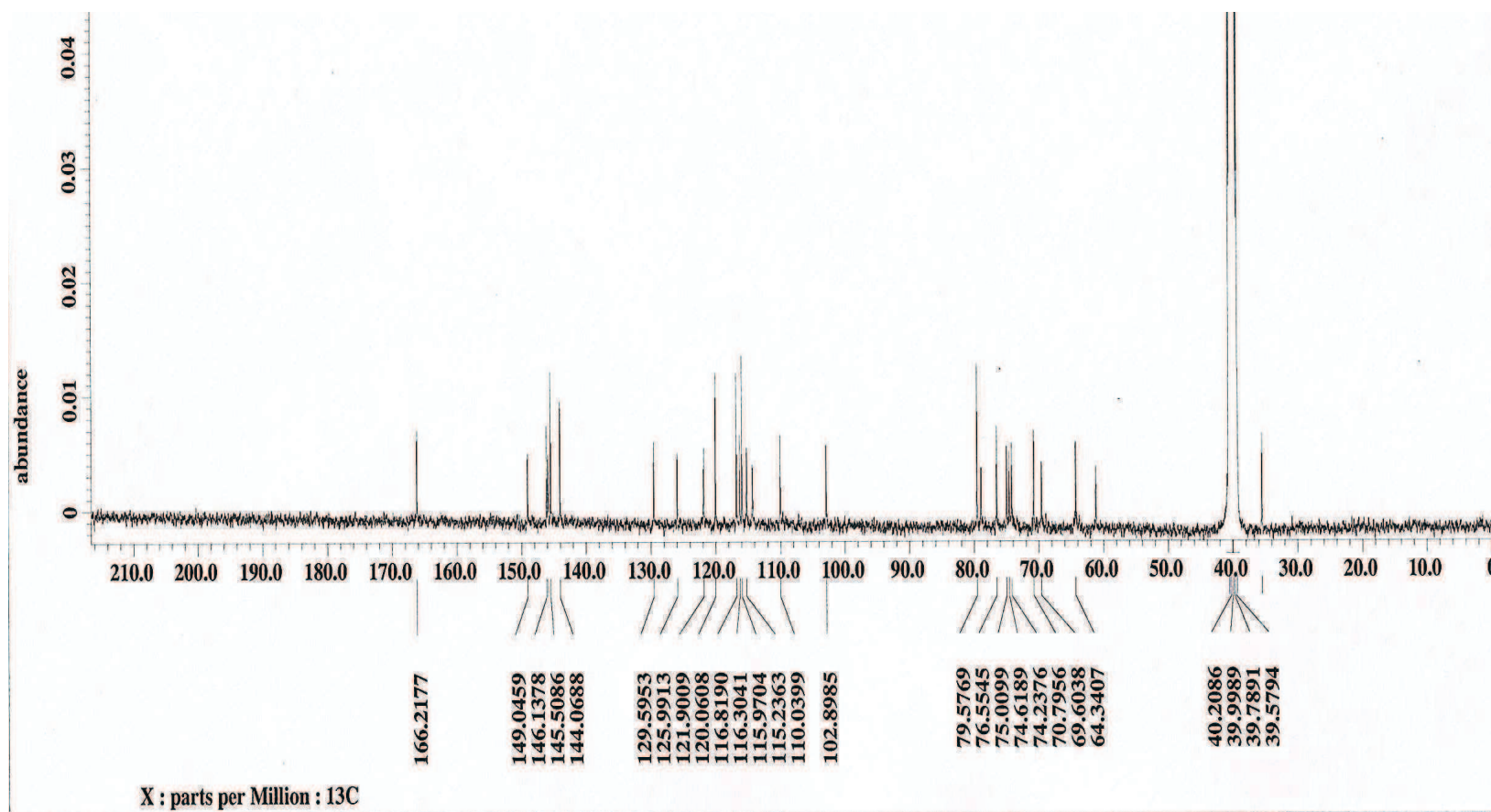
Figure 4.68: Carbon NMR spectrum of Compound PP-2 (measured in CD$_3$SOCD$_3$).
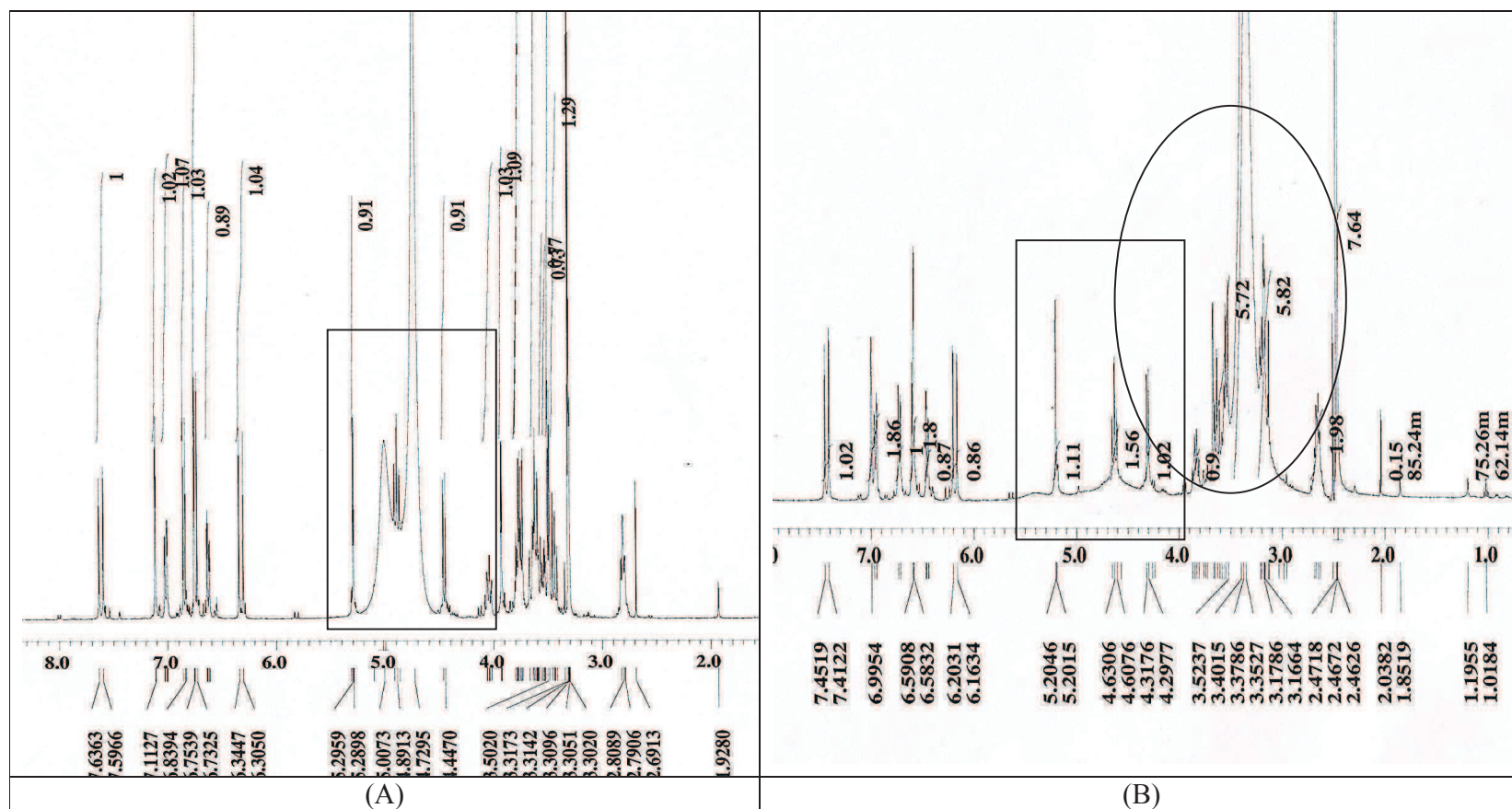
Figure 4.69: Comparison of enlarged proton NMR spectrum of PP-2, measured in (A) D₂O and CD₃OD (B) CD₃SOCD₃. The square indicates the comparison of the group of protons, while the circle indicates the presence of Hydrogen-Oxygen-Deuterium (HOD) in the solution.

Table 4.18: Carbon and proton chemical shifts and HMBC correlation for PP-2.

	^{13}C NMR	^{1}H NMR	HMBC
		Aglycone	
C-1	130.5		
CH-2	116.2	6.76, d (*J*=2.1)	C-6, C-7
C-3	144.4		
C-4	142.9		
CH-5	115.5	6.75, d (*J*=8.3)	C-1, C-3
CH-6	120.5	6.63, dd (*J*=2.1, 8.3)	C-2, C-4, C-7
CH$_2$-7	34.9	2.81, t (*J*=7.3)	C-1, C-2, C-6, C-8
CH$_2$-8	71.1	3.7-3.8; 4.05, m	C-1
		Core sugar	
CH-1"	102.5	4.46, d (*J*=8.0)	C-8
CH-2"	74.3	3.57, m	
CH-3"	80.8	3.70-3.80, m	C-2", C-4"
CH-4"	69.3	4.89, m	C-2", C-3", C-9'''
CH-5"	74.0	3.45, m	C-1", C-3"
CH$_2$-6"	60.8	3.53; 3.67, m	
		Apiosyl unit	
CH-1'	110.2	5.29, d (*J*=2.4)	C-4',C-3"
CH-2'	77.0	3.93, d (*J*=2.4)	
C-3'	79.4	Quartenary C	
CH$_2$-4'	73.7	3.59; 3.70-3.80, m	C-1', C-2', C-3'
CH$_2$-5'	63.8	3.45-3.53 m	C-2', C-3', C-4'
		Caffeoyl unit	
C-1'''	126.4		
CH-2'''	114.2	7.12, d (*J*=1.8)	C-3''', C-4''', C-6'''
C-3'''	145.2		
C-4'''	148.2		
CH-5'''	115.6	6.85, d (*J*=8.3)	C-1''', C-3''', C-4'''
CH-6'''	122.3	7.02, dd (*J*=1.8, 8.3)	C-2''', C-4'''
CH-7'''	146.7	7.62, d (*J*=15.9)	C-6''', C-8''', C-9'''
CH-8'''	113.7	6.32, d (*J*=15.9)	C-1''', C-9'''
C-9'''	167.7		

Chemical shifts are in (δ) in ppm, multiplicities and coupling constant in Hz in parentheses.
PP-2 was measured in D$_2$O and CD$_3$OD.
Multiplicity caused by overlapping and poorly-resolved ^{1}H signals.

Table 4.19: Carbon chemical shifts of PP-2, calceoralarioside E (Damtoft *et al*., 1993), nuomioside A (Kasai *et al*., 1991), and cusianoside A (Tanaka *et al*., 2004).

	^{13}C NMR			
	PP-2	**calceoralarioside E**	**nuomioside A**	**cusianoside A**
Aglycone				
C-1	130.5	131.6	129.1	129.0
CH-2	116.2	115.6	116.1	116.2
C-3	144.4	145.8	144.8	144.9
C-4	142.9	144.3	143.3	143.4
CH-5	115.5	116.8	115.3	115.7
CH-6	120.5	121.6	119.4	119.4
CH_2-7	34.9	36.5	35.0	34.9
CH_2-8	71.1	72.2	70.2	70.2
Core sugar				
CH-1"	102.5	103.9	102.9	102.4
CH-2"	74.3	75.5	74.4	74.0
CH-3"	80.8	81.6	78.9	78.6
CH-4"	69.3	70.6	69.0	69.2
CH-5"	74.0	75.8	73.6	74.5
CH_2-6"	60.8	62.5	60.7	60.7
Apiosyl unit				
CH-1'	110.2	111.4	109.5	109.5
CH-2'	77.0	78.4	76.0	76.1
C-3'	79.4	80.6	78.5	78.9
CH_2-4'	73.7	75.2	73.6	73.6
CH_2-5'	63.8	66.0	63.8	63.8
Caffeoyl unit				
C-1'''	126.4	127.7	125.4	125.5
CH-2'''	114.2	115.0	114.8	114.7
C-3'''	145.2	146.5	145.5	145.5
C-4'''	148.2	149.4	148.3	148.4
CH-5'''	115.6	116.6	115.7	115.4
CH-6'''	122.3	123.4	121.2	121.2
CH-7'''	146.7	148.0	145.2	145.2
CH-8'''	113.7	116.6	113.8	113.9
C-9'''	167.7	168.7	165.6	165.6

PP-2 was measured in D_2O and CD_3OD. Calceoralarioside E was measured in CD_3OD (500 MHz), while nuomioside A (100 MHz) and cusianoside A (125 MHz) were measured in CD_3SOCD_3.

Table 4.20: Proton chemical shifts of PP-2, nuomioside A (Kasai *et al*., 1991), and cusianoside A (Tanaka *et al*., 2004).

	PP-2	**nuomioside A**	**cusianoside A**
		^{1}H NMR	

Aglycone

	PP-2	**nuomioside A**	**cusianoside A**
C-1			
CH-2	6.76 d(2.1)	6.69 d(1.9)	6.62 s
C-3			
C-4			
CH-5	6.75 d(8.3)	6.7 d(8.1)	6.77 d(7.9)
CH-6	6.63 dd(2.1,8.3)	6.57 dd(1.9,8.1)	6.5 d(7.9)
CH_2-7	2.81 t(7.3)	2.77; 2.75 ddd(7.2,8.8,9)	2.71 m
CH_2-8	3.70-3.80, 4.05 m	3.71; 3.95 ddd(7.2,8.8,8.8)	3.63; 3.88 m

Core sugar

	PP-2	**nuomioside A**	**cusianoside A**
CH-1"	4.46 d(8.0)	4.36 d(7.8)	4.35 d(7.3)
CH-2"	3.57 m	3.27 dd(7.8,9.3)	3.22 dd(7.3,9.8)
CH-3"	3.70-3.80 m	3.74 dd(9.3,9.5)	3.67 dd(9.2,9.8)
CH-4"	4.89 m	4.68 dd(9.5,9.6)	4.68 dd(9.8,9.8)
CH-5"	3.45 m	3.53 ddd(1.7,6,9.6)	3.43-3.47 (3H overlapped)
CH_2-6"	3.53; 3.67 m	3.42; 3.47 dd(6,10.7); (1.7, 10.7)	

Apiosyl unit

	PP-2	**nuomioside A**	**cusianoside A**
CH-1'	5.29 d(2.4)	5.26 d(1.7)	5.25 br s
CH-2'	3.93 d(2.4)	3.77 d(1.7)	3.71 br s
C-3'			
CH_2-4'	3.59; 3.70-3.80 m	3.49; 3.7 d(9)	3.18; 3.24 d(10.4)
CH_2-5'	3.45-3.53 m	3.25; 3.28 d(10.8)	3.47; 3.59 d(9.2)

Caffeoyl unit

	PP-2	**nuomioside A**	**cusianoside A**
C-1'''			
CH-2'''	7.12 d(1.8)	7.1 d(1.4)	7.05 s
C-3'''			
C-4'''			
CH-5'''	6.85 d(8.3)	6.83 d(8.2)	6.63 d(7.9)
CH-6'''	7.02 dd(1.8,8.3)	7.05 dd(1.4,8.2)	6.99 d(7.9)
CH-7'''	7.62 d(15.9)	7.53 d(15.8)	6.21 d(15.9)
CH-8'''	6.32 d(15.9)	6.29 d(15.8)	7.47 d(15.9)
C-9'''			

Chemical shifts are in (δ) in ppm, multiplicities and coupling constant in Hz in parentheses.
PP-2 was measured in D_2O and CD_3OD. Nuomioside A (400 MHz) and cusianoside A (500 MHz) were measured in CD_3SOCD_3.
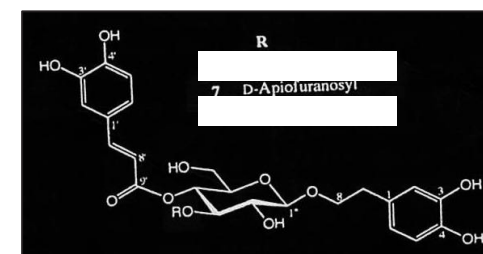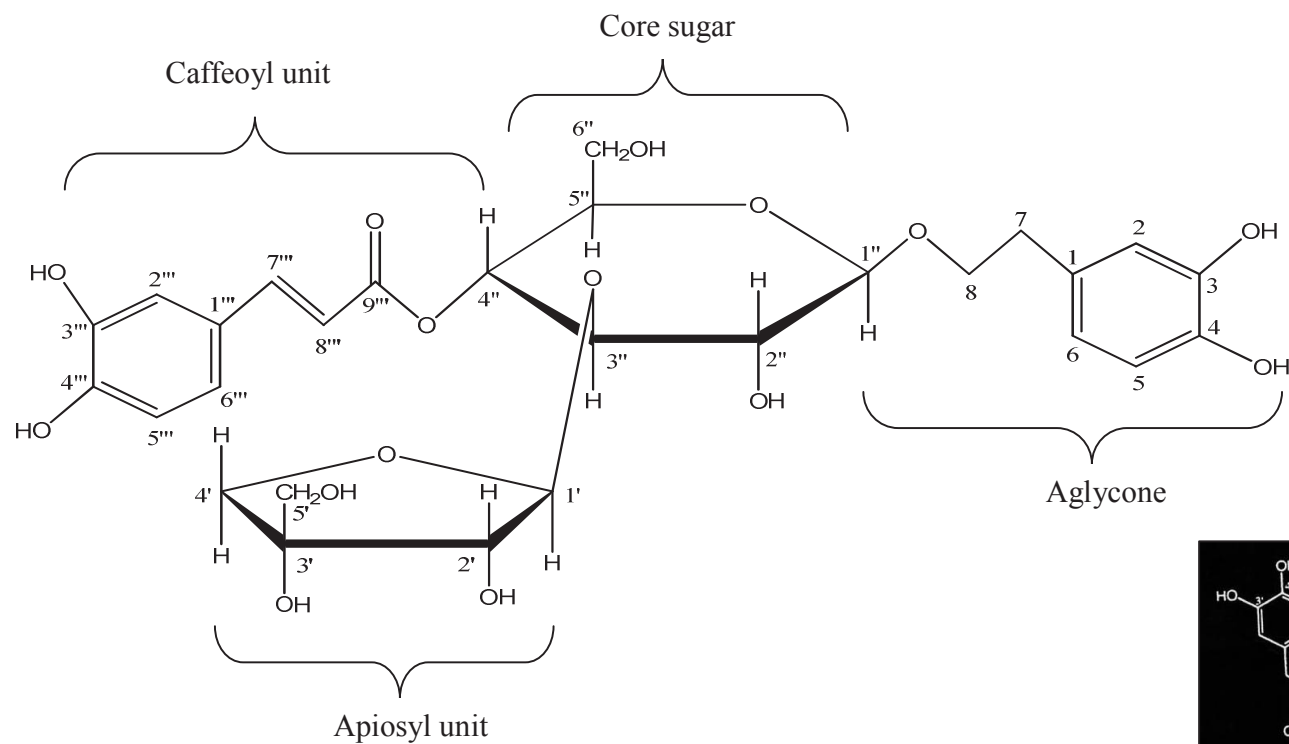
Figure 4.70: Molecular structure of PP-2, 3, 4-dihydroxyphenethyl-(3"-O-β-D-apiofuranosyl-4"-O-caffeoyl)-β-D-glucopyranoside. The structure on right bottom is cusianoside A (Tanaka *et al.*, 2004).

38.1 mg PP-3 (18.14%) was isolated from 210 mg of leaf F-5 in the form of brownish amorphous powder (Figure 4.71). The LC-mass spectrum has a molecular ion peak at m/z 623 [M-H]$^-$ and dimeric signal at m/z 1246.8 [2M-H]$^-$ in negative ion mode with calculated molecular weight of 624, suggesting the molecular formula of $C_{29}H_{36}O_{15}$. Other fragment ion peaks were observed at 579, 516, 461 [M-caffeoyl unit-H]$^-$, 415, 311 [461-rhamnose]$^-$, 162, 161[315–aglycone unit-H$_2$O]$^-$ and 135 [315-hexose-H$_2$O]$^-$ (Figures 4.72 and 4.73). The UV spectra of PP-3 were highly similar to PP-2, with absorption maxima at 199, 217, and 332 nm, confirming their phenolic nature (Figure 4.74). Examinations of the IR spectrum demonstrated bands at 3416 (hydroxyl groups), 2929 (C-H), 1686 (C=O), 1616 (C=C), 1524 (aromatic rings), 1435, 1369, 1270, 1200, 1155 (C-O stretching), 1118, 1096, 1067, 1037, 1019, 916, 809, and 731 cm^{-1} (Figure 4.75).

The chemical shifts of compound PP-3 were almost the same as those of PP-2. The ^{1}H NMR spectrum (Figure 4.76) exhibited the characteristic signal of caffeoyl unit (3 aromatic protons for an AMX system, and a carbonyl carbon) and 3, 4 dihydroxyphenylethanol unit (3 aromatic protons as ABX system and a methylene carbon). The downfield signal of H-4" at δ 4.67 and the HMBC correlation between H-4" and C-9"' (δ 166.3) showed that the caffeoyl unit was bonded to the C-4" of the central glucose unit, as demonstrated in PP-2. The signals of anomeric protons appeared at δ 4.32 (d, J=7.9 Hz) and δ 4.99 (s), indicating the disaccharide structure. However, the secondary methyl signal at δ 0.92 (d, J=6.1 Hz) suggested the presence of rhamnosyl residue attaching to the

core glucose unit, rather than apiosyl unit in PP-2. The large J_{H1-H2} value (7.9 Hz) of the anomeric proton of glucopyranoside, signified its β-configuration. Compared with corresponding β-glycosides, α-glycosides resonate at downfield position by 0.3 to 0.5 ppm and smaller coupling constant (Agrawal, 1992) and this confirmed the α-configuration of rhamnosyl unit in PP-3, which gave singlet ^{1}H signal at δ 4.99. The H-7'''of caffeoyl unit is coupled *trans* across the double bond to the H-8''' (J=15.9 Hz). The low field position of C-3" (δ 79.6) of glucose showed long-range correlation with the anomeric proton of rhamnose (δ 4.99) in the HMBC spectrum revealing the site of interglycosidic linkage. In ^{13}C NMR spectrum (Figure 4.77), there are only 27 carbon signals observed, and this could be due to the overlapping of carbon chemical shifts. This was confirmed by the examination of HMQC spectrum at δ 75.0, indicating the correlation of the particular carbon with 2 different types of protons (Figure 7.13b) and at δ 146.2 with the splitting of carbon signal into two very close peaks (Figure 7.13f).

All the chemical shifts data (Tables 4.22 to 4.23) of PP-3 are comparable to verbacoside (Andrary *et al*., 1982; Gafner *et al*., 1997) and acteoside (Kitagawa *et al*., 1984) indicated the existence of similar skeleton of structure. On the basis of these data, the structure of PP-3 was established as 3,4-dihydroxyphenethyl-(3"-O-α-L-rhamnopyranosyl-4"-O-caffeoyl)-β-D-glucopyranoside (Figure 4.80).
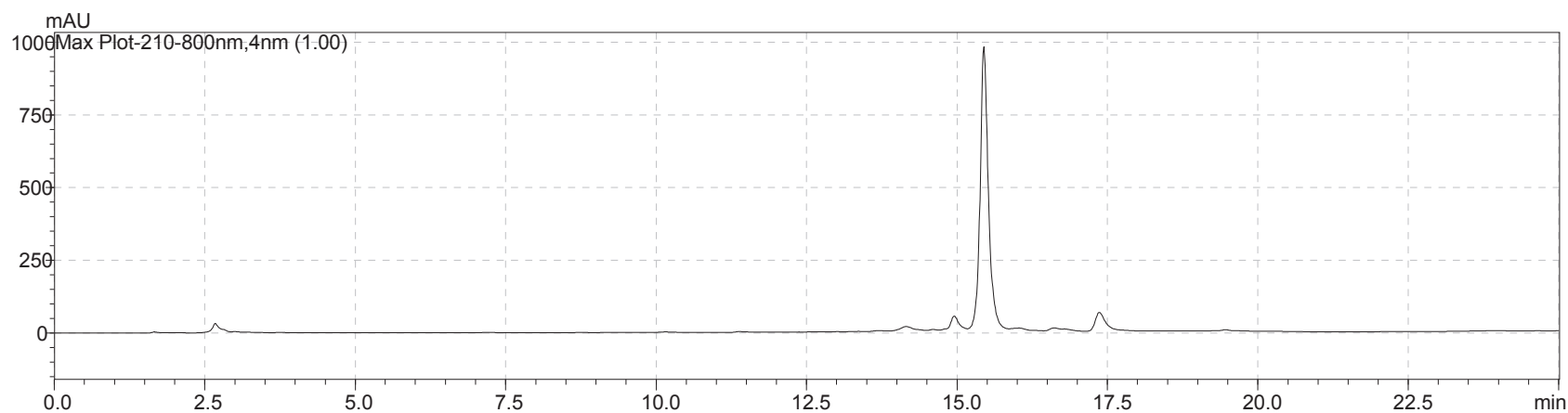
Figure 4.71: High performance liquid chromatography analysis of Compound PP-3. Stationary phase: Chromolith RP-18 analytical column 100-4.6 mm. Mobile phase: 0-7 min (7% CH$_3$CN: 93% H$_2$O); 7-10 min (20% CH$_3$CN: 80% H$_2$O); 10-15 min (35% CH$_3$CN: 65% H$_2$O); 15-17 min (60% CH$_3$CN: 40% H$_2$O; 17-23 min (7% CH$_3$CN: 93% H$_2$O). Flow rate: 0.6 ml/min. Spectral scan 210 nm to 800 nm. About 85% of peak purity was achieved.
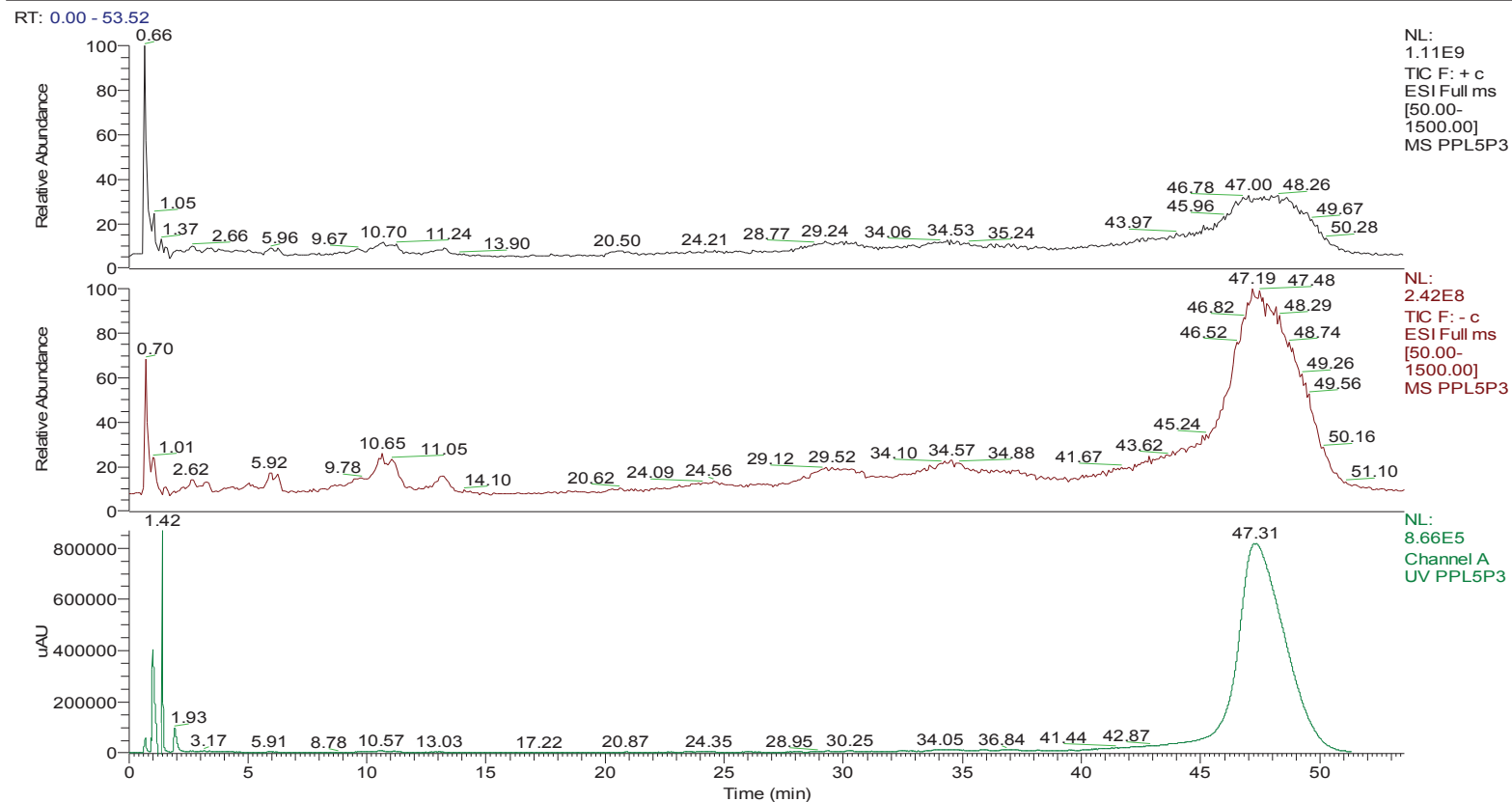
Figure 4.72: Liquid chromatography-mass spectroscopy analysis of Compound PP-3. (-)-MS showed stronger peak signal than (+)-MS does. From top to lowest: positive ion mode-ESI, negative ion mode-ESI, UV liquid chromatography.
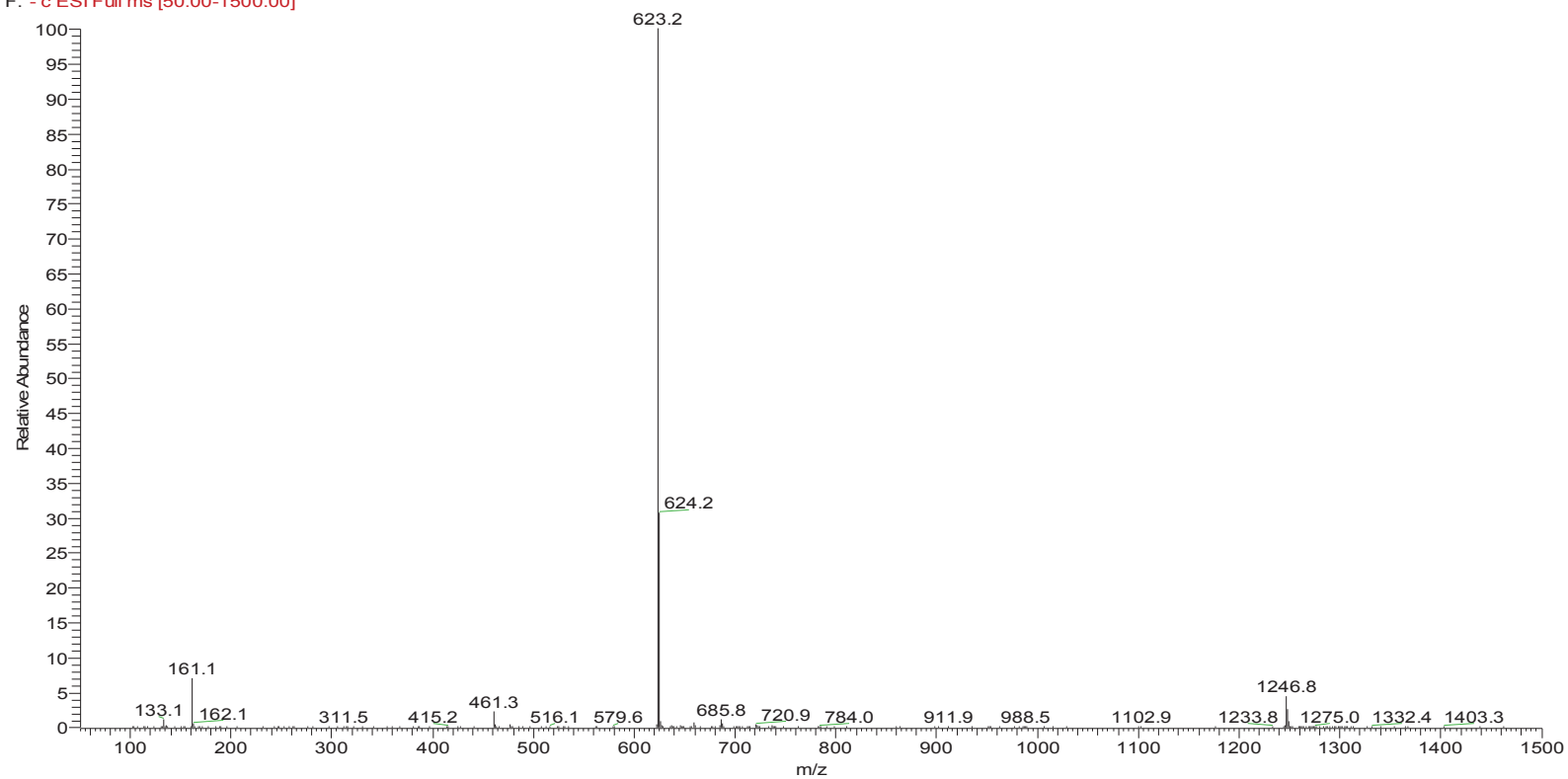
Figure 4.73: Mass spectrum of Compound PP-3. The LC-mass spectrum has a molecular ion peak at m/z 623 [M-H]⁻ and dimeric signal ion at m/z 1246.8 [2M-H]⁻ in negative ion mode.
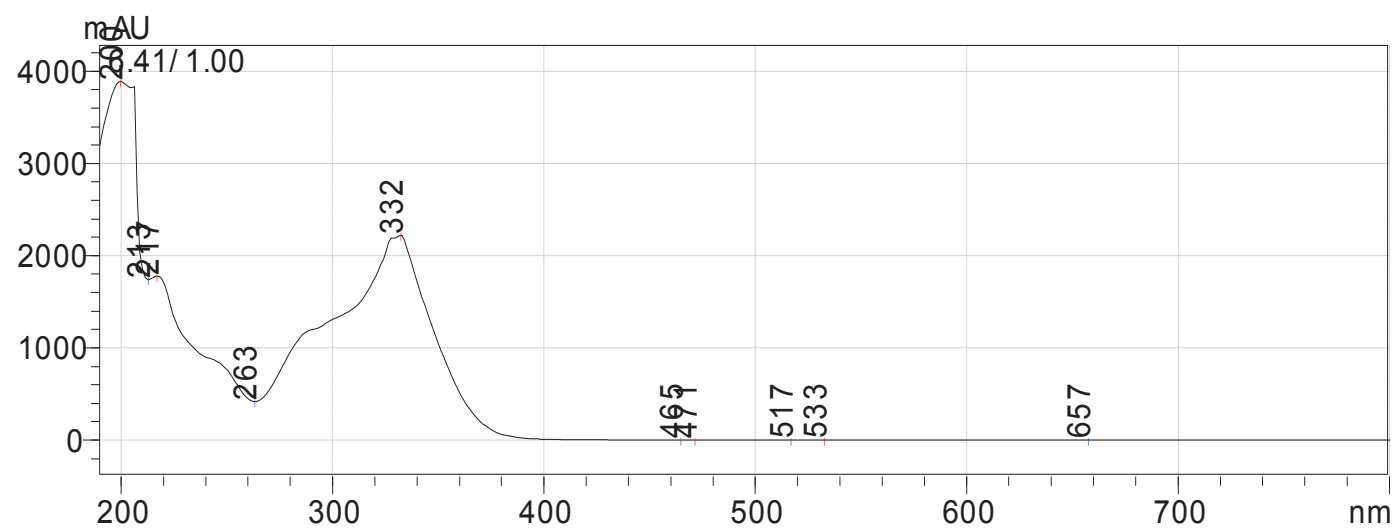
Figure 4.74: UV-Vis Spectrum of Compound PP-3.
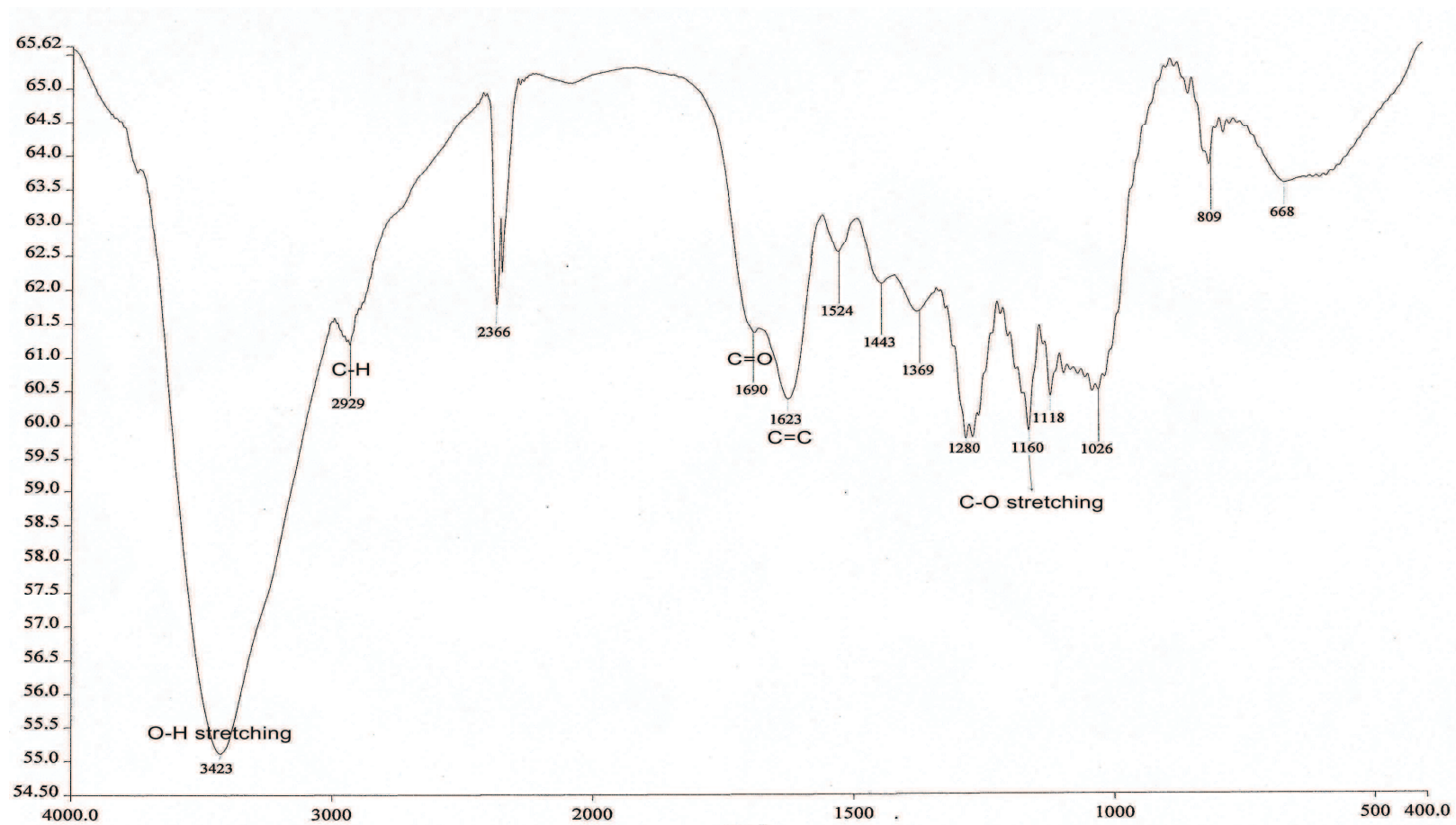
Figure 4.75: Infrared spectrum of Compound PP-3.

Figure 4.76 (a): Proton NMR spectrum of Compound PP-3. Please refer to following figures (b) and (c) for enlarged spectra.
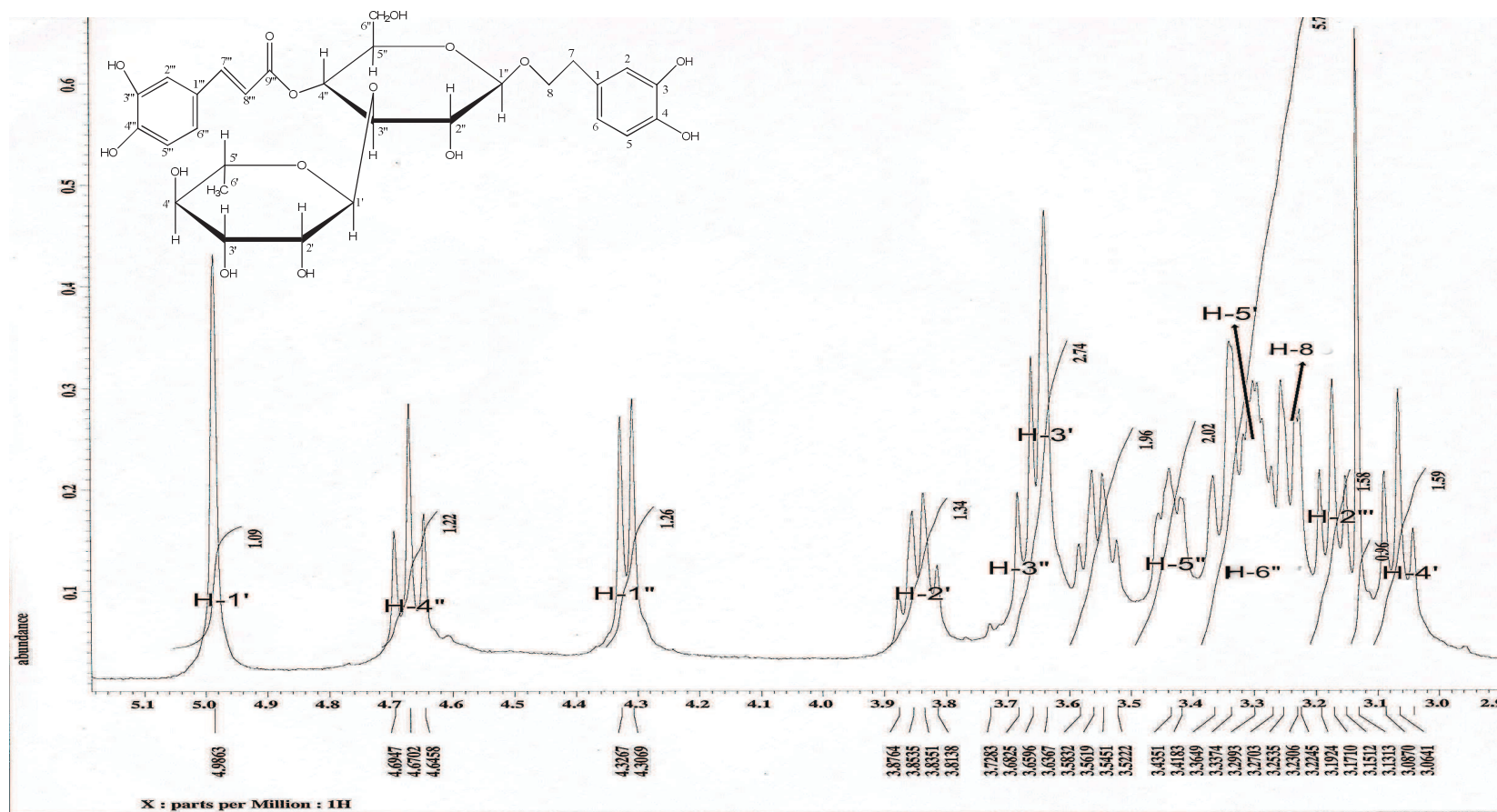
Figure 4.76 (b): Proton NMR spectrum of Compound PP-3 (extended view).
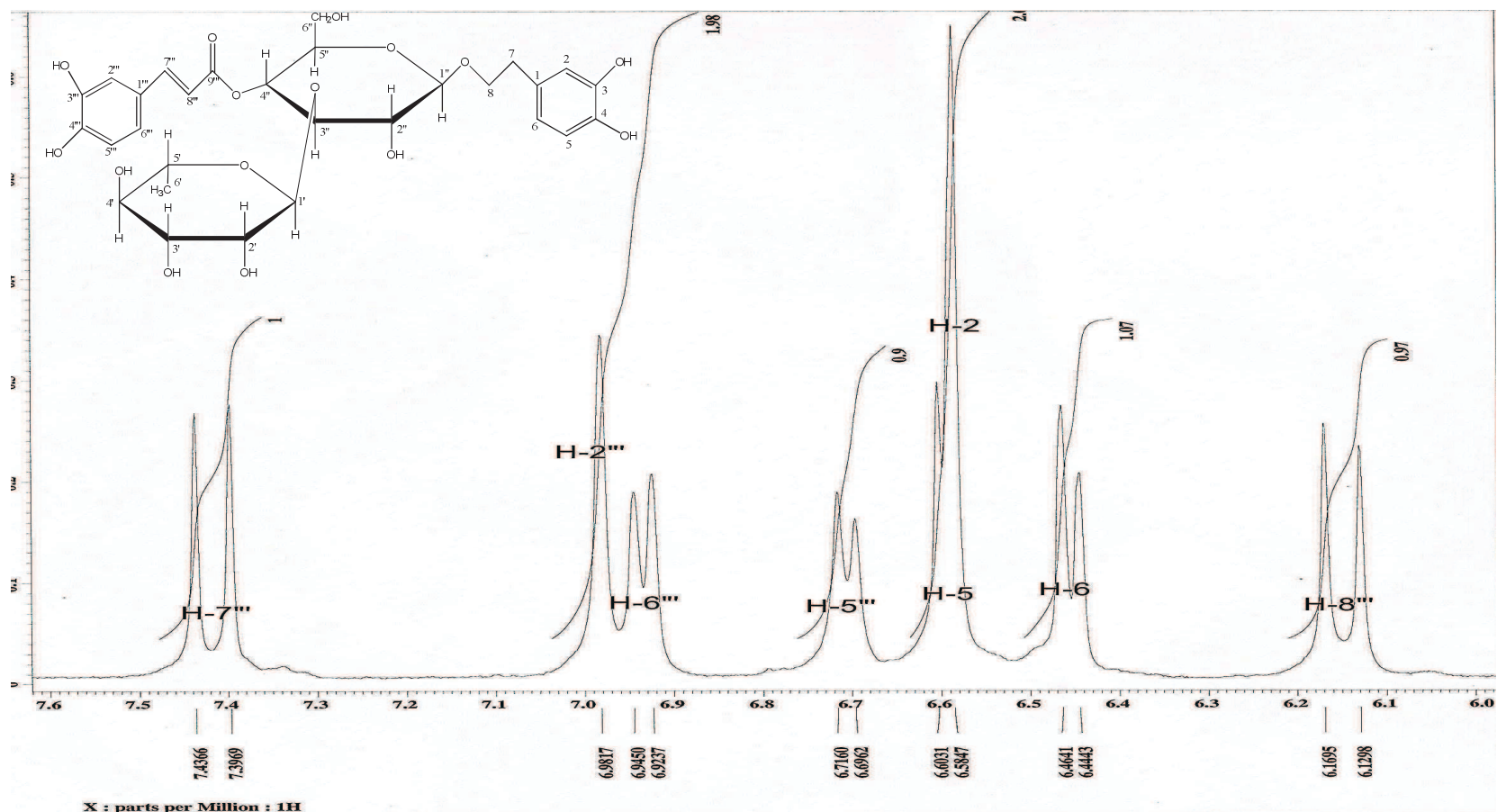
Figure 4.76 (c): Proton NMR spectrum of Compound PP-3 (extended view).
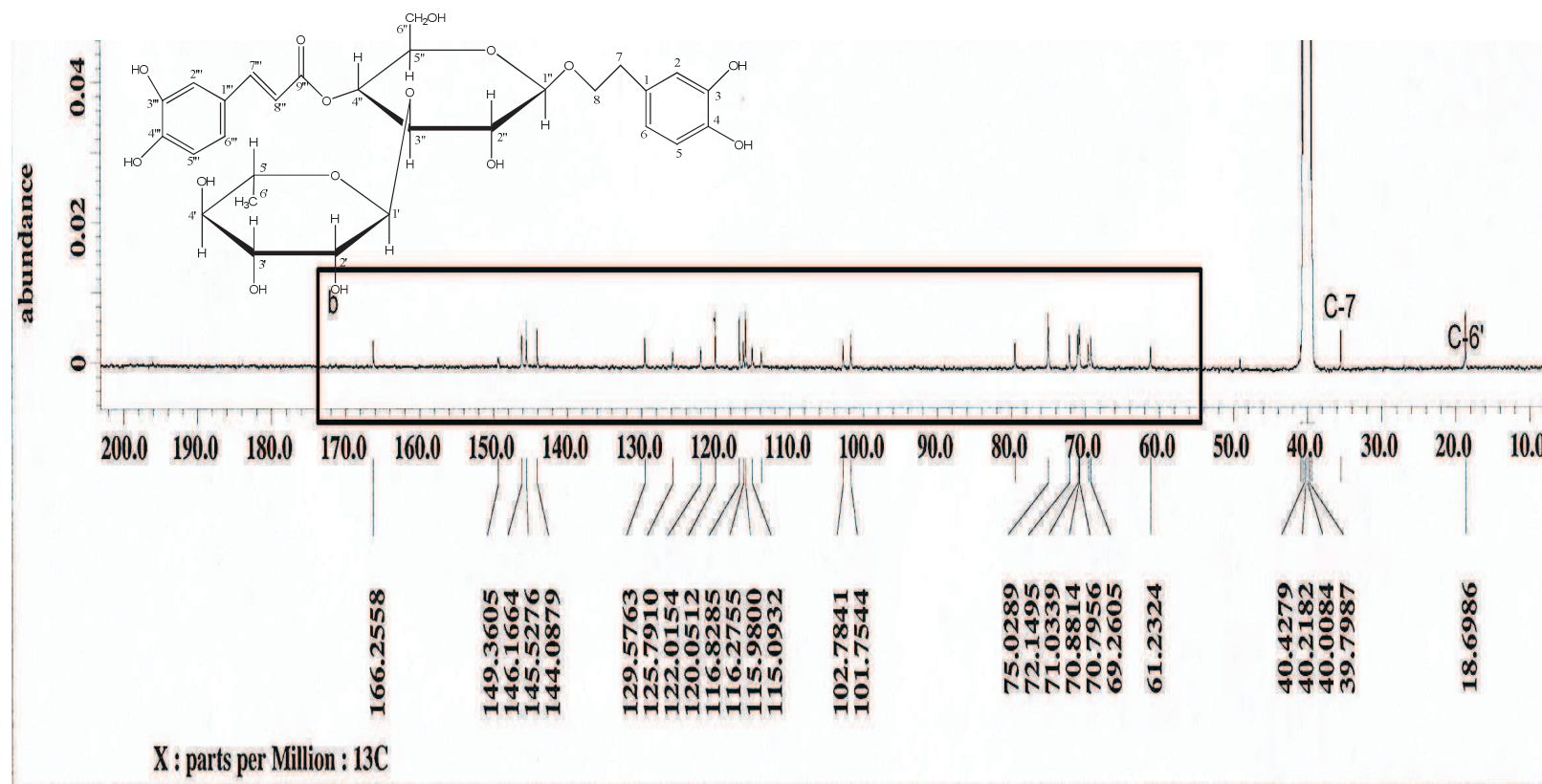
Figure 4.77 (a): Carbon NMR spectrum of Compound PP-3. Please refer to following figure (b) for enlarged spectra.
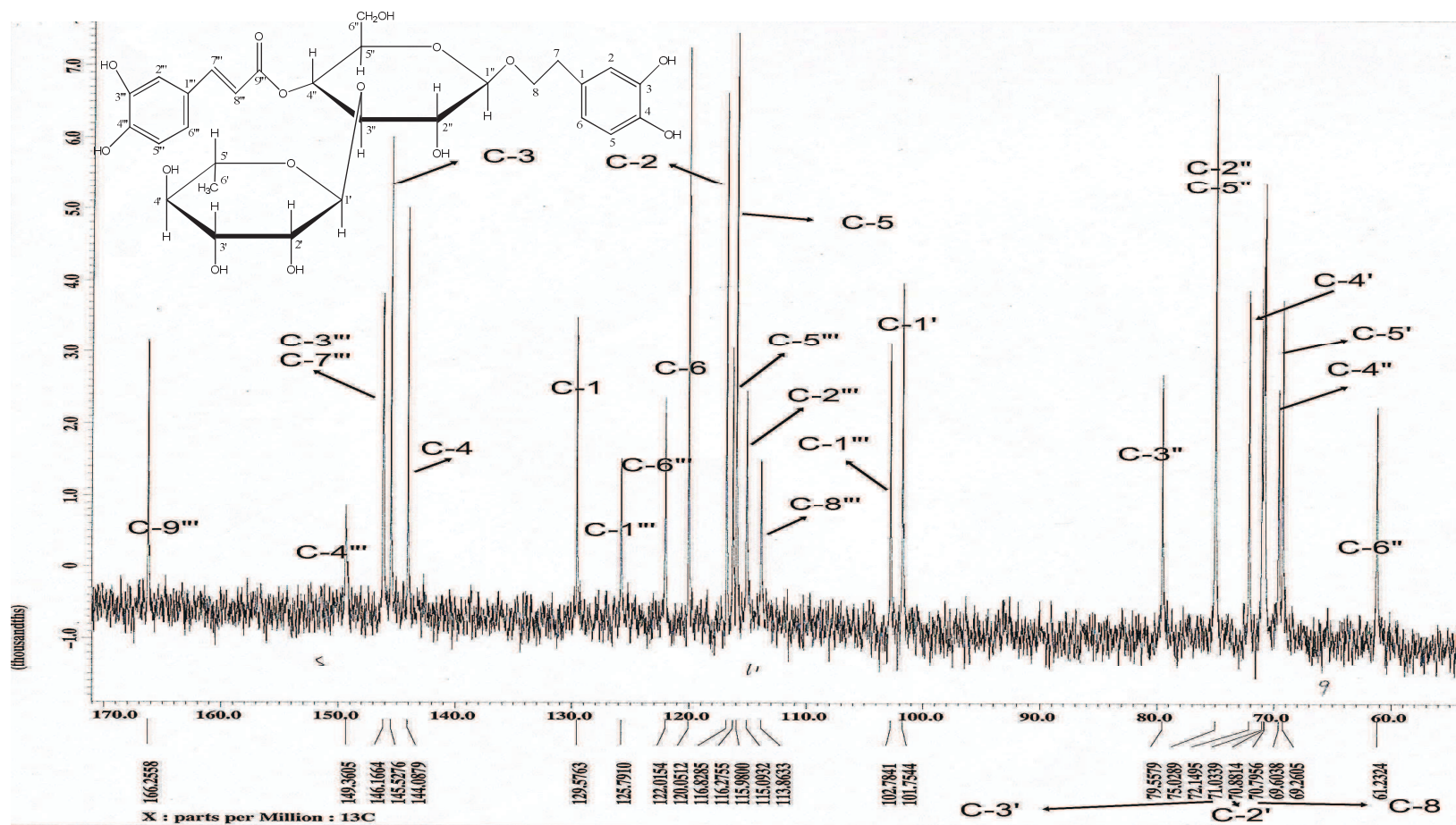
Figure 4.77 (b): Carbon NMR spectrum of Compound PP-3 (extended view).
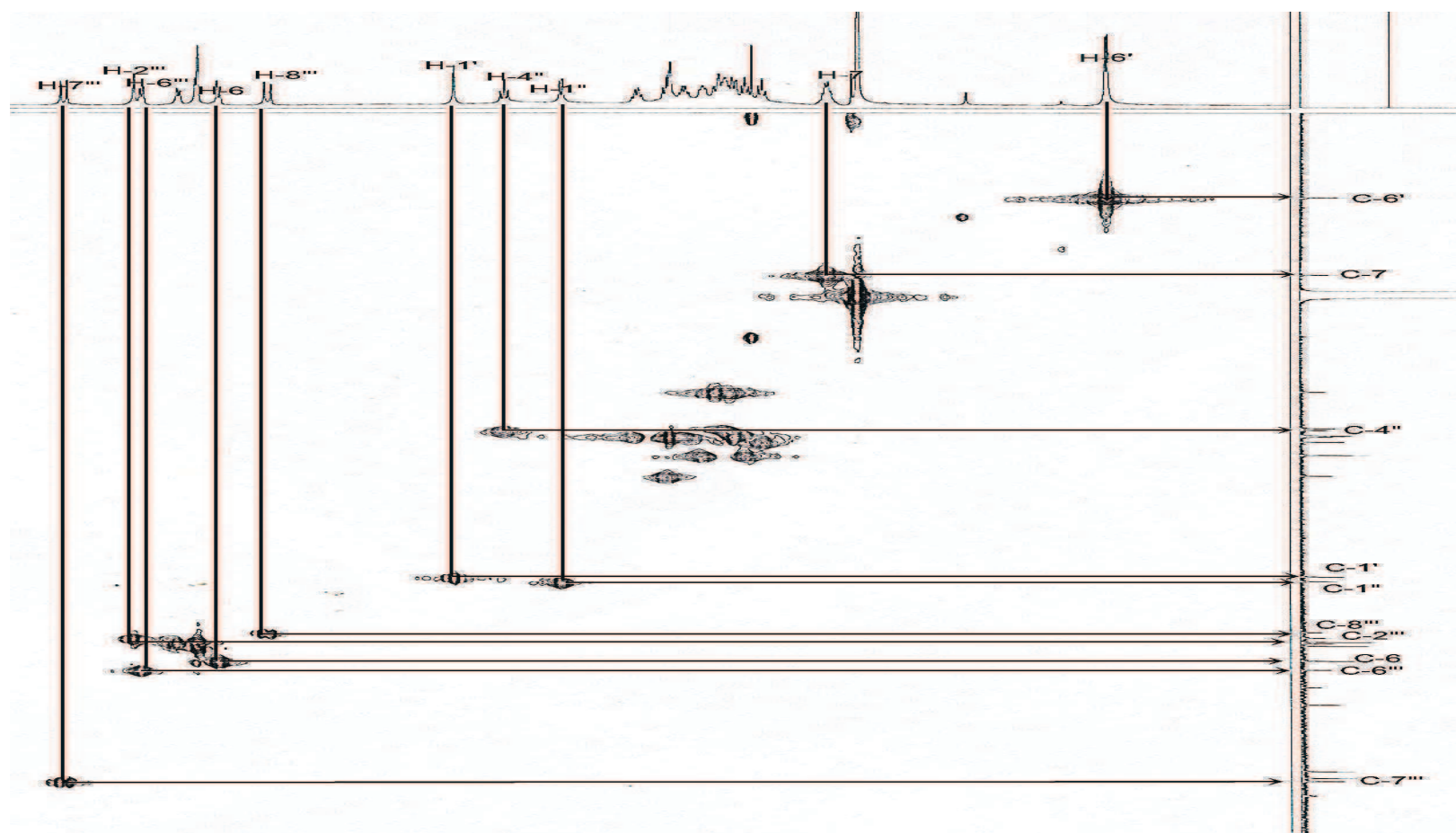
Figure 4.78: HMQC spectrum of Compound PP-3. Please refer to Appendix C: Figures 7.13 (a-f) for enlarged spectra.
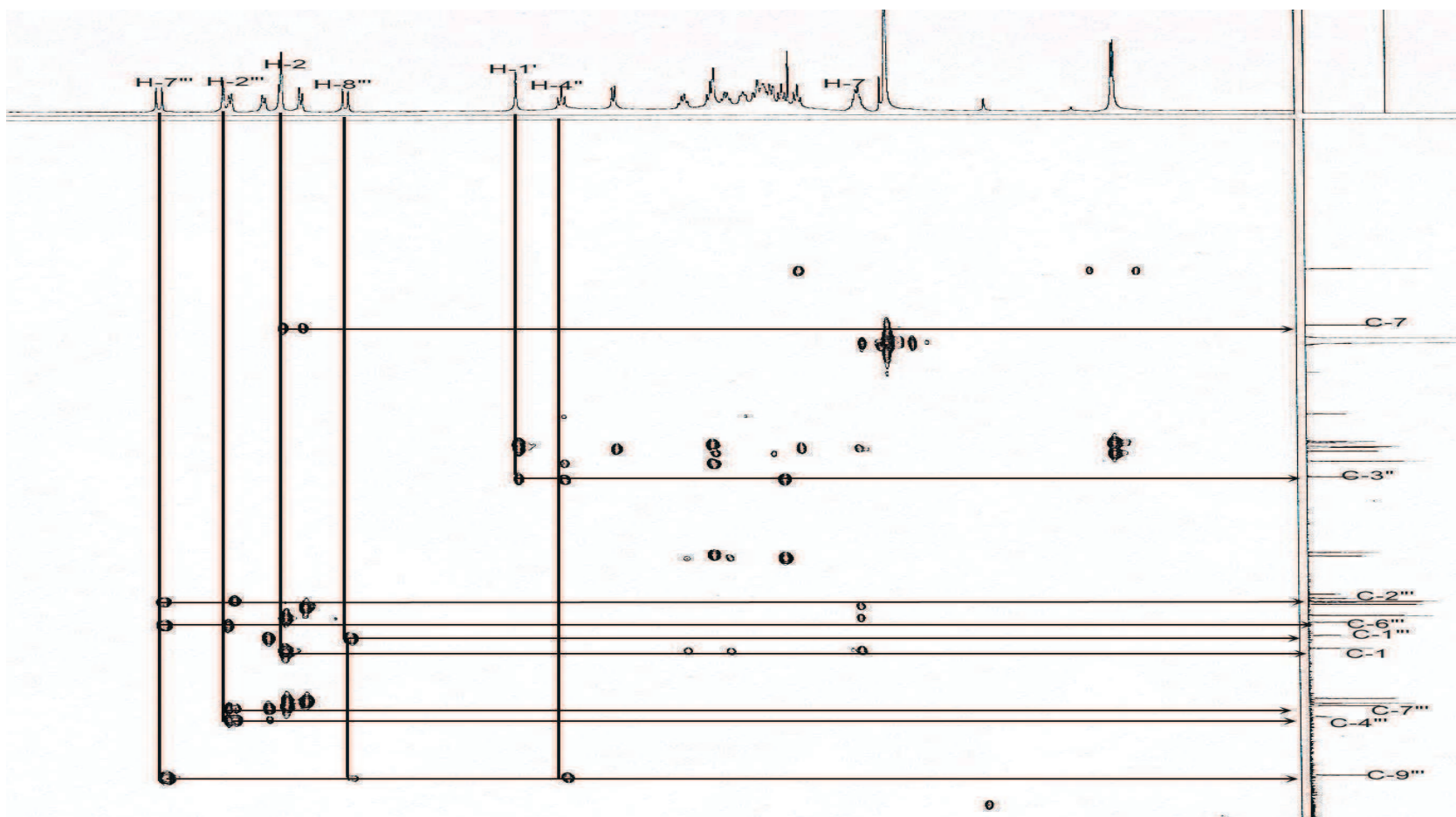
Figure 4.79: HMBC spectrum of Compound PP-3. Please refer to Appendix C: Figures 7.14 (a-g) for enlarged spectra.

Table 4.21: Carbon and proton chemical shifts and HMBC correlation for PP-3.

	^{13}C NMR	^{1}H NMR	HMBC
		Aglycone	
C-1	129.6		
CH-2	116.8	6.58, s	C-1, C-7
C-3	145.5		
C-4	144.1		
CH-5	116.0	6.59, d(J=7.7)	C-3, C-6
CH-6	120.1	6.45, d(J=7.7)	C-2, C-4, C-7
CH$_2$-7	35.5	2.66, m	C-1, C-2, C-6, C-8
CH$_2$-8	70.9	3.22-3.25, m	
		Core sugar	
CH-1"	102.8	4.32, d(J=7.9)	C-8
CH-2"	*75.0	3.15-3.19, m	C-1", C-3"
CH-3"	79.6	3.68-3.72, m	C-2", C-4", C-1'
CH-4"	69.6	4.67, t(J=9.8)	C-2", C-3", C-9'''
CH-5"	*75.0	3.41-3.44, m	
CH$_2$-6"	61.2	3.25-3.34, m	
		Rhamnosyl unit	
CH-1'	101.8	4.99, s	C-3", C-2'
CH-2'	70.8	3.82-3.88, m	
CH-3'	71.0	3.64-3.66, m	C-4'
CH-4'	72.1	3.06-3.09, m	C-3', C-6'
CH-5'	69.3	3.25-3.29, m	
CH$_3$-6'	18.7	0.92, d(J=6.1)	C-4', C-5'
		Caffeoyl unit	
C-1'''	125.8		
CH-2'''	115.1	6.98, s	C-4''', C-6''', C-7'''
C-3'''	*146.2		
C-4'''	149.4		
CH-5'''	116.3	6.70, d(J=8.2)	C-1''', C-3''', C-4'''
CH-6'''	122.0	6.93, d(J=8.2)	C-2''', C-4''', C-7'''
CH-7'''	*146.2	7.42, d(J=15.9)	C-2''', C-6''', C-9'''
CH-8'''	113.9	6.15, d(J=15.9)	C-1''', C-9'''
C-9'''	166.3		

Chemical shifts are in (δ) in ppm, multiplicities and coupling constant in Hz in parentheses.
PP-3 was measured in CD$_3$SOCD$_3$. *indicates the duplication of carbon signals.
Multiplicity caused by overlapping and poorly-resolved ^{1}H signals.

Table 4.22: Carbon chemical shifts of PP-3, verbascoside ([1]Andrary et al., 1982; [2]Gafner et al., 1997), and acteoside (Kitagawa et al., 1984).

	^{13}C NMR			
	PP-3	**Verbascoside[1]**	**Verbascoside[2]**	**Acteoside**
	Aglycone			
C-1	129.6	131.6	131.4	131.4
CH-2	116.8	117.5	116.5	116.2
C-3	145.5	145.6	144.7	145.9
C-4	144.1	144.1	146.1	144.4
CH-5	116.0	116.8	117.1	117.0
CH-6	120.1	121.7	121.2	121.1
CH_2-7	35.5	36.0	36.6	36.3
CH_2-8	70.9	72.1	72.3	72
	Core sugar			
CH-1"	102.8	102.4	104.2	104
CH-2"	75.0	74.6	76.2	75.8
CH-3"	79.6	79.2	81.6	81.5
CH-4"	69.6	69.2	70.5	70.2
CH-5"	75.0	74.6	76.0	75.8
CH_2-6"	61.2	60.8	62.3	62.2
	Rhamnosyl unit			
CH-1'	101.8	101.3	103.0	102.8
CH-2'	70.8	70.6	72.3	72.0
CH-3'	71.0	70.5	72.0	72.0
CH-4'	72.1	71.8	73.8	73.7
CH-5'	69.3	68.8	70.4	70.2
CH_3-6'	18.7	18.2	18.5	18.2
	Caffeoyl unit			
C-1'''	125.8	127.4	127.6	127.5
CH-2'''	115.1	115.8	114.7	115.2
C-3'''	146.2	146.4	149.8	146.6
C-4'''	149.4	149.3	146.8	149.5
CH-5'''	116.3	114.7	116.5	116.4
CH-6'''	122.0	123.4	123.2	123.0
CH-7'''	146.2	148.1	148.0	147.8
CH-8'''	113.9	117.0	115.2	114.6
C-9'''	166.3	169.5	168.3	168.2

PP-3 was measured in CD_3SOCD_3. Verbascoside[1] was measured in D_2O and $(CD_3)_2CO$ (62.86 MHz), while Verbascoside[2] was measured in CD_3OD (50 MHz) and acteoside was measured in CD_3OD (15 MHz).

Table 4.23: Proton chemical shifts of PP-3, verbascoside ([1]Andrary *et al*., 1982; [2]Gafner *et al*., 1997), and acteoside (Kitagawa *et al*., 1984).

	PP-3	Verbascoside[1]	Verbascoside[2]	Acteoside
	^{1}H NMR			
Aglycone				
C-1				
CH-2	6.58 s	6.62 s	6.67 d(1.8)	
C-3				
C-4				
CH-5	6.59 d(7.7)	6.48 d(8)	6.63 d(8)	
CH-6	6.45 d(7.7)	6.62 d(8)	6.54 dd(8,2)	
CH_2-7	2.66 m	2.72 m(8)	2.77 t(7.6)	2.77 t(7)
CH_2-8	3.22-3.25 m	3.60; 3.88 m(8,9)	3.94; 3.71 m	
Core sugar				
CH-1"	4.32 d(7.9)	4.33 d(7.5)	4.41 d(7.7)	4.35 d(8)
CH-2"	3.15-3.19 m	3.22 dd(7.5,9)		
CH-3"	3.68-3.72 m	3.70 t(9-9.5)	3.62 dd(10.7,10)	
CH-4"	4.67 t(9.8)	4.72 t(9.5)	3.35-3.5	
CH-5"	3.41-3.44 m	3.45 m	3.50-3.60	
CH_2-6"	3.25-3.34 m	3.70; 3.45	4.51; 4.34 dd(11.8,2; 11.8, 5.7)	
Rhamnosyl unit				
CH-1'	4.99 s	5.03 d(1)	5.01 d(1.3)	5.17 br s
CH-2'	3.82-3.88 m	3.70 dd(1,2.5)	3.94-4.00	
CH-3'	3.64-3.66 m	3.3 dd(2.5,9.5)	3.69 dd(9.5,2.9)	
CH-4'	3.06-3.09 m	3.12 t(9.5)	3.35-3.45	
CH-5'	3.25-3.29 m	3.36 m	3.85-3.95	
CH_3-6'	0.92 d(6.1)	1.01 d(6)	1.25 d(6.1)	1.10 d(6)
Caffeoyl unit				
C-1'''				
CH-2'''	6.98 s	7.00 s	7.15 d(1.7)	
C-3'''				
C-4'''				
CH-5'''	6.70 d(8.2)	6.74 d(8)	6.79 d(8.3)	
CH-6'''	6.93 d(8.2)	6.93 d(8)	7.01 dd(8.3,1.7)	
CH-7β'''	7.42 d(15.9)	7.43 d(16)	7.61 d(15.9)	7.55 d(15)
CH-8α'''	6.15 d(15.9)	6.18 d(16)	6.38 d(15.9)	6.23 d(15)
C-9'''				

Chemical shifts are in (δ) in ppm, multiplicities and coupling constant in Hz in parentheses.
PP-3 was measured in CD_3SOCD_3 Verbascoside[1] was measured in D_2O and $(CD_3)_2CO$ (250 MHz), while Verbascoside[2] was measured in CD_3OD (200 MHz) and acteoside was measured in CD_3OD.
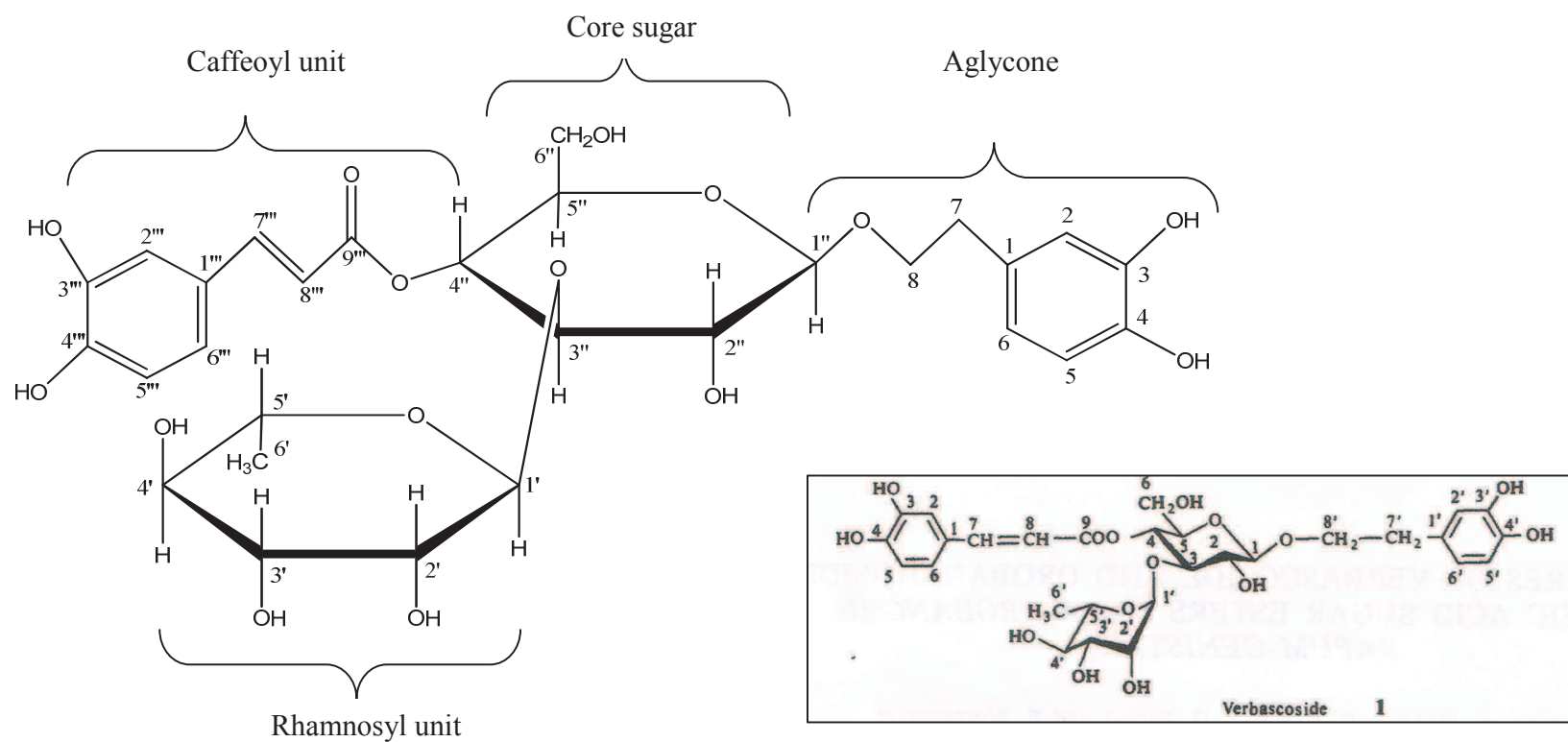
Figure 4.80: Molecular structure of PP-3, 3, 4-dihydroxyphenethyl-(3"-O-α-L-rhamnopyranosyl-4"-O-caffeoyl)-β-D-glucopyranoside. The structure on right bottom is verbascoside (Andrary *et al.*, 1982).

4.7   IC$_{50}$ Determination of DPPH Free Radical Scavenging Activity

Based on the preliminary screening result, leaf and rhizome F-5 were active in inhibition of DPPH free radicals (Table 4.12). The isolated compounds, together with the reference standards were subjected to five-point DPPH free radical scavenging serial dilution assay (Tables 4.24 and 4.25). PP-2 and PP-3 showed strong antiradical activity with IC$_{50}$ values of 15.25 µg/ml, 16.25 µg/ml, respectively (Figures 4.84 and 4.85), while PP-1 attained an inhibition rate of 50% at the concentration of 34 µg/ml (Figure 4.83). The corresponding IC$_{50}$ values of quercitin and L-ascorbic acid were 7.5 µg/ml and 11 µg/ml (Figures 4.81 and 4.82).

Table 4.24: Percentage inhibition of quercitin and L-ascorbic acid via DPPH-free radical scavenging assay at various concentrations.

Reference standard	Concentrations (μg/ml)	Percentage of inhibition ± SD (%)
Quercitin	50	92.09 ± 0.55
	25	91.74 ± 0.06
	12.5	82.05 ± 8.39
	6.25	39.39 ± 8.71
	3.125	13.69 ± 3.74
L-ascorbic acid	50	93.45 ± 0.28
	25	93.42 ± 0.20
	12.5	57.59 ± 7.48
	6.25	21.09 ± 9.79
	3.125	6.88 ± 3.36

DPPH free radical scavenging activity was expressed as percentage ± standard deviation of three independent experiments.
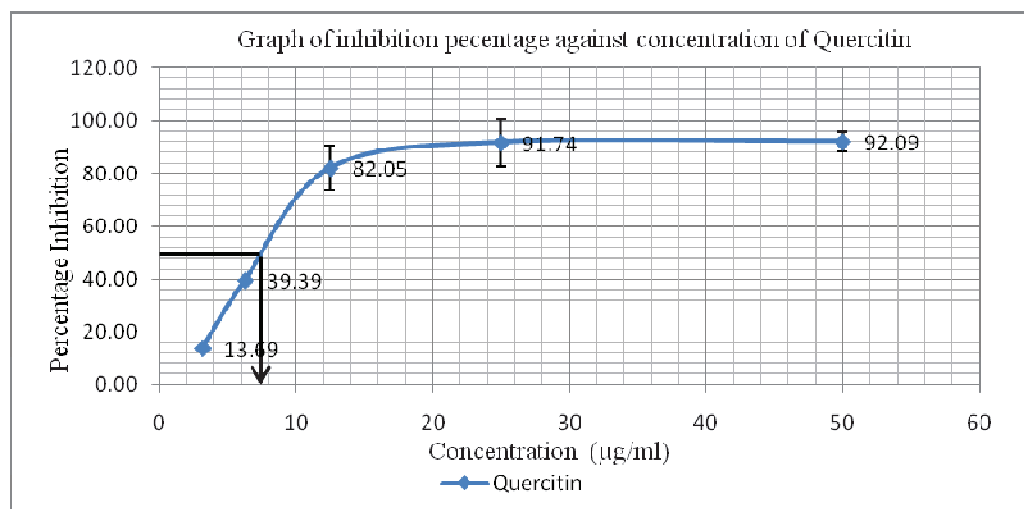
Figure 4.81: DPPH free radical scavenging activity of Quercitin at various concentrations and IC_{50} is 7.5 µg/ml. The scavenging activity was presented as percentage inhibition ± standard deviation (%).
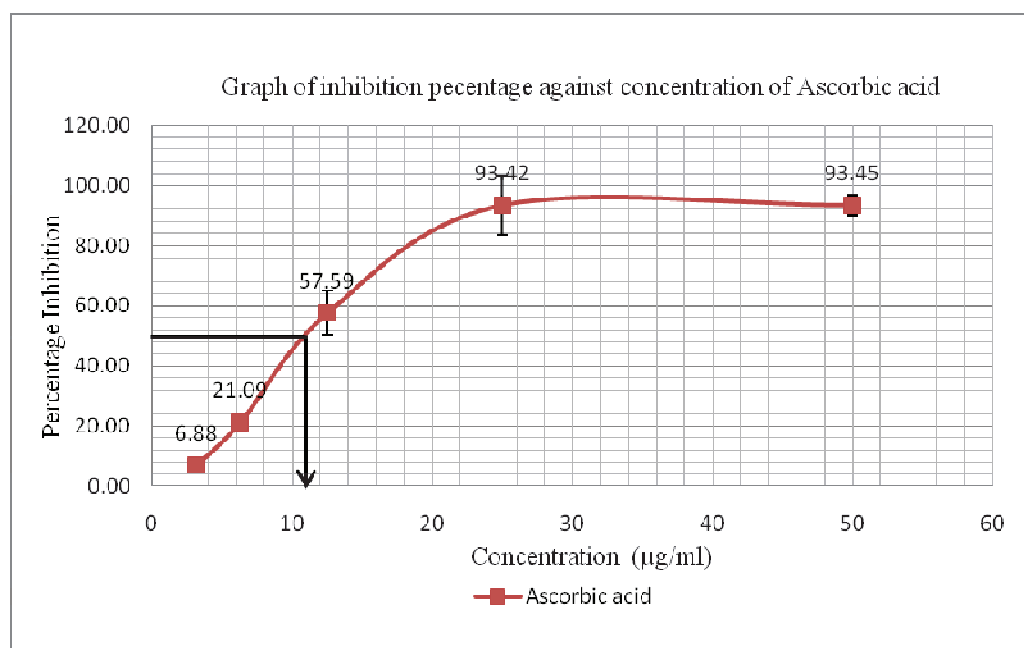
Figure 4.82: DPPH free radical scavenging activity of Ascorbic acid at various concentrations and IC_{50} is 11 µg/ml. The scavenging activity was presented as percentage inhibition ± standard deviation (%).

Table 4.25: Percentage inhibition of PP-1, PP-2 and PP-3 via DPPH-free radical scavenging assay at various concentrations.

Compounds	Concentrations (μg/ml)	Percentage of inhibition ± SD (%)
PP-1	50	81.83 ± 4.40
	25	32.27 ± 6.65
	12.5	10.06 ± 4.68
	6.25	1.07 ± 6.63
	3.125	-10.66 ± 0.44
PP-2	50	90.96 ± 0.47
	25	76.46 ± 12.16
	12.5	39.52 ± 5.46
	6.25	11.69 ± 2.05
	3.125	3.86 ± 5.70
PP-3	50	91.00 ± 0.79
	25	75.91 ± 12.85
	12.5	34.63 ± 7.90
	6.25	12.11 ± 6.80
	3.125	2.13 ± 3.33

DPPH free radical scavenging activity was expressed as percentage ± standard deviation of three independent experiments.
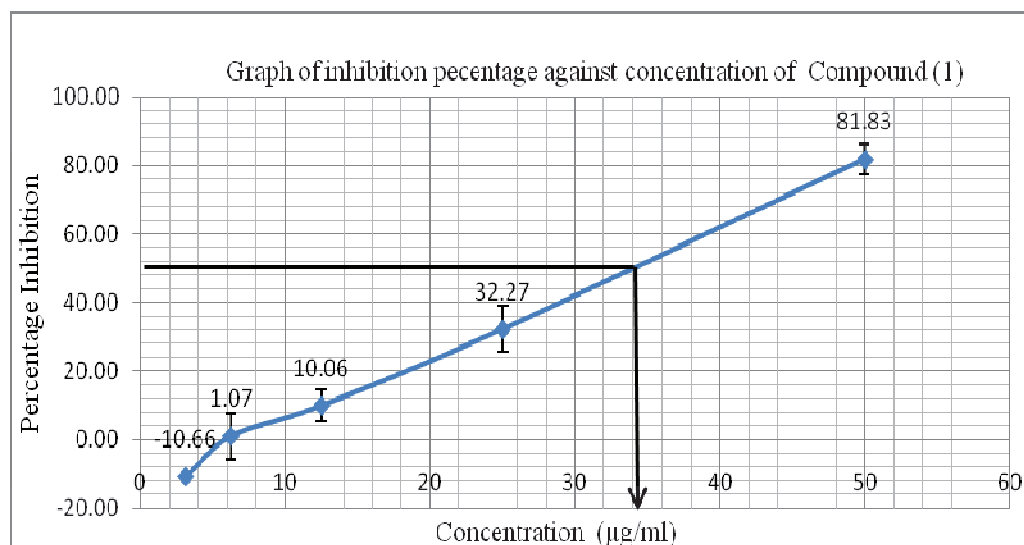
Figure 4.83: DPPH free radical scavenging activity of PP-1 at various concentrations and IC_{50} is 34 µg/ml. The scavenging activity was presented as percentage inhibition ± standard deviation (%).
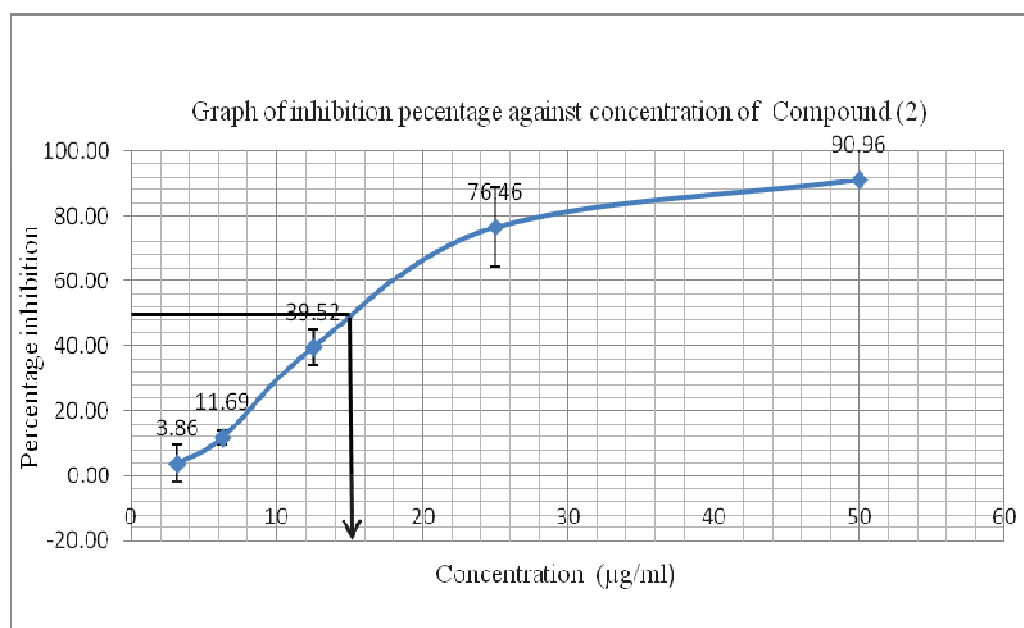
Figure 4.84: DPPH free radical scavenging activity of PP-2 at various concentrations and IC_{50} is 15.25 µg/ml. The scavenging activity was presented as percentage inhibition ± standard deviation (%).
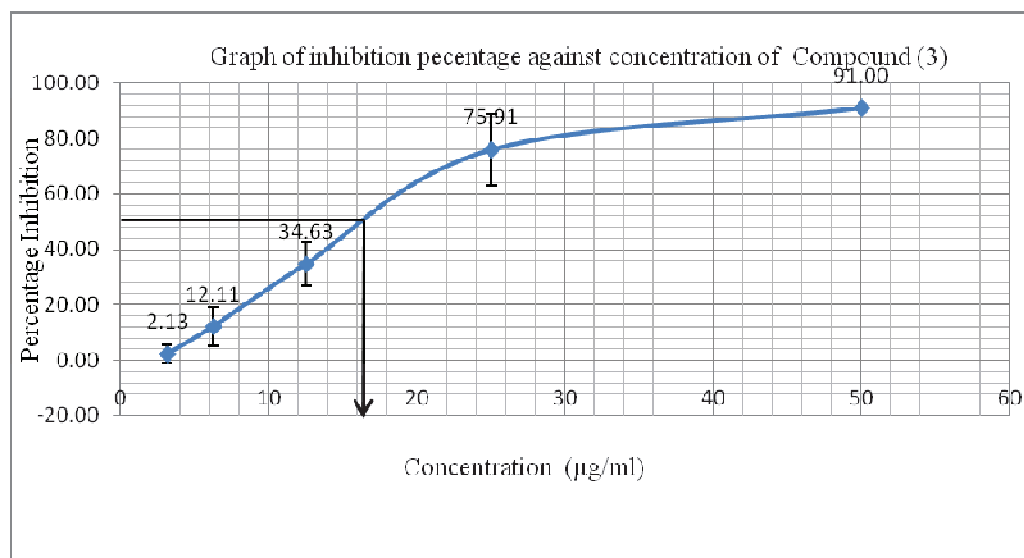
Figure 4.85: DPPH free radical scavenging activity of PP-3 at various concentrations and IC$_{50}$ is 16.25 µg/ml. The scavenging activity was presented as percentage inhibition ± standard deviation (%).

4.8   IC$_{50}$ Determination of Cytotoxicity against K-562 Cell Line

Three isolated compounds, together with the reference standards were subjected to five-point MTT serial dilution assay (Tables 4.26 and 4.27). PP-1, PP-2, and PP-3 exhibited strong cytotoxic activity against K-562 cell line with 50% of cell killing rate at concentration of 18 µg/ml, 16.5 µg/ml, 17 µg/ml, respectively (Figures 4.88 to 4.90). The corresponding IC$_{50}$ values obtained for doxorubicin and cisplastin were 1.1 µg/ml and 1.5 µg/ml (Figures 4.86 and 4.87). Morphology of cells after treated with control drugs, doxorubicin and cisplastin are shown in Plate 4.1 to Plate 4.4, while cell morphology after treated with PP-1, PP-2, and PP-3 are demonstrated in Plate 4.5 to Plate 4.10.
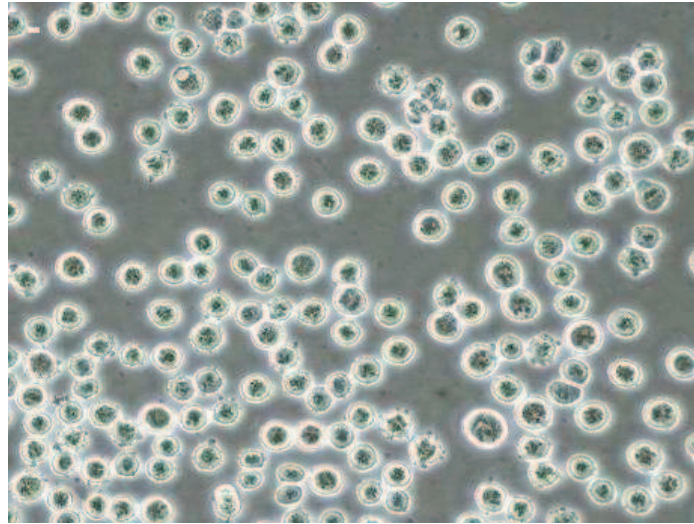
Plate 4.1: Morphology of K-562 cells (positive control), incubated in RPMI-1640 medium for 72 hours (200x). All cells were round and multinucleated.
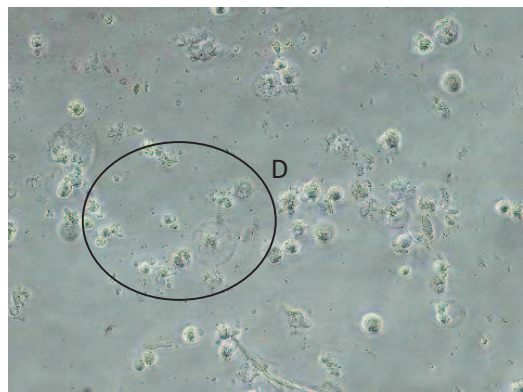
(A) 1 µg/ml

(B) 0.5 µg/ml
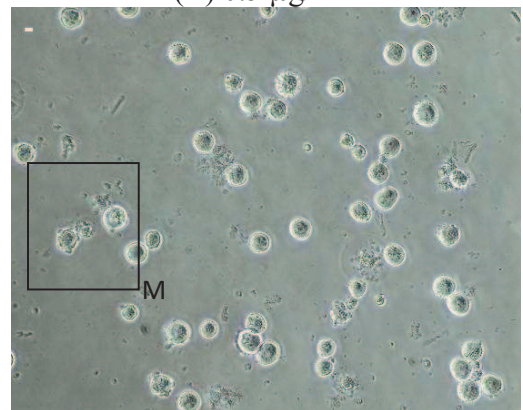
(C) 0.25 µg/ml

(D) 0.125 µg/ml

Plate 4.2 (A, B, C, D): Morphology of K-562 cells treated with various concentrations of doxorubicin after 72 hours (200x). Note: D= dead cells, M= membrane blebbing cells.
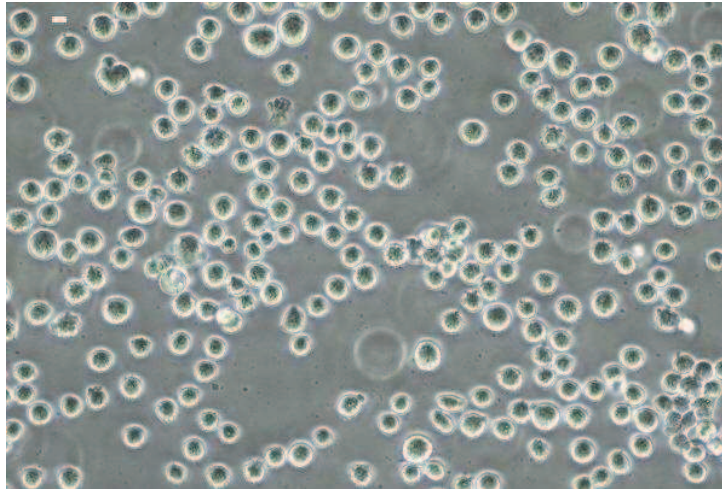
Plate 4.3: Morphology of K-562 cells (positive control), incubated in RPMI-1640 medium for 72 hours (200x). All cells were round and multinucleated.
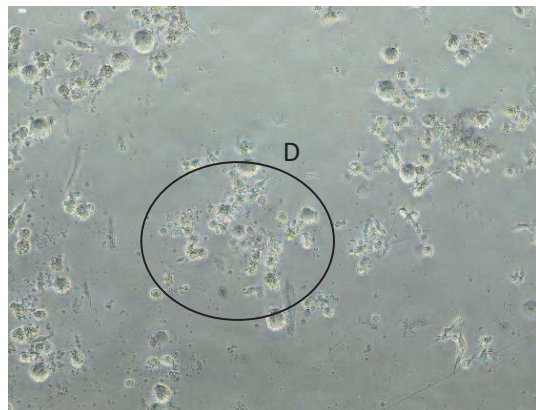
(A) 1 µg/ml

(B) 0.5 µg/ml
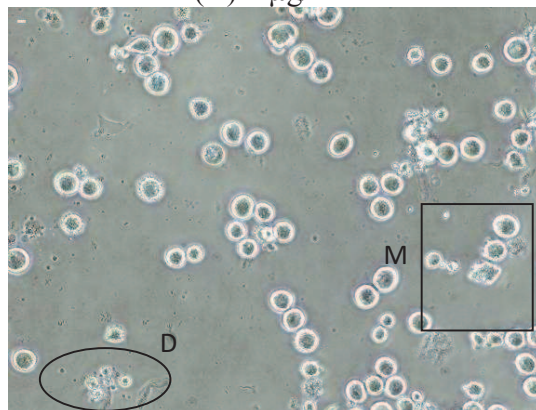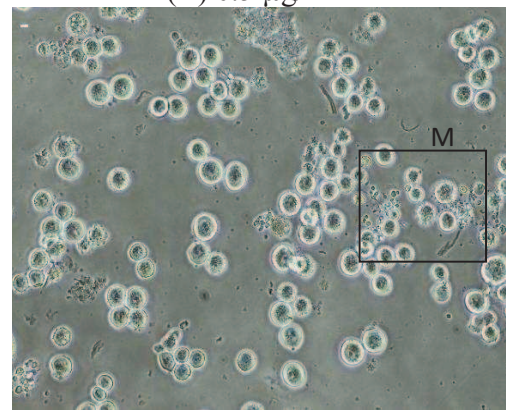
(C) 0.25 µg/ml

(D) 0.125 µg/ml

Plate 4.4 (A, B, C, D): Morphology of K-562 cells treated with various concentrations of cisplastin after 72 hours (200x). Note: D= dead cells, M= membrane blebbing cells.

Table 4.26: Cell viability of K-562 cells after treated with Doxorubicin and Cisplastin at various concentrations.

Reference standard	Concentrations (µg/ml)	Cell Viability ± SD (%)
Doxorubicin	1	7.59 ± 0.61
	0.5	7.85 ± 1.44
	0.25	22.55 ± 3.99
	0.125	46.28 ± 3.28
	0.0625	59.18 ± 4.19
	0.03125	64.54 ± 4.41
Cisplastin	10	3.72 ± 0.96
	5	15.73 ± 1.14
	2.5	37.20 ± 3.47
	1.25	55.59 ± 2.17
	0.625	71.00 ± 8.94
	0.3125	81.37 ± 1.88

Cell viability was expressed as percentage ± standard deviation value of three independent experiments.
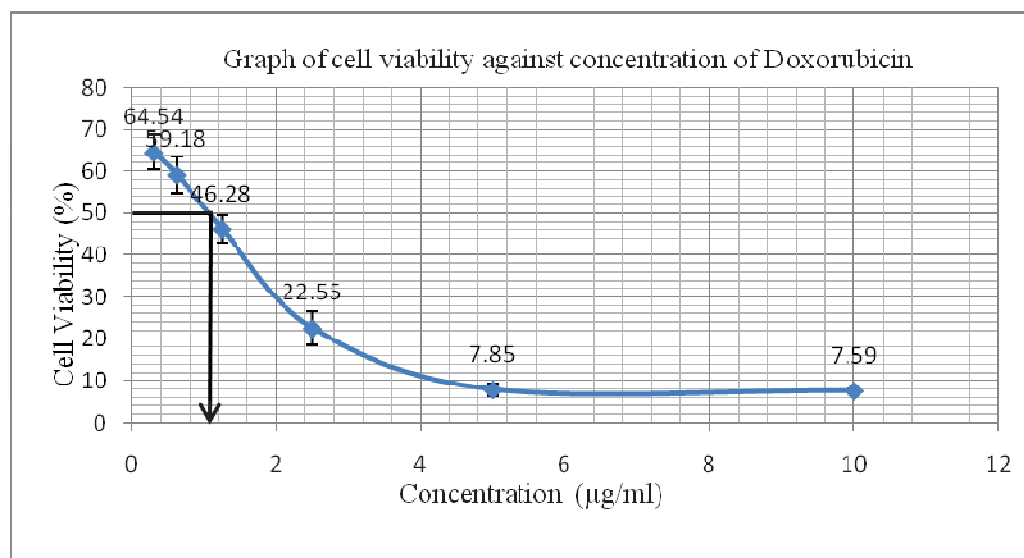
Figure 4.86: Cell viability of K-562 cells after treated with Doxorubicin at various concentrations and IC$_{50}$ is 1.1 µg/ml. The cytotoxic activity was expressed as cell viability ± standard deviation (%).
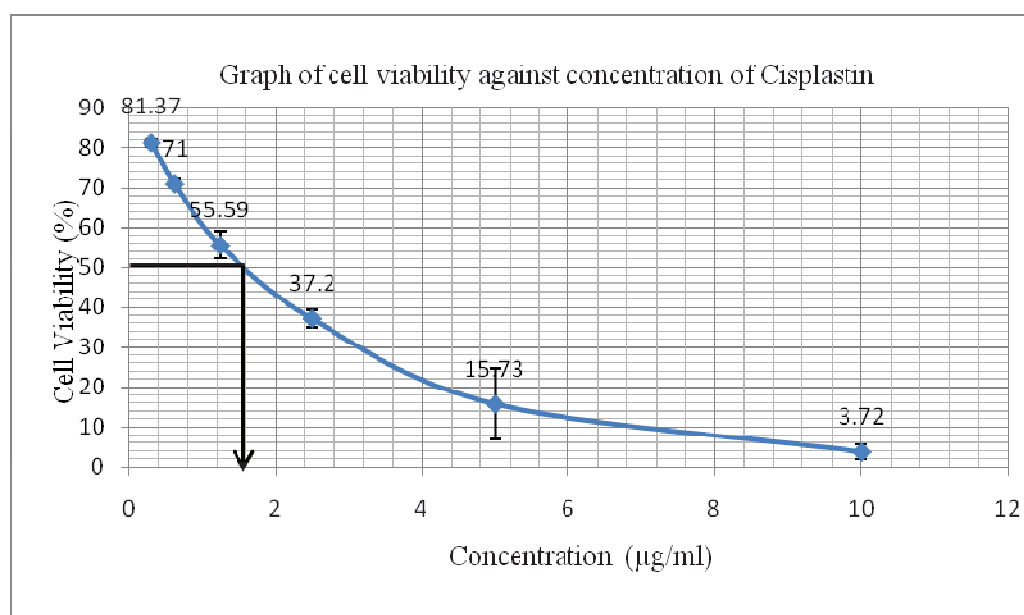
Figure 4.87: Cell viability of K-562 cells after treated with Cisplastin at various concentrations and IC$_{50}$ is 1.5 µg/ml. The cytotoxic activity was expressed as cell viability ± standard deviation (%).
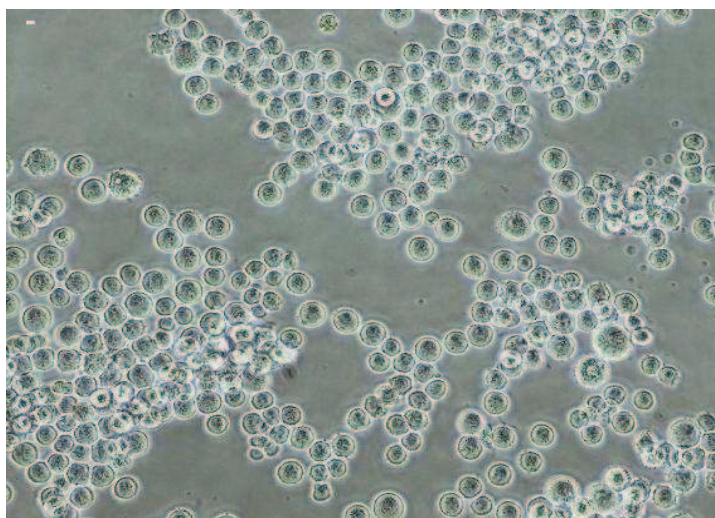
Plate 4.5: Morphology of K-562 cells (positive control), incubated in RPMI-1640 medium for 72 hours (200x). All cells were round and multinucleated.
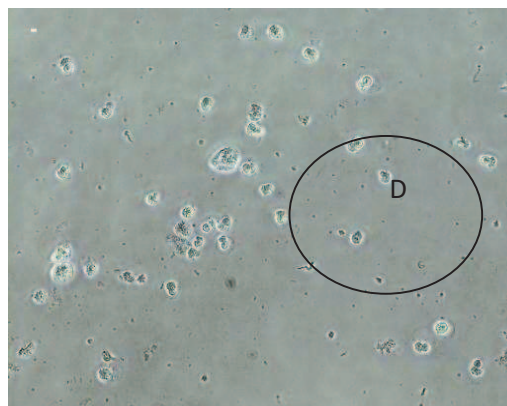
(A) 50 µg/ml
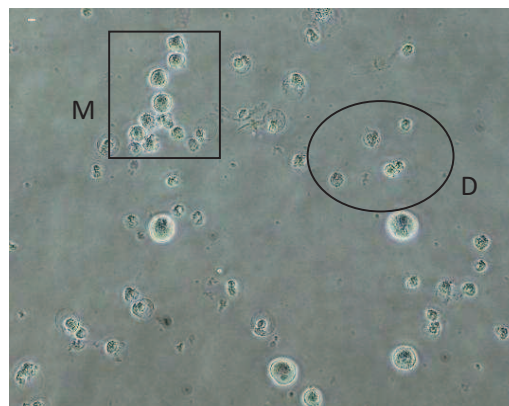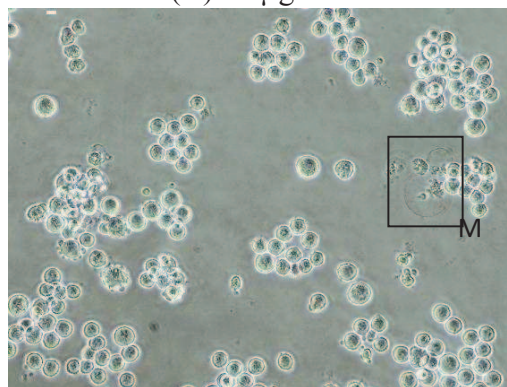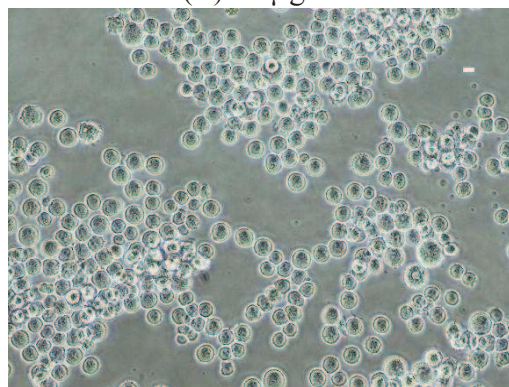
(B) 25 µg/ml

(C) 12.5 µg/ml

(D) 6.25 µg/ml

Plate 4.6 (A, B, C, D): Morphology of K-562 cells treated with various concentrations of compound PP-1 after 72 hours (200x). Note: D= dead cells, M= membrane blebbing cells.
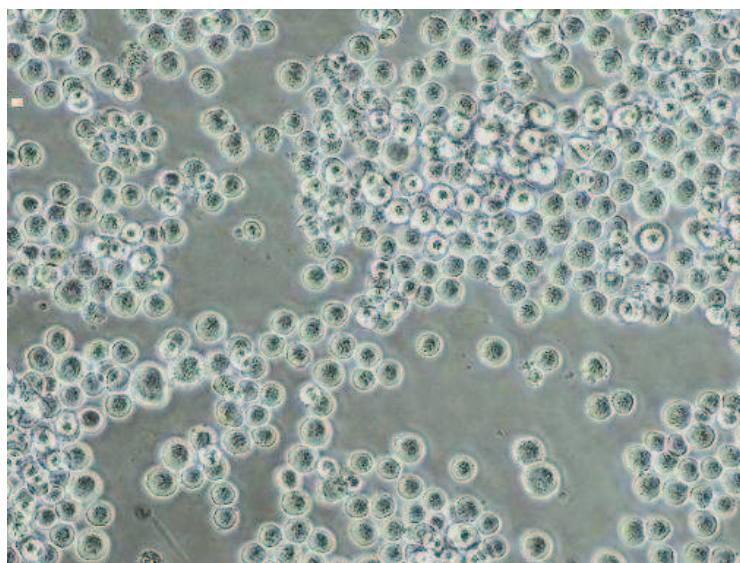
Plate 4.7: Morphology of K-562 cells (positive control), incubated in RPMI-1640 medium for 72 hours (200x). All cells were round and multinucleated.

(A) 50 µg/ml
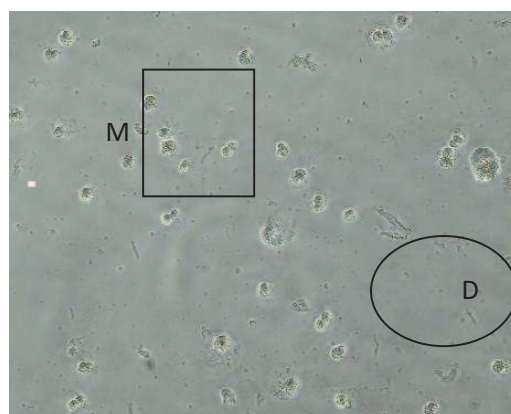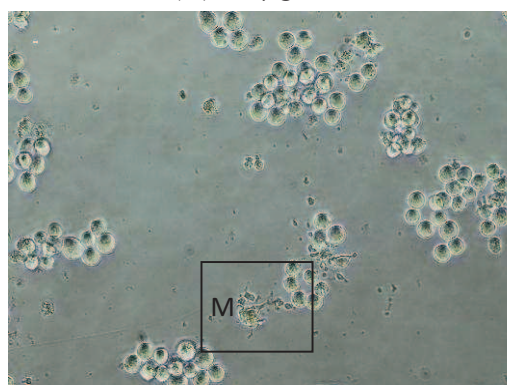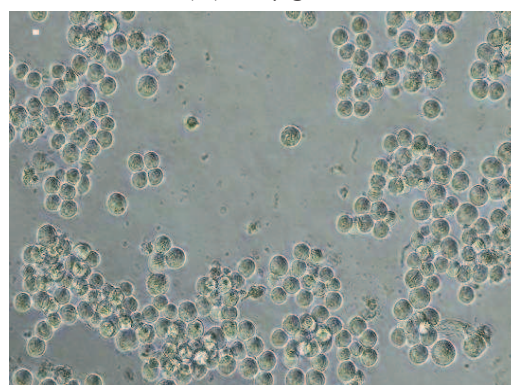
(B) 25 µg/ml

(C) 12.5 µg/ml

(D) 6.25 µg/ml

Plate 4.8 (A, B, C, D): Morphology of K-562 cells treated with various concentrations of compound PP-2 after 72 hours (200x). Note: D= dead cells, M= membrane blebbing cells.
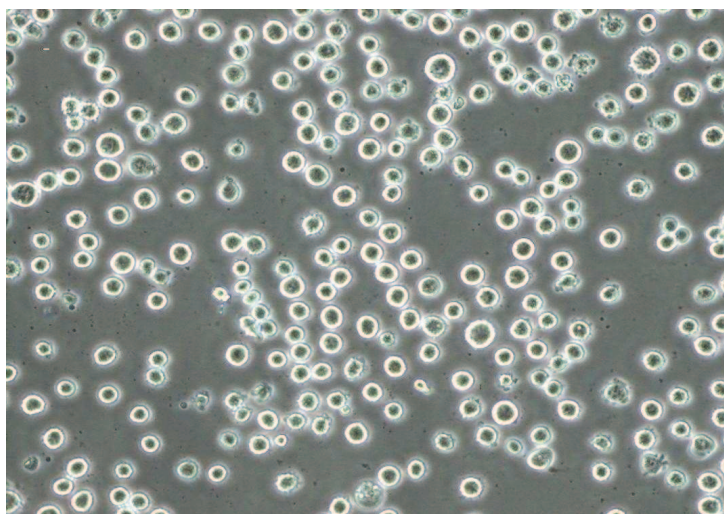
Plate 4.9: Morphology of K-562 cells (positive control), incubated in RPMI-1640 medium for 72 hours (200x). All cells were round and multinucleated.
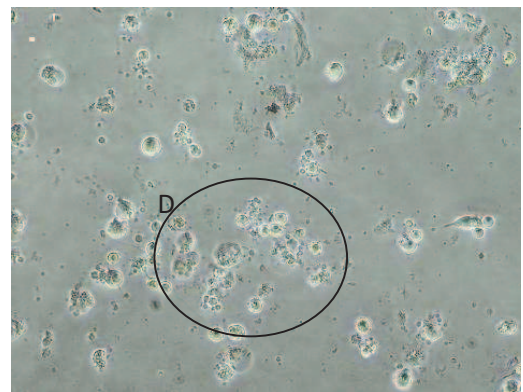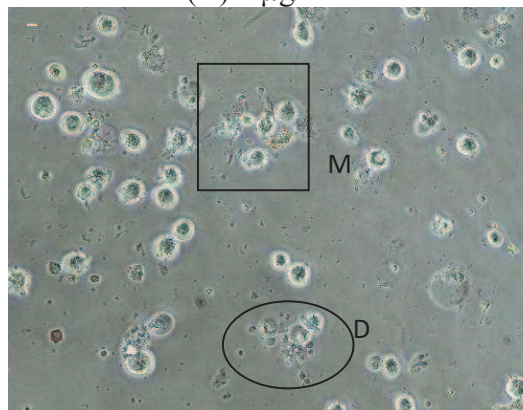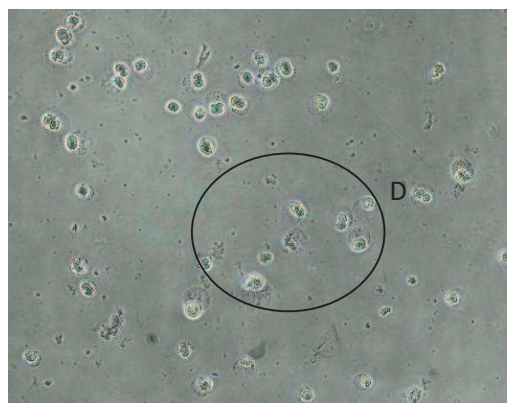

(A) 50 µg/ml
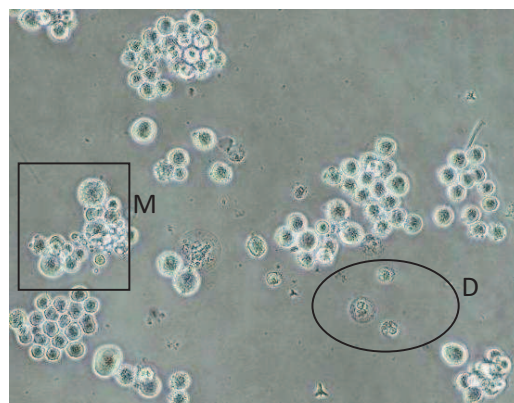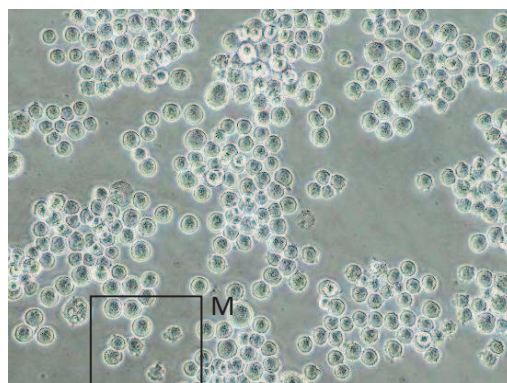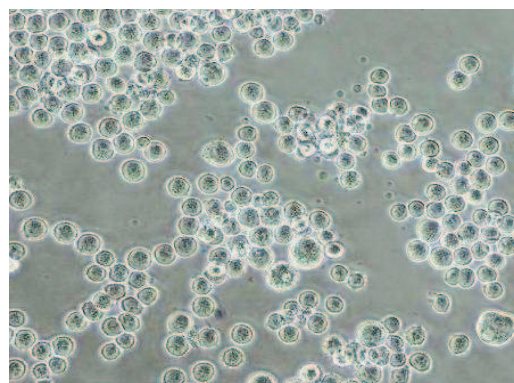
(B) 25 µg/ml

(C) 12.5 µg/ml

(D) 6.25 µg/ml

Plate 4.10 (A, B, C, D): Morphology of K-562 cells treated with various concentrations of compound PP-3 after 72 hours (200x). Note: D= dead cells, M= membrane blebbing cells.

Table 4.27: Cell viability of K-562 cells after treated with PP-1, PP-2, PP-3 at various concentrations.

Compounds	Concentrations (μg/ml)	Cell Viability ± SD (%)
PP-1	50	8.13 ± 2.02
	25	25.17 ± 8.15
	12.5	80.55 ± 17.64
	6.25	91.77 ± 8.31
	3.125	96.68 ± 8.87
PP-2	50	6.80 ± 2.76
	25	10.15 ± 2.62
	12.5	81.07 ± 5.37
	6.25	90.47 ± 11.92
	3.125	92.10 ± 11.34
PP-3	50	7.21 ± 1.35
	25	18.50 ± 4.27
	12.5	71.47 ± 11.36
	6.25	72.11 ± 8.51
	3.125	76.26 ± 10.93

Cell viability was expressed as percentage ± standard deviation value of three independent experiments.
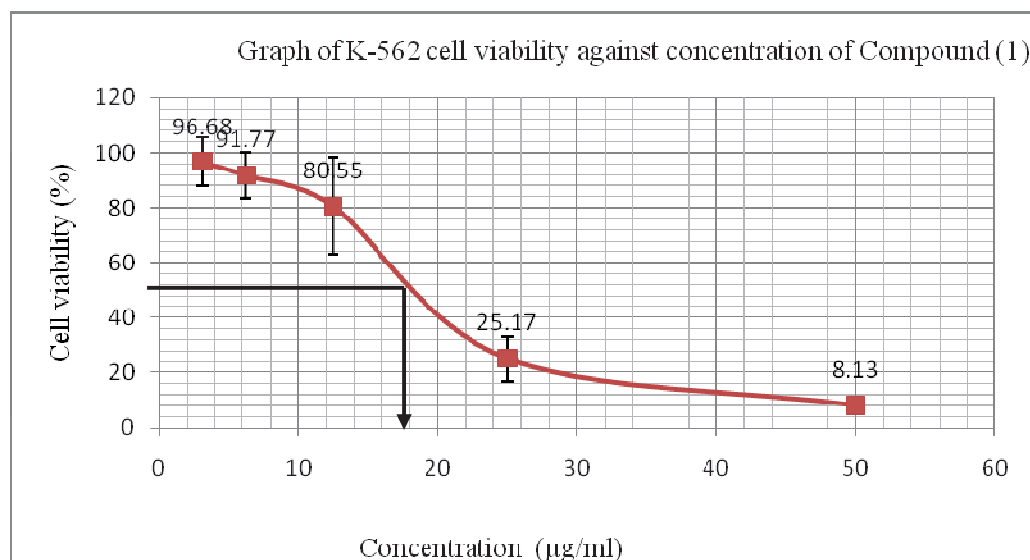
Figure 4.88: Cell viability of K-562 cells after treated with PP-1 at various concentrations and IC_{50} is 18 µg/ml. The cytotoxic activity was expressed as cell viability ± standard deviation (%).
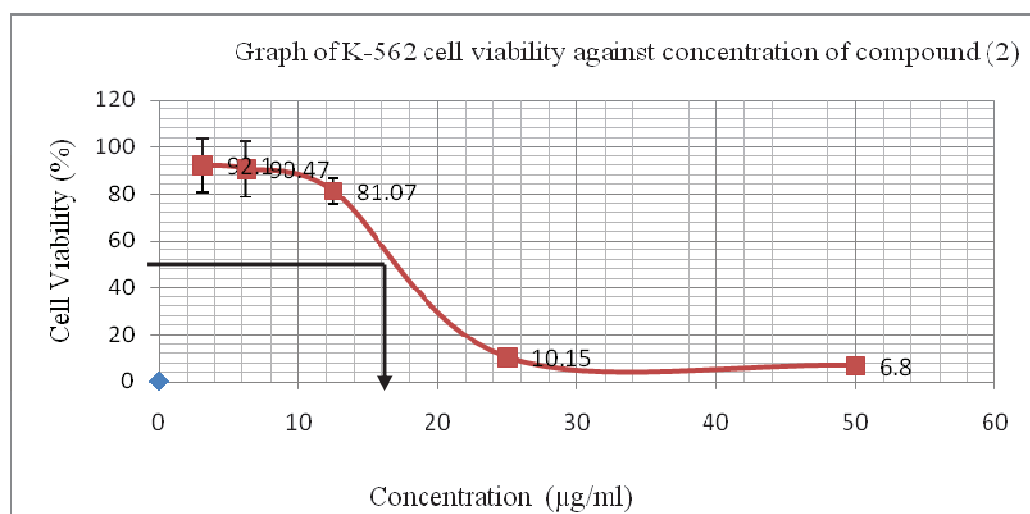
Figure 4.89: Cell viability of K-562 cells after treated with PP-2 at various concentrations and IC_{50} is 16.5 µg/ml. The cytotoxic activity was expressed as cell viability ± standard deviation (%).
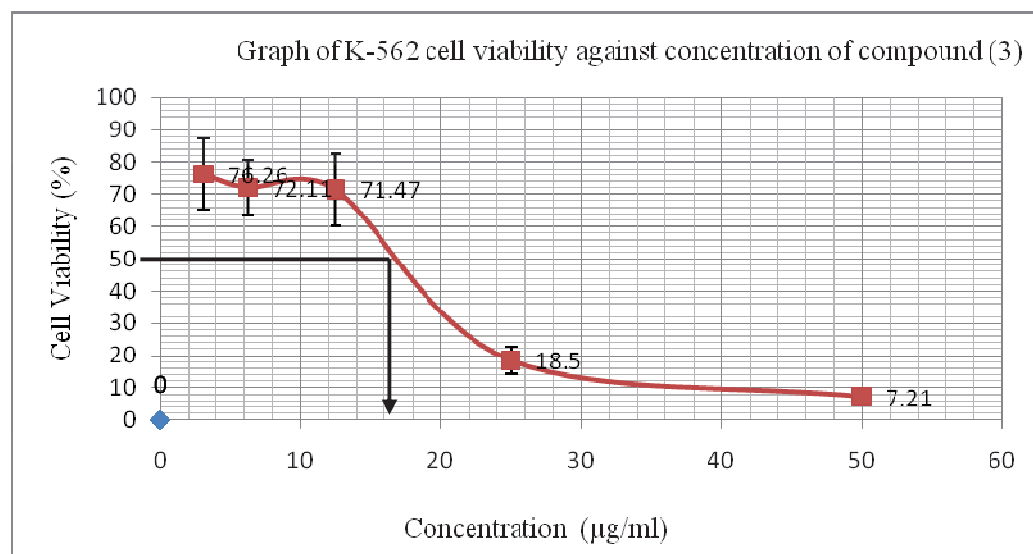
Figure 4.90: Cell viability of K-562 cells after treated with PP-3 at various concentrations and IC_{50} is 17 µg/ml. The cytotoxic activity was expressed as cell viability ± standard deviation (%).

CHAPTER 5

DISCUSSIONS

Fingerprinting analysis of the bioactive compounds as a whole formulation to yield a common fingerprint profile in first dimension is essential. With the intention to enhance the drug discovery efficacy and provide a rapid understanding of the pharmacological profiles of the potential plant, the development of well defined fingerprints is needed. The documentation of phytochemical fingerprints can facilitate to identify the morphological and geographical variations in medicinal raw plant materials (Sunita and Abhishek, 2008). An all-embracing chemical fingerprint profile may be impossible to be created, but a representative fingerprint pattern is expected to be established first, followed by other fingerprints as the new evidence demand (Xie *et al*., 2006). In this context, the first dimensional fingerprint profile serves as the representative fingerprint, while the second dimensional profile affords a more comprehensive picture of the active group of constituents in the plant.

5.1 Sample Preparation

Herbal raw materials are complex matrices, generating countless number of metabolites with diverse functional groups and solubility. The protocols of extraction as well as sample preparation are the key factor to yield informative fingerprints of herbal medicines (Liang *et al*., 2004). Maceration *in vacuo* with appropriate solvent governed by the nature of the target phytochemicals is desirable prior to fractionation of the active constituents. In this context, extraction that covers a broad range of compounds is preferred, in order to develop a non-selective first dimensional fingerprint profile. For a total extraction, a polar organic solvent, methanol was employed in the attempt to extract as many constituents as possible. The extraction with alcoholic solvent increases the efficiency of extracting large amount of constituents owing to different polarity (Satyajit *et al*., 2005). Widmer *et al.* (2008) also stated that employment of polar solvent could yield meaningful fingerprints with many intense zones without interference with sample matrix.

Subsequently, the methanolic crude extract was re-dissolved in water and fractionated according to the solubility properties of the constituents. In the present study, the Solid Phase Extraction (SPE) method was chosen, rather than liquid-liquid extraction (LLE) technique and conventional gravity column chromatography for fractionation purpose. To yield a distinctive fingerprint profile for each active fraction, the preparation of consistent fractions is essential.

The pre-packed SPE columns with uniform chemically-modified silica particles provide high extraction efficiencies as well as constant and reproducible results. Reversed phase stationary phase composing of silica bonded saturated hydrocarbon C18 chains was utilized in this case and the elution mechanisms, i.e. the mobile phase and extraction conditions were optimized. Due to the non-specificity of reversed phase extraction, a wide range of compounds would be retained (Phenomenex, 2008). Most of the herbal tinctures were traditionally prepared by steeping the plant materials in water or aqueous alcohol, which favours the extraction of hydrophilic compounds (Sena *et al*., 2009). The reversed phase extraction was performed to yield polar analytes from the aqueous matrix. Hence, an aqueous environment was prepared to achieve the optimal retention, where the sample was dissolved with water and methanol in proportion of 9:1 (v/v). The cartridges were washed with an aqueous mixture in 5% of methanol after sample loading. The crude extracts were fractionated by eluting with 100% water, followed by increasing proportions of methanol and lastly dichloromethane, consecutively, to yield 11 fractions. Acidified methanol with 2M of nitric acid was served as last elution solvent, with the purpose of eluting any retained amine group compounds. As stated by Phenomenex (2008), the silica based sorbents may contain some un-reacted silanols that may provide acidic and polar bonding reactions.

5.2 HPTLC as Fingerprint Developing Tool

The profiling of relative amounts of the active ingredients found in herbal material happened to be a comprehensive approach for the purpose of species authentication, identification and evaluation of the quality of herbal medicine (Xie *et al.,* 2006). World Health Organization has confirmed the employment of chromatographic fingerprinting method as strategy of quality assessment of herbal products (1991). Many analytical techniques that are able to provide the recognition pattern of a complete set of analytes were suggested (Xie *et al*., 2007; Fiehn, 2008; García-Pérez *et al*., 2008; Ni *et al*., 2008; Suzuki *et al*., 2008; Yang *et a*l., 2008). However, many of the fingerprint techniques employed sophisticated equipments and were time-consuming; the methods described do not meet the requirement for routine identification of raw material (Widmer *et al*., 2008). HPTLC is advantageous in terms of high sample throughput with low operating cost, rapid sample preparation, short analysis time, and analytical assurance by means of the validation according to the optimized conditions (Rathi *et al*., 2008).

In the current project, the fingerprint profiles of planar chromatography (HPTLC) combining with digital scanning profiling of the rhizome and leaf parts of *Paraboea paniculata* were developed to identify and distinguish both parts in detail. The first dimensional fingerprint profiles of crude leaf and rhizome were established as picture-like images of HPTLC at the wavelength of 254 nm and 366 nm, under white light after chemical derivatization as well as digital scanning

profiles from 200 nm to 800 nm. The second dimensional fingerprint patterns would be the active cytotoxic fractions of both leaf and rhizome. These second dimensional HPTLC images and the peak-to-peak distributions in the digital scanning profiles explain the distribution of the active ingredients in both parts. The crude extract might be dominated by a small number of highly concentrated metabolites; thus the second dimensional pattern allows the profiling of active fraction that contains trace metabolites (Kopka *et al*., 2004). By converting the HPTLC image to digital scanning fingerprint, all the peak intensities of peak profiles were in concurrence with the bands and their brightness of the TLC images. Thus, the peak profiles can be easily evaluated by comparison of a characteristic pattern, including the peaks intensities and peak-to-peak ratios (Chen *et al*., 2006).

5.2.1 Optimization of TLC Conditions

Due to the off-line principle of planar chromatography, individual manual steps are involved together with discrete devices employed for sample application, plate development, derivatization as well as documentation. The operating parameters of all devices were optimized and kept constant throughout the establishment of fingerprint profiles, in order to obtain reproducible and stable results.

At the early step, after the samples were sprayed on plate, the twin-trough chamber was saturated with one wall fitted with filter paper and wetted with developing solvent, for 20 minutes. This allows the chamber to reach its equilibration of the developing solvent with its vapour. The added procedure of saturating the chamber with mobile phase is essential before plate conditioning in order to yield good resolution and well defined bands (Rumalla *et al*., 2008).

The developed plate was then pre-conditioned by placing the plate on the other wall of the chamber, in order to achieve equilibration between the gas phases in tank with surface of stationary phase. An increase in the activity of the stationary phase is achieved by implementing the step of preconditioning the plate with developing solvents before plate development.

A known marker compound (reference) was employed for all plates' development, in order to calibrate the scanned fingerprint profile of each system. Curcumin, quercitin, and stigmasterol were used to ensure the reproducibility of the fingerprint profiles obtained.

5.2.2 Selection of Stationary and Mobile Phases

For TLC separation, the mobile phase controls the separation, while stationary phase provides a media for analyte interaction. An appropriate gradient of developing solvent (i.e., types of solvents and ratios) for a chosen sorbent is

required to provide separation over a wide polarity range (Gocan *et al*., 1996). The silica gel was chosen at the first choice, as it is by far the most widely used adsorbent. In optimizing the mobile phase systems, approximately 10 neat solvents were chosen as mobile phase for separation in the first place. The three solvents that give the best separation will be selected for further ratio adjustment to achieve the optimum separation, which is in the R_f range of 0.2 to 0.5. As for complex substances, the R_f range of 0.1 to 0.8 is expected for distinct separation (Nyiredy *et al*., 1985). All the TLC plates employed containing the fluorescence indicator F_{254} emit, thus, substances that absorb UV 254 nm are visible as dark bands on the plate. The substances are noticeable as colour fluorescent zones against the dark background when the compounds excited by UV 366 nm (Reich and Widmer, 2009).

Since crude leaf and rhizome composed of complex ingredients, the first dimensional fingerprint profile demonstrated should give the most number of peaks. In present study, the attempt of double development with the employment of two different mobile phases on the same adsorbent was demonstrated, for the purpose of profiling the ingredients in crude extracts (Figures 5.1 a and b). After two times of development, it was found to be effective in resolving the complex substances by separating the compounds in a wide range of polarity in single TLC plate. However, it was not recommended due to the stability issues, long duration and low reproducibility (the more steps involved in the method, for example, development and drying steps, the more variation).
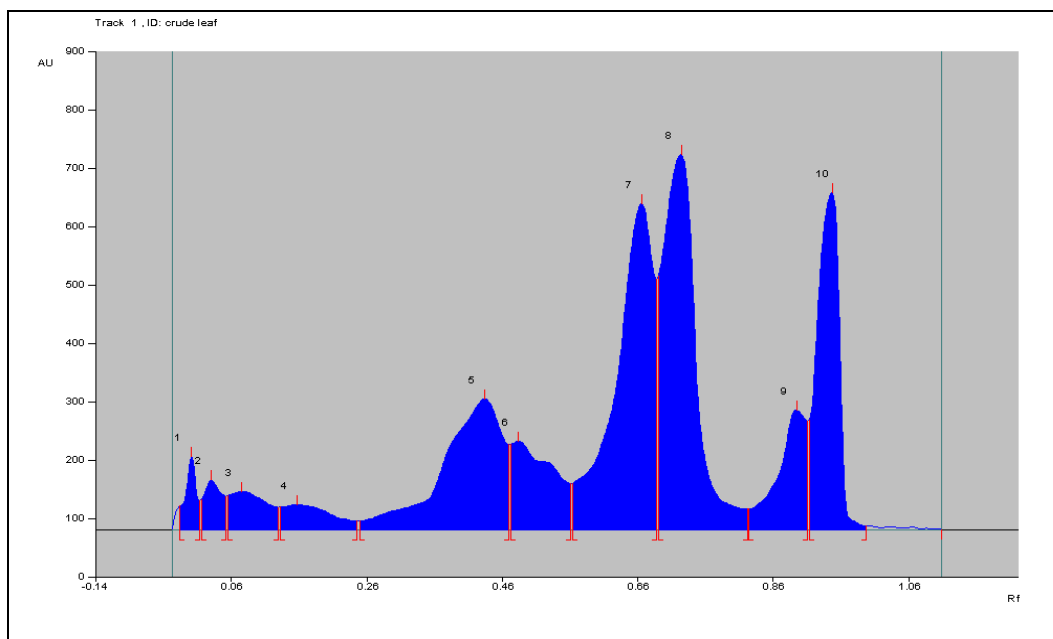
Figure 5.1(a): HPTLC first development fingerprint profile of leaf crude extract. Stationary phase: HPTLC Si 60 F_{254}. Mobile phase: ethyl acetate: methanol: acetonitrile: water: acetic acid (77%: 11%: 5.5%: 5.5%: 1%). UV 254 nm.
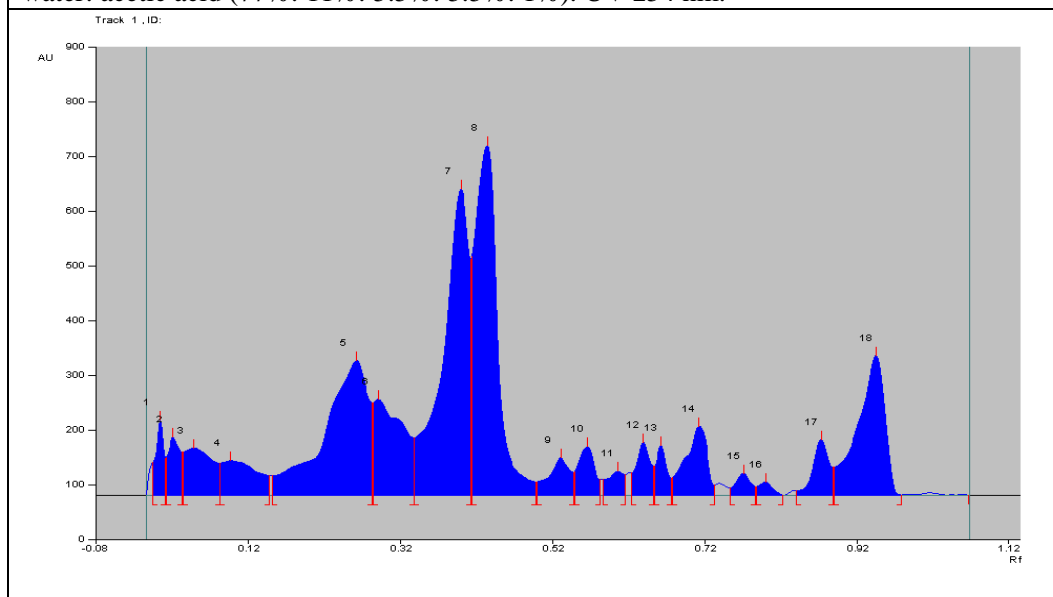
Figure 5.1(b): HPTLC second development fingerprint profile of leaf crude extract. Stationary phase: HPTLC Si 60 F_{254}. Mobile phase: dichloromethane: hexane (90%: 10%). UV 254 nm.

Thus, for the first dimensional plate development, which targeting on crude extracts, different proportions of solvent systems were examined as developing solvents, and ethyl acetate, methanol, water in the proportion of 7.5: 1.4: 1.1 yielded the best separated peaks profile (Figures 4.1 and 4.2). Silica normal phase HPTLC plates were used, as the silanol groups, -Si-OH in the structure allows stationary phase to interact with a wide range of analytes (Reich and Schibli, 2007).

For the SPE-separated active fractions, satisfactory separations were achieved with the employment of reversed phase 18 stationary phase. Compared to silica gel 60 plates, reversed phase 18 TLC plate is less polar and more hydrophobic. They generally act like deactivated silica gel and less affinity to water. It resulted in minimal spot tailing and better peak resolution after separation, for polar analytes. By employing the chemically modified silica gel plates (Reversed phase 18 TLC, in this context), solvent system of high polarity such as water and acetonitrile in higher proportion was chosen as developing solvent, since the polarity of the stationary phase is low and harmful reagents can be avoided (Ohno *et al.*, 2006). Figure 5.2 showed the HPTLC chromatogram of leaf SPE-separated fraction 5 with silica gel 60 as stationary phase, and it was obviously seen that the baseline resolution could not be achieved and significant tailing for separated peaks was observed, with the same concentration and volume of sample applied.

Figure 5.2: HPTLC fingerprint profile of leaf SPE-separated fraction 5. Stationary phase: HPTLC Si 60 F_{254}. Mobile phase: ethyl acetate: acetonitrile: methanol: water (75%: 12.5%: 6.25%: 6.25%). UV 254 nm.
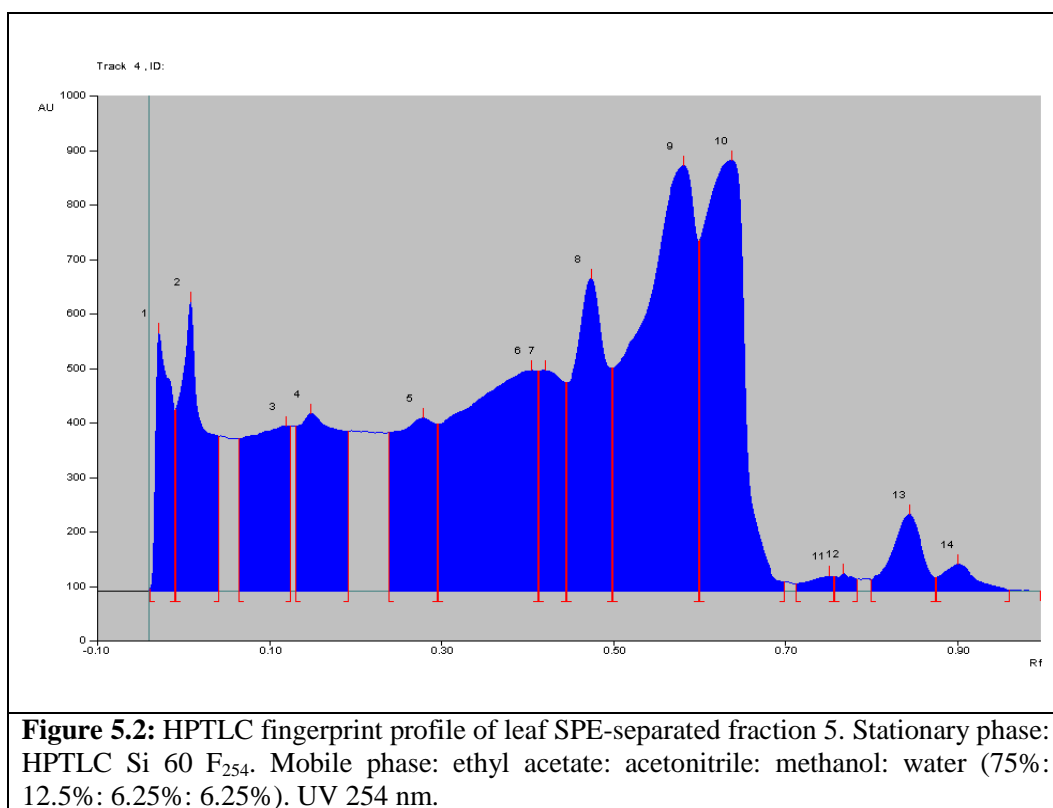
By optimizing the developing solvents with the stationary phase chosen, all components in the active fractions were distinctively separated without any tailing and diffuseness. Since the cytotoxic SPE-separated fractions 4, 5 and 7 (Figures 4.5, 4.10, 4.12, 4.13) were more polar in nature, their fingerprint profiles were developed in higher polarity of developing solvents on silica RP-18 stationary phase. As for cytotoxic leaf SPE-separated fraction 12, due to its nature of reduced affinity on silica bonded phase, it was separated in mobile phase of hexane: acetone (70%: 30%), on the silica TLC plate (Figure 4.7).

In present study, the first dimensional separation for crude extracts are performed on silica gel, while the second dimensional separation for partially separated fractions are established on C-18 bonded silica gel, except for the case of leaf SPE-separated fraction 12. The establishment of fingerprint profile in two dimensional approaches with the employment of two different types of stationary phases might offer the possibility of separating the mixture that covers wide range of polarity.

For TLC, simple charring of the compounds on plate surface using the relative derivatization reagents offer a simple and rapid method for optical detection of these non-visible compounds under white light. Sulphuric acid in cold methanol is effective for generating a rich-informative fluorescence fingerprint (Chen *et al.*, 2006). Due to many of the bands were not UV active and had lower absorption maxima values (Sukumar *et al.*, 2008), most bands could be detectable under visible range after charring the developed plates with sulphuric reagent and vanillin reagent (Figures 4.3, 4.6, 4.8, 4.11, 4.14).

5.2.3 Comparison of Peaks Profile

Well resolved fingerprint profiles of the active fractions in both leaf and rhizome of *Paraboea paniculata* were demonstrated. Each developed plate possessed distinct chromatographic characteristics, for example colour and R_f value of the bands.

It is interesting to note that when compared to the fingerprint profiles of leaf and rhizome SPE-separated fractions 5 (both also fractionated at ratio of 60% water: 40% methanol via SPE) (Figure 4.6), both fractions possessed a common peak pattern, under the same developing solvent system. However, intensity of the later eluted peak of rhizome SPE-separated fraction 5 was much significant, when compared to the leaf fraction. The same peak of leaf SPE-separated fraction 5 demonstrated a marked decreased in relative. This may explain the chemical distribution in both fractions is not equivalent, although they might possess the similar type of constituents.

As for the fingerprint profile of rhizome SPE-separated fraction 7, it appeared as few faint zones and barely distinguishable from the baseline, which is not sufficient for definitive differentiation (Figures 4.13 and 4.14). Its scarce amount of ingredients in the fraction become obvious when evaluated with the obtained weight data, fraction 7 only consists of 0.81% of the overall weight. It is very little in amount, and difficult to be further justified for identity, although it showed strong cytotoxic activity against K-562 cell line.

In the case of leaf SPE-separated fraction 12, one of the peaks found in the fingerprint profile has the exact peak position and pattern as the reference standard, stigmasterol (Figure 4.8). The overlapping of both peaks suggests the presence of sterol-typed compound in the related fraction. It could be further justified when the fraction 12 was subjected to GC-MS analysis (Figure 4.44).

The analyzed spectrum showed the presence of stigmasterol and beta-sitosterol in fraction 12.

HPTLC profile of three isolated constituents spiked with each other under two developing systems was demonstrated in Figures 4.36 and 4.37. The three pure substances were mixed and applied on the first and second tracks; all the substances demonstrated distinctive bands and not overlapping to each other. The compounds were identified by comparison of their R_f values and UV spectra, under the same analytical condition. Each of the compound corresponding bands on TLC plate was scanned from 200 nm to 700 nm with spectrodensitometer to record the UV-Vis spectrum. The maximum absorption wavelength of 279 nm, 329 nm, and 332 nm were obtained from the spectra of PP-1, PP-2 and PP-3, respectively (Figures 5.3 a and b). Thus, wavelength of 279 nm for PP-1 and 330 nm for PP-2 and PP-3 were chosen as the screening wavelength of the substances. The R_f values for PP-1, PP-2, and PP-3 were 0.65, 0.41 and 0.39, developed in their respective mobile phases. The maximum wavelength, spectrum pattern, as well as the recorded R_f value can be used for future investigation of the similar main component in crude extract, rapidly and accurately (Ohno *et al*., 2006).
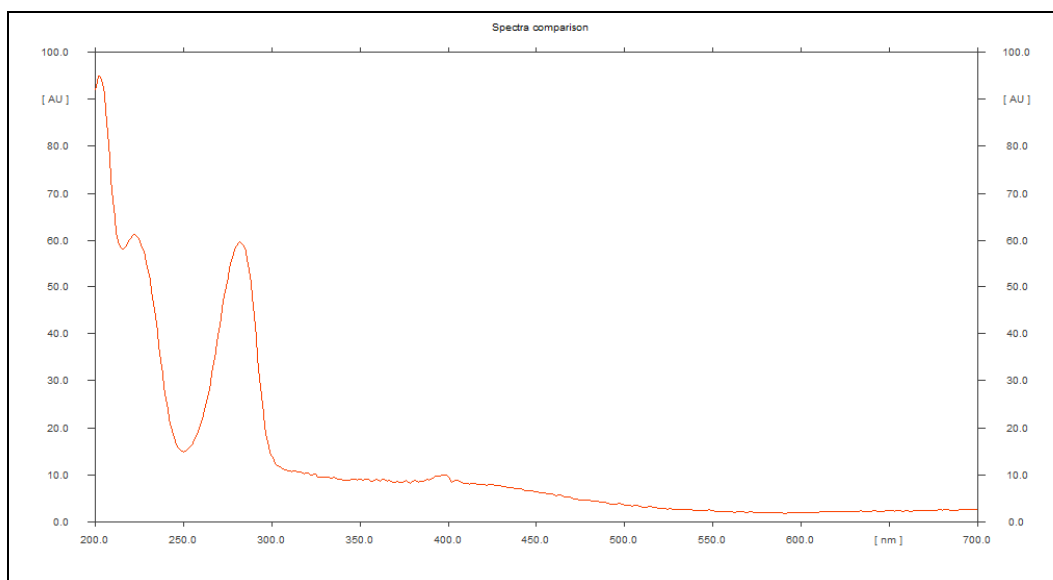
Figure 5.3 (a): UV-Vis spectrum of PP-1 with maximum wavelength of 279 nm, generated by HPTLC spectral scan.
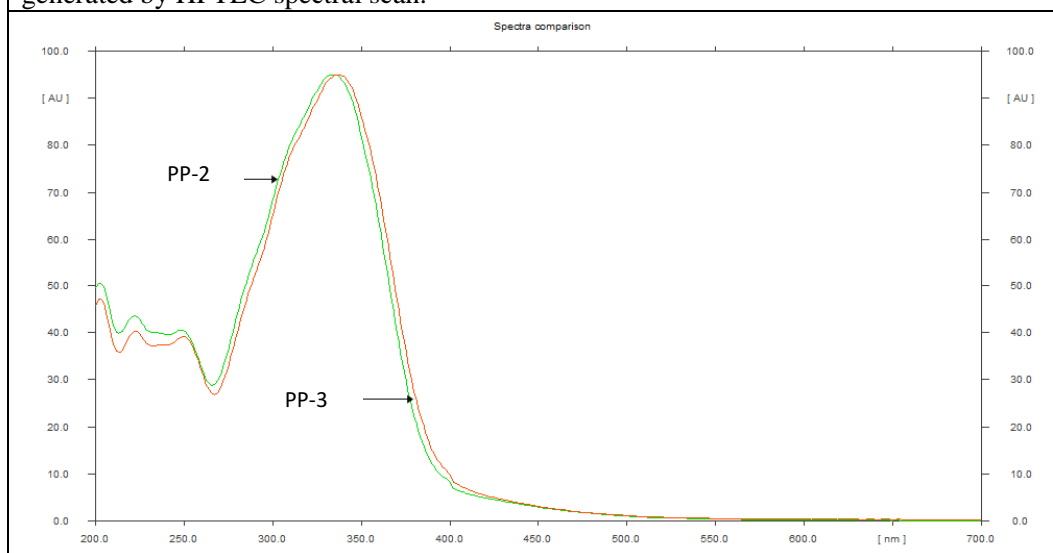
Figure 5.3 (b): UV-Vis spectra of PP-2 with maximum wavelength of 329 nm and PP-3 with maximum wavelength of 332 nm, generated by HPTLC spectral scan.

5.3   Validation of Method

Method validation is the formal proof which the method is suitable for particular use (Reich and Schibli, 2007). It aims to demonstrate the method performance characteristics, where within limits; the method still can yield predictable results with the same sample. It allows the small differences attributed by the samples due to natural variability, and not method uncertainty. There are a few validation parameters for qualitative analysis: precision, robustness, stability, and specificity (EMEA, 2006). Precision and robustness tests are analysed in term of standard deviation and relative standard deviation of the retention time and the acceptable measure was performed as suggested by Reich and Schibli (2007).

The parameter of precision is the system suitability test to ensure the constant performance of samples on plates. It could be divided into precision on a plate (repeatability), on different plates (intra-day precision), and on different days (inter-day precision). Precision on a plate describes the homogeneity of every chromatography step across the plate. It was measured for few prominent zones of each fingerprint profile in triplicate analysis of the same sample on the same plate. An acceptable measure is that the R_f values across the plate do not deviate more than 0.01. Results are summarized in Table 4.4, and all precision values (n=3) were lower than 0.01. As for the precision on different plates, it refers to same sample analysis on the influence of different plates on the same day. It was determined by applying the sample solutions of three analyses on three

individual plates and the mean R_f value (n=9) of three plates vary not more than 0.02. Table 4.5 illustrates the deviation of all precision values were within the range. Inter-day precision refers to the environmental effects and human influence to the fingerprint profile generated. It was determined on two other days (one plate prepared during repeatability test, one plate prepared on the next three days, and the last plate was performed on the following three days). The average R_f values between plates on different days should deviate less than 0.05. Result showed all inter-day precision values were not more than 0.05 (Table 4.6).

Robustness is the ability to tolerate variation of parameters, without significant changes in the fingerprint profiles (Reich and Schibli, 2007). By introducing small changes in the volume of developing solvent, equilibration time between gas phase and stationary phase, type of chamber, development distance and dosage speed of sample applicator, any changes caused by the substitution is investigated. Volume of developing solvent was performed in 5 ml, and 15 ml in place of 10 ml and the acceptable criterion for the variation of R_f would be less than 0.05. Few values of Table 4.7 were higher than 0.05. The results showed the best solvent volume in one of the troughs was 10 ml or less, 15 ml of developing solvent would be too much until cover the application line of the plate, causing shifting of application position. Equilibration time of gas phase and stationary phase was performed in 10 minutes and 30 minutes, instead of 20 minutes. There are no significant effects implied, as illustrated in Table 4.8. As for the type of chamber used, flat bottom chamber in comparable size (10 x 10 cm) was

substituted for the specified twin-trough chamber. Table 4.9 demonstrated that the mean R_f value of the prominent peaks deviated more than 0.05 between both type of chambers. Thus, this suggests the consistent use of the similar chamber throughout the fingerprint establishment is necessary. The developing distance was extended to 75 mm and 80 mm, rather than 70 mm from the lower edge of the plate (Table 4.10), and the dosage speed of sample applicator was performed in 150 nl/s and 200 nl/s, which normally in 100 nl/s (Table 4.11). Both parameters gave no significant change of effects, and all the values were within the range.

The stability of samples during analysis was established to facilitate the investigation of any sample degradation. Stability of the analytes before chromatography was assessed in term of the consistence of the same sample prepared in solution at different time and from different batches. The reasonable criterion would be the samples are stable prior to chromatography and no additional zones or decomposition of analytes is observed. The same sample of different batches was stable on the TLC plate for at least 3 hours at room temperature (Figure 4.15 to Figure 4.19). Stability of analytes during chromatography was investigated by turning the developed plate 90 degrees to the right and developed for the second time with fresh similar developing solvent. The method is stable during chromatography if all zones are located at the diagonal connecting to the application position with the intersection of the two solvent fronts. Figures 4.20 to 4.26 illustrate the stability of all samples during plate development and no additional bands were observed, as shown in 2-

dimensional chromatography. As for the stability of analytes after chromatography, it was assessed by evaluating the chromatographic result repeatedly in several time points. After the plate development, the peak profiles were stable for at least 1 hour (Figures 4.27 to 4.33).

Last but not least, specificity of the method was assessed by comparing different sets of same sample, in order to investigate their similarity. In this study, the pure constituents would be served as the point of reference, and compared to the profiles of crude extract and partially purified fraction (Figures 4.34 and 4.35). The specificity of the pure compounds in crude extract and semi-purified fraction was confirmed by comparing the overlaying position, colour and zone intensity of interest bands. The method was specific, as all raw material samples showed the interest bands corresponding with the isolated compounds.

5.4   Determination of Radical Scavenging Activity in *Paraboea paniculata*

Free radicals include superoxide radicals, hydroxyl radicals, peroxyl radicals and singlet oxygen; have associated with many disease conditions. DPPH is one of the free radicals generally used for the routine analysis of the free radical scavenging activity of the plants. The routine used spectrophotometric method measures the radical scavenging activity in total, but it lacks of the ability to locate the anti-oxidant compound of a mixture. The TLC-DPPH method is simple and suitable for distinguishing active from non-active compounds in natural

extract after TLC separation (Yrjönen *et al.*, 2003). Determination of radical scavenging activity by TLC-DPPH *in situ* method would detect the active compound in bright yellow band under purple background. Pozharitskaya *et al.* (2007) has reported the applied concentration of reference compounds in 0.5 mg/ml and sample solutions in 1 mg/ml on TLC plate. However, for screening purpose, many studies have used the supernatant as sample solutions, without specifying their concentration (Camag Laboratory, 2009; Yrjoren *et al.*, 2003). Thus, in this study, the concentration of 0.5 mg/ml was employed for sample solutions and standard reference, quercitin, in order not to eliminate any potential substances. Figure 5.4 shows the active fraction, leaf SPE-separated fraction 5 in 0.5 mg/ml gives the most observable bands after stained with DPPH solution.

Figure 5.4: TLC-DPPH *in situ* of leaf SPE-separated fraction 5; quercitin as reference standard. Stationary phase: TLC Si 60 RP18 F_{254}S. Mobile phase: ethyl acetate: methanol: water (40%:35%:35%). Under white light. From left to right: track 1: quercitin 100 μg/ml; track 2 to 3, Leaf F-5 100 μg/ml; track 4 to 5, Leaf F-5 250 μg/ml; track 6 to 7, Leaf F-5 500 μg/ml.
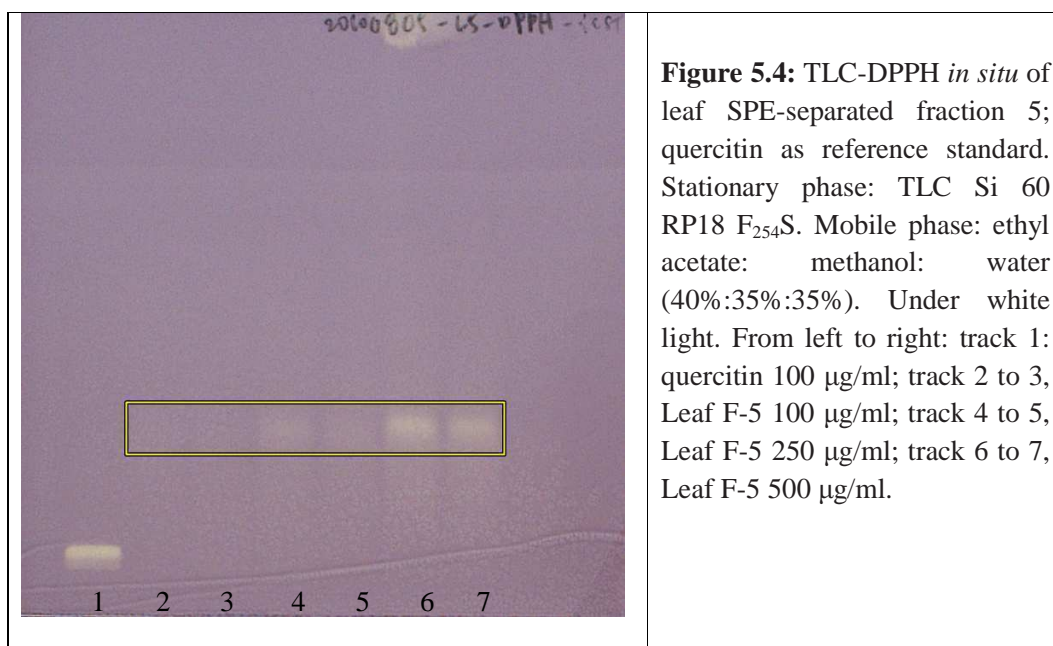
The widely used spectrophotometric DPPH method was employed as reference method, so that the selectivity of the anti-oxidant compound towards DPPH on TLC plates could be determined. In this context, both methods correlated well where, leaf F-5 and rhizome F-5 (60% water: 40% methanol) are very active in quenching of the DPPH radicals on TLC-DPPH method and spectrophotometric assay. Results obtained from the TLC-DPPH method showed that leaf F-5 and rhizome F-5 (0.5 mg/ml) exhibiting strong activity as thick yellow bands appeared right after staining with DPPH in methanol solution (Figure 4.39). This suggests the principal compound of both fractions is responsible for the antioxidant activity of *Paraboea paniculata*. In spectrophotometric assay, leaf and rhizome F-5 were able to quench up to 80% of DPPH free radical at the concentration of 50 µg/ml (Table 4.12). Rhizome F-7 and leaf F-12 showed no obvious yellow band under the same condition (Figures 4.41 and 4.42), corresponding to -8.22% and 44.26% of free radical inhibition rate (Table 4.12). Rhizome F-4 (80% water: 20% methanol) showed faded yellow thin band (Figure 4.40) and the inhibition rate was 30.64% (Table 4.12). These findings are in accordance with the statement suggested by Ravishankara *et al.* (2002); polar fractions were more likely constituted by phenolic compounds, which active in DPPH radical scavenging activity, than the non-polar fractions. Research has indicated that the intensity of yellow band depend on the amount and nature of scavengers in the sample (Pozharitskaya *et al.*, 2008). Thus, the amount of stoichiochemistry units that attributed to the anti-oxidant activity in rhizome F-4 would be probably lesser than F-5 does.

Moreover, the adjusted application volume may affect the detection of antioxidant activity (Camag Laboratory, 2009). Therefore, the same chromatographic condition was applied in all fractions. Quercitin and curcumin served as the reference standards, because of their distinguished strong DPPH free radical scavenging ability. Due to the polarity nature of the fractions, RP-TLC was employed for leaf F-5, rhizome F-4, F-5 and F-7. However, the active bands of leaf and rhizome F-5 were unstable on RP-TLC plate and started to fade after staining, and this led to poor peak shapes against the faded purple background (Figure 4.39). The declining intensity of the developing colour has rendered the RP-TLC-DPPH method be less effective for quantitative analysis and rapid processing the developed plates is necessary (Yrjönen *et al*., 2003). In this context, the TLC-DPPH *in situ* method has facilitated the bioassay-guided-isolation of potent antioxidant compounds.

The evaluation of chromatographic patterns after staining with DPPH solution enhances the chance of isolating target analyte(s) that possess free radical scavenging activity. Compounds PP-2 and PP-3, two caffeic acid esters of phenylethanoid glycosides (CPGs), and PP-1, a phenylethanoid glycoside (PhGs) were isolated from leaf F-5 and rhizome F-4, correspondingly. The dose of PP-2 and PP-3 required for scavenging 50% of DPPH radical were 15.25 µg/ml and 16.25 µg/ml, respectively, while PP-1 showed an inhibition rate of 50% at 34 µg/ml (Figures 4.83, 4.84, 4.85). Compounds PP-1, PP-2 and PP-3 contain free phenolic hydroxyl groups in their structures, and these groups were reported to

function as electron or hydrogen donors (Lafka *et al.*, 2007). Compounds PP-2 and PP-3 which possess an extra caffeoyl unit in their structures showed stronger free radical scavenging ability than PP-1, thus implying the presence of additional dihydroxy moieties stabilized the free radical and involved in the electron delocalization (Es-Safi *et al.*, 2007). The high free radical scavenging activity of PP-2, and PP-3 could be attributed to the hydroxyl groups from their diphenol and glycosides structures. Study has demonstrated that the number of hydroxyl groups in phenol affects the hydrogen donating ability of the compound. Phenolic antioxidants generally function as a terminator of oxidation chain, by interfere the chain propagation reactions with rapid donation of the hydrogen atom to free radicals (Lafka *et al.*, 2007). The scavenging activity of the compounds would serve as responsible mechanism of the anti-inflammatory, healing and anti-tumour activities (Gálvez *et al.*, 2006).

Cuneataside C (Chang and Case, 2005), which possesses highly similar structural configuration as PP-1, has showed strong antioxidant activity by inhibiting the lipid peroxidation in rat liver microsomes (Lin *et al.*, 2007). Calceolarioside E (PP-2) and acteoside (PP-3) have also found to inhibit superoxide radical in PMA-stimulated neutrophil granulocytes (Hennebelle *et al.*, 2007). Study on the structure-activity relationship showed that caffeic acid and 3, 4-diphenylethanoid obtained after hydrolysis gave significant neuroprotective activity, nitric oxide and DPPH free radical scavenging activities, with EC_{50} values lower than the positive control, α-tocopherol (Koo *et al.*, 2006). It also

suggested the aglycones reduce ROS production from cells, by enhancing the anti-oxidative defence system. Previous review by Gálvez *et al.* (2006) has stated the direct influence of the number and position of hydroxyl groups to anti-oxidant activity of a compound, while converse effect with the increasing number of higher monosaccharide moieties.

5.5   Determination of Cytotoxic Activity in Isolated Compounds

In this study, MTT (3-(4, 5-dimethylthiazol-2-yl)-2, 5-diphenyl tetrazolium bromide) colorimetric assay was adopted as a simple mean to measure proliferation, viability and activation of K-562 cell line (Mosmann, 1983). The determination of cell viability via MTT assay is dependent on the enzymatic reaction of mitochondria in living cells. K-562, a human chronic myelogenous leukemic cell line, was used as an *in vitro* model for studying the effects of cell killing of *Paraboea paniculata* against hematopoietic cells. The preliminary screening of the cytotoxic activity of the crude leaf and rhizome fractions, together with all SPE-separated fractions revealed that both crude and five sub-fractions were cytotoxic against K-562 cell line. The active cytotoxic fractions were employed for further metabolite fingerprinting establishment (Figure 4.43).

Compound PP-1 is a decaffeoyl derivative of PP-2, where its structure lacks of the ester-link caffeic acid that PP-2 and PP-3 possess. Nevertheless, PP-1, PP-2, and PP-3 showed similar degree of cytotoxicity, with the IC_{50} values of 18

μg/ml, 16.5 µg/ml, and 17 µg/ml, respectively (Figures 4.88, 4.89, 4.90). The results obtained in the present study support the statement by Nagao *et al*. (2001), where caffeic acid contributed minor effect on anti-proliferative activity. Additionally, acteoside, PP-3 was found to induce apoptosis in human promyelocytic leukaemia HL-60 cells by induction of G_1 cell cycle arrests through down-regulation of CDK4- and CDK6- associated kinase activities, and also induction of differentiation by increasing TGF-β1 signalling (Inoue *et al*., 1998; Lee *et al*., 2007). This could suggest the same mechanism of killing action of the compounds against K-562 cell line, due to the similar cell morphological changes observed under microscopic investigation (Plates 4.5 to 4.10). Acteoside induced apoptosis on HL-60 cell line has revealed the characteristics of cell shrinkage, disappearance of microvillus and chromatin condensation (Inoue *et al*., 1998). The 50% of HL-60 cell killing concentration was 26.7 µg/ml (Inoue *et al*., 1998), and 38.3 µM (Lee *et al*., 2007), which are almost the same as the value obtained for K-562 cell line (17 µg/ml) and were categorized as moderate cytotoxic (> 30%; < 70% of cell viability) in this study. According to National Cancer Institute guideline (Lee and Houghton, 2005), the threshold of significance for pure compound is less than 4 µg/ml, and less than 20 µg/ml for crude extracts.

Acteoside, is a phenylethanoid glycoside that widely found in plants and has shown a wide range of biological activities. There are several reports on the inhibition effect of acteoside on proliferation of P-388 cells (mouse lymphoid

neoplasm) (Herbert and Maffrind, 1991), B16F10 cells (murine melanoma) (Nagao *et al*., 2001), MK-1 cells (adenocarcinoma) (Abe *et al*., 2002), dRLh-84 cells (rat hepatoma), and S-180 cells (sarcoma) but not against primary cultured rat hepatocytes (Saracoglu *et al*., 1995), indicating the selectivity of acteoside in its cytotoxicity between normal and cancer cells. The inhibitory effect of acteoside against PKC was suggested to be the contribution factor of the cytotoxic activity (Herbert and Maffrind, 1991). PKC is involved in signalling pathway that allows cellular responses to extracellular stimuli which involved in cell proliferation, differentiation and apoptosis. Acteoside also showed suppressive effect on lung metastasis of B16 melanoma cells, which is believed to be closely related to its anti-oxidant activity, NO inhibition synthesis and cytotoxic activity exhibited by the compound (Ohno *et al*., 2002). In another study done by Saracoglu *et al.* (1995) has claimed the biphasic effect of acteoside on cancer cells, which are the cytotoxic and cytostatic effects dependent on different cell types. Cytotoxicity is the activity with decreased cell number caused by cell death, while cytostatic indicates the cell-growth inhibitory activity, which suppress the increased cell number without causing cell death. Therefore, these lay great variations of mechanism following the PP-1, PP-2, and PP-3 induced cell death.

Polyphenols are known to elicit pro-oxidant action due to its capability of binding to metal ion and causing cell damage. The compounds with catechol-like aromatic rings are known to induce cellular damage through hydrogen peroxide production (Tyson and Martell, 1972). The experimental data on structure-activity

relationship studies (Saracoglu *et al*., 1995; Nagao *et al*., 2001; Abe *et al*., 2002; Lee *et al*., 2007) suggested that the anti-proliferative activities of phenylethanoid glycosides are affected by the ortho-dihydroxy aromatic (phenolic) systems, the number of free hydroxyl groups, the type and location of the sugar moieties within the structure. However, report by Abe *et al.* (2002) declined the influence of sugar moiety on the cytotoxic activity. A latter study by Lee *et al.* (2007) has further confirmed the type of sugar is a crucial cytotoxic feature.

5.6   The Distribution of Caffeoyl Phenylethanoid Glycosides (CPGs) in the Family of Gesneriaceae

Paraboea paniculata is a member of the family of Gesneriaceae, subfamily of Cyrtandriodeae, and the tribe of Didymorcarpeae. Members of Gesneriaceae have not much subjected to chemical works and mostly served as ornamental plants (Jensen, 1996).

Flavonoids, phenylpropanoids, anthocyanins are the common compounds isolated from the family of Gesneriaceae, (Lowry, 1972; Kang *et al*., 2010) and chalcones, aurones, and quinones are restricted to the genera of Cyrtandroideae (Harborne, 1966; Kvist and Pedersen, 1986). Flavonols and iridoid glucosides are completely absent from Gesneriaceae (Harborne, 1966; Jensen, 1996). Previous studies done within the members of Gesneriaceae, which 46 species were investigated by chromatography (Harborne, 1966) and 590 species of 91 genera were studied by ESR spectroscopy (Kvist and Pedersen, 1986), have shown that

214

caffeoyl phenylpropanoid glycosides (CPGs) are commonly found in the family. Acteoside is abundantly present in the family; however, not many of this group of compounds was isolated (Damtoft and Jensen, 1994).

Study by Jensen (1996) has reported that the rare groups of CPGs with pentose as auxiliary sugars may be an advance characteristic in the family of Gesneriaceae. The present study showed evidence that CPG with apiose as auxiliary sugar (PP-2) was isolated, apart from acteoside. This is the first report on the isolation of a phenylethanoid glycoside and two CPGs and their biological activities in the *P. paniculata* found in Malaysia.

The fingerprint profiles of other ethno medicinally screened plants that deposited in Natural Product Library of UTAR could be developed with the hyphenation of SPE-HPTLC, for future reference. Similar species of *Paraboea* could be subjected to the same approach to unravel any similar bioactivities of plant species through pattern recognition. Understanding the detailed mechanisms underlying the suppression of K-562 cell proliferation by the isolated compounds should be further emphasized. Other bioassays focusing on anti-inflammatory, anti-angiogenesis and anti-invasion should be employed to support the justification for the isolated compounds to be regarded as anti-cancer agents.

CHAPTER 6

CONCLUSIONS

In the study, two dimensional fingerprint profiles establishment with the employment of solid phase extraction method as interface and planar thin layer chromatography method for systematic pattern documentation was successfully demonstrated. The unique picture liked images of HPTLC and digital scanning profiles of crude fractions and each active SPE-separated fraction provide comprehensive chemical profiles reflective of the active group of constituents in *Paraboea paniculata*. The distinct fingerprint profiles observed can be used as function of differentiation of active ingredients in same plant species or different parts of plant. The optimized HPTLC method was validated and all the validation parameters were within the performance's limits, indicating the current method can be used to yield the predictable result with the same samples.

This study also revealed that the free radical scavengers in complex mixture or semi-purified fractions can be identified with post chromatographic derivatization of TLC plates by DPPH free radicals after fingerprint development. The active profiles identified via TLC-DPPH *in situ* method were correlated well with the results generated by the routine used spectrophotometric DPPH method. Leaf and rhizome SPE-separated F-5 were found to quench up to 80% of DPPH free radical at the concentration of 50 µg/ml. As for rhizome fraction 4 and

fraction 7, as well as leaf fraction 12, all showed moderate to weak free radical scavenging activity.

The simultaneous determination of the structure of active compounds in the present study has yielded three phenylethanoid glycosides, namely 3,4-dihydroxyphenethyl-(3"-O-β-D-apiofuranosyl)-β-D-glucopyranoside (PP-1), 3,4-dihydroxyphenethyl-(3"-O-β-D-apiofuranosyl-4"-O-caffeoyl)-β-D-glucopyranoside (PP-2), and 3,4-dihydroxyphenethyl-(3"-O-α-L-rhamnopyranosyl-4"-O-caffeoyl)-β-D-glucopyranoside (PP-3), from rhizome SPE-separated F-4 and leaf F-5. The structure of the isolated compounds has been elucidated based on the spectroscopic analysis, including mass spectroscopy, FT-IR and two-dimensional NMR spectroscopic data. Compounds PP-2 and PP-3 are as potent as quercitin and ascorbic acid, with 50% of free radical scavenging ability at the concentration of 15.25 µg/ml and 16.25 µg/ml, respectively, while PP-1 showed moderate free-radical scavenging activity with 50% inhibition rate at 34 µg/ml. Compounds PP-1, PP-2, and PP-3 exhibited similar degree of cytotoxic against K-562 cell line, with IC_{50} values of 18 µg/ml, 16.5 µg/ml, and 17 µg/ml, correspondingly.

The current study is the first attempt to investigate the chemical profiles and biological activities of *Paraboea paniculata*. The three isolated phenylethanoid glycosides emerge to be promising anti-tumour agents, prompting the future study to investigate the cell death mode of K-562 cell line and the exact

structural-activity relationship of the three potential compounds. These results suggest that 3,4-dihydroxyphenethyl-(3"-O-β-D-apiofuranosyl)-β-D-glucopyranoside (PP-1), 3,4-dihydroxyphenethyl-(3"-O-β-D-apiofuranosyl-4"-O-caffeoyl)-β-D-glucopyranoside (PP-2), and 3,4-dihydroxyphenethyl-(3"-O-α-L-rhamnopyranosyl-4"-O-caffeoyl)-β-D-glucopyranoside (PP-3) might be used as the lead compounds for leukaemia cancer treatment.

LIST OF REFERENCES

Abe, F., Nagao, T. and Okabe, H. (2002). Antiproliferative constituents in plants 9. Aerial parts of *Lippia dulcis* and *Lippia canescens*. *Biol. Pharm. Bull.,* 25 (7), 920-922.

Abe, K. and Matsuki, N. (2000). Measurement of cellular 3-(4, 5-dimethylthiazol-2-yl)-2, 5,-diphenyltetrazolium bromide (MTT) reduction activity and lactate dehydrogenase release using MTT. *Neuroscience research,* 38, 325-329.

Agrawal, P. K. (1992). NMR spectroscopy in the structural elucidation of oligosaccharides and glycosides. *Phytochemistry*, 31, 3307-3330.

American Cancer Society (2008). *Cancer organizations team up for global cancer fight*.
URL: http://www.cancer.org/docroot/NWS/content/NWS_1_1x_Leading Cancer_Organizations_Team_Up_For_Global_Cancer_Fight.asp.
Assessed on 14th January 2010.

American Herbal Pharmacopeoia (AHP) (2009). URL: http://www.herbal-ahp.org/hptlc.htm. Assessed on 15th January 2010.

Andrary, C., Wylde, R., Laffite, C., Privat, G. and Winternitz, F. (1982). Structures of verbascoside and orobanchoside caffeic acid sugar esters from *Orobanche rapum*-genistae. *Phytochemistry*, 21 (5), 1123-1127.

Ankli, A., Reich, E. and Steiner, M. (2008). Rapid high-performance thin-layer chromatographic method for detection of 5% adulteration of black cohosh with *Cimicifuga foetida*, *C. heracleifolia*, *C. dahurica*, or *C. americana*. *Journal of AOAC international*, 91, 1257-1260.

ARBEC (2003). *Natural product and biotechnology*. URL: http://www.arbec.com.my/indigenious.htm. Assessed on 14th January 2010.

Avendano, C. and Menendez, J. C. (2008). Medicinal chemistry of anticancer drugs. In: *Other approaches to targeted therapy*. (pp. 341-347). Amsterdam: Elsevier.

Babich, H., and Borenfreund, E. (1991). Cytotoxicity of T-2 toxin and its metabolites determined with the neutral red cell viability assay. *Applied and environmental microbiology,* 57 (7), 2101-2103.

Balunas, M. J. and Kinghorn, A. D. (2005). Drug discovery from medicinal plants. *Life sciences,* 78, 431-441.

Camag Laboratory (2009). *Application note: HPTLC screening method for antioxidant properties of substances in various matrices using DPPH.* Switzerland.

Campbell, N. A. and Reece, J. B. (2005). Biology (7th ed.). In: *Regulation of the cell cycle* (pp. 224-229). San Francisco: Pearson Education.

Cao, Y., Wang, L., Yu, X. and Ye, J. (2006). Development of the chromatographic fingerprint of herbal preparations Shuang-Huang-Lian oral liquid. *Journal of pharmaceutical and biomedical analysis*, 41, 845-856.

Cashman, J. R. (1996). Drug discovery and drug metabolism. *Drug discoveries and therapeutics*, 1 (5), 209-216.

Chabner, B. A. and Roberts, T. G. (2005). Chemotherapy and the war on cancer. *Nature reviews*, 5, 65-72.

Chang, J. and Case, R. (2005). Phenolic glycosides and ionone glycoside from the stem of *Sargentodoxa cuneata. Phytochemistry*, 66, 2752-2758.

Chen, P., Ozcan, M. and Harnly, J. (2007). Chromatographic fingerprint analysis for evaluation of Gingko biloba products. *Analytical and bioanalytical chemistry*, 389, 251-261.

Chen, S, Liu, H, Tian, R., Yang, D., Chen, S., Xu, H., Chan, A. S. C. and Xie, P. (2006). High performance thin layer chromatographic fingerprints of isoflavonoids for distinguishing between *Radix puerariae lobate* and *Radix puerariae thomsonii. Journal of chromatography A*, 1121, 114-119.

Chen, S. T., Dou, J., Temple, R., Agarwal, R., Wu, K. and Walker, S. (2008). New therapies from old medicines. *Nature biotechnology*, 26 (10), 1077-1083.

Chen, X., Kong, L., Su, X., Fu, H., Ni, J., Zhao, R. and Zou, H. (2004). Separation and identification of compounds in Rhizoma chuanxiong by comprehensive two-dimensional liquid chromatography coupled to mass spectrometry. *Journal of chromatography A*, 1040, 169-178.

Cho, H. J., Kim, J. D., Lee, W. Y., Chung, B. C. and Choi, M. H. (2009). Quantitative metabolic profiling of 21 endogenous corticosteroids in urine by liquid chromatography-triple quadrupole-mass spectrometry. *Analytica chimica acta*, 632, 101-108.

Christian, M. and Custodio M. D. (2008). Neuromuscular complications of cancer and cancer treatments. *Physical medicine and rehabilitation clinics of North America*, 19 (1), 27-45.

Ciesla, L., Bogucka-kocka, A., Hajnos, M., Petruczynik, A. and Waksmundzka-hajnos, M. (2008). Two-dimensional thin-layer chromatography with adsorbent gradient as a method of chromatographic fingerprinting of furanocoumarins for distingushing selected varieties and forms of *Heracleum spp. Journal of chromatography A*, 1207, 160-168.

Ciesla, L. and Waksmundzka-hajnos, M. (2009). Two-dimensional thin-layer chromatography in the analysis of secondary plant metabolites. *Journal of chromatography A*, 1216, 1035-1052.

Claude, B., Morin, P., Lafosse, M., Belmont, A. S. and Haupt, K. (2008). Selective solid-phase extraction of a triterpene acid from a plant extract by molecularly imprinted polymer. *Talanta*, 75, 344-350.

Committee of National Pharmacopoiea (2000). *Pharmacopoeia of PR China.* Beijing: Press of chemical industry.

Cordell, G. A. (1995). Changing strategies in natural products chemistry. *Current opinion in phytochemistry*, 40 (6), 1585-1612.

Cragg, G. M., Kingston, D. G. I. and Newman, D. J. (2005). *Anticancer agents from natural products.* Boca Raton: Taylor and Francis Group.

Cragg, G. M. and Newman, D. J. (2005). Plants as a source of anti-cancer agents. *Journal of ethnopharmacolgy*, 100, 72-79.

Cree, I. A. and Andreotti, P. E. (1997). Measurement of cytotoxicity of ATP-based luminescence assay in primary cell cultures and cell lines. *Toxicology in vitro*, 11, 553-556.

Damtoft, S., Franzyk, H., Jensen, S. R. and Nielsen, B. J. (1993). Iridoids and verbascosides in Retzia. *Phytochemistry*, 34 (1), 239-243.

Damtort, S. and Jensen, S. R. (1994). Three phenylethanoid glucosides of unusual structure from *Chirita sinensis* (Gesneriaceae). *Phytochemistry*, 37 (2), 441-443.

Development therapeutics program (DTP) (2009). *DTP human tumor cell line screen*. URL:http://dtp.nci.nih.gov/branches/btb/ivclsp.html. Accessed on 14th January 2010.

Di, X., Chan, K. K. C., Leung, H. W. and Huie, C. W. (2003). Fingerprint profiling of acid hydrolyzates of polysaccharides extracted from the fruiting bodies and spores of Lingzhi by high performance thin layer chromatography. *Journal of chromatography A*, 1018, 85-95.

Erenpreisa, J. and Cragg, M. S. (2007). Cancer: A matter of life cycle? *Cell biology international*, 31, 1507-1510.

Espinosa, E., Zamora, P., Feliu, J. and Baron, M. G. (2003). Classification of anticancer drugs- a new system based on therapeutic targets. *Cancer treatment reviews*, 29, 515-523.

Es-Safi, NE., Kollmann, A., Khlifi, S. and Ducrot, PH. (2007). Antioxidative effect of compounds isolated from *Globularia alypum* L. structure-activity relationship. *LWT*, 40, 1246-1252.

European Medicines Agency (EMEA). (2001). *Note for guidance on quality of herbal medicinal product.* London.

European Medicines Agency (EMEA). (2006). *Note for guidance on validation of analytical procedures: text and methodology (CPMP/ICH/381/95: ICH Topic Q2[R1]).* URL: http://www.ema.europa.eu/docs/en_GB/document_library/Scientific_ guideline/2009/09/WC500002662.pdf. Accessed on 23rd March 2010.

Fiehn, O. (2008). Extending the breadth of metabolite profiling by gas chromatography coupled to mass spectrometry. *Trends in Analytical Chemistry*, 27 (3), 261-269.

Fotakis, G. and Timbrell, J. A. (2005). *In vitro* cytotoxicity assays: Comparison LDH, neutral red, MTT and protein assay in hepatoma cell lines following exposure to cadmium chloride. *Toxicology letters*, 160 (2), 171-177.

Gafner, S., Wolfender, JL., Nianga, M. and Hostettmann (1997). Phenylpropanoid glycosides from *Newbouldia laevis* roots. *Phytochemistry*, 44 (4), 687-690.

Gallo, F. R., Multari, G., Giambenedetti, M. and Federici, E. (2008). Chemical fingerprinting of *Lawsonia inermis* L. using HPLC, HPTLC and densitometry. *Phytochemical analysis*, 19, 550-559.

Gálvez, M., Martín-Cordero, C. and Ayuso, M. J. (2006). Pharmacological activities of phenylpropanoid glycosides. *Studies in Natural Products Chemistry*, 33, 675-718.

Gao, J., Ren, P., Yang, Z. and Li, Q. (2006). The pollination ecology of *Paraboea rufescens* (Gesneriaceae): a buzz-pollinated tropical herb with mirror-image flowers. *Annals of botany*, 97, 371-376.

García-Pérez, I., Vallejo, M., García, A., Legido-Quigley, C. and Barbas, C. (2008). Metabolite fingerprinting with capillary electrophoresis. *Journal of Chromatography A*, 1204, 130-139.

Gerlier, D. and Thomasset, D. (1986). Use of MTT colorimetric assay to measure cell activation. *Journal of immunological methods*, 94, 57-63.

Giddings, J. C. (1984). Two-dimensional separation: concept and promise. *Analytical chemistry*, 56 (12), 1258-1270.

Gocan, S., Cimpan, G. and Muresan, L. (1996). Automated multiple development thin layer chromatography of some plant extracts. *Journal of pharmaceutical and biochemical analysis*, 14, 1221-1227.

Gong, W., Cao, Y. and Wang, Y. (2008). Analysis of pharmaceutical samples of *Resina draconis* by HPLC-PAD. *Phytochemical analysis*, 19, 499-505.

Gonzalez, R. J. and Tarloff, J. B. (2001). Evaluation of hepatic subcellular fractions for Alamar blue and MTT reductase activity. *Toxicology in vitro*, 15, 257-259.

Gore, M. and Russell, R. (2003). *Cancer in primary care.* New York: Martin Dunitz.

Harborne, J. B. (1966). Comparative biochemistry of flavonoids-II. 3-desoxyanthocyanins and their systematic distribution in ferns and gesnerads. *Phytochemistry*, 5, 589-600.

Hawryl, M. A., Soczewinski, E. and Dzido, T. H. (2000). Separation of coumarins from *Arzhangelica officinalis* in high-performance liquid chromatography and thin-layer chromatography systems. *Journal of chromatography A*, 886, 75-81.

Hennebelle, T., Sahpaz, S., Gressier, B., Joseph, H. and Bailleul, F. (2007). Antioxidant and neurosedative properties of polyphenols and iridoids from *Lippia alba*. *Phytotherapy Research*, 22, 256-258.

Herbert, JM. and Maffrind, JP. (1991). Tumor cell adherence to cultured capillary endothelial cells is promoted by activators of protein kinase C. *Biochemical Pharmacology*, 42 (1), 163-170.

Holbeck, S. L. (2004). Update on NCI *in vitro* drug screen utilities. *European journal of cancer*, 40, 785-793.

Hordegen, P., Cabaret, J., Hertberg, H., Langhans, W. and Maurer, V. (2006). *In vitro* screening of six antihelmintic plant products against larval *Harmonchus contortus* with a modified methyl-thiazolyl-tetrazolium reduction assay. *Journal of ethnopharmacology*, 108, 85-89.

Hu, H. B. and Fan, J. (2008). A new neolignan glycosides from the roots of *Acanthopanax brachypus*. Molecules, 13.

Inoue, M., Sakuma, Z., Ogihara, Y. and Saracoglu, I. (1998). Induction of apoptotic cell death in HL-60 cells by acteoside, a phenylpropanoid glycoside. *Biol. Pharm. Bull.*, 21 (1), 81-83.

Ishii, T. and Yanagisawa, M. (1998). Synthesis, separation and NMR spectral analysis of methyl apiofuranosides. *Carbohydrate research*, 313, 189-192.

Jadhav, A. N., Rumalla, C. S., Avula, B. and Khan, I. A. (2007). HPTLC method for determination of 20-hydroxyecdysone in *Sida rhombifolia* L. and dietary supplements. *Chromatographia*, 66, 797-800.

Jensen, S. R. (1996). Caffeoyl phenylethanoid glycosides in *Sanango racemosum* and in the Gesneriaceae. *Phytochemistry*, 43 (4), 777-783.

Jiang, X., Horst, A., Lima, V. and Schoenmakers, P. J. (2005). Comprehensive two-dimensional liquid chromatography for the characterization of functional acrylate polymers. *Journal of chromatography A*, 1076, 51-61.

Kancheva, V. D., Boranova, P. V., Nechev, J. T. and Manolov, I. I. (2010). Structure-activity relationships of new 4-hydroxy bis-coumarins as radical scavengers and chain-breaking antioxidants. *Biochimie*, 1-9.

Kang, WY., Chen, L. and Zang, XY. (2010). Sesquiterpenes and triterpenes from *Aeschynanthus mengxinggensis*. *Chemistry of Natural Compounds,* 46 (4), 661-663.

Kasai, R., Ogawa, K., Ohtani, K., Ding, JK., Chen, PQ., Fei, CJ. and Tanaka, O. (1991). Phenolic glycosides from Nuo-Mi-Xang-Cao, a chinese Acanthaceous herb. *Chem. Pharm. Bull.,* 39 (4), 927-929.

Kemsley, J. N. (2009). Modernizing TLC. *Chemical & engineering news*, 87 (20), 11-18.

Kitagawa, S., Tsukamoto, H., Hisada, S. and Nishebe, S. (1984). Studies on the Chinese Crude Drug "*Forsythiae Fructus*."VII. A New Caffeoyl Glycoside from Forsythia viridissima. *Chem. Pharm. Bull.*, 32 (3), 1209-1213.

Koo, K. A., Kim, S. H., Oh, T. H. and Kim, Y. C. (2006). Acteoside and its aglycones protect primary cultures of rat cortical cells from glutamate-induced excitotoxicity. *Life Sciences*, 79, 709-716.

Kopka, J., Fernie, A., Weckwerth, W., Gibon, Y. and Stitt, M. (2004). Metabolite profiling in plant biology: platforms and destinations. *Genome Biology*, 5 (6), 109.

Kufe, D. W., Pollock, R. E., Holland, Weichselbaum, R. R., Bast, R. C., Gansler, T. S., Holland, J. F., and Frei, E. (2003). *Holland-Frei Cancer medicine* (6th Ed.). Hamilton (ON): BC Decker.

Kumar, V., Mukherjee, K., Kumar, S., Mal, M. and Mukherjee, P. K. (2008). Validation of HPTLC method for the analysis of taraxerol in *Clitoria ternatea*. *Phytochemical analysis*, 19, 244-250.

Kvist, L. P. and Pedersen, J. A. (1986). Distribution and taxonomic implications of some phenolics in the family of Gesneriaceae determined by EPR spectroscopy. *Biochemical systematics and ecology*, 14 (4), 385-405.

Lafka, TI, Sinanoglou, V. and Lazos, E. S. (2007). On the extraction and antioxidant activity of phenolic compounds from winery wastes. *Food Chemistry*, 104, 1206-1214.

Lategan, C. A., Campbell, W. E., Seaman, T. and Smith, P. J. (2009). The bioactivity of novel furanoterpenoids isolated from *Siphonochilus aethiopicus*. *Journal of ethnopharmacology*, 121, 92-97.

Lee, C. C. and Houghton, P. (2005). Cytotoxicity of plants from Malaysia and Thailand used traditionally to treat cancer. *Journal of Ethnopharmacology*, 100, 237-243.

Lee, K. W., Bode, A. M. and Dong, Z. (2011). Molecular targets of phytochemicals for cancer prevention. *Nature reviews. Cancer*, 11, 211-218.

Lee, KW., Kim, H. J., Lee, Y. S., Park, HJ, Choi, JW, Ha, J. and Lee, KT. (2007). Acteoside inhibits human promyelocytic HL-60 leukeamia cell proliferation via inducing cell cycle arrest at G0/G1 phase and differentiation into monocyte. *Carcinogenesis*, 28 (9), 1928-1936.

Lee, S. K., Mbwambo, Z. H., Chung, H. S., Luyengi, L., Gamez, E. J., Mehta, R. G., Kinghorn, A. D. and Pezzuto, J. M. (1998). Evaluation of the Antioxidant Potentioal of Natural Products. *Combinatorial Chemistry & High Throughput Screening*, 35-46.

Liang, Y. Z., Xie, P. and Chan, K. (2004). Quality control of herbal medicines. *Journal of chromatography B*, 812, 53-70.

Lin, S., Wang, S., Liu, M., Gan, M., Li, S., Yang, Y., Wang, Y., He, W. and Shi, J. (2007). Glycosides from the stem bark of *Fraxinus sieboldiana. Journal of Natural Product*, 70, 817-823.

Liu, L., Li, YF. and Cheng, YY. (2008). A method for the production and characterization of fractionated libraries from Chinese herbal formulas. *Journal of Chromatography B*, 862, 196–204.

Lowry, J. B. (1972). Anthocyanins of some Malaysian members of the Gesneriaceae. *Phytochemistry*, 11, 3267-3269.

Lupulescu, A. (2001). *Cancer cell metabolism and cancer treatment.* Netherlands: Harwood Academic Publishers.

MAKNA (2008). *The latest cancer statistics*. URL: http://www.makna.org.my/cancerstatistics.asp. Accessed on 14th January 2010.

Melnick, R. L., Huff, J., Barrett, J. C., Maronpot, R. R., Lucier, G. and Portier, C. J. (1993). Cell proliferation and chemical carcinogenesis: symposium overview. *Environmental health perspectives*, 101 (Suppl 5), 3-8.

Micheal W. D. (2006). Some common-sense corollaries. In: *Modern HPLC fot practising scientists.* (pp.12). New Jersey: Wiley-Interscience.

Molyneux, P. (2003). The use of the stable free radical diphenylpicryl-hydrazyl (DPPH) for estimating antioxidant activity. *Songklanakarin J. Sci. Technol.*, 26 (2), 211-219.

Mosmann, T. (1983). Rapid colorimetric assay for cellular growth and survival: Application to proliferation and cytotoxicty assays. *Journal of immunological methods*, 65, 55-63.

Nagao, T., Abe, F. and Okabe, H. (2001). Antiproliferative constituents in the plants 7. Leaves of *Clerodendron bungei* and leaves and bark of *C. trichotomum*. *Biol. Pharm. Bull.*, 24 (11), 1338-1341.

National Cancer Institute (2003). *Cancer treatments*. URL: http://www.cancer.gov/cancertopics/treatment. Assessed on 13th January 2010.

National Cancer Institute (2006). *Loss of normal growth control*. URL: http://www.cancer.gov/cancertopics/understandingcancer/cancer. Assessed on 13th January 2010.

National Cancer Institute (2010). *Defining cancer*. URL: http://www.cancer.gov/cancertopics/cancerlibrary/what-is-cancer. Accessed on 3rd May 2011.

Ni, Y., Peng, Y. and Kokot, S. (2008). Fingerprinting of complex mixtures with the use of high performance liquid chromatography, inductively coupled plasma atomic emission spectroscopy and chemometrics. *Analytica chimica acta*, 616, 19-27.

Nobili, S., Lippi, D., Witort, E., Donnini, M., Bausi, L., Mini, E. and Capaccioli, S. (2009). Natural compounds for cancer treatment and prevention. *Pharmacological research*, 59, 365-378.

Nyiredy, SZ., Meier, B., Erdelmeier, C. A. J. and Sticher, O. (1985). "PRISMA". A geometrical design for solvent optimization in HPLC. *Journal of high resolution chromatography*, 8 (4), 186-188.

Ohno, T., Inoue, M., Ogihara, Y. and Saracoglu, I. (2002). Antimetastatic activity of acteoside, a phenylethanoid glycoside. *Biol. Pharm. Bull.*, 25 (5), 666-668.

Ohno, T., Mikami, E. and Oka, H. (2006). Analysis of crude drugs using reversed-phase TLC/scanning densitometry. (II) Identification of ginseng, red ginseng, gentian, Japanese gentian, pueraria root, gardenia fruit, schisandra fruit and ginger. *Journal of Nat. Med.*, 60, 141-145.

Ortholand, J. and Ganesan, A. (2004). Natural products and combinatorial chemistry: back to the future. *Current opinion in chemical biology*, 8, 271-280.

Pereira, C. A. M., Yariwake, J. H., Lancas, F. M., Wauters, J. N., Monique, T. and Angenot, L. (2004). A HPTLC densitometric determinatioon of flavonoids from *Passiflora alata*, *P. edulis*, *P. incarnate* and *P. caerulea* and comparison with HPLC method. *Phytochemical analysis*, 15, 241-248.

Phenomenex (2008). *SPE reference manual and users guide.* California.

Pirozynski (2006). 100 years of lung cancer. *Respiratory medicine*, 100, 2073-2084.

Pozharitskaya, O. N., Ivanova, S. A., Shikov, A. N. and Makarov, V. G. (2006). Separation and quantification of terpenoids of *Boswellia serrata* Roxb. extract by planar chromatography techniques (TLC and AMD). *Journal of separation science*, 29, 2245-2250.

Pozharitskaya, O. N., Ivanova, S. A., Shikov, A. N. and Makarov, V. G. (2007). Separation and evaluation of free radical-scavenging activity of phenol components of *Emblica officinalis* extract by using an HPTLC-DPPH method. *Journal of Separation Science*, 30, 1250-1254.

Pozharitskaya, O. N., Ivanova, S. A., Shikov, A. N. and Makarov, V. G. (2008). Separation and free radical-scavenging activity of major curcuminoids of *Curcuma longa* using HPTLC-DPPH method. *Phytochemical Analysis*, 19, 236-243.

Prakash, A. (2001). Antioxidant activity. *Agric Food Chem*, 19 (2), 701-705.

Rathi, A., Srivastava, N., Khatoon, S. and Rawat, A. K. S. (2008). TLC determination of strychnine and brucine of *Strychnos nux vomica* in ayurveda and homeopathy drugs. *Chromatographia*, 67, 607-613.

Ravishankara, M. N., Shrivastava, N., Padh, H. and Rajani, M. (2002). Evaluation of antioxidant properties of root bark of *Hemidesmus indicus* R. Br. (Anantmul). *Phytomedicine*, 9, 153-160.

Reich, E. and Schibli, A. (2007). *High-performance thin-layer chromatography for the analysis of medicinal plants.* New York: Thieme Medical Publishers.

Reich, E. and Widmer, V. (2009). Plant analysis 2008-Planar chromatography. *Planta medica*, 75, 711-718.

Rocha, A. B., Lopes, R. M. and Schwartsmann, G. (2001). Natural products in anticancer therapy. *Current opinion in pharmacology*, 1, 364-369.

Roche Applied Science (2005). Cell proliferation kit I (MTT). URL: http://www.roche-applied-science.com/pack-inert/145007a. Assessed on 9th September 2010.

Rochfort, S., Caridi, D., Stinton, M., Trenerry, V. C. and Jones, R. (2006). The isolation and purification of glucoraphanin from broccoli seeds by solid phase extraction and preparative high performace liquid chromatography. *Journal of chromatography A*, 1120, 205-210.

Royal Horticultural Society. (2004). *The use of limestone in horticulture.* Surrel.

Rumalla, C. S., Avula, B., Shukla, Y. J., Wang, Y. H., Pawar, R. S., Smillie, T. J. and Khan, I. A. (2008). Chemical fingerprint of Hoodia species, dietary supplements, and related genera by using HPTLC. *Journal of Separation science*, 31, 3959-3964.

Russo, A., Cardile, V., Lombardo, L., Vanella, L., Vanella, A. and Garbarino, J. A. (2005). Antioxidant activity and antiproliferative action of methanolic extract of *Geum quellyon* Sweet roots in human tumor cell lines. *Journal of Ethnopharmacology*, 100, 323-332.

Saha, K., Lajis, N. H., Israf, D. A., Hamzah, A. S., Khozirah, S., Khamis, S. and Syahida, A. (2004). Evaluation of antioxidant and nitric oxide inhibitory activities of selected Malaysian medicinal plants. *Journal of Ethnopharmacology*, 92, 263-267.

Saracoglu, I., Inoue, M., Calis, I. and Ogihara, Y. (1995). Studies on constituents with cytotoxic and cytostatic activity of two Turkish medicinal plants *Phlomis armeniaca* and *Scutellaria salviifolia. Biol. Pharm. Bull.*, 18 (10), 1396-1400.

Satyajit D. S., Zahid L. and Alexander I. G. (2005). Natural products isolation: Second edition. In: *Extraction of plant natural products*. (pp. 29-37). New jersey: Humana Press.

Schaneberg, B. T., Crockett, S., Bedir, E. and Khan, I. A. (2003). The role of chemical fingerprinting: application to Ephedra. *Phytochemistry*, 62, 911-918.

Schrijvers, D. L. (2003). Extravasation: a dreaded complication of chemotherapy. *Annals of Oncology*, 14 (3), iii26-iii30.

Sena, F. J. G., Nimmo, S. L., Xavier, H. S., Barbosa-Filho, J. M. and Cichewicz, R. H. (2009). Phenylethanoid and lignan glycosides from polar extracts of Lantana, a genus of Verbenaceous plants widely used in traditional herbal therapies. *Journal of Natural Product*, 72, 1344-1347.

Simonovska, B., Vovk, I., Andrensek, S., Valentová, K. and Ulrichová, J. (2003). Investigation of phenolic acids in yacon (*Smallanthus sonchifolius*) leaves and tubers. *Journal of Chromatography A*, 1016, 89-98.

Soepadmo, A. (1998). Limestone, quartzite and ultramatic vegetation. In: *The encyclopedia of Malaysia plants.* (pp. 26-27). Singapore: Archipelago press.

Stepp, J. R. and Moerman, D. E. (2001). The importance of weeds in ethnopharmacology. *Journal of ethnopharmacology*, 75, 19-23.

Sukumar, D., Arimboor, R. and Arumughan, C. (2008). HPTLC fingerprinting and quantification of lignans as markers in sesame oil and its polyherbal formulations. *Journal of Pharmaceutical and Biomedical Analysis*, 47, 795-801.

Sunita, A. and Abhishek, S. (2008). A comparative evaluation of phytochemical fingerprints of *Asteracantha longifolia* Nees. using HPTLC. *Asian journal of plant sceinces*, 7 (6), 611-614.

Suzuki, H., Sasaki, R., Ogata, Y., Nakamura, Y., Sakurai, N., Kitajima, M., Takayama, H., Kanaya, S., Aoki, K., Shibata, D. and Saito, K. (2008). Metabolic profiling of flavonoids in *Lotus japonicus* using liquid chromatography Fourier transform ion cyclotron resonance mass spectrometry. *Phytochemistry*, 69, 99-111.

Tam, K. F., Ng, T. Y., Liu, S. S., Tsang, P. C. K., Kwong, P. W. K. and Ngan, H. Y. S. (2004). Potential application of ATP cell viability assay in the measurement of intrinsic radio-sensitivity in cervical cancer. *Gynaecologic oncology*, 96, 765-770.

Tan, H. Y. (2008). *Ethnomedicinal approach in screening of cytotoxic phytochemicals from local medicinal plants.* Bachelor degree final year project, University Tunku Abdul Rahman, Malaysia.

Tan, K. H. (2009). *Isolation and purification of potential anti-tumour-promoting compound(s) from Paraboea paniculata.* Bachelor degree final year project, University Tunku Abdul Rahman, Malaysia.

Tanaka, T., Ikeda, T., Kaku, M., Zhu, XH., Okawa, M., Yokomizo, K., Uyeda, M. and Nohara, T. (2004). A new lignan glycoside and phenylethanoid glycosides from *Strobilanthes cusia* Bremek. *Chem. Pharm. Bull.*, 52 (10), 1242-1245.

Tannock, I. F., Hill, R. P., Bristow, R. G. and Harrington, L. (2005). Cell death and apoptosis. In: *The basic science of oncology* (fourth ed.). (pp. 258-260). New York: McGraw-Hill Medical.

Tian, R., Xie, P. and Lie, H. (2009). Evaluation of traditional chinese herbal medicine: Chaihu (*Bupleuri radix*) by both high performance liquid chromatographic and high performance thin layer chromatographic fingerprint and chemometric analysis. *Journal of chromatography A*, 1216, 2150-2155.

Toi, L. R. (2008). *Ethnomedicinal approach in screening of cytotoxicity and DPPH radical scavenging activities of local medicinal plants.* Bachelor degree final year project, University Tunku Abdul Rahman, Malaysia.

Tsuda, H., Ohshima, Y., Nomoto, H., Fujita, K., Matsuda, E., Iigo, M., Takasuka, N. and Moore, M. A. (2004). Cancer Prevention by Natural Compounds. *Drug Metab. Pharmacokin.,* 19 (4), 245-263.

Tuzimski, T. and Soczewinski, E. (2002). Correlation of retention parameters of pesticides in normal- and reversed-phase systems and their utilization for the separation of a mixture of 14 triazines and urea herbicides by means of two-dimensional thin-layer chromatography. *Journal of chromatography A*, 961, 277-283.

Tysnes, B. B. and Bjerkvig, R. (2007). Cancer initiation and progression: involvement of stem cells and the microenvironment. *Biochimica et biophysica acta*, 1775, 283-297.

Tyson, C. A. and Martell, A. E. (1972). Kinetics and mechanism of the metal chelate catalyzed oxidation of pyrocatechols. *J. Am. Chem. Soc.*, 94 (3), 939-945.

Ueda, J., Tezuka, Y., Banskota, A. H., Tran, Q. L., Tran, Q. K., Harimaya, Y., Saiki, I. and Kadota, S. (2002). Antiproliferative activity of Vietnamese medicinal plants. *Biological and Pharmaceutical Bulletin*, 25 (6), 753-760.

U.S. Food and Drug Administration (FDA) (2000). *FDA guidance for industry-botanical drug products (draft guidance).* Rockville: MD.

Wang, W., Pan, K., Li, Z., Weitzman, A. L. and Skog, L. E. (1998). *"Paraboea" in flora of China* (Vol. 18). Beijing: Science press and Missouri botanical garden press.

Wang, X., Peng, Y., Xu, L., Xiao, W., Xiao, P. and Liu, Y. (2009). Triterpenes and triterpene glycosides from aerial part of *Paraboea glutinosa*. *Zhong guo zhong yao za zhi*, 34 (10), 1228-1230.

Weinberg, R. A. (2007). *The biology of cancer.* New York: Garland Science, Taylor & Francis Group.

Weyermann, J., Lochmann, D. and Zimmer, A. (2005). A practical note on the use of cytotoxicity assays. *International journal of pharmaceutics*, 288, 360-376.

Wiart, C. (2007). Medicinal Rubiaceae (I). In: *Ethnopharmacology of medicinal plants.* (pp.168). New jersey: Humana press.

Widmer, V., Reich, E. and DeBatt, A. (2008). Validated HPTLC method for identification of *Hoodia gordonii*. *Journal of planar chromatography*, 21 (1), 21-26.

World Health Organization (WHO) (1991). *Guidelines for the assessment of herbal medicines.* Geneva.

Xie, P., Chen, S., Liang, Y., Wang, X., Tian, R. and Upton, R. (2006). Chromatographic fingerprint analysis – a rational approach for quality assessment of traditional Chinese herbal medicine. *Journal of Chromatography A*, 1112, 171-180.

Xie, G., Zhao, A., Li, P., Li, L. and Jia, W. (2007). Fingerprint analysis of Rhizome chuanxiong by pressurized capillary electrochromatography and high performance liquid chromatography. *Biomedical chromatography*, 21, 867-875.

Yang, T., Yang, Y. H., Yang, J. Y., Chen, B. M., Duan, J. P., Yu, S. P., Ouyang, H. T., Cheng, J. P. and Chen, Y. X. (2008). Fingerprint of *Hedyotis diffusa* Willd. by HPLC-MS. *Phytochemical analysis*, 19, 487-492.

Yong, T. K. (2003). *Plants face rising rate of extinction: public should be educated on the need to conserve rare and endangered species.* Malaysia: New sunday times.

Yrjönen, T., Peiwu, L., Summanen, J. ,Hopia, A. and Vuorela, H. (2003). Free radical-scavening activity of phenolics by reversed-phase TLC. *JAOCS*, 80, 9-14.

Yuliana, N. D., Khatib, A., Choi, Y. H. and Verpoorte, R. (2011). Metabolomics for bioactivity assessment of natural products. *Phytotherapy research*, 25, 157-169.

Zheng, XK., Li, J., Feng, WS., Bi, YF., Ji, CR. (2003). Isolation and structural identification of phenylethanoid glycosides from *Corallodiscus flabellate*. *Acta pharmaceutica sinica*, 38 (2), 116-119.
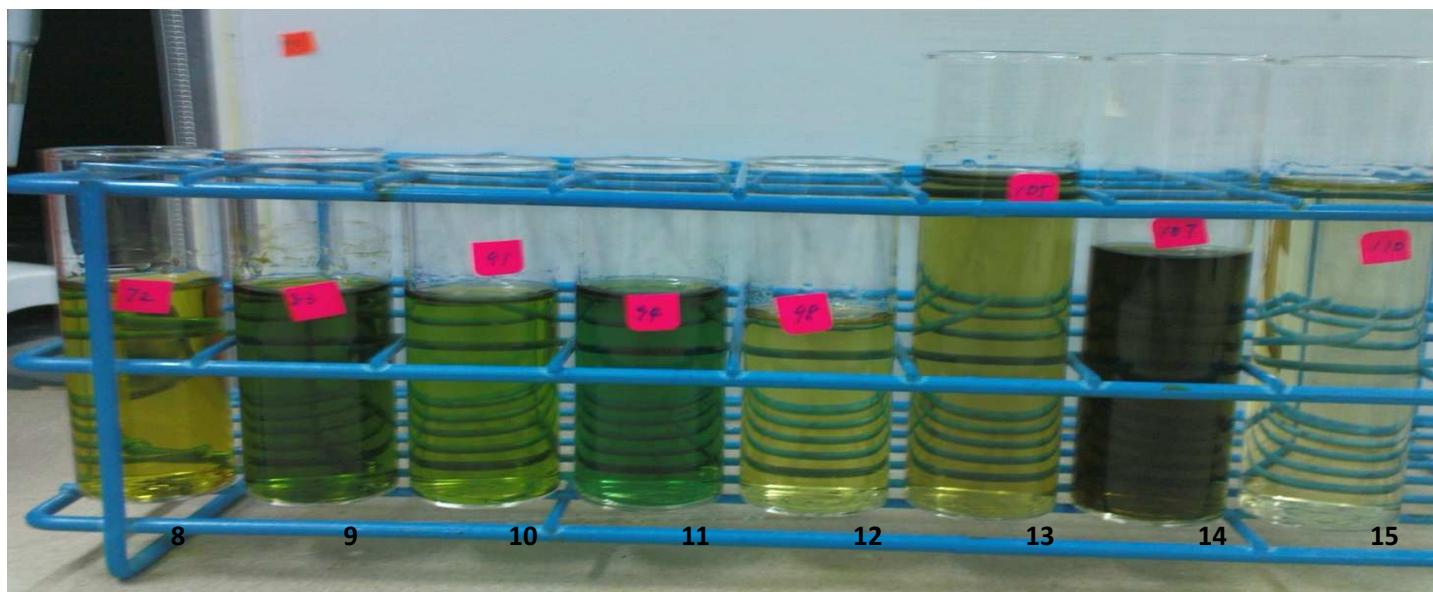
Figure 7.1: Separation of fractions 8 to 15 of crude leaf of *P. paniculata* based on different colours of band eluted.

Figure 7.2: Zones selected in fingerprint profile of leaf crude extract for evaluation of method validation.

Figure 7.3: Zones selected in fingerprint profile of rhizome crude extract for evaluation of method validation.

Figure 7.4: Zones selected in fingerprint profile of rhizome SPE-separated fraction 4 for evaluation of method validation.

Figure 7.5: Zones selected in fingerprint profile of rhizome SPE-separated fraction 5 for evaluation of method validation.

Figure 7.6: Zones selected in fingerprint profile of rhizome SPE-separated fraction 7 for evaluation of method validation.
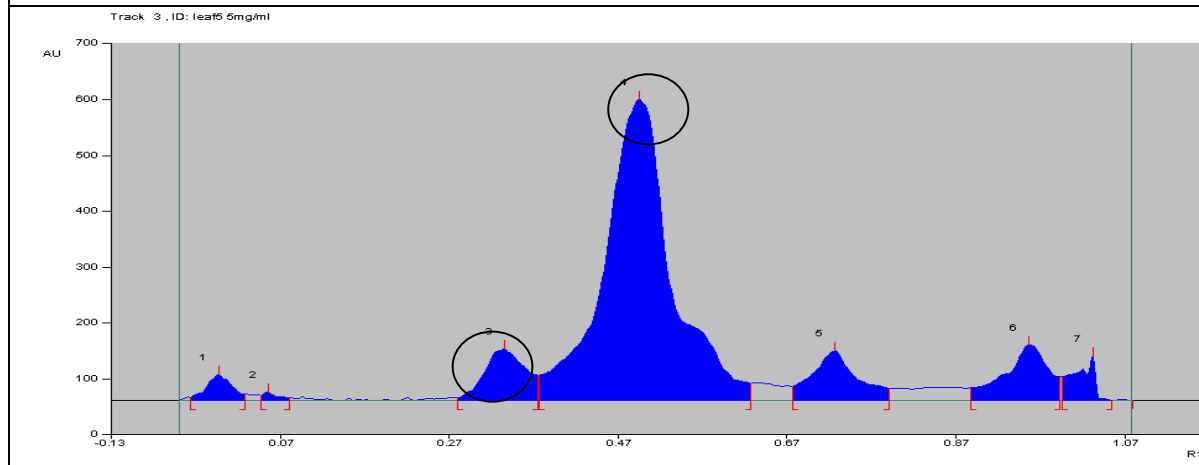
Figure 7.7: Zones selected in fingerprint profile of leaf SPE separated-fraction 5 for evaluation of method validation.

Figure 7.8: Zones selected in fingerprint profile of leaf SPE-separated fraction 12 for evaluation of method validation.
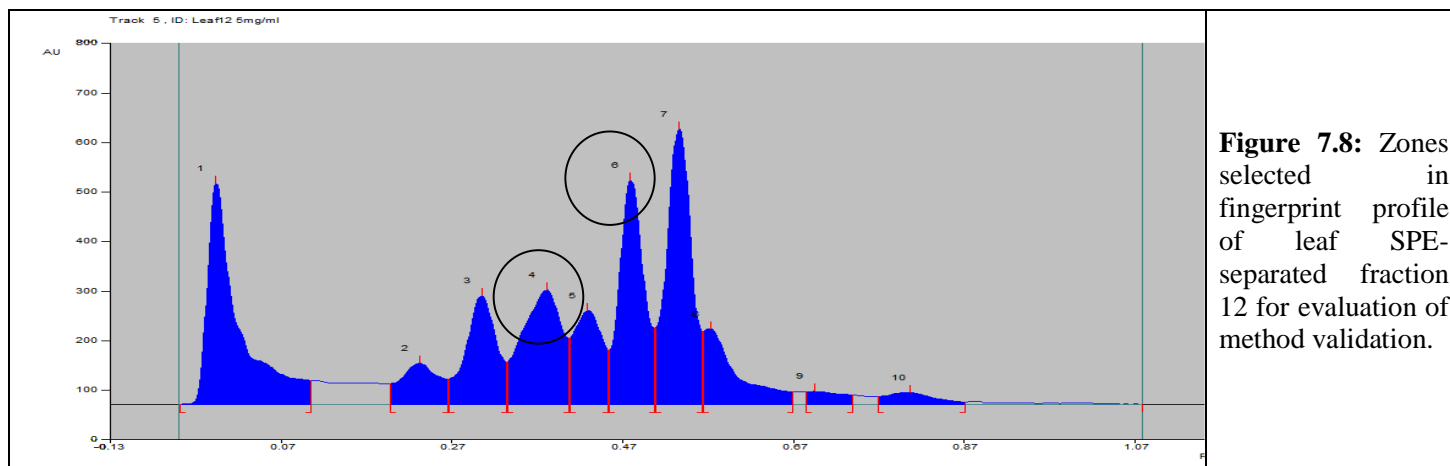
The selected zones present in the chromatogram could be declared as characteristic peaks of the active sample.
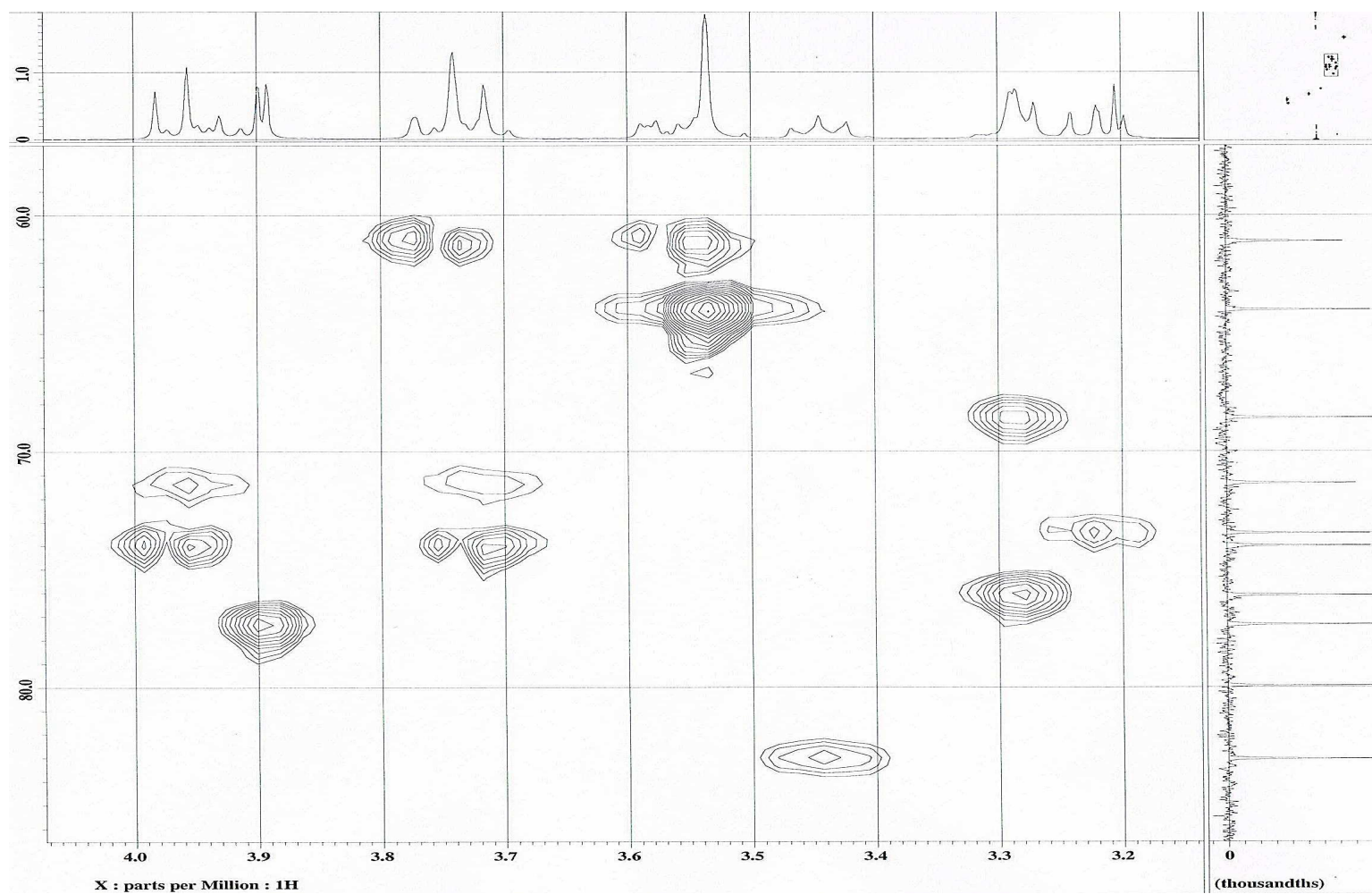
Figure 7.9 (a): Enlarged HMQC spectrum of Compound PP-1.
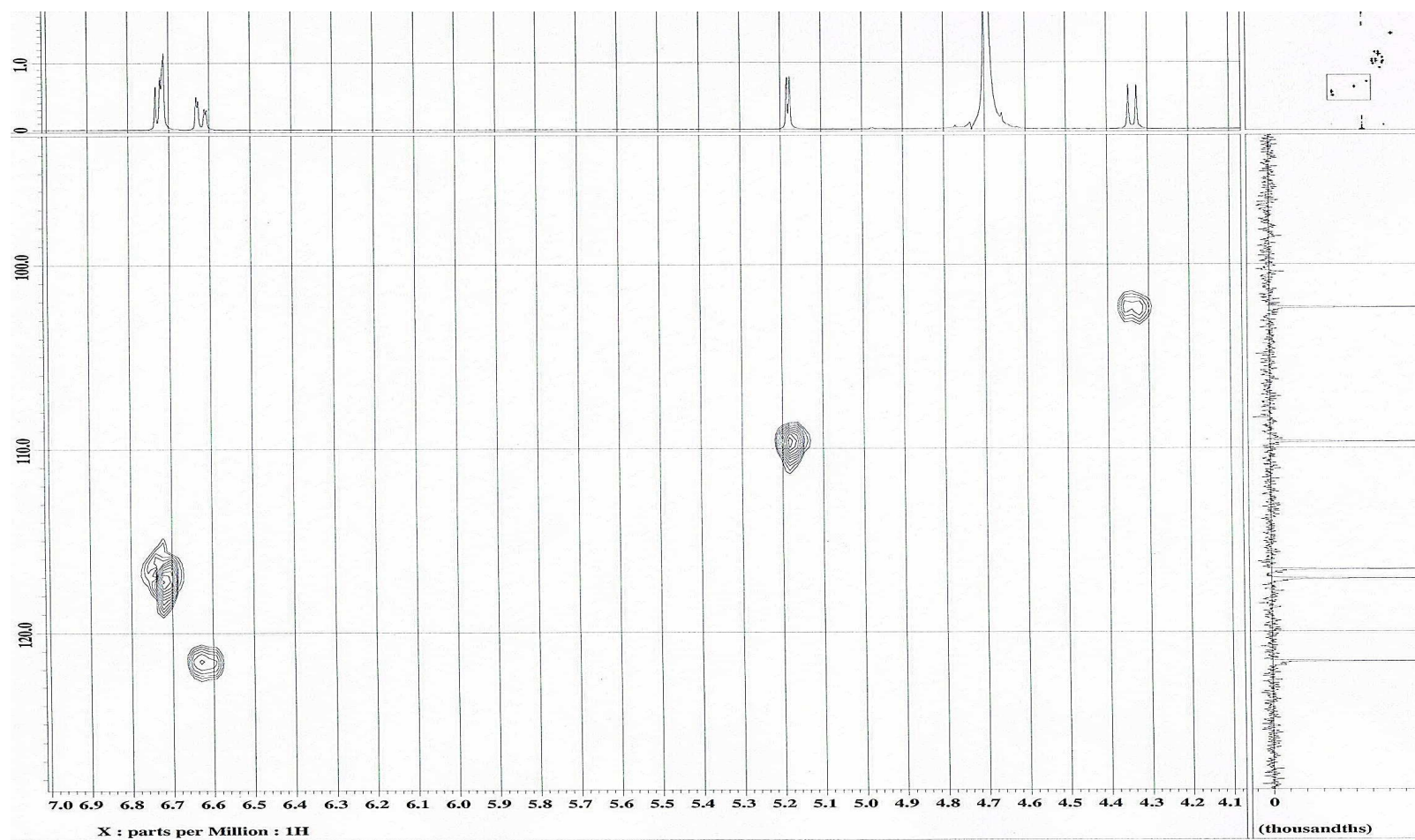
Figure 7.9 (b): Enlarged HMQC spectrum of Compound PP-1.
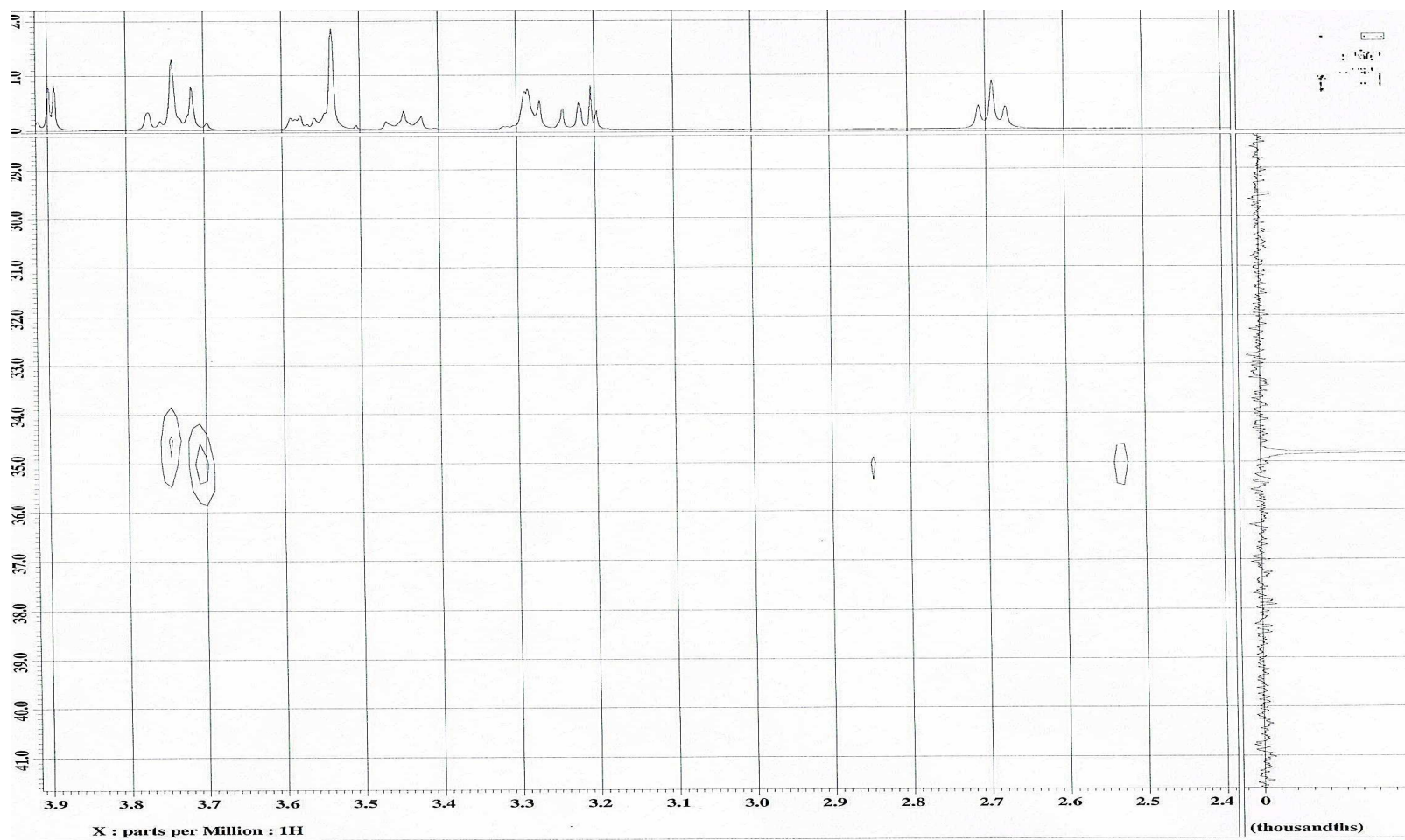
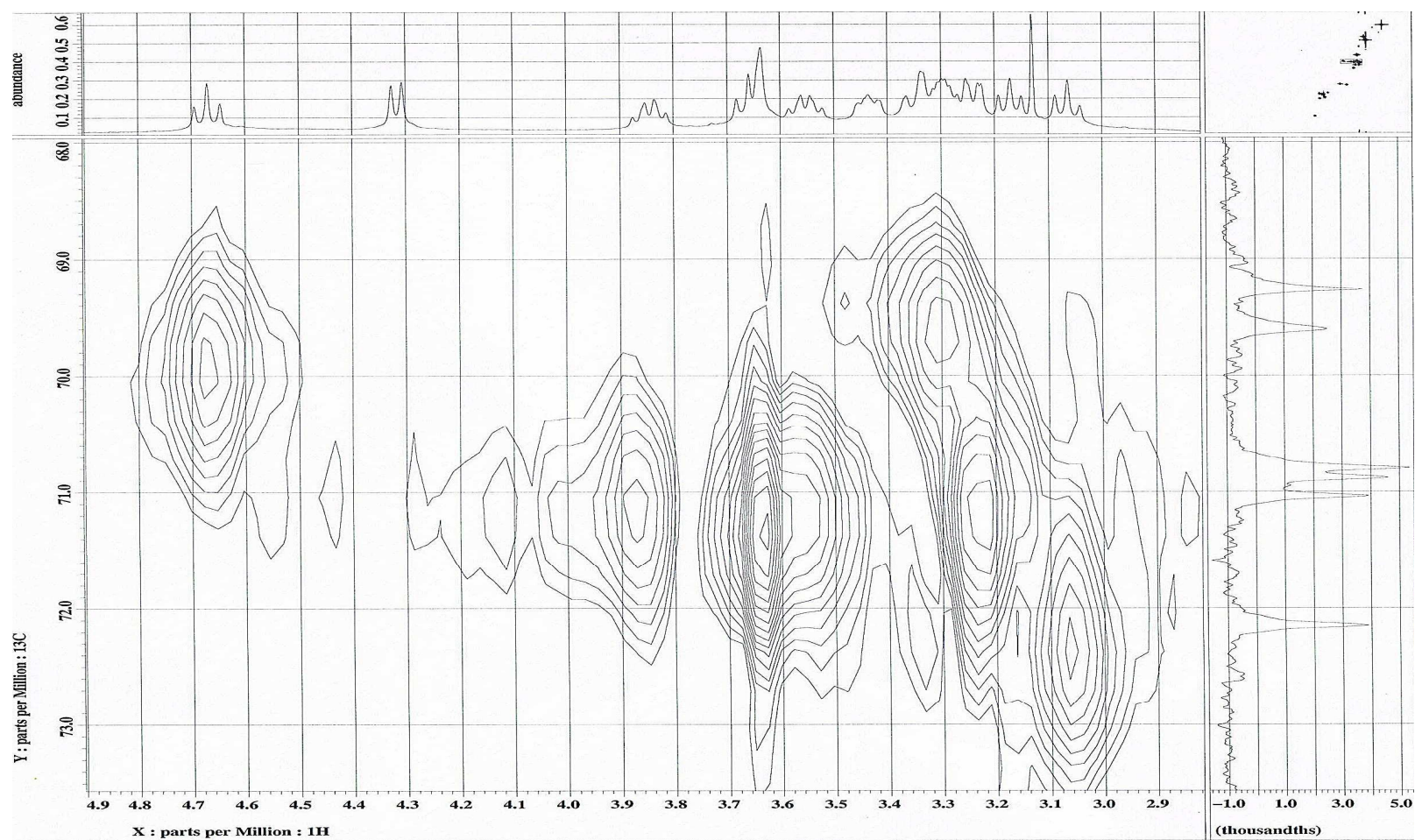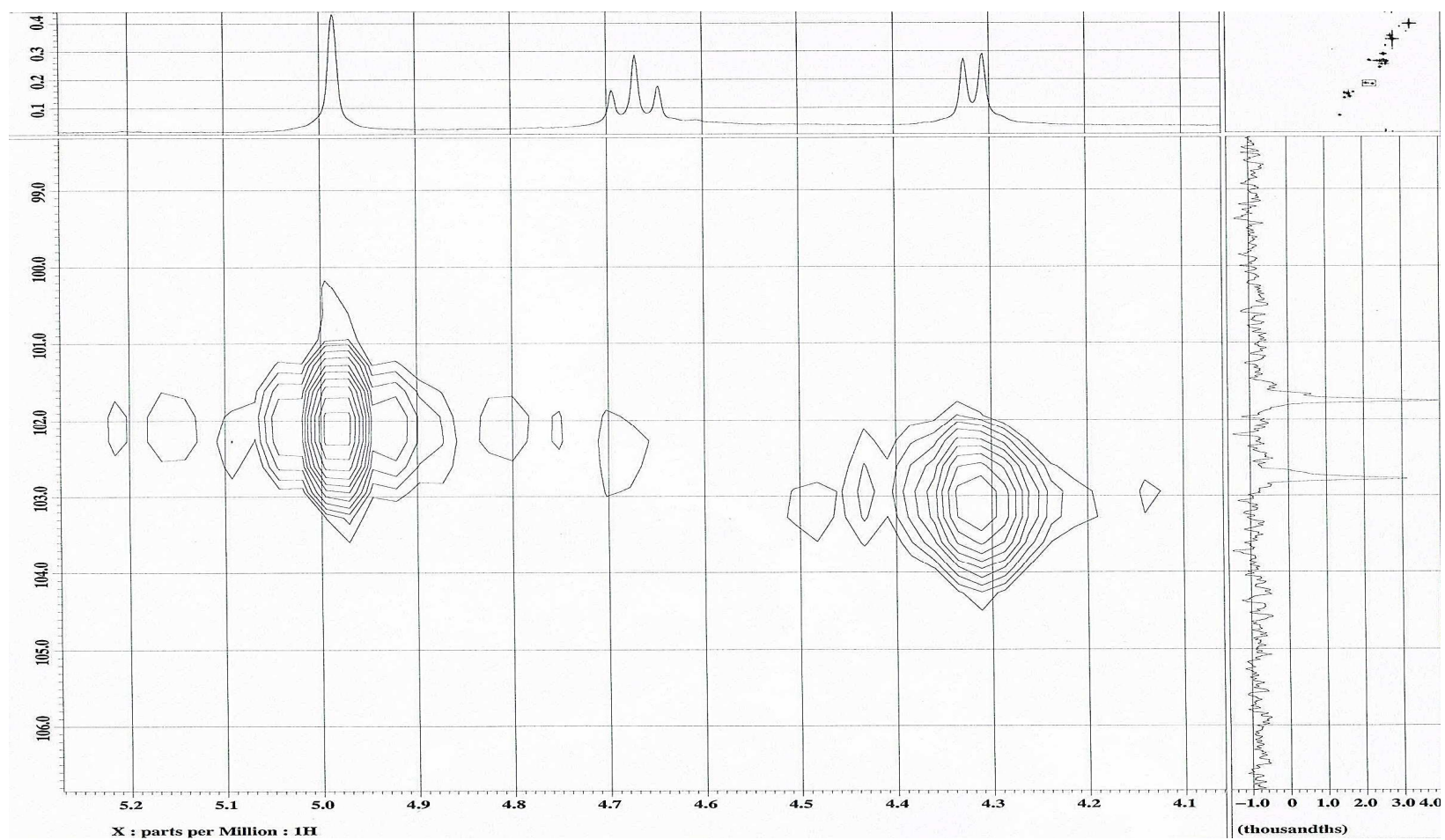**Figure 7.10 (a):** Enlarged HMBC spectrum of Compound PP-1.
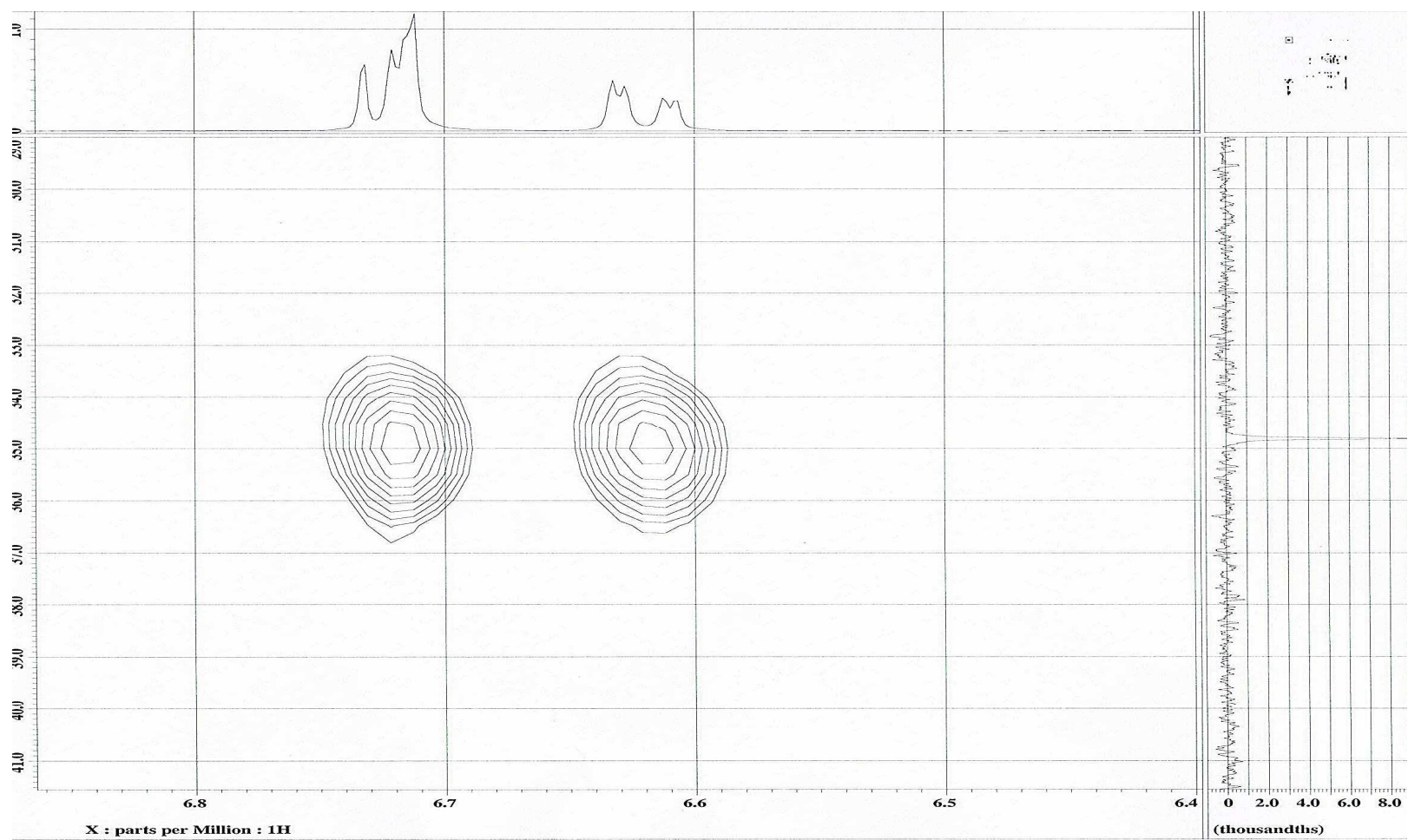
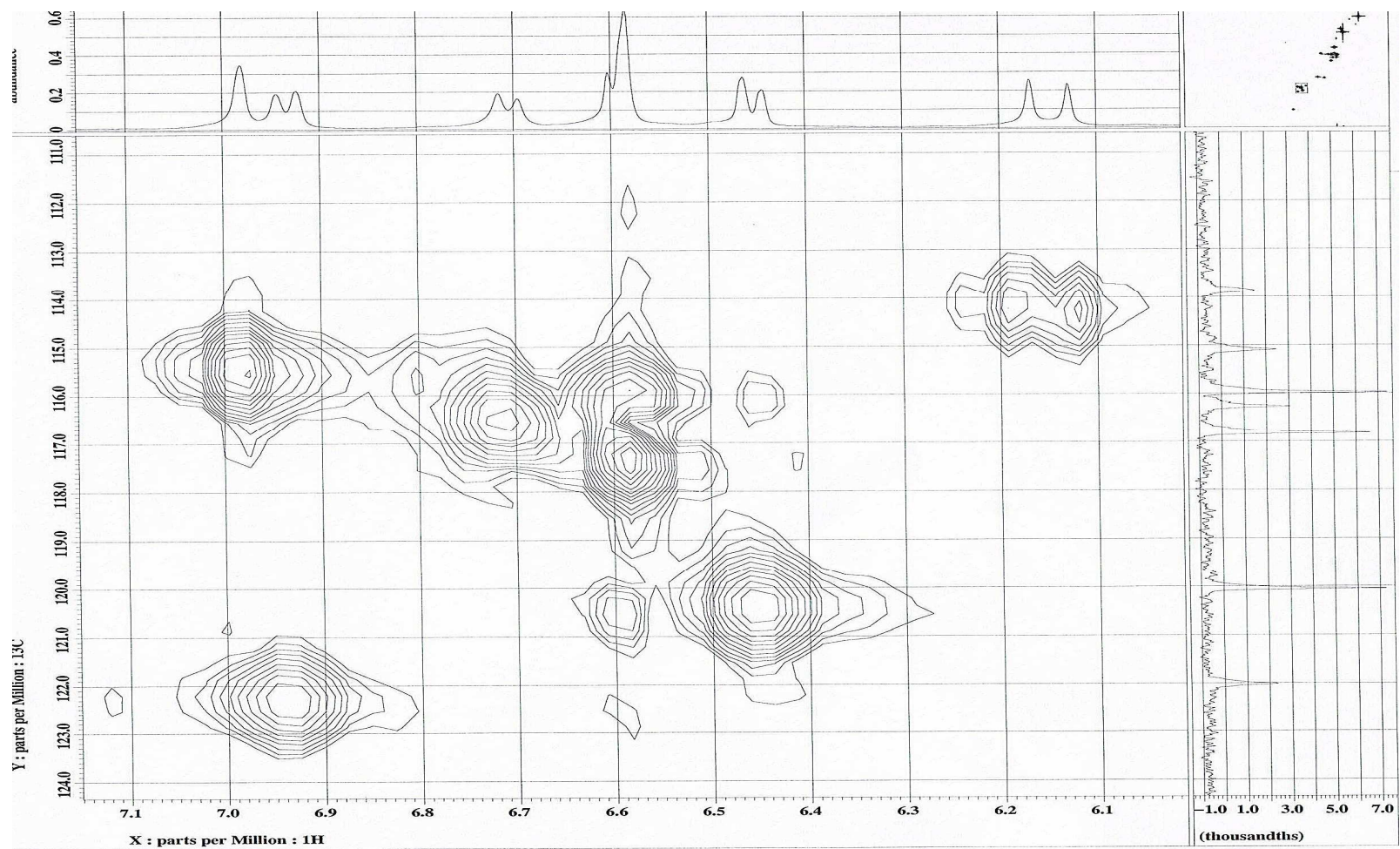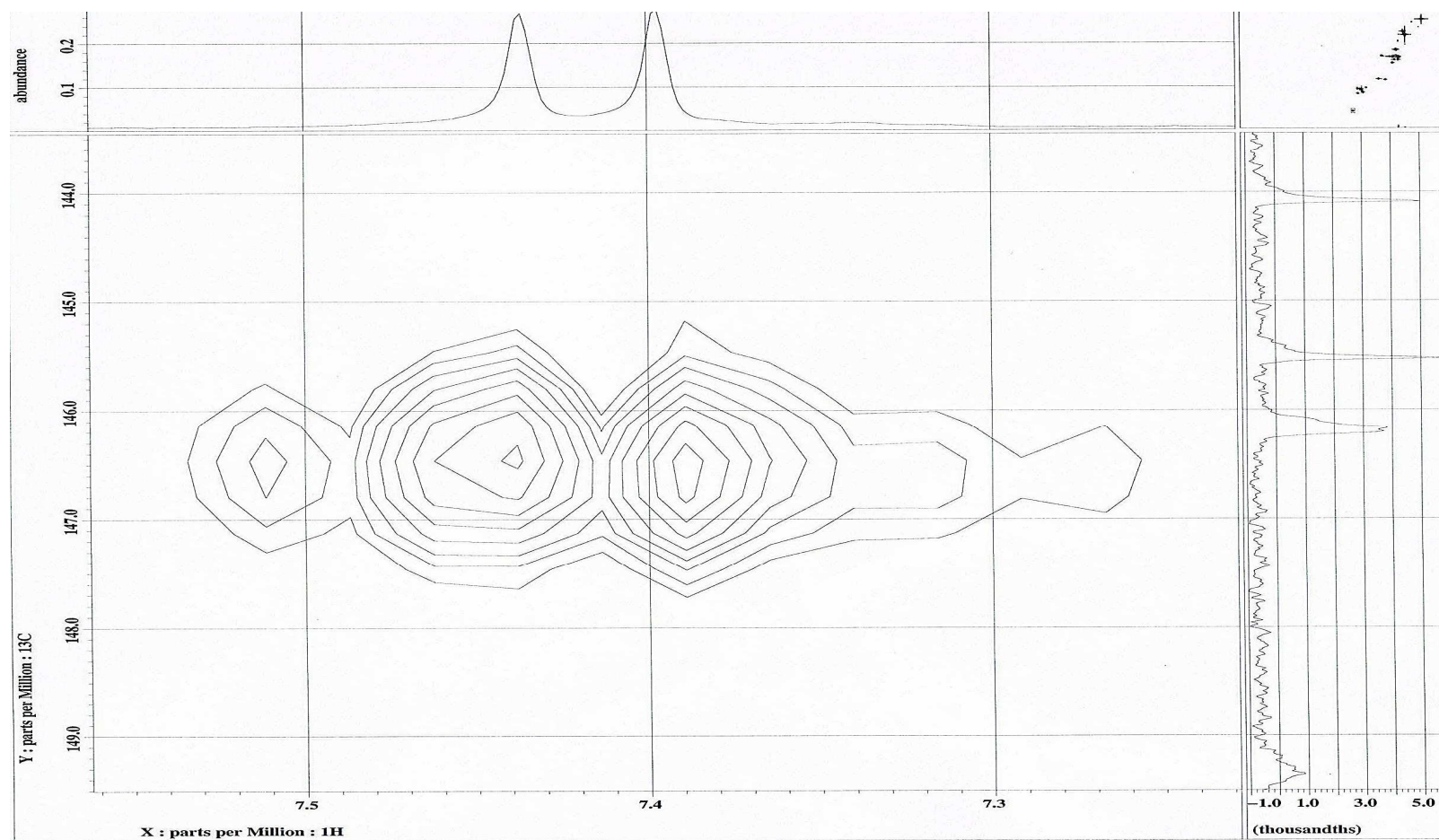**Figure 7.10 (b):** Enlarged HMBC spectrum of Compound PP-1.
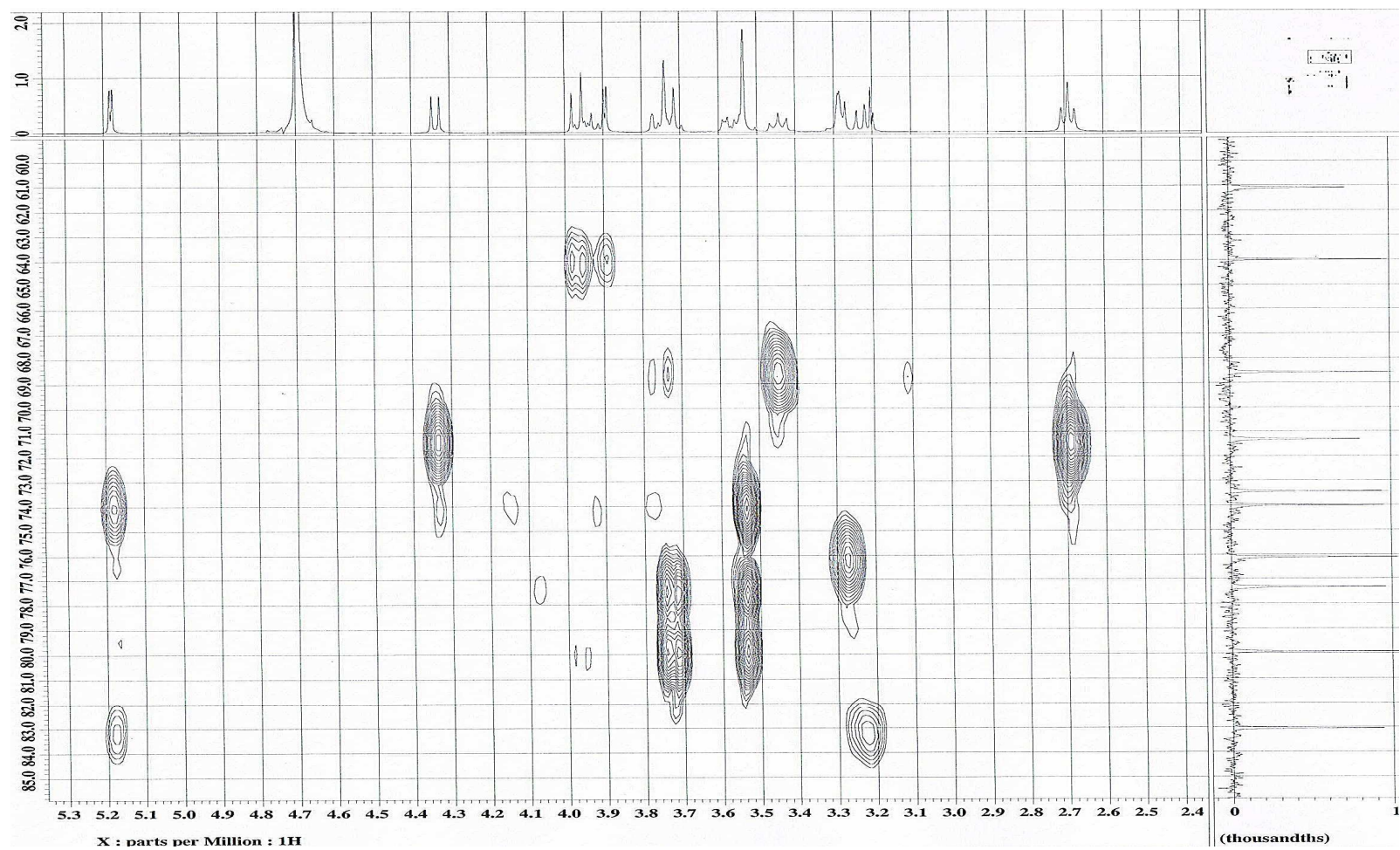
Figure 7.10 (c): Enlarged HMBC spectrum of Compound PP-1.
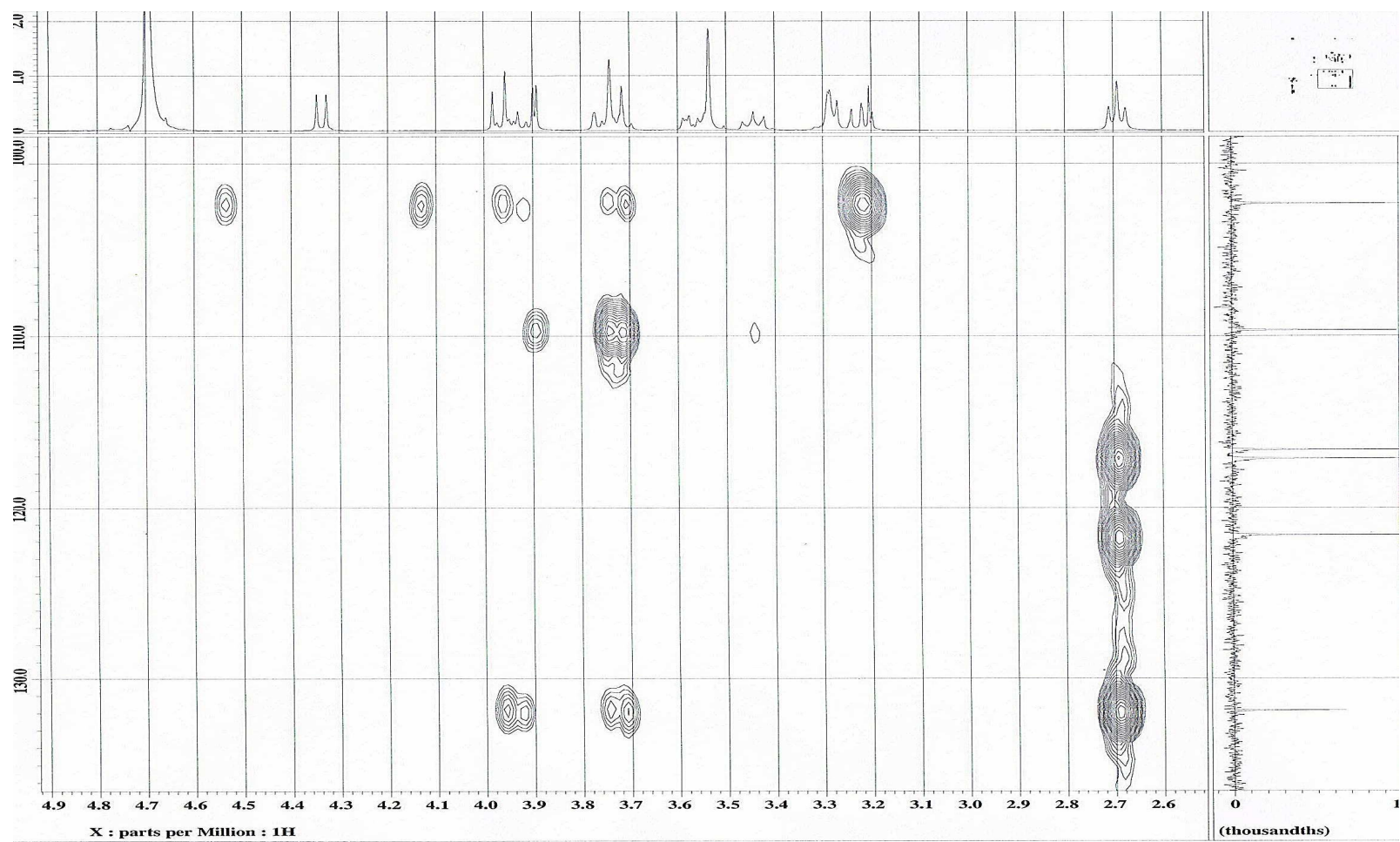
Figure 7.10 (d): Enlarged HMBC spectrum of Compound PP-1.
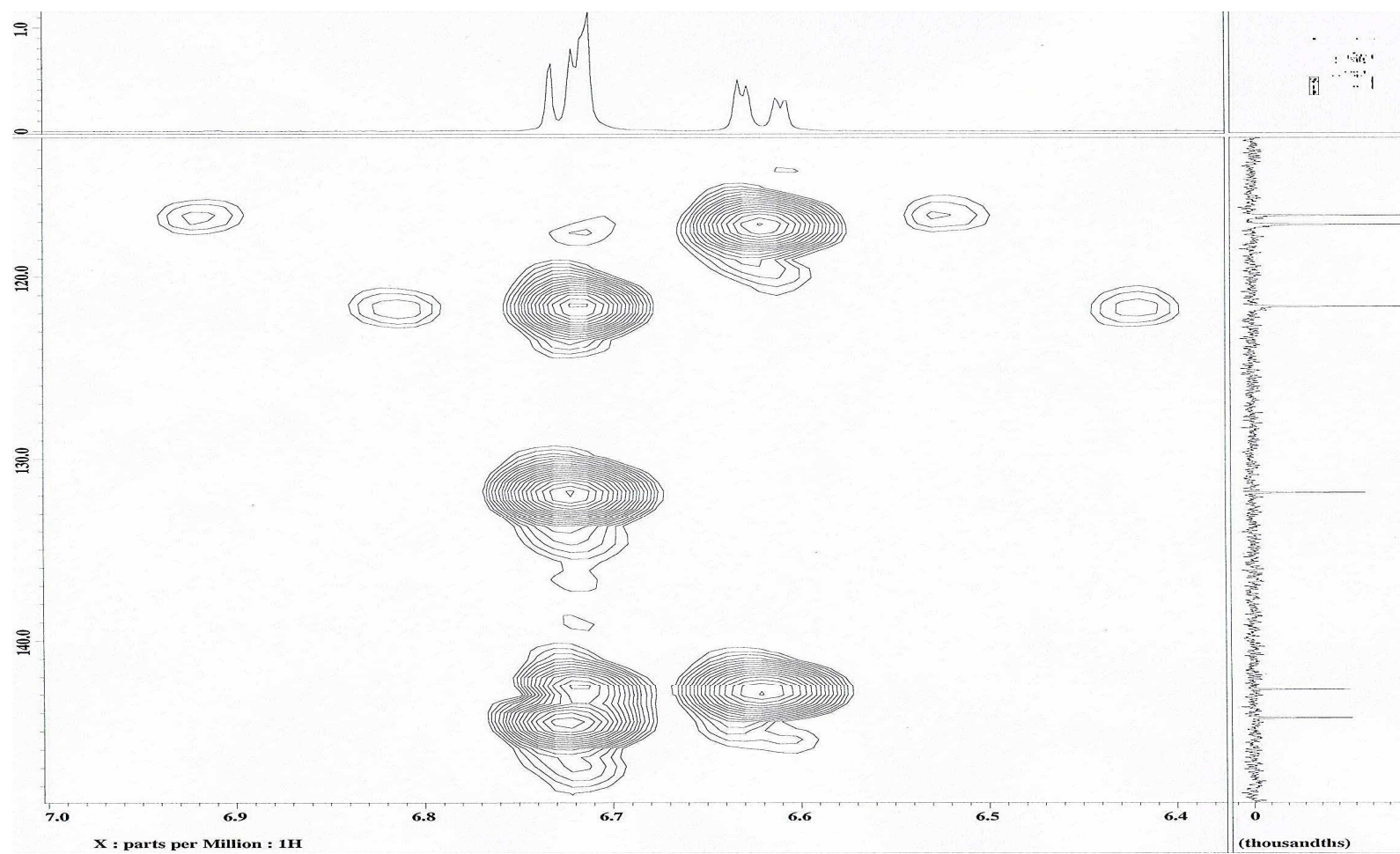
Figure 7.10 (e): Enlarged HMBC spectrum of Compound PP-1.
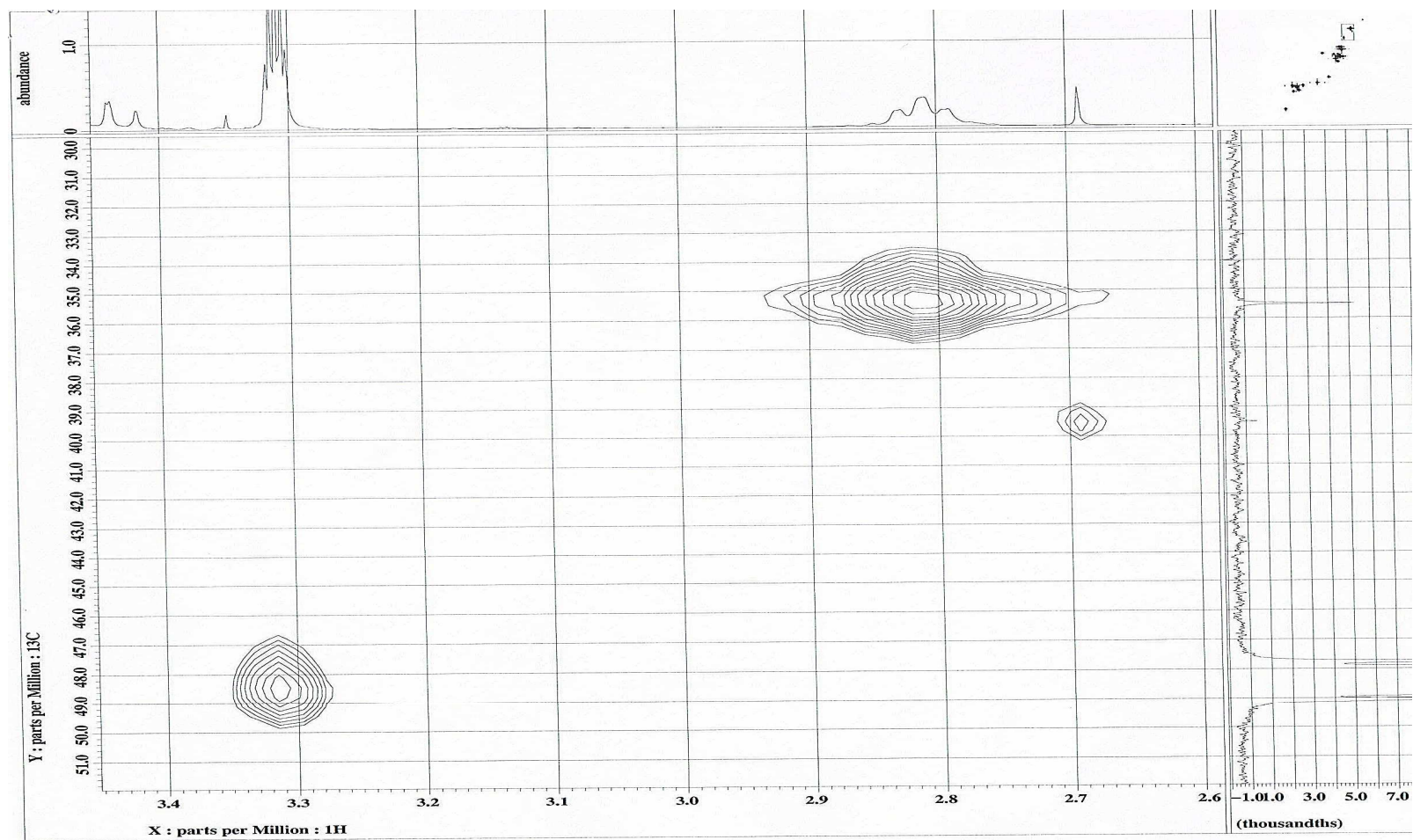
Figure 7.11(a): Enlarged HMQC spectrum of Compound PP-2.
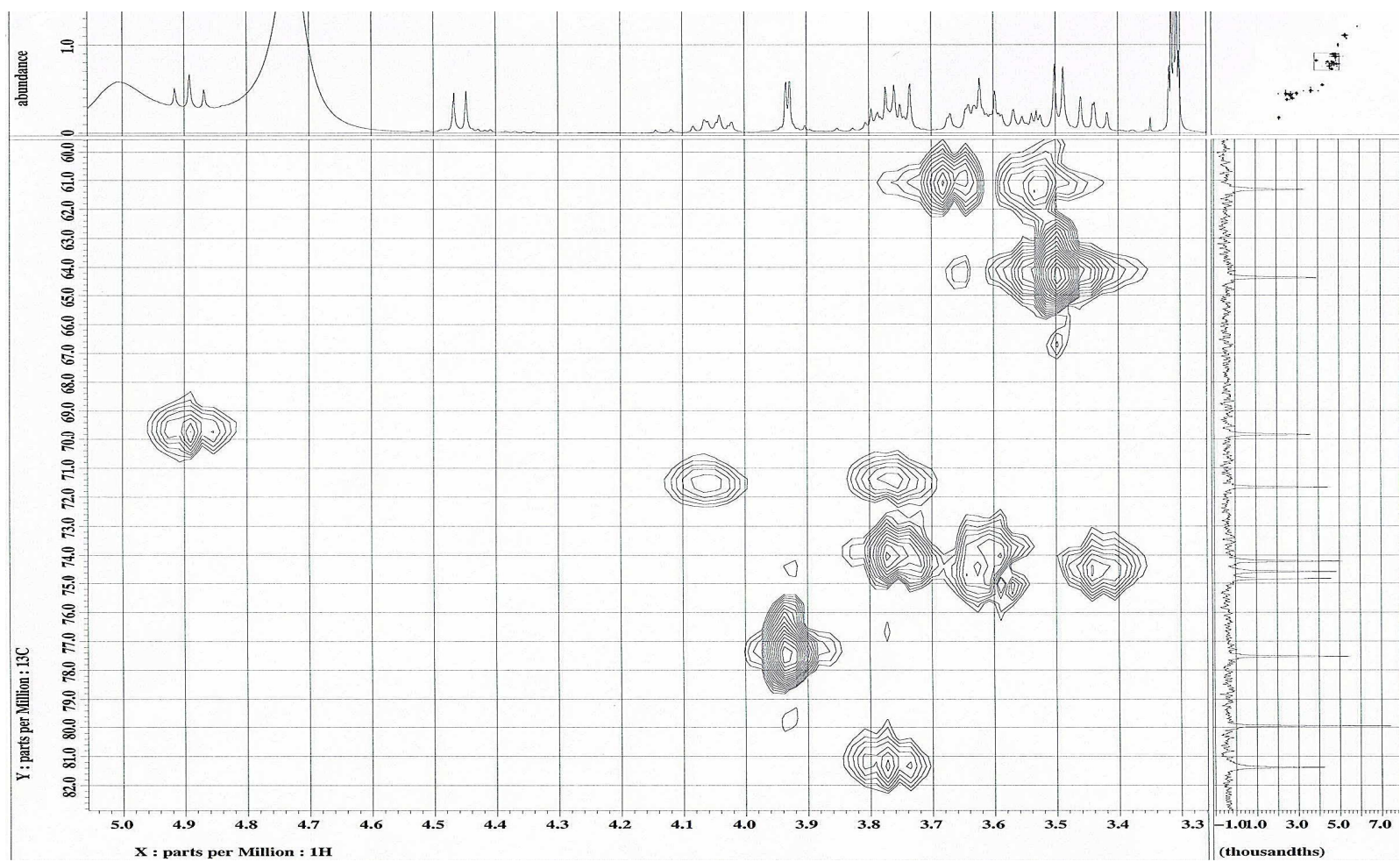
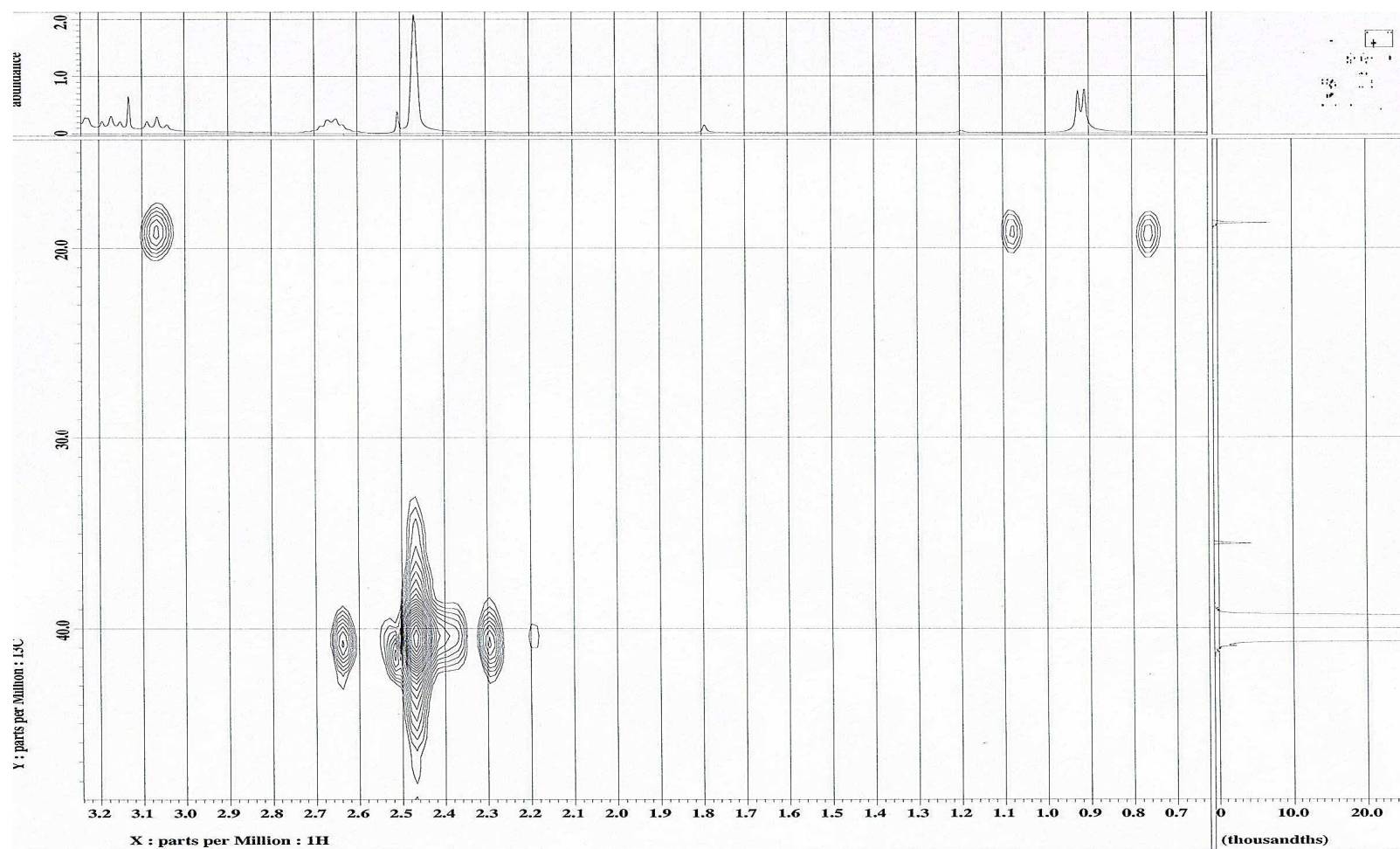**Figure 7.11(b):** Enlarged HMQC spectrum of Compound PP-2.
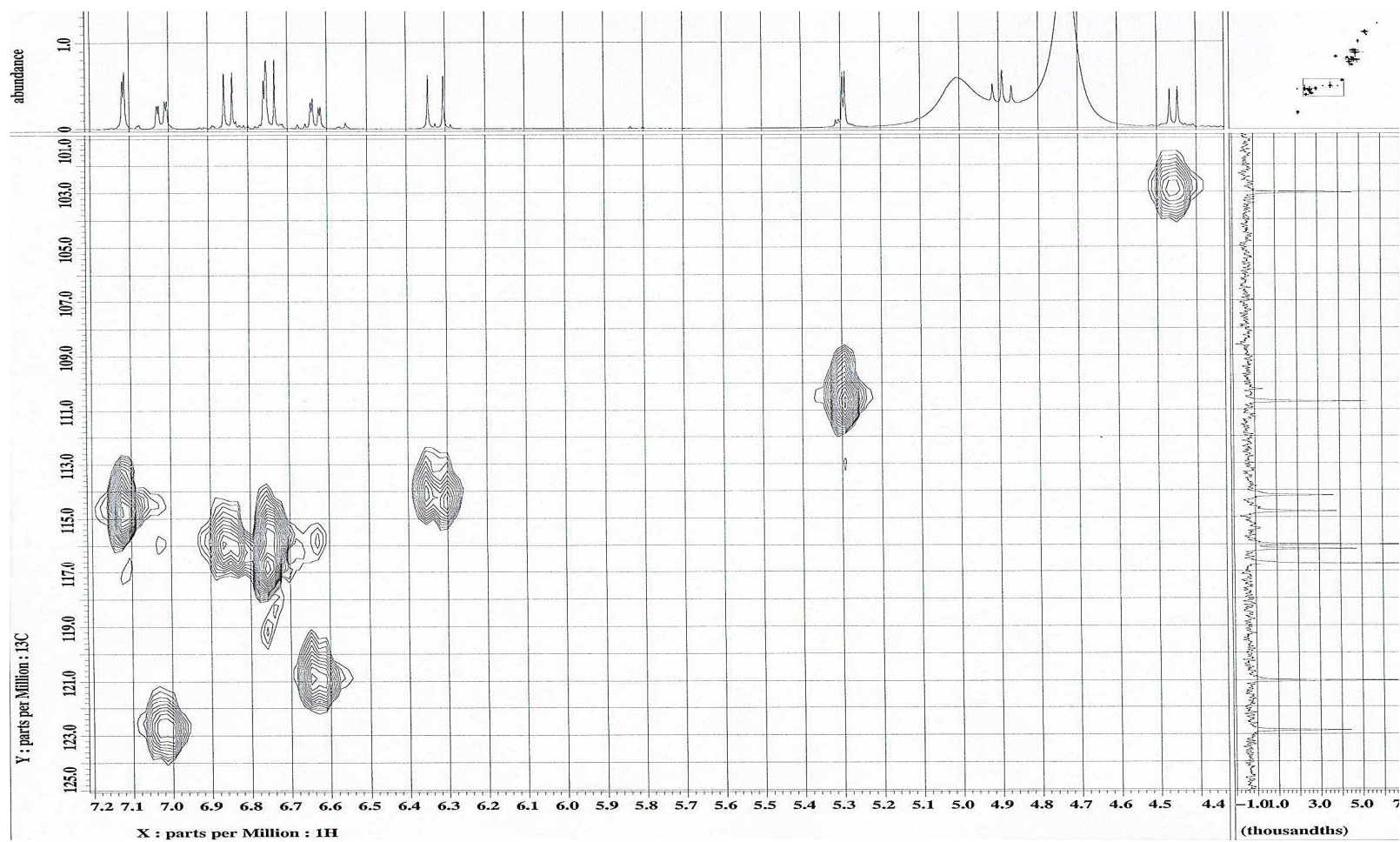
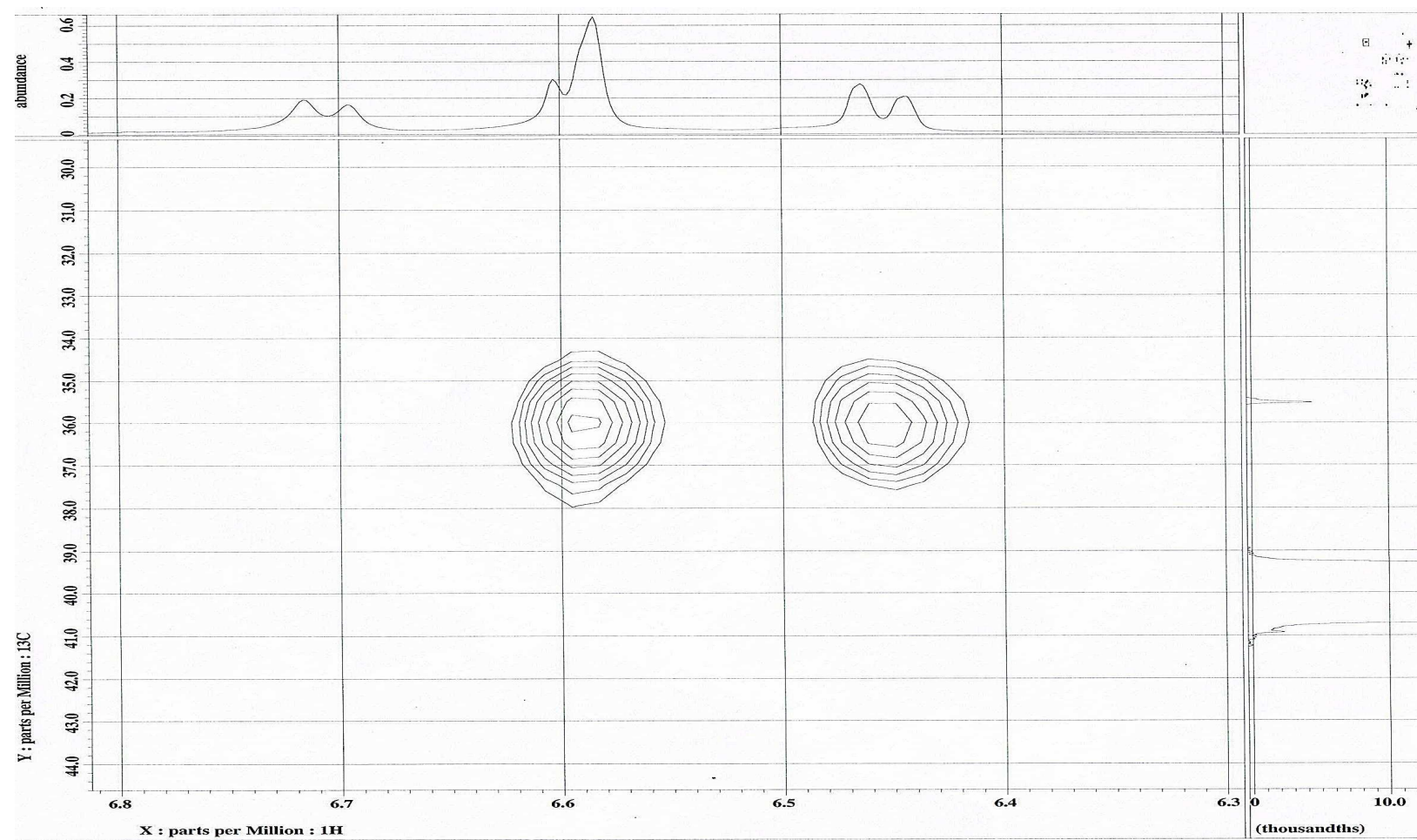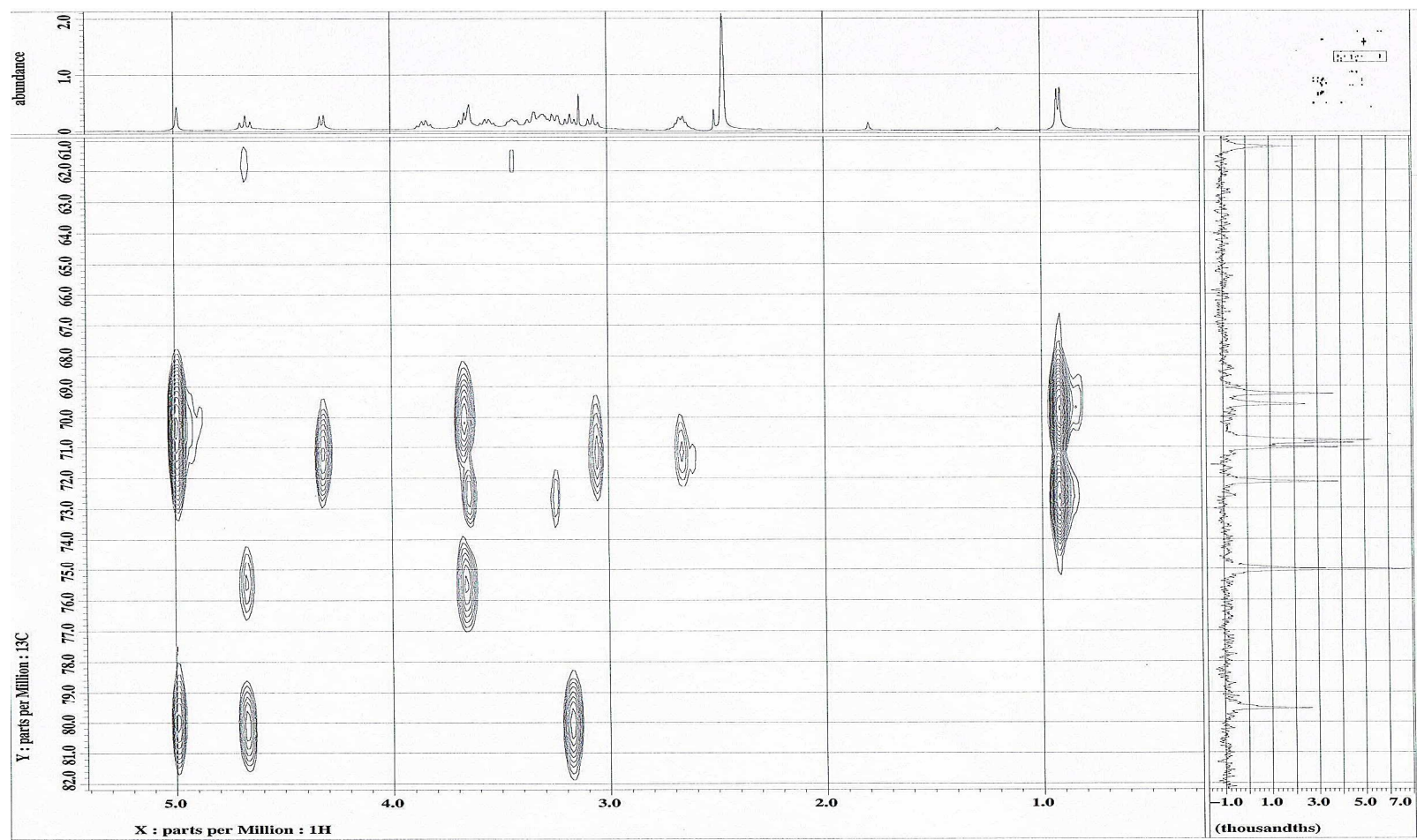**Figure 7.11(c):** Enlarged HMQC spectrum of Compound PP-2.
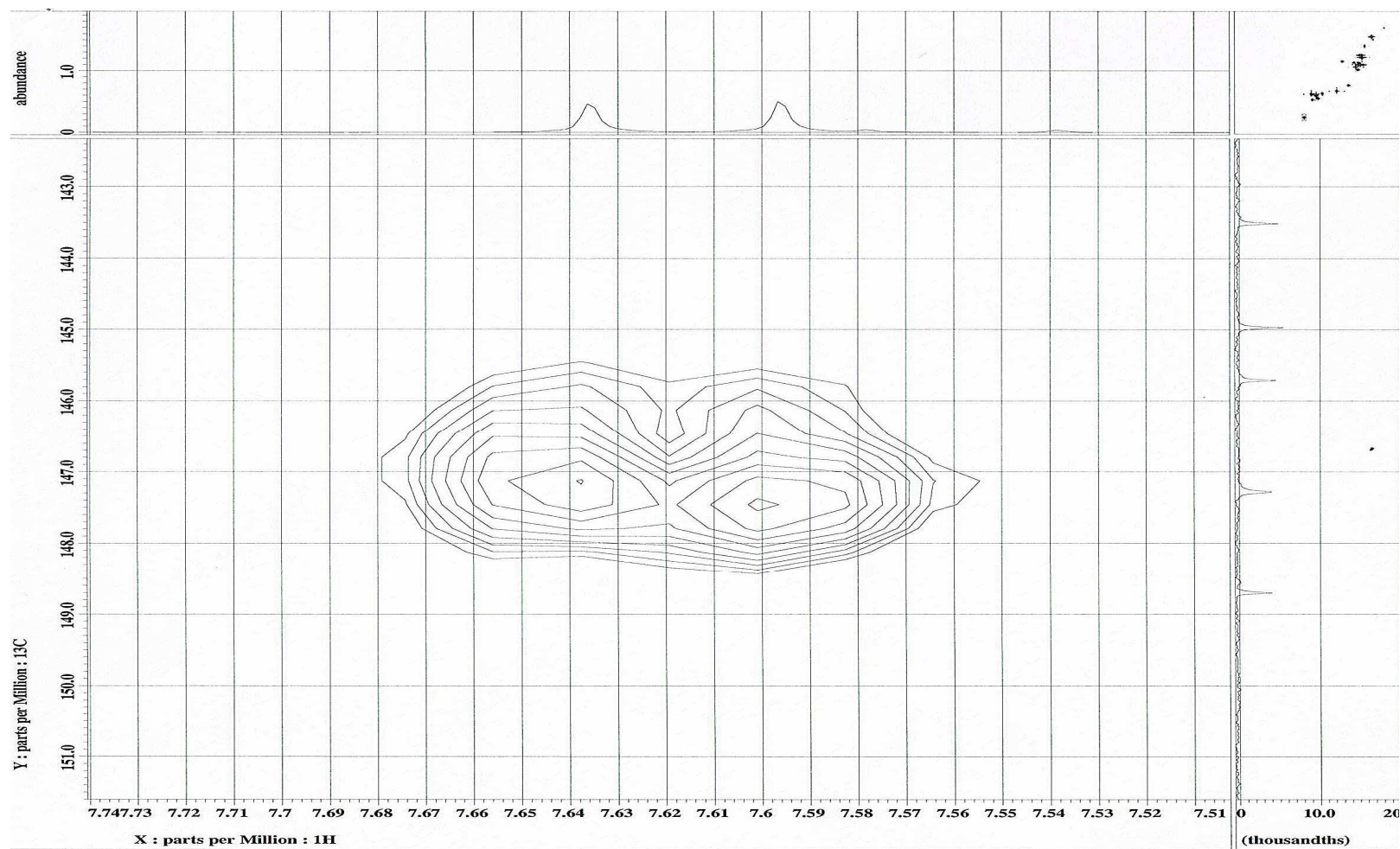
Figure 7.11(d): Enlarged HMQC spectrum of Compound PP-2.
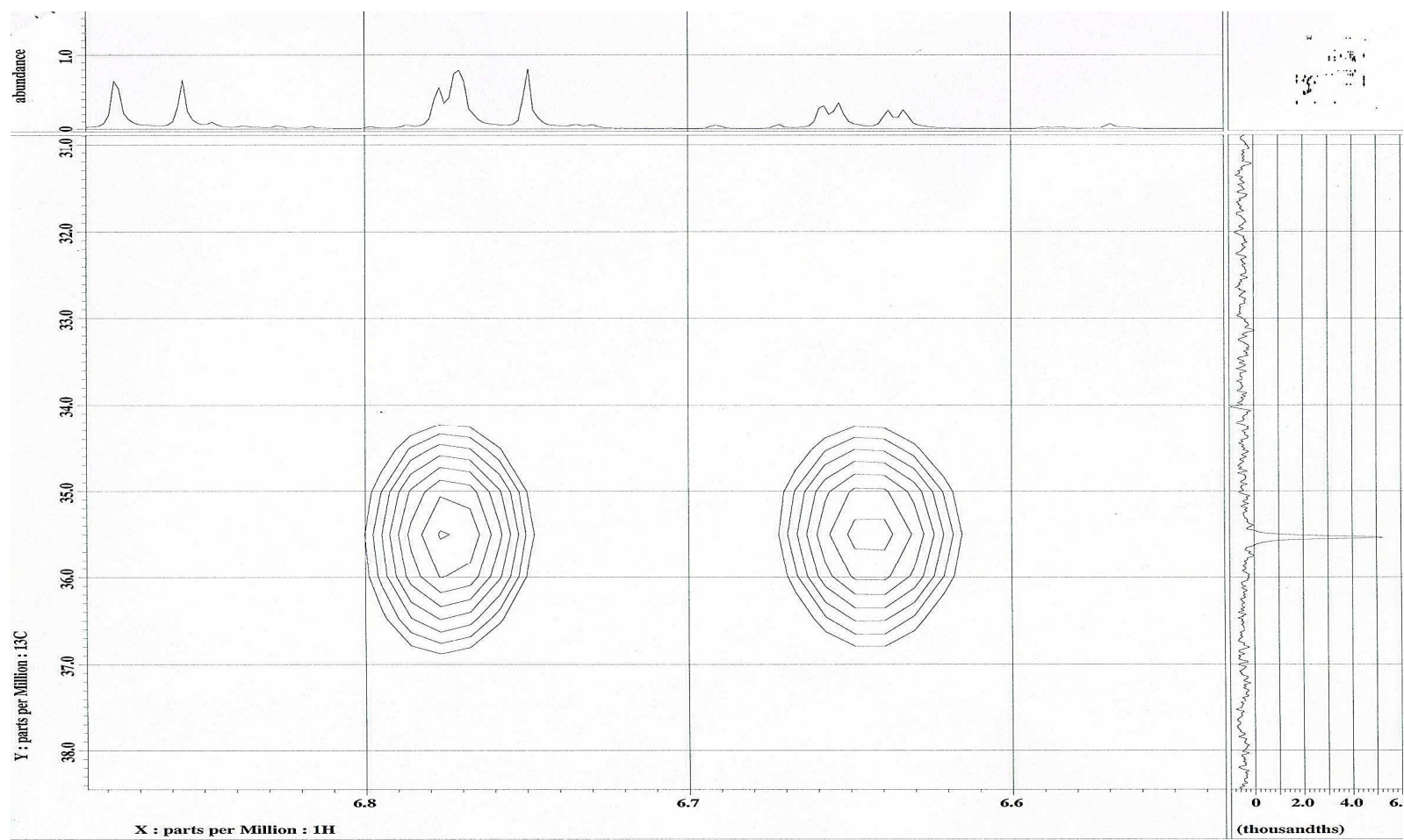
Figure 7.12(a): Enlarged HMBC spectrum of Compound PP-2.
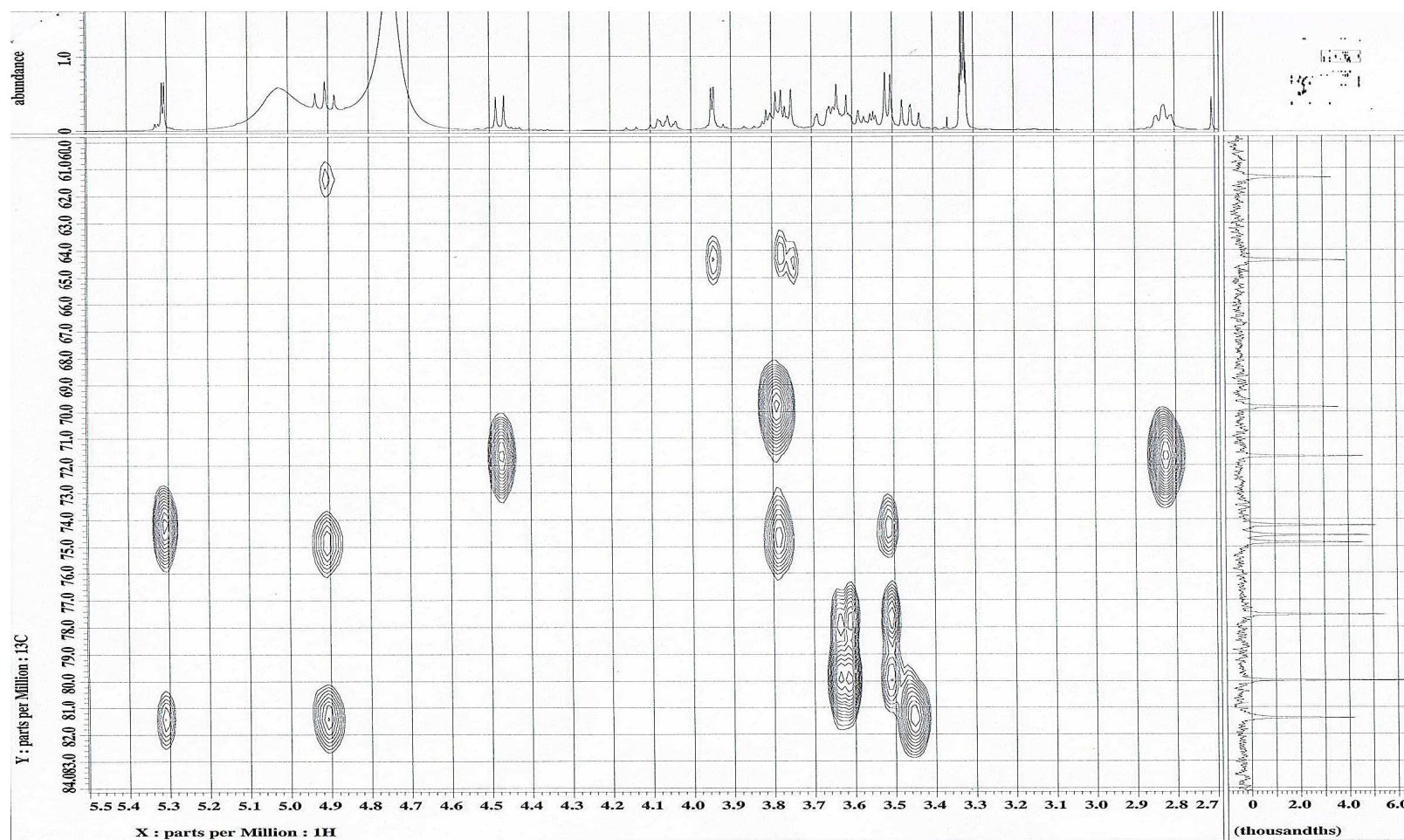
Figure 7.12(b): Enlarged HMBC spectrum of Compound PP-2.
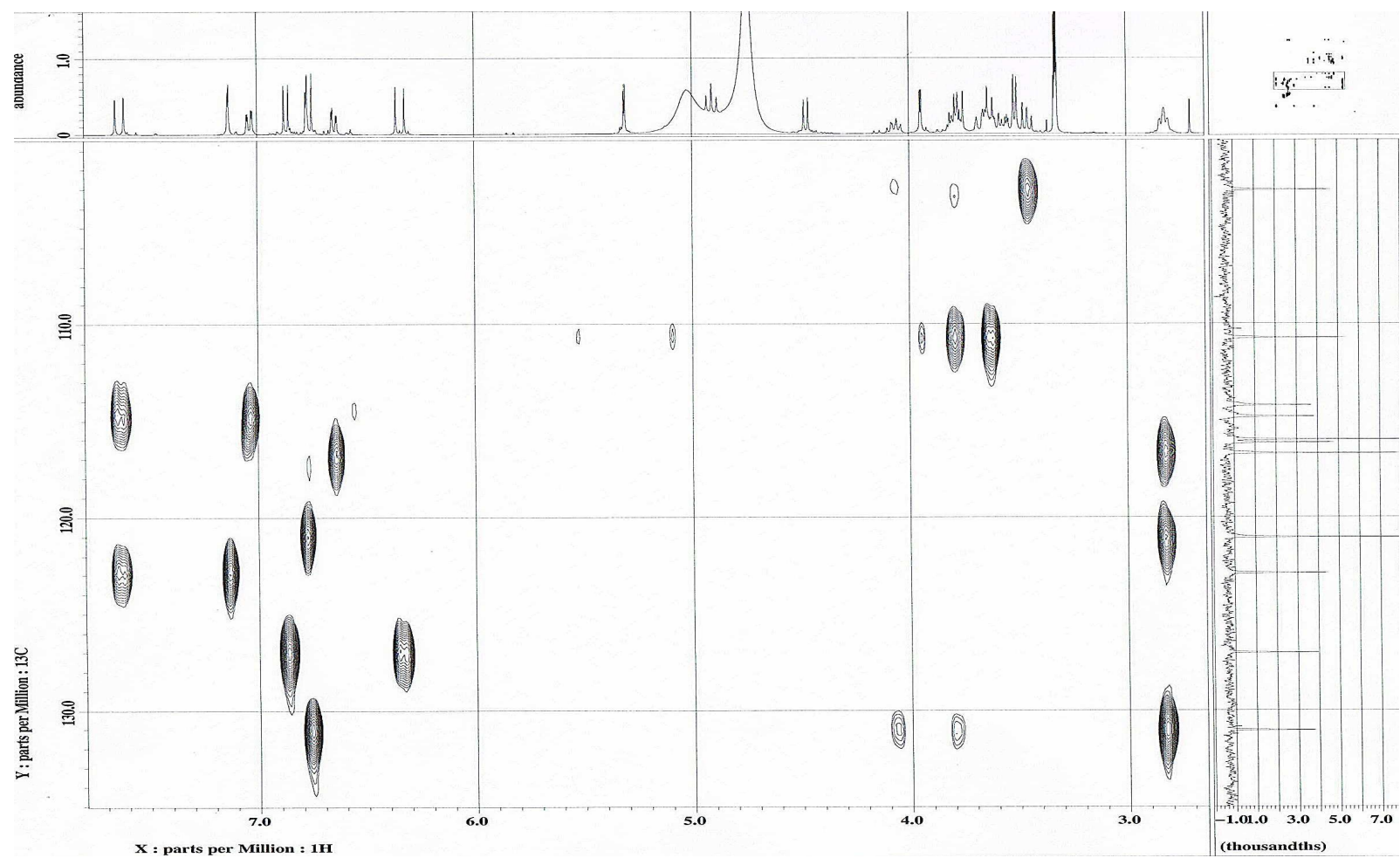
Figure 7.12(c): Enlarged HMBC spectrum of Compound PP-2.
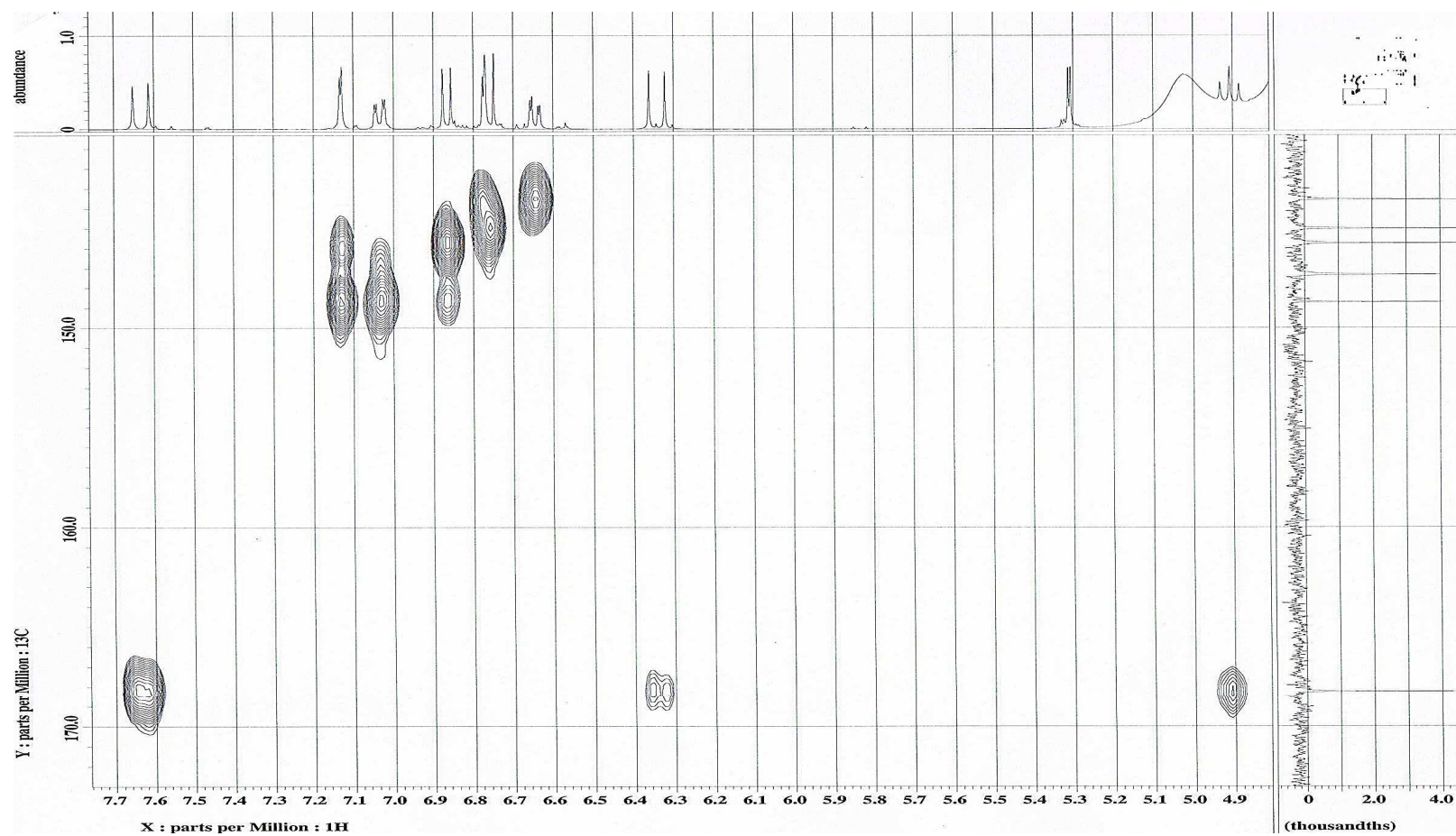
Figure 7.12(d): Enlarged HMBC spectrum of Compound PP-2.
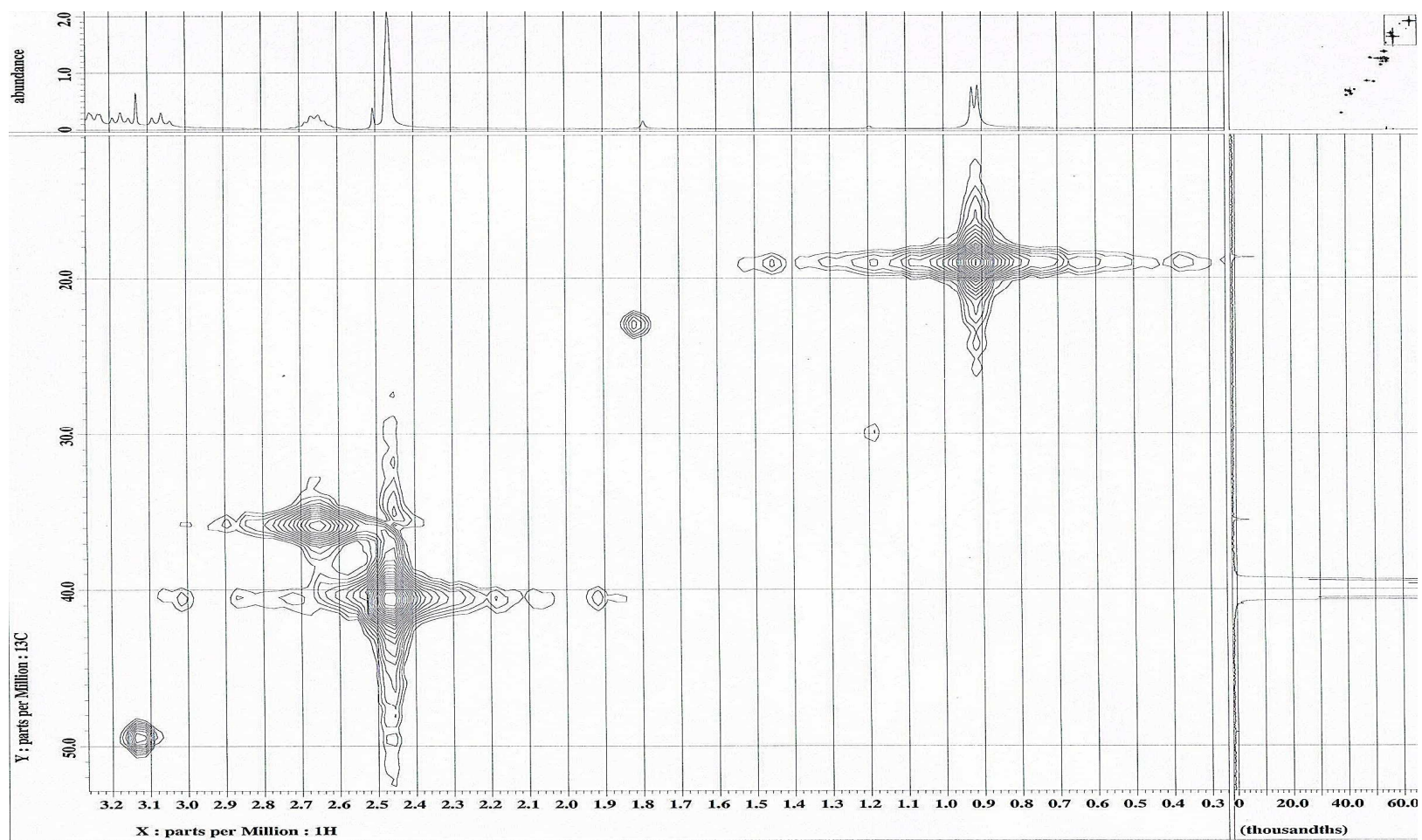
Figure 7.13 (a): Enlarged HMQC spectrum of Compound PP-3.
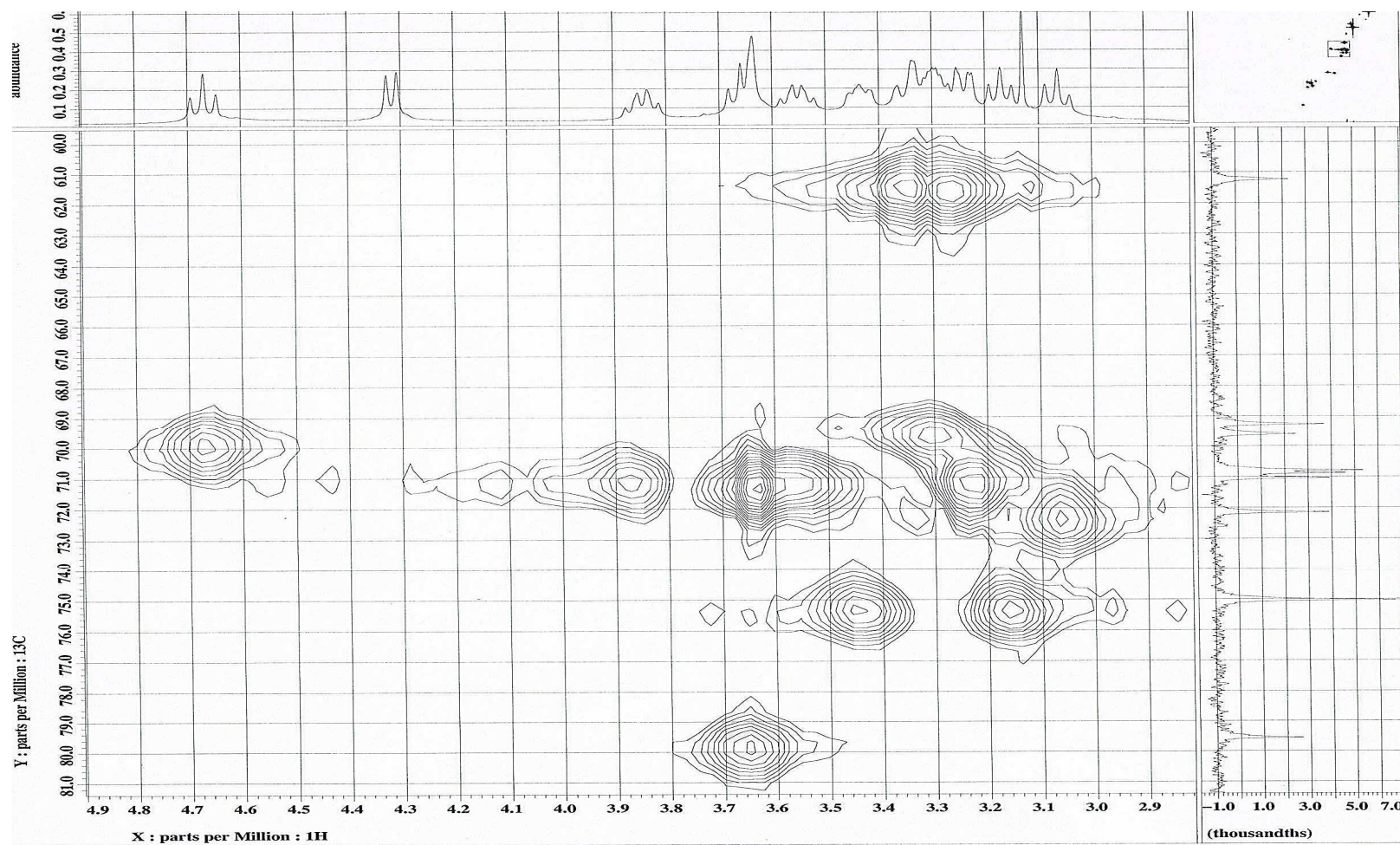
Figure 7.13 (b): Enlarged HMQC spectrum of Compound PP-3.

Figure 7.13(c): Enlarged HMQC spectrum of Compound PP-3.

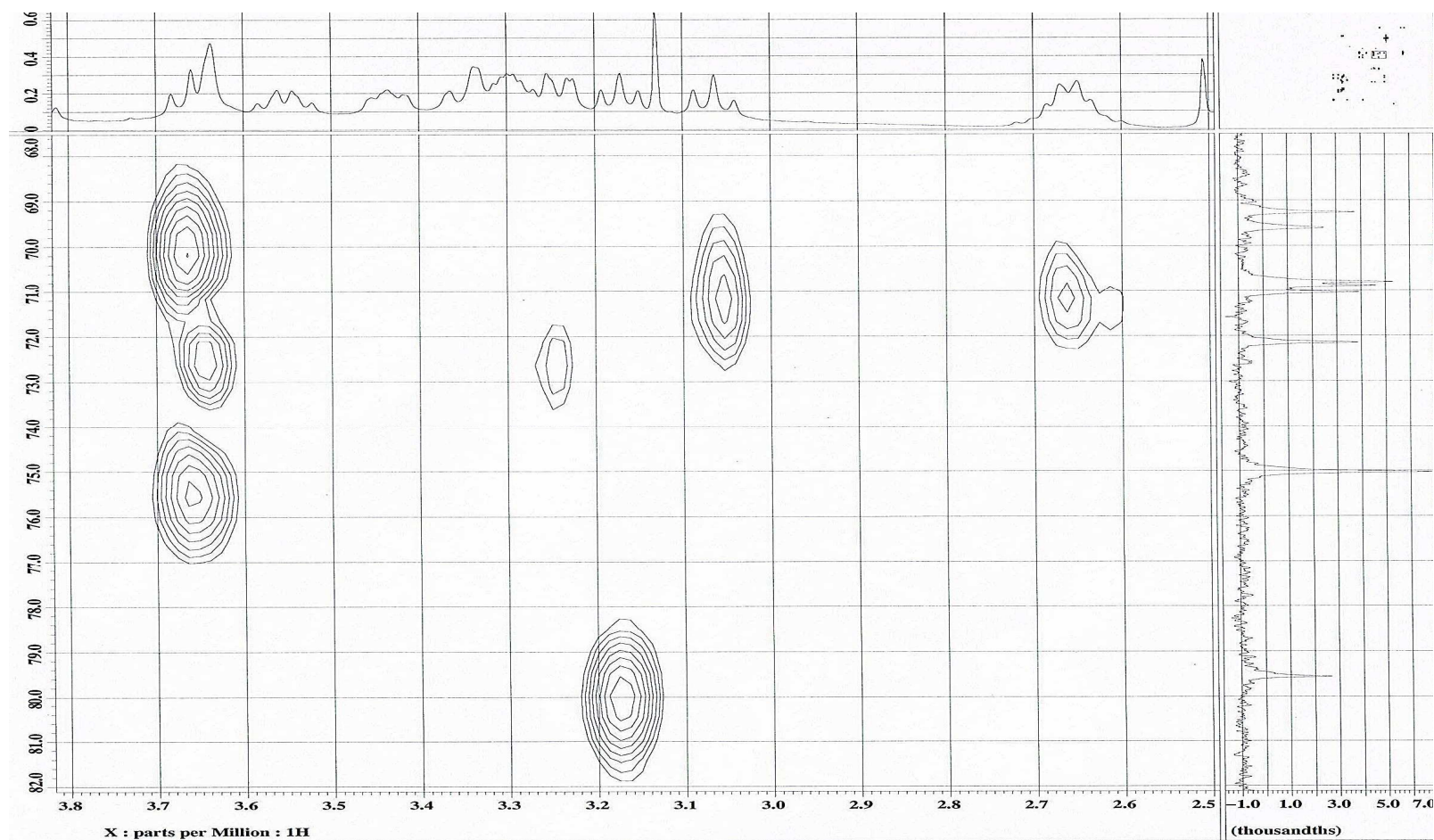**Figure 7.13(d):** Enlarged HMQC spectrum of Compound PP-3.

Figure 7.13(e): Enlarged HMQC spectrum of Compound PP-3.

Figure 7.13(f): Enlarged HMQC spectrum of Compound PP-3.

Figure 7.14(a): Enlarged HMBC spectrum of Compound PP-3.

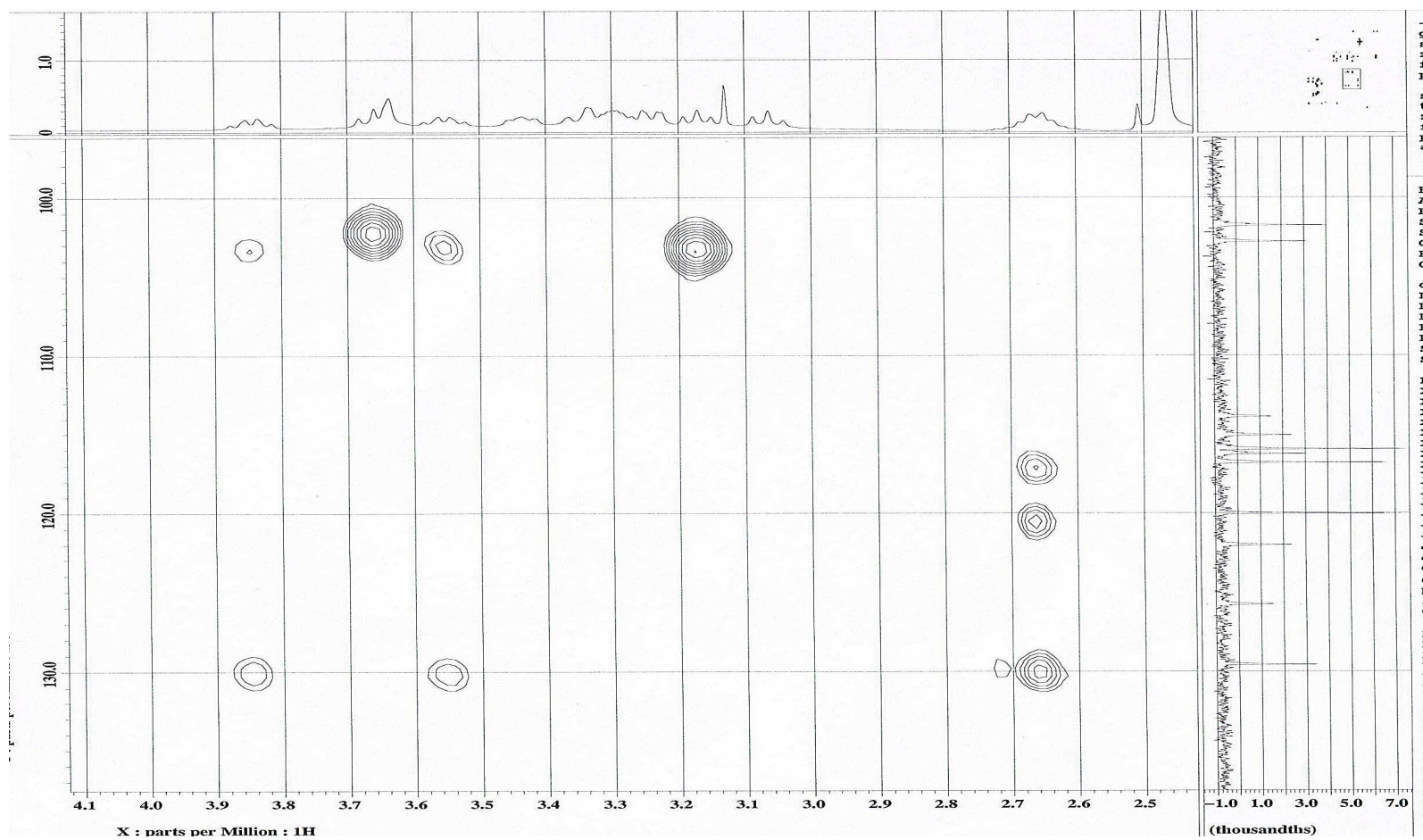**Figure 7.14(b):** Enlarged HMBC spectrum of Compound PP-3.

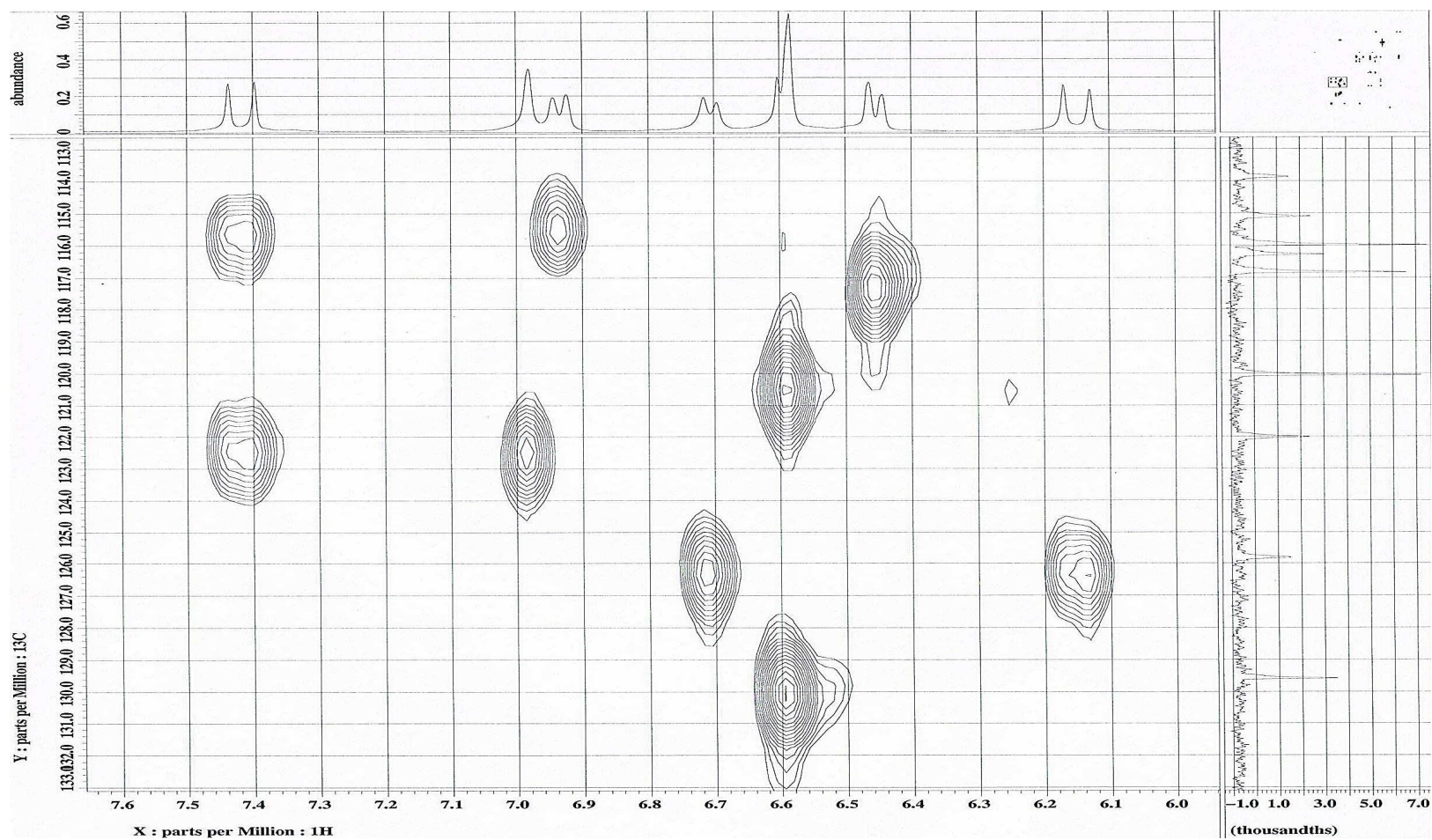**Figure 7.14(c):** Enlarged HMBC spectrum of Compound PP-3.

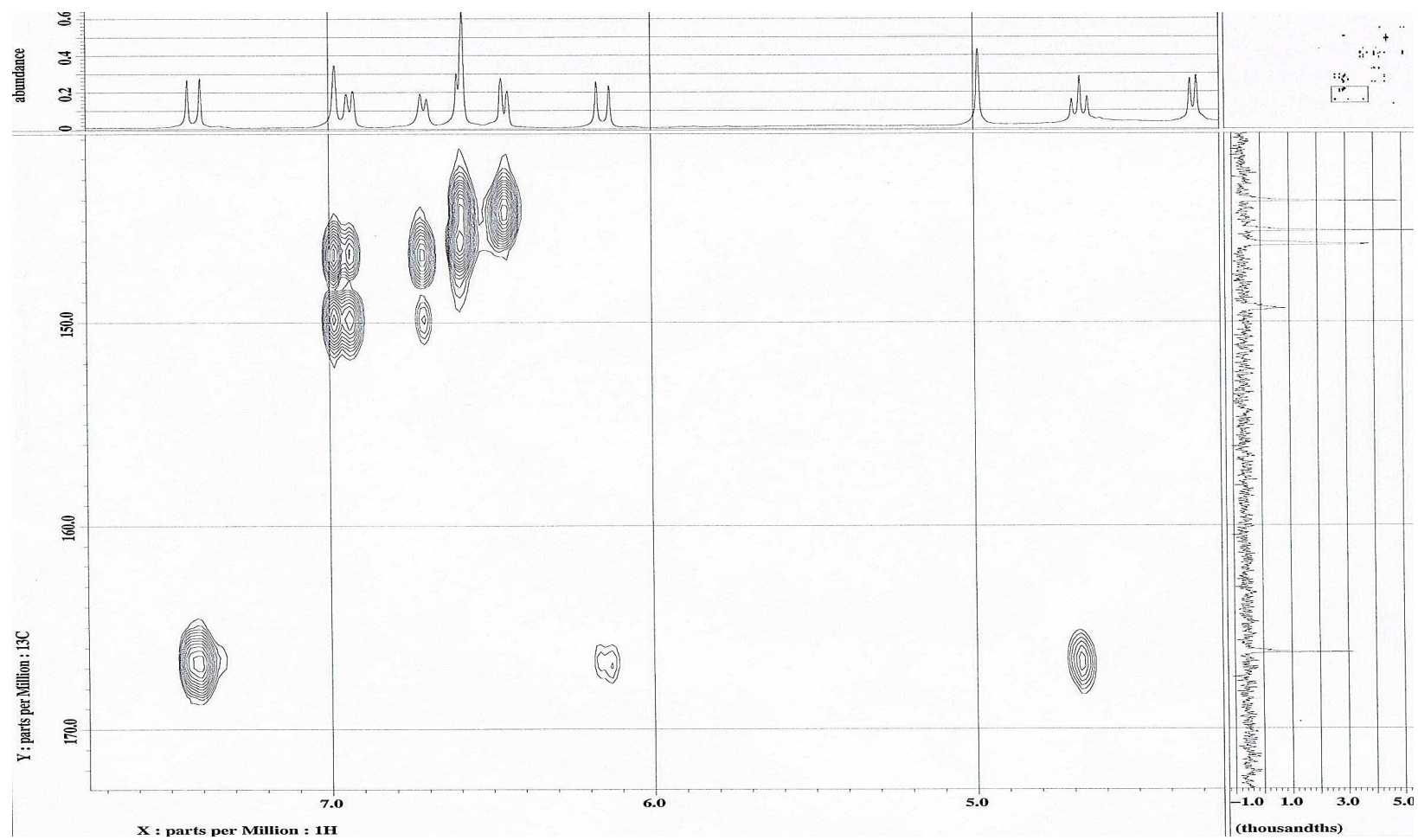**Figure 7.14(d):** Enlarged HMBC spectrum of Compound PP-3.

Figure 7.14(e): Enlarged HMBC spectrum of Compound PP-3.

Figure 7.14(f): Enlarged HMBC spectrum of Compound PP-3.

Figure 7.14(g): Enlarged HMBC spectrum of Compound PP-3.